National Library
of Canada

Bibliothèque nationale
du Canada

Canadian Theses Service

Service des thèses canadiennes

Ottawa, Canada
K1A 0N4

NOTICE

The quality of this microform is heavily dependent upon the quality of the original thesis submitted for microfilming. Every effort has been made to ensure the highest quality of reproduction possible.

If pages are missing, contact the university which granted the degree.

Some pages may have indistinct print especially if the original pages were typed with a poor typewriter ribbon or if the university sent us an inferior photocopy.

Previously copyrighted materials (journal articles, published tests, etc.) are not filmed.

Reproduction in full or in part of this microform is governed by the Canadian Copyright Act, R.S.C. 1970, c. C-30.

AVIS

La qualité de cette microforme dépend grandement de la qualité de la thèse soumise au microfilmage. Nous avons tout fait pour assurer une qualité supérieure de reproduction.

S'il manque des pages, veuillez communiquer avec l'université qui a conféré le grade.

La qualité d'impression de certaines pages peut laisser à désirer, surtout si les pages originales ont été dactylographiées à l'aide d'un ruban usé ou si l'université nous a fait parvenir une photocopie de qualité inférieure.

Les documents qui font déjà l'objet d'un droit d'auteur (articles de revue, tests publiés, etc.) ne sont pas microfilmés.

La reproduction, même partielle, de cette microforme est soumise à la Loi canadienne sur le droit d'auteur, SRC 1970, c. C-30.

NL-339 (r. 88/04)

Canada

THE UNIVERSITY OF ALBERTA

RHODIUM COMPLEXES IN CARBON-HYDROGEN ACTIVATION

BY

© CHANCHAL KUMAR GHOSH

A THESIS
SUBMITTED TO THE FACULTY OF GRADUATE
STUDIES AND RESEARCH IN PARTIAL FULFILLMENT
OF THE REQUIREMENTS FOR THE DEGREE
OF DOCTOR OF PHILOSOPHY

DEPARTMENT OF CHEMISTRY

EDMONTON, ALBERTA

FALL 1988

Permission has been granted to the National Library of Canada to microfilm this thesis and to lend or sell copies of the film.

The author (copyright owner) has reserved other publication rights, and neither the thesis nor extensive extracts from it may be printed or otherwise reproduced without his/her written permission.

L'autorisation a été accordée à la Bibliothèque nationale du Canada de microfilmer cette thèse et de prêter ou de vendre des exemplaires du film.

L'auteur (titulaire du droit d'auteur) se réserve les autres droits de publication; ni la thèse ni de longs extraits de celle-ci ne doivent être imprimés ou autrement reproduits sans son autorisation écrite.

ISBN 0-315-45667-1

THE UNIVERSITY OF ALBERTA

RELEASE FORM

NAME OF AUTHOR	CHANCHAL KUMAR GHOSH
TITLE OF THESIS	RHODIUM COMPLEXES IN CARBON-HYDROGEN ACTIVATION
DEGREE FOR WHICH THESIS WAS PRESENTED	DOCTOR OF PHILOSOPHY
YEAR THIS DEGREE GRANTED	1988

Permission is hereby granted to THE UNIVERSITY OF ALBERTA LIBRARY to reproduce single copies of this thesis and to lend or sell such copies for private, scholarly or scientific research purposes only.

The author reserves other publication rights, and neither the thesis nor extensive extracts from it may be printed or otherwise reproduced without the author's written permission.

Chanchal k. Ghosh

Permanent Address:

Jabni, Shirgram
Faridpur, Bangladesh

Dated 19 August 1988

THE UNIVERSITY OF ALBERTA

FACULTY OF GRADUATE STUDIES AND RESEARCH

The undersigned certify that they have read, and recommend to the Faculty of Graduate Studies and Research, for acceptance, a thesis entitled RHODIUM COMPLEXES IN C-H ACTIVATION submitted by CHANCHAL KUMAR GHOSH in partial fulfillment of the requirements for the degree of Doctor of Philosophy in Chemistry.

W A G Graham
Supervisor

John Hogg

R B Jordan

Ronald G Cavell

William D. Jones
External Examiner

Date 19 August 1988

ABSTRACT

Synthesis, properties and carbon-hydrogen activation reactions of pyrazolylborate complexes of rhodium have been investigated.

The tris(dimethylpyrazolyl)borato complex $(HBPz^*_3)Rh(CO)_2$ (**1**, Pz* = 3,5-dimethylpyrazol-1-yl) reacted with a variety of tertiary phosphines to give the corresponding new class of monophosphine derivatives $(HBPz^*_3)Rh(CO)(PR_3)$ (**4**). Solution infrared spectra indicated that the $HBPz^*_3$ ligand is bidentate in **4**, which are therefore 16-electron Rh (I) complexes. ^{1}H NMR spectra indicated two fluxional processes; an intermediate involving tridentate $HBPz^*_3$ was proposed to explain the low temperature fluxional process.

Ultraviolet irradiation of a benzene solution of **1** rapidly and quantitatively activated benzene affording $(HBPz^*_3)Rh(CO)(H)(C_6H_5)$ (**6**). A solution of **6** in benzene-d_6 undergoes exchange above room temperature forming $(HBPz^*_3)Rh(CO)(D)(C_6D_5)$ (**8a**) and it follows first-order kinetics.

Photolysis of **1** in cyclohexane using an inert gas purge quantitatively afforded $(HBPz^*_3)Rh(CO)(H)(C_6H_{11})$ (**17**), fully characterized as its more stable chloro derivative $(HBPz^*_3)Rh(CO)(Cl)(C_6H_{11})$ (**18**). Cyclohexane in **17** was rapidly and quantitatively displaced by benzene at 25°C forming **6**. Saturation of cyclohexane solution of **17** with CH_4 at 25°C established an equilibrium between **17** and $(HBPz^*_3)Rh(CO)(H)(CH_3)$ (**19**) in which the equilibrium constant favoring methane activation was 190. A combination of kinetic and equilibrium data enabled relative bond strengths to be estimated, with the result Rh-Ph > Rh-CH_3 > Rh-cyclohexyl.

Irradiation of **4b** (PR_3 = PMe_2Ph) in benzene afforded mainly $(HBPz*_3)Rh(H)(C_6H_5)(PMe_2Ph)$ (**32**), while in cyclohexane orthometallation of the phenyl group occurred.

Complexes $(HBPz*_3)Rh(CO)(\eta^2\text{-olefin})$ (Olefin = ethylene, **34a**, propylene, **34b**) have been prepared and shown to be four coordinate in solution. These complexes activate solvent benzene in the dark at 75-105°C forming **6** in high yield. Thermolysis of the above complexes in cyclohexane gave binuclear hydrido species (**38**).

Photolysis of **34a** in benzene yielded both **6** and $(HBPz*_3)Rh(CO)(Et)(Ph)$ (**39**). Carbonylation of **39** in cyclohexane afforded $(HBPz*_3)Rh(CO)(COEt)(Ph)$ (**40**) as the major product; reaction of **40** with $ZnBr_2$ afforded propiophenone in 82% yield.

Irradiation of **1** in cyclohexane using cyclopropane purge afforded rhodacyclobutane (**45**). Thermolysis of **45** in benzene gave **6** along with propylene and cyclopropane. Carbonylation of **45** at 25°C yielded rhodacyclopentanone (**47**). Further carbonylation of **47** at 75°C afforded the rhodacyclohexadione (**49**).

ACKNOWLEDGEMENTS

The author is sincerely grateful to Dr. W.A.G. Graham for his invaluable guidance, dedication, encouragement and especially for his enthusiasm which has been a continual source of inspiration throughout the course of this work.

The author also wishes to express his appreciation to:

Dr. Graham's research group past and present, for assistance in many ways. In particular I would like to thank Dr. G.J. Sunley for discussion on carbonylation reactions, Dr. J.K. Hoyano, Dr. A.D. McMaster, Dr. J.M. Sullivan, Dr. D.P.S. Rodgers, Dr. M. Thomas, Dr. E. Ditzel, Dr. I.M. Saez and Mr. L.B. Gan for many helpful suggestions, assistance and friendship. A special thanks to Mr. R. Krentz for many stimulating discussions, help, friendship and also for proof-reading the manuscript.

Dr. T. Nakashima and the NMR staff, especially Mr. G. Bigam and Mr. T. Brisbane for NMR spectra of consistently high quality.

Mr. J. Olekszyk and Mr. A. Jodhan for obtaining mass spectra.

Dr. Bill Kiel and Dr. Gong-Yu Kiel who have made my time in Edmonton much more enjoyable.

Ms. Nola Shaw for her patience and expertise in the preparation of this manuscript.

The University of Dhaka for allowing me to complete my graduate studies.

TABLE OF CONTENTS

CHAPTER PAGE

I INTRODUCTION....1

References....11

II PHOSPHINE ADDITION REACTIONS....13

Section 1 Introduction....14

Section 2 Synthesis and properties of pyrazolylborate rhodium complexes....17

Section 3 Phosphine addition reactions and fluxional behaviour....24

Section 4 Experimental....45

References....53

III ARENE C-H ACTIVATION....55

Section 1 Introduction....56

Section 2 Benzene activation and the properties of the hydridophenyl product....64

Section 3 Activation of other aromatic hydrocarbons....81

Section 4 Mechanism of C-H activation - some speculation....87

Section 5 Chemically assisted C-H activation....90

Section 6 Experimental....94

References....102

IV ALKANE C-H ACTIVATION....................................105
Section 1 Introduction......................................106
Section 2 Activation of dihydrogen and cyclohexane.......117
Section 3 Acyclic alkane activation.......................139
Section 4 Experimental......................................147
References 157

V C-H ACTIVATION BY MONOPHOSPHINE DERIVATIVES...............161
Section 1 Introduction......................................162
Section 2 C-H activation by $(HBPz^*{}_3)Rh(CO)(PMe_2Ph)$.......166
Section 3 Experimental......................................172
References 180

VI OLEFIN COMPLEXES..181
Section 1 Introduction......................................182
Section 2 Synthesis and properties of olefin complexes...185
Section 3 Thermal C-H activation...........................201
Section 4 Novel photochemical reaction of the carbonyl-ethylene complex...............................210
Section 5 Functionalization using carbon monoxide........217
Section 6 Experimental......................................227
References 240

VII METALLACYCLES...243
Section 1 Introduction......................................244
Section 2 Synthesis and characterization of metallacycles.....................................249

Section 3 Thermolysis of metallacycles....................255
Section 4 Functionalization of metallacycles.............268
Section 5 Experimental...................................278
References 285

VIII DISCUSSION AND CONCLUSIONS..............................288
References 296

LIST OF TABLES

TABLE PAGE

CHAPTER II

2.I ν_{CO} of the Phosphine Complexes....................................26

2.II Spin Saturation Transfer Data for $(HBPz^*_3)Rh(CO)(PMe_2Ph)$ (**4b**)....................................37

2.III Line Broadening Data for $(HBPz^*_3)Rh(CO)(PMe_2Ph)$ (**4b**).....40

CHAPTER III

3.I Rate Constants for Exchange of Benzene-d_6 with $(HBPz^*_3)Rh(CO)(H)(C_6H_5)$ (**6**)....................................72

3.II UV-VIS Spectral Data....................................87

CHAPTER IV

4.I Rate Constants for the Reaction of $(HBPz^*_3)Rh(CO)(H)(Cy)$ (**17**) at Different $[CyH]/[C_6H_6]$ Ratios....................................126

CHAPTER V

5.I Crystal Data for $(HBPz^*_3)\overline{Rh(Cl)\{P(Me)_2C}_6H_4\}$ (**33**).......176

5.II Bond Lengths for **33**....................................177

5.III Bond Angles for **33**....................................178

CHAPTER VI

6.I Spin Saturation Transfer Data for $(HBPz^*_3)Rh(CO)(\eta^2\text{-}C_2H_4)$ (**34a**)....192

6.II Line Broadening Data for **34a**....193

6.III Relative Yields of Ethyl Phenyl (**39**) and Phenyl Hydride (**6**)....214

6.IV Crystal Data for $(HBPz^*_3)Rh(CO)(Et)(Ph)$ (**39**)....234

6.V Bond Lengths for **39**....235

6.VI Bond Angles for **39**....236

LIST OF FIGURES

FIGURE PAGE

CHAPTER II

II.1 Infrared spectrum of $(HBPz^*_3)Rh(CO)_2$ **(1)**................21

II.2 ^{1}H NMR spectrum of $(HBPz^*_3)Rh(CO)(PMe_2Ph)$ **(4b)**..........27

II.3 ^{1}H NMR spectrum of $(H_2BPz^*_2)Rh(CO)(PMe_2Ph)$ **(5b)**.........29

II.4a ^{1}H SST difference spectrum of $(HBPz^*_3)Rh(CO)(PMe_2Ph)$ **(4b)**..35

II.4b ^{1}H SST difference spectrum of $(HBPz^*_3)Rh(CO)(PMe_2Ph)$ **(4b)**..36

II.5 Eyring plot of ^{1}H rate constant data for $(HBPz^*_3)Rh(CO)(PMe_2Ph)$ **(4b)**.............................39

CHAPTER III

III.1 ^{1}H NMR spectrum of $(HBPz^*_3)Rh(CO)(H)(C_6H_5)$ **(6)** at ambient temperature..................................66

III.2 ^{1}H NMR spectrum of $(HBPz^*_3)Rh(CO)(H)(C_6H_5)$ at -20°C.....67

III.3 2-D NMR spectrum of $(HBPz^*_3)Rh(CO)(H)(C_6H_5)$ in the phenyl region...69

III.4 Rate of benzene exchange for $(HBPz^*_3)Rh(CO)(H)(C_6H_5)$ **(6)** in C_6D_6 at 42°C....................................71

III.5 Eyring plot for the exchange of $(HBPz^*_3)Rh(CO)(H)(C_6H_5)$ **(6)**............................73

CHAPTER IV

IV.1 First-order rate plot for the reaction of $(HBPz*_3)Rh(CO)(H)(Cy)$ (**17**) with C_6H_6....................124

IV.2 Plot of $1/k_{obsd}$ versus $[CyH]/[C_6H_6]$ ratios for the reaction of $(HBPz*_3)Rh(CO)(H)(Cy)$ (**17**)................127

IV.3 Energy profile for the reaction of $(HBPz*_3)Rh(CO)(H)(Cy)$ with C_6H_6........................128

IV.4 Infrared spectrum showing the equilibrium between $(HBPz*_3)Rh(CO)(H)(Cy)$ (**17**) and $(HBPz*_3)Rh(CO)(H)(CH_3)$ (**19**)..130a

CHAPTER V

V.1 ^1H NMR spectrum of $(HBPz*_3)Rh(Ph)(Cl)(PMe_2Ph)$ (**31**).....168

V.2 Crystal structure of $(HBPz*_3)Rh(Cl)(PMe_2C_6H_4)$ (**33**).....171

CHAPTER VI

VI.1 Mechanism for exchange between benzene-d_6 and coordinated ethylene in $(\eta\text{-}C_5H_5)Rh(C_2H_4)_2$..............183

VI.2 Eyring plot of ^1H rate constant data for $(\eta^2\text{-}HBPz*_3)Rh(CO)(\eta^2\text{-}C_2H_4)$ (**34a**)......................194

VI.3 ^1H NMR spectrum of $(HBPz*_3)Rh(CO)(C_8H_{14})$ (**37**)..........198

VI.4 ^1H NMR spectrum of binuclear hydrido species (**38**)......206

VI.5 ^{13}C NMR spectrum of binuclear hydrido species (**38**).....207

VI.6 Crystal structure of $(HBPz*_3)Rh(CO)(Et)(Ph)$ (**39**).......212

VI.7 A view of ethyl phenyl complex (**39**) along B-Rh pseudo three-fold axis..................................213

CHAPTER VII

VII.1 ^{13}C NMR spectrum of methyl-substituted metallacyclobutane (**46A**)..............................254

VII.2 Plot of normalized concentration of metallacyclobutane (**45**), pentadeuterophenyl deuteride (**8a**) and η^2-propylene complex (**34b**) versus time........256

VII.3 First-order plot for the reaction of metallacyclobutane (**45**) with benzene-d_6................258

VII.4 First-order plot for the reaction of (HBPz$^*_3$)Rh(CO)(η^2-propylene) (**34b**) with benzene-d_6.....259

VII.5 Plot of concentration of η^2-propylene complex (**34b**) versus time at different k_1/k_3 ratios..................261

VII.6 Infrared spectrum of rhodacyclohexadione (**49**)..........274

VII.7a ^{13}C NMR spectrum of rhodacyclohexadione (**49**)...........276

VII.7b ^{13}C NMR spectrum of rhodacyclohexadione (**49**)...........277

LIST OF ABBREVIATIONS

Me	methyl
Et	ethyl
Ph	phenyl
THF	tetrahydrofuran
COD	1,5 cyclooctadiene
t-Butyl	tertiary butyl
Cp	η^5-cyclopentadienyl, C_5H_5
Cp*	η^5-pentamethylcyclopentadienyl, C_5Me_5
Pz	pyrazolyl-1-yl, $C_3H_3N_2$
Pz*	3,5-dimethylpyrazol-1-yl, $C_5H_7N_2$
APT	attached proton test
RF	radio frequency
FID	free induction decay
Mz	equilibrium magnetization (z component)
δ	chemical shift in ppm's from tetramethylsilane
SST	spin saturation transfer

CHAPTER I

INTRODUCTION

This Thesis describes the synthesis and properties of tris(dimethylpyrazolyl)borato complexes of rhodium. The main concern of this work is to investigate the potential of this class of complex in carbon-hydrogen (C-H) activation. Before describing C-H activation, a brief discussion of the tris(pyrazolyl)borate ligand will be presented.

Tris(pyrazolyl)borate ligand

The tris(pyrazolyl)borate ligand was first reported in 1967.[1] The use of this novel ligand to form complexes with a variety of transition metals has been described.[2] The two most common and extensively investigated of these ligands are derived from the unsubstituted pyrazole, and 3,5-dimethyl substituted pyrazole. These have a formal similarity to cyclopentadienide anion ($C_5H_5^-$) and pentamethylcyclopentadienide anion ($C_5Me_5^-$). For example, tris(pyrazolyl)borate anion and cyclopentadienide anion are uninegative six electron donors, the electrons being derived from three nitrogen lone pairs in tris(pyrazolyl)borate anion or the aromatic sextet in $C_5H_5^-$.

The framework of tris(pyrazolyl)borate ligand is shown in the sketches in eq. 1-1. 1 is the hydrotris(pyrazol-1-yl)borato ligand, abbreviated $HBPz_3$; 2 is the hydrotris(3,5-dimethylpyrazol-1-yl)borato ligand, $HBPz^*_3$ (the asterisk indicates methyl groups replacing two hydrogen atoms on each of the pyrazole rings).

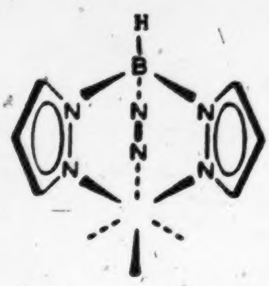

$(HBPz_3)$

1

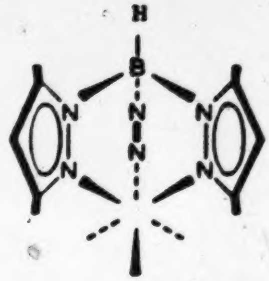

$(HBPz^*_3)$

2

(1-1)

Previous investigations[3] of the coordination chemistry of unsubstituted tris(pyrazolyl)borate ligand ($HBPz_3^-$) had shown that, in most cases, dinuclear rhodium species formed preferentially to mononuclear ones. Thus in the present investigation, the 3,5-dimethyl derivative of pyrazole has been used to synthesize mononuclear tris(3,5-dimethylpyrazolyl)borato complexes $(HBPz^*_3)Rh(CO)(L)$ (L = carbon monoxide, tertiary phosphines, olefins) and the potential of these rhodium complexes for C-H activation has been explored. The dicarbonyl, $(HBPz^*_3)Rh(CO)_2$, was first briefly mentioned in 1971 reported by Trofimenko[4] and later examined cursorily by Powell et al.[5]

An interesting aspect of tris(pyrazolyl)borate ligand is that it can bond to transition metals in different ways. For example, it may function as a bidentate ligand (two of three available nitrogen atoms coordinated to metal) or in a tridentate fashion (all three nitrogen atoms coordinated to metal). It is convenient to have a shorthand notation to describe the number of nitrogen atoms attached to the metal. A system of notation originally suggested by Cotton[6] for carbocyclic ligands will be adapted for this purpose. The number of nitrogen atoms bonded to the metal is specified by a prefix such as monohapto, dihapto, trihapto. Abbreviations for these prefixes are η^1, η^2, η^3.

Effective atomic number rule

The 18-electron rule provides a simple way of estimating the stability and reactivity of many types of complexes. This rule was initially formulated by Sidgwick[7] in 1934, after a study of the binary carbonyls. Few exceptions are known among compounds containing π-acid ligands. A molecular orbital viewpoint of the 18-electron rule has been provided by Mitchell and Parish.[8] The eighteen electrons to which the rule refers are considered to be in the nine valence shell orbitals of the metal atom (five (n-1)d orbitals, one ns orbital, and three np orbitals). More precisely, it can be said that the electrons are placed in the molecular orbitals formed from these atomic orbitals. These electrons comprise those donated by the ligands together with the d electrons of the metal ion in the appropriate oxidation state. To apply 18-electron rule to a specific case like $Mo(CO)_6$, one can say that Mo is six groups from the left hand side of the Periodic Table, and thus has six valence electrons. Each carbon monoxide ligand donates an electron pair, so that molybdenum can be considered to obey the 18-electron rule $(6 + (6 \times 2) = 18)$.

A number of reactions proceed via 16-electron, coordinatively unsaturated intermediate, generated by heat or ultraviolet light (eq.

1-2).[9]

$$W(CO)_6 \xrightarrow[\text{or } \Delta]{h\nu,\ -CO} [W(CO)_5] \xrightarrow{L} W(CO)_5L \qquad (1\text{-}2)$$

The 16-electron $[W(CO)_5]$ species is known to be involved in the simple substitution of one ligand by another.

Stable 16-electron complexes of the later transition metals (Rh, Ir, Pd, Pt), all d^8 in their compounds, are more the rule than the exception. These are square planar complexes, and the origin can be traced qualitatively to the large energy gap between $d_{x^2-y^2}$ and the next lower orbital that emerges even in simple crystal field theory.[10] One of the most famous of these 16-electron complexes is the four-coordinate iridium compound $ClIr(CO)(PPh_3)_2$.[11] It is considered to be made up of a Cl^- ion, and Ir^+, and three neutral ligands (ligands may be either neutral or negative, and each is considered to donate a pair of electrons to the metal). Neutral iridium (nine groups from the left hand side of the Periodic Table) would have nine valence electrons. Hence Ir^+, or as it is usually represented, Ir (I), will have eight electrons. Thus the electron count is (8 + 4 x 2) = 16e. This iridium complex is a stable species, but its reactions are dominated by its tendency to achieve an 18e configuration. This can be shown by the landmark reaction[11] in which hydrogen was activated (eq. 1-3).

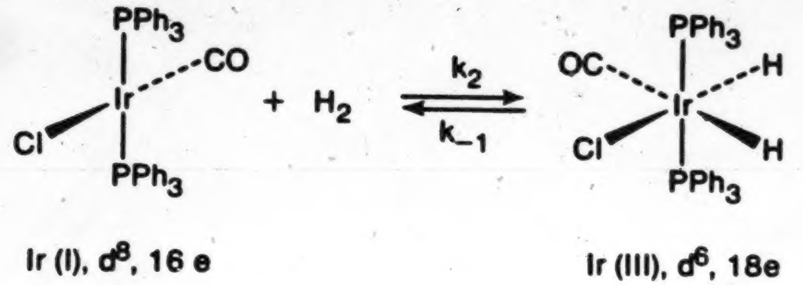

(1-3)

The eq. 1-3 illustrates the known geometric arrangement of ligands, square planar in the reactant and octahedral in the product. The reactant $ClIr(CO)(PPh_3)_2$ is a 16e Ir (I) complex, the Roman numerical representing iridium's oxidation state. The product complex $ClIr(H)_2(CO)(PPh_3)_2$ has three negative ligands (Cl^-, H^-, H^-) and since the compound is unchanged overall, the metal oxidation state must be counted as +3 or Ir (III). Since Ir (III) would have six electrons and 12-electron (6 x 2) are donated by ligands, the product is an 18e complex. The forward reaction in eq. 1-3 is called an oxidative addition (Ir is oxidized from I to III and hydrogen adds to it); the reverse reaction (eq. 1-3) is called reductive elimination.

Tris(3,5-dimethylpyrazolyl)borato complexes $(HBPz^*_3)Rh(CO)(L)$ (L = CO, PR_3, olefin) might exist as four-coordinate, 16-electron square planar rhodium (I) complexes, or as trigonal bipyramidal five-coordinate 18-electron species depending upon the mode of attachment of the tris(pyrazolyl)borate ligand. The coordination chemistry and dynamic behaviour of the above complexes will be addressed in the present investigation.

Carbon-hydrogen activation

The activation and subsequent functionalization of C-H bonds under mild and homogeneous conditions are currently attracting a great deal of interest. Only in recent years have significant advances in the stoichiometric activation of saturated hydrocarbons been achieved. However, catalytic activation of C-H bonds resulting in useful and selective functionalization of saturated hydrocarbons remains a challenging objective to organometallic chemists.

It is useful to regard dihydrogen as a model for C-H bonds in activation processes. Hydrogen, like saturated hydrocarbons, is chemically unreactive in many reactions even when there is a strong thermodynamic driving force for the reaction. For example, hydrogenation of olefin[12] (eq. 1-4) proceeds only when a catalyst is present.

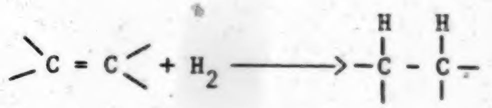

$$>C=C< + H_2 \longrightarrow -\overset{H}{\underset{|}{\overset{|}{C}}}-\overset{H}{\underset{|}{\overset{|}{C}}}- \qquad (1\text{-}4)$$

$\Delta H = -33$ kcal

Finely divided transition metals were once exclusively used as catalysts in this reaction. This process is heterogeneous and the catalyst is considered to activate hydrogen, presumably in a series of steps beginning with adsorption on the metal surface.

Since the 1960's, Wilkinson's catalyst [$ClRh(PPh_3)_3$] has become known as an effective and widely used homogeneous hydrogenation catalyst.[13] Details of how the catalyst activates the substrate can be more readily determined in the homogeneous system than for heterogeneous catalysts. The pathway for hydrogenation is shown in eq. 1-5 for a soluble transition metal complex represented by [M].

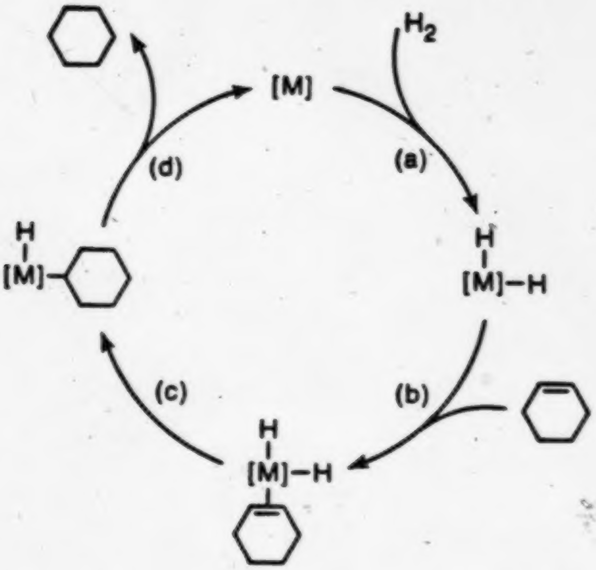

(1-5)

The step a in eq. 1-5 is the activation of hydrogen, in which H-H bond is broken and two new M-H bonds are formed. This is followed by: binding of the olefin to an available site on the metal (step b in eq. 1-5); insertion of bound olefin into a metal-hydrogen bond (step c); and finally elimination of the saturated hydrocarbon (step d). The unique feature of a catalytic cycle is that all steps occur rapidly and consecutively.

Activation of saturated hydrocarbons by well defined, intermolecular oxidative addition processes has been known only since 1982, although the activation of other saturated molecules, including

H_2, is widespread and has been extensively studied.[14,15]

Several approaches to C-H activation have been categorized by Halpern[16] as follows:

1. Electrophilic displacement

$$M^n + X\text{-}Y \longrightarrow M^nX^- + Y^+ \qquad (1\text{-}6)$$

2. Oxidative addition

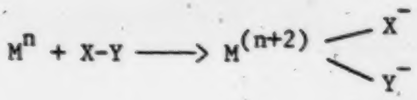

$$M^n + X\text{-}Y \longrightarrow M^{(n+2)} \begin{array}{l} \diagup X^- \\ \diagdown Y^- \end{array} \qquad (1\text{-}7)$$

3. Homolytic displacement

$$M^n + X\text{-}Y \longrightarrow M^{(n+1)}X^{\bullet} + Y^{\bullet} \qquad (1\text{-}8)$$

4. Nucleophilic displacement

$$M^n + X\text{-}Y \longrightarrow M^{(n+2)}\, X^- + Y^- \qquad (1\text{-}9)$$

Of these general modes, electrophilic displacement and oxidative addition have been identified for H_2 and were suggested[16] to be applicable to C-H activation. The approach to C-H activation involving oxidative addition will be considered in the present investigation.

Pyrazolylborate-transition-metal chemistry has developed extensively but has not previously intersected the area of carbon-hydrogen activation. Rhodium in one form or another is the basis for many catalytic processes. By virtue of its position in the Periodic Table and its general importance in catalysis, rhodium was considered a promising basis for this new C-H activating system. Moreover pentamethylcyclopentadienyl rhodium complexes had been shown to activate C-H bonds.[17]

The question of how the compounds formed in the initial C-H activation step can be converted to functionalized end products will also be addressed in this Thesis.

References for Chapter I

1. S. Trofimenko, J. Am. Chem. Soc., 89 (1967) 3170.
2. (a) S. Trofimenko, Acc. Chem. Res., 4 (1971) 17.
   (b) S. Trofimenko, Chem. Rev., 72 (1972) 497.
   (c) S. Trofimenko, Prog. Inorg. Chem., 34 (1986) 115.
3. (a) D.J. O'Sullivan and F.J. Lalor, J. Organomet. Chem. 65 (1974) C47.
   (b) N.F. Borkett and M.I. Bruce, J. Organomet. Chem., 65 (1974) C51.
   (c) M. Cocivera, T.J. Desmond, G. Ferguson, B. Kaitner, F.J. Lalor and D.J. O'Sullivan, Organometallics, 1 (1982) 1125.
4. S. Trofimenko, Inorg. Chem., 10 (1971) 1372.
5. S. May, P. Reinsalu and J. Powell, Inorg. Chem., 19 (1980) 1582.
6. F.A. Cotton, J. Am. Chem. Soc., 90 (1968) 6230.
7. N.V. Sidgwick and R.W. Bailey, Proc. Roy. Soc., 144 (1934) 521.
8. P.R. Mitchell and R.V. Parish, J. Chem. Ed., 46 (1969) 811.
9. C.A. Tolman, Chem. Soc. Reviews, 1 (1972) 337.
10. F.A. Cotton and G. Wilkinson, Adv. Inorg. Chem., 4th Ed. Wiley and Sons, (1980) 643.
11. L. Vaska and J.W. DiLuzio, J. Am. Chem. Soc., 84 (1962) 679.
12. R.E. Harmon, S.K. Gupta and D.J. Brown, Chem. Rev., 73 (1973) 21.
13. J.A. Osborn, F.H. Jardine, J.F. Young and G. Wilkinson, J. Chem. Soc., (A) (1966) 1711.
14. J. Halpern, Ann. Rev. Phys. Chem., 16 (1965) 103.
15. B.R. James, "Homogeneous Hydrogenation", Wiley, New York, 1977.
16. J. Halpern, Inorg. Chim. Acta, 100 (1985) 41.
17. (a) W.D. Jones and F.J. Feher, J. Am. Chem. Soc., 106 (1984) 1650.

(b) W.D. Jones and F.J. Feher, J. Am. Chem. Soc., 107 (1985) 620.

CHAPTER II

PHOSPHINE ADDITION REACTIONS

Section 1

INTRODUCTION

The hydrotris (pyrazol-1-yl)- and (3,5-dimethylpyrazol-1-yl)borato ligands were first prepared by Trofimenko,[1] who has pointed out that this novel and important class of ligands may function as a bidentate ligand or in a tridentate fashion.[2,3] The analogy between tris(pyrazolyl)borate anion ($HBPz_3^-$) and the cyclopentadienide anion ($C_5H_5^-$) has also been drawn by Trofimenko.[2] The comparison arises from the fact that both ligands are uninegative six electron donors, the electrons being derived from three nitrogen lone pairs in $HBPz_3^-$ or the aromatic sextet in $C_5H_5^-$. A similar analogy can be drawn between hydrotris (3,5-dimethylpyrazol-1-yl)borate anion ($HBPz*_3^-$) and the pentamethylcyclopentadienide anion ($C_5Me_5^-$).

An important bis(olefin) rhodium (I) complex $(HBPz_3)Rh(C_2H_4)_2$ was first reported by Trofimenko.[4] On the basis of NMR results, he proposed that the structure was like that of $(acac)Rh(C_2H_4)_2$ (acac is the acetylacetonate anion), a well-known sixteen electron (16e) complex, rather than $(C_5H_5)Rh(C_2H_4)_2$, a five-coordinate eighteen electron (18e) structure.

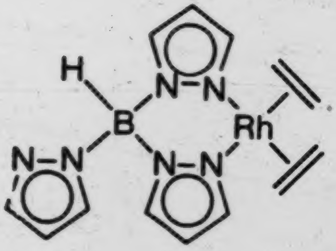

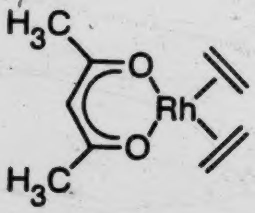

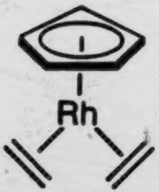

Since the three Pz ligands were equivalent on the NMR timescale, he argued that some fluxional process would have to be involved if it did not have the 18e structure where all three Pz ligands coordinated to rhodium.

Over the past 15 to 20 years the structural[5-8] and chemical[8-10] properties of these and related complexes have received some attention. In this context it is interesting to note Lalor's[11] work on the $(BPz_4)Rh(COD)$ complex (BPz_4 denotes tetrakis(1-pyrazolyl)borate ion), in which NMR equivalence of the four Pz groups was found. This of course does not tell much about the state of rhodium, which on the NMR evidence could be either four- or five-coordinate. Another important observation by Lalor was that Ph_3P readily displaced C_2H_4 from $(HBPz_3)Rh(C_2H_4)_2$ or $(BPz_4)Rh(C_2H_4)_2$; he considered this as evidence for a 16e structure, since displacement of C_2H_4 from $(C_5H_5)Rh(C_2H_4)_2$ by phosphines has a high activation energy. In the case of $(BPz_4)Rh(CO)(I)_2$, Lalor[11] found two distinct Pz environments in a 3:1 ratio in the NMR. From this observation he supports a "tri-N-hapto" structure with a dangling Pz group. A number of other five-coordinate rhodium diene complexes of the type $(BPz_4)Rh(diene)$ have more recently been reported and characterized structurally by X-ray crystallography.[12]

Using the 3,5-dimethyl derivative of pyrazole, Trofimenko[13] synthesized $(HBPz^*_3)Rh(COD)$ and $(HBPz^*_3)Rh(CO)_2$ and found three equivalent Pz* ligands in the NMR. From the NMR results Trofimenko again favoured a 16e, four-coordinate rhodium, but did not rule out the possibility of five-coordination. Since then the nature of $(HBPz^*_3)Rh(CO)_2$ in the solid state or in solution has not been conclusively resolved.

In 1980, an improved procedure for the synthesis of $(HBPz*_3)Rh(CO)_2$ was reported by Powell et al.,[14] who explored some of its reactions. The reaction of I_2 with $(HBPz*_3)Rh(CO)_2$ to yield $(HBPz*_3)Rh(CO)(I)_2$, an oxidative addition, was reported. Reactions with tertiary phosphines and arsines were mentioned briefly, but the reaction products were not characterized and according to the authors[14] the NMR spectrum of these compounds were broad and irreproducible.

It appeared from the literature that nothing had been done with $(HBPz*_3)Rh(CO)_2$ since 1980. To have a secure basis for C-H activation studies with the complex, it was of interest to investigate its nature in solution and to examine in detail some of the chemistry of this interesting compound, such as phosphine addition reactions.

The nature of $(HBPz*_3)Rh(CO)_2$ in solution and the new class of monophosphine derivatives $(HBPz*_3)Rh(CO)(PR_3)$ for a variety of tertiary phosphines and their NMR fluxional behaviour will be discussed in this Chapter. The intent of this work was to provide background for work on carbon-hydrogen activation.

Section 2

SYNTHESIS AND PROPERTIES OF PYRAZOLYLBORATE RHODIUM COMPLEXES

Dicarbonyl $(HBPz^*_3)Rh(CO)_2$ (1) was synthesized as an orange-yellow crystalline solid in 69% yield by reacting $[Rh(CO)_2Cl]_2$ with $K[HBPz^*_3]$ in the dark using toluene as a solvent. The compound has been fully characterized by elemental analysis and spectroscopic methods. 1 appears to be slightly air-sensitive in the solid state and is also sensitive to light and air in solution. A much better elemental analysis has been obtained for 1 than that reported previously.[14] In addition some of the physical properties of 1 reported earlier[14] differ from the present observations. The reported infared spectrum (IR) listed only one absorption band in the carbonyl stretching region (ν_{CO}): 2045 cm^{-1} (solvent not mentioned). In the present work, the IR of 1 in *n*-hexane shows two ν_{CO} bands at 2055, 1981 cm^{-1}, as one would expect.

The ^{1}H NMR spectra of 1 at ambient temperature and also at -90°C showed the equivalence of three Pz* ligands, in agreement with the early report of Trofimenko.[13] This NMR result is not informative as to whether 1 has a five-coordinate 18e or a four-coordinate 16e structure. The two likely five-coordinate forms are trigonal bipyramidal (TBP) and square pyramidal (SP). The five- and four-coordinate forms are sketched below:

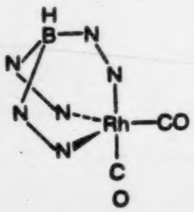

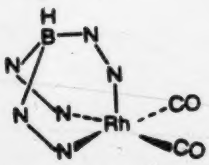

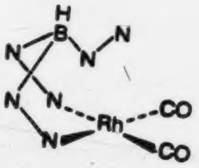

For the five-coordinate forms, structures with two equivalent and one unique pyrazole ring can be drawn based on either geometry. In SP geometry the two equivalent ligands would occupy cis positions in the basal plane. Alternatively, for TBP geometry, the unique pyrazole ring would occupy an axial position and the two equivalent ligands equatorial positions. In summary, the ^1H NMR does not distinguish the following:

(i) a fluxional five-coordinate form

(ii) a fluxional four-coordinate form

(iii) a rapidly interconverting mixture of four- and five-coordinate forms.

Nature of $(HBPz^*_3)Rh(CO)_2$ (1) in Solution

At this point, IR spectra of some known and unambiguously four-coordinate dicarbonyl rhodium compounds were examined in the carbonyl stretching region. The timescale of infrared spectroscopy is much faster than that of dynamic processes considered possible here, and was expected to shed some light on the problem. A well known 16e four-coordinate square planar complex is $(acac)Rh(CO)_2$[15] with reported IR ν_{CO}, (petroleum ether) at 2083, 2015 cm^{-1}. Another example of a four-coordinate 16e complex is $Et_2B(Pz)_2Rh(CO)_2$,[16] with reported ν_{CO}(Nujol) at 2080, 2020 cm^{-1}. It appeared that the reported ν_{CO} of both four-coordinate rhodium (I) complexes were very similar, and that these values are much higher (ca. 30-35 cm^{-1}) than those observed in case of 1. It thus appeared that 1 might be five-coordinate in hexane solution.

It appeared that the best comparison would be with the closely related bispyrazole complex $(H_2BPz^*_2)Rh(CO)_2$ (**2**), necessarily a four-coordinate complex. Accordingly, $(H_2BPz^*_2)Rh(CO)_2$ was synthesized following with slight modification the procedure utilized by Bonati et al.[17] The compound was characterized by elemental analysis and spectroscopic methods. The IR spectrum in n-hexane shows ν_{CO} at 2079 and 2013 cm^{-1}, very similar to the other previously mentioned four-coordinate complexes and much higher than the ν_{CO} of 1.

From the direct comparison of ν_{CO} in a number of four-coordinate dicarbonyl rhodium (I) complexes with the ν_{CO} of 1 it is reasonable to conclude that 1 has a five-coordinate 18e structure in solution (non-polar solvent) as sketched below:

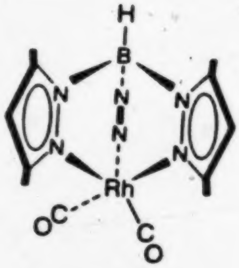

(η^3-HBPz$^*_3$)Rh(CO)$_2$

The η^3 (Greek eta) notation indicates that three nitrogen atoms of three pyrazole rings are attached to rhodium.

In general, one would expect that ν_{CO} in five-coordinate complexes would be lower than those of four-coordinate complexes. For (η^3-HBPz$^*_3$)Rh(CO)$_2$, coordination of the third pyrazolyl group to rhodium would increase the electron density on the metal; as a result the extent of back-donation from Rh to CO increases, and the C≡O bond becomes weaker. Thus ν_{CO} is expected to shift to lower wavenumber relative to

$(\eta^2\text{-HBPz*}_3)\text{Rh(CO)}_2$, where only two pyrazolyl groups are donating to rhodium.

Another very important and interesting observation was made by McMaster[18] regarding the IR spectrum of 1 in a polar solvent (CH_2Cl_2). The IR spectra for 1 in cyclohexane and also in CH_2Cl_2 are shown in Fig. II.1 for comparison. Four ν_{CO}'s are present in the IR spectrum of 1 in CH_2Cl_2. The weak bands at higher ν_{CO} (2080, 2012 cm^{-1}) are very similar to those of $(H_2BPz*_2)Rh(CO)_2$ (2082, 2013 cm^{-1}) in CH_2Cl_2. The more intense bands at lower ν_{CO} (2058, 1982 cm^{-1}) can reasonably be assigned to $(\eta^3\text{-HBPz*}_3)\text{Rh(CO)}_2$. McMaster[18] also demonstrated that the appearance of the weak bands (2082, 2012 cm^{-1}) was reversible, not a result of some reaction. He removed the CH_2Cl_2 and took the sample up in _n_-hexane or cyclohexane, and the bands were no longer seen. It is therefore likely that in dichloromethane, $(HBPz*_3)Rh(CO)_2$ (1) exists as an equilibrium mixture of $(\eta^3\text{-HBPz*}_3)\text{Rh(CO)}_2$ and $(\eta^2\text{-HBPz*}_3)\text{Rh(CO)}_2$. At equilibrium, the five-coordinate geometry is very much favoured.

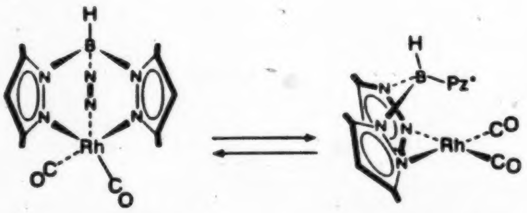

$(\eta^3\text{—HBPz*}_3)\ \text{Rh(CO)}_2$
18 electrons

$(\eta^2\text{—HBPz*}_3)\text{Rh(CO)}_2$
16 electrons

The value of the equilibrium constant is estimated as $K_{eq}(CH_2Cl_2) \cong 0.01$, from which $\Delta G° \cong 3.0$ kcal mol^{-1} (at 25°C). In view of this small and somewhat solvent dependent free energy difference, reactions of 1 could involve either form, even in a nonpolar solvent where the fraction

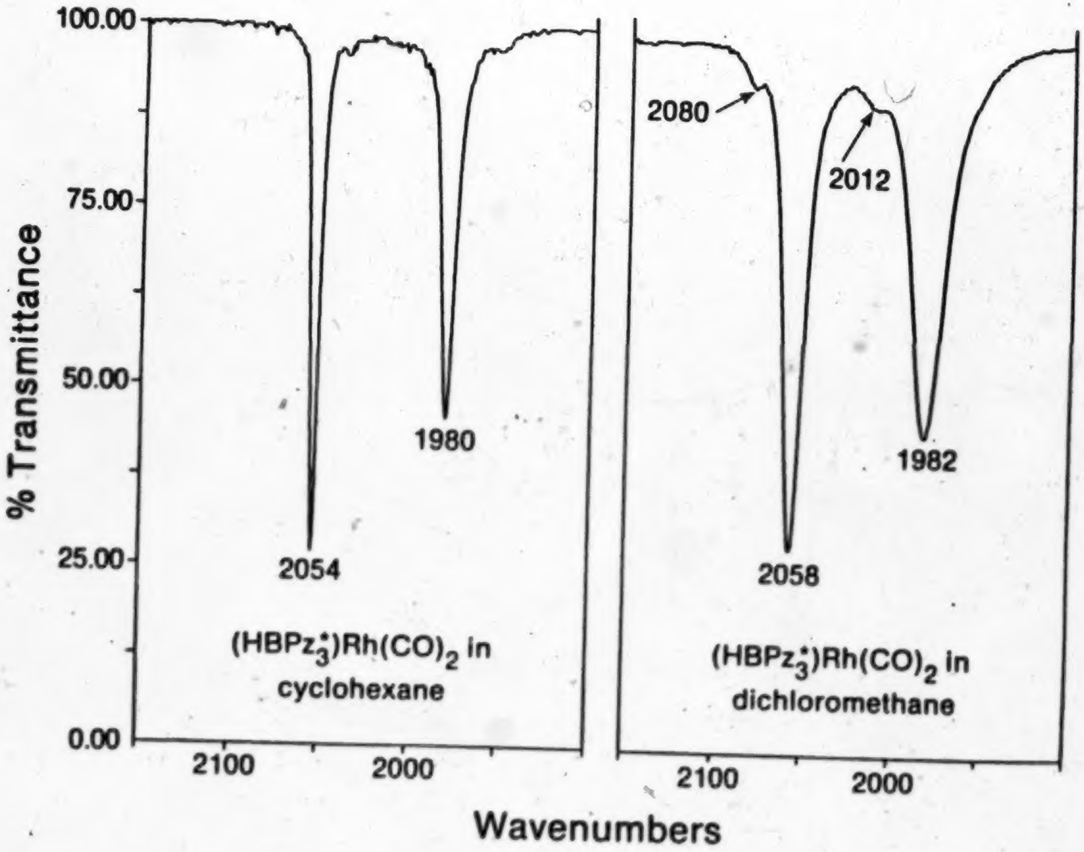

Figure II.1 Infrared spectra of (HBPz*$_3$)Rh(CO)$_2$ (1) in cyclohexane and CH_2Cl_2.

of 16e form is too small for detection by IR. ^1H NMR spectra of 1 in CD_2Cl_2 give no evidence even at -90°C for a second form, so it is reasonable to conclude that the kinetic barrier for interconversion of the 16e and 18e forms of 1 is low as well. Unfortunately, all attempts to obtain crystals of 1 suitable for x-ray diffraction were unsuccessful; even the crystal structure would not have established the situation in solution, however.

Thermal decomposition of $(HBPz^*_3)Rh(CO)_2$ (1)

Compound 1 decomposed in the temperature range 215-220°C during examination of its melting point. The IR spectrum of the decomposed product in n-hexane was quite clean, exhibiting two new terminal ν_{CO} (2067, 2000 cm^{-1}), and this led to a more detailed investigation of the thermolysis products. The experiment was again performed by heating a larger quantity of 1 in an NMR tube (5 mm) in a silicone oil bath at 220°C for approximately 15 minutes. The IR spectrum indicated the presence of the same new compound as was obtained in the melting point tube. The compound was purified by chromatography on a Florisil column.

The mass spectrum suggested the formula $C_{27}H_{37}N_{10}O_2B_1Rh_2$, which was consistent with elemental analysis. The ^1H NMR spectrum indicated a transition-metal bonded hydrogen (δ-12.31) coupled to two nonequivalent rhodium atoms (J=15.6 Hz, J=6.1 Hz), and three sets of pyrazole resonances in a 1:2:2 ratio. On the basis of elemental analysis and spectroscopic evidences the new dinuclear species is formulated as $(HBPz^*_3)(Pz^*_2)Rh_2(CO)_2H$, either **3a** or **3b**. Two possible structures are proposed for 3 as shown below.

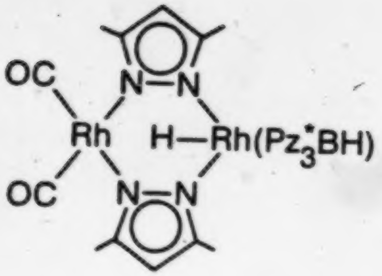
OC
N=N
Rh
H—Rh(Pz*3BH)
OC
N=N

3a

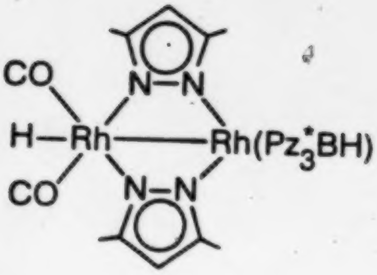
CO
N=N
H—Rh
Rh(Pz*3BH)
CO
N–N

3b

Attempts to obtain x-ray quality crystals were unsuccessful.

Section 3

PHOSPHINE ADDITION REACTIONS AND FLUXIONAL BEHAVIOUR

$(HBPz^*_3)Rh(CO)_2$ (**1**) reacted rapidly and quantitatively at room temperature with one equivalent of a variety of tertiary phosphines to give the new class of monophosphine derivatives formulated as $(HBPz^*_3)Rh(CO)(PR_3)$ (eq. 2-1).

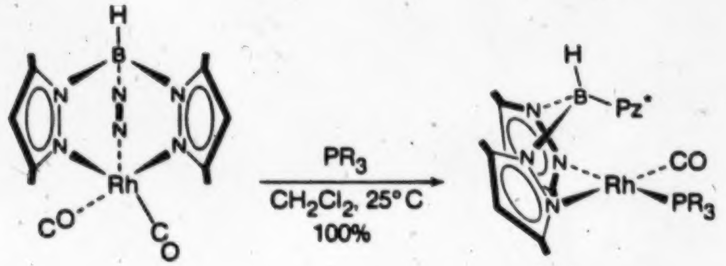

(2-1)

$(\eta^3\text{-}HBPz^*_3)Rh(CO)_2$

$(\eta^2\text{-}HBPz^*_3)Rh(CO)(PR_3)$

1

4a : R = Me

4b : PR_3 = PMe_2Ph

4c : PR_3 = $PMePh_2$

4d : R = Ph

4e : PR_3 = PEtMePh

The IR spectrum, mass spectrum and elemental analysis are consistent with the above formulation. This class of monophosphine derivatives is extremely air sensitive in solution (especially **4a**) and moderately air sensitive in the solid state. The bis pyrazolylmonophosphine complexes $(H_2BPz^*_2)Rh(CO)(PR_3)$ (**5**) have also been synthesized and characterized where necessary for comparison; their properties will be discussed later in this section. The IR ν_{CO} of the phosphine complexes are summarized in Table 2.I.

IR spectra of complexes 4 exhibit ν_{CO} bands very similar to those of the related bis(pyrazolyl)borate phosphine complexes (5). For example, the ν_{CO} for $(HBPz^*_3)Rh(CO)(PMe_2Ph)$ (**4b**) in n-hexane is 1978 cm^{-1}, and the related $(H_2BPz^*_2)Rh(CO)(PMe_2Ph)$ (**5b**) complex has the ν_{CO} at 1979 cm^{-1} in the same solvent. The comparison of ν_{CO} establishes that the potentially tridentate $HBPz^*_3$ ligand is bidentate in $(HBPz^*_3)Rh(CO)(PR_3)$ (4) complexes, which are therefore 16e Rh(I).

^1H NMR spectra of $(HBPz^*_3)Rh(CO)(PR_3)$ (4) at ambient temperature show three equivalent Pz* rings indicating one or more fluxional processes which average all three Pz* resonances. Upon cooling, the single ^1H NMR signals observed at ambient conditions exhibit splitting.

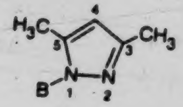

The resonance due to the 4-H ring protons (**4b**) at δ 5.83 splits into signals at δ 5.92 and δ 5.79 in 1:2 intensity ratio. At the same time the $3\text{-}CH_3$ and $5\text{-}CH_3$ peaks each split into pairs of signals of intensity ratio 3:6. The temperature required for this decoalescence depends on the phosphine (-40°C for **4a** (PMe_3), -65°C for **4b** (PMe_2Ph), -75°C for **4c** ($PMePh_2$)).

In other words, on cooling the ^1H NMR spectra of $(HBPz^*_3)Rh(CO)(PR_3)$ complexes show two sets of pyrazole rings in 1:2 ratio. Some representative spectra are shown in Fig. II.2. In this

Table 2.I ν_{CO} of the Phosphine Complexes

Compound	ν_{CO} (n-hexane) cm^{-1}
$(HBPz^*_3)Rh(CO)(PMe_3)$ (**4a**)	1973
$(HBPz^*_3)Rh(CO)(PMe_2Ph)$ (**4b**)	1978
$(HBPz^*_3)Rh(CO)(PMePh_2)$ (**4c**)	1983
$(HBPz^*_3)Rh(CO)(PPh_3)$ (**4d**)	1983
$(HBPz^*_3)Rh(CO)(PEtMePh)$ (**4e**)	1973
$(H_2BPz^*_2)Rh(CO)(PMe_3)$ (**5a**)	1975
$(H_2BPz^*_2)Rh(CO)(PMe_2Ph)$ (**5b**)	1979

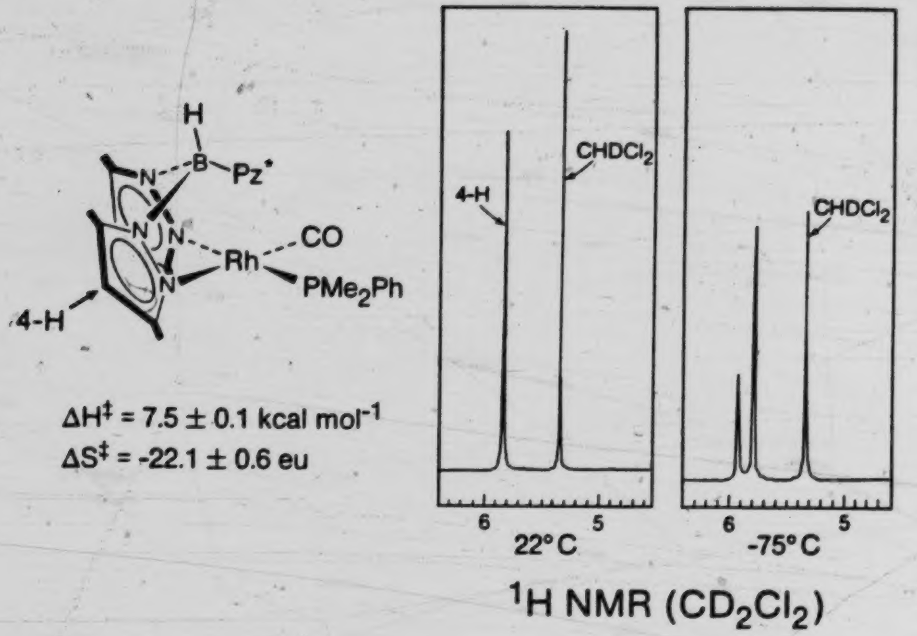

$\Delta H^{\ddagger} = 7.5 \pm 0.1$ kcal mol^{-1}
$\Delta S^{\ddagger} = -22.1 \pm 0.6$ eu

Figure II.2 ^{1}H NMR spectra of (HBPz*$_3$)Rh(CO)(PMe$_2$Ph) (**4b**) in the 4-H region at ambient temperature and at -75°C.

series of tertiary monophosphine derivatives, the ^1H NMR spectrum of **4d** decoalescence of only the 4-H protons occurs at -90°C while even at -105°C the methyl signals remain broad. There is an apparent inverse correlation of the barrier for ring interchange with the bulkiness of the phosphine ligand; although from the phosphines studied, the correlation could be between the barrier and the basicity of the phosphine.

The ^1H NMR spectra of square planar $(H_2BPz^*_2)Rh(CO)(PMe_3)$ (**5a**) and $(H_2BPz^*_2)Rh(CO)(PMe_2Ph)$ (**5b**) (Fig. II.3) indicated two nonequivalent Pz* rings (in each case) as expected. Therefore, one would expect three nonequivalent Pz* signals in the low temperature limiting spectra of $(HBPz^*_3)Rh(CO)(PR_3)$ if it has a four-coordinate square planar geometry. However, three nonequivalent Pz* rings were not observed at the lowest accessible temperatures (-95°C). The infrared spectra nevertheless indicate a four-coordinate square planar geometry with no other species at sufficient concentration to detect. It is reasonable to propose that the observed fluxional process involves a five-coordinate intermediate, which is trigonal bipyramidal and has a plane of symmetry, viz,

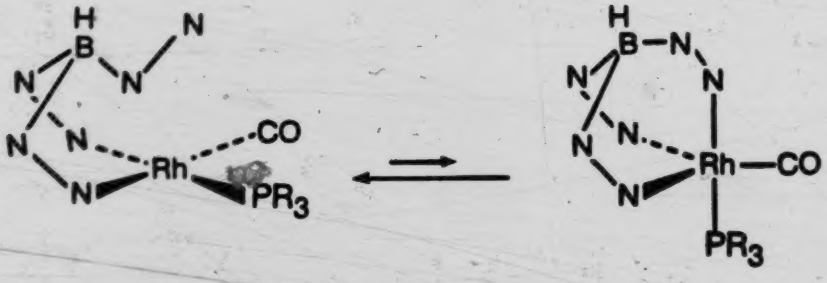

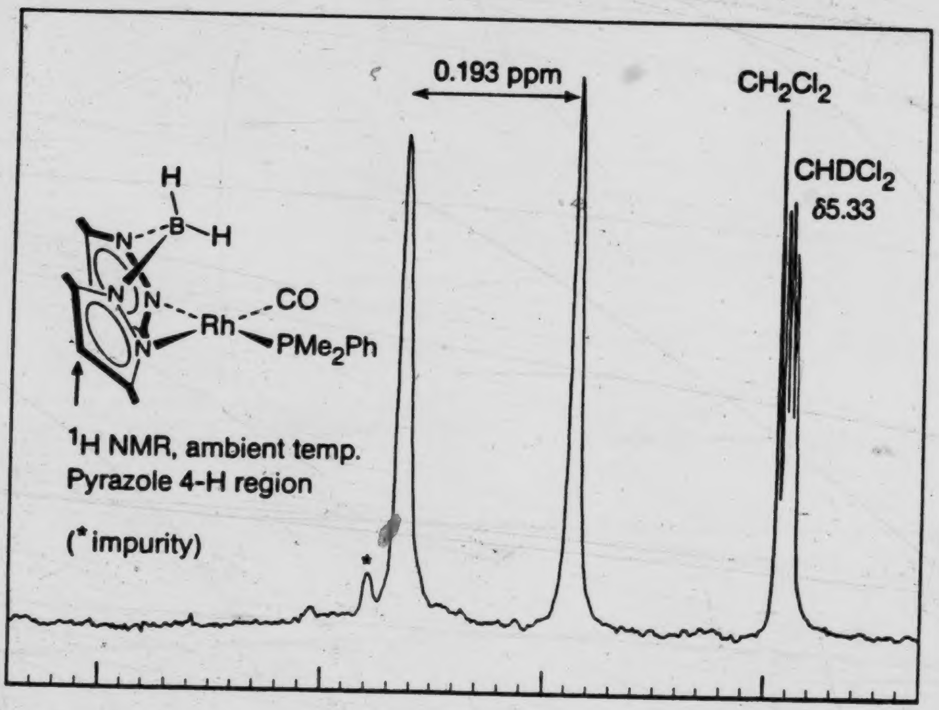

Figure II.3 ^{1}H NMR spectrum of $(H_2BPz^*_2)Rh(CO)(PMe_2Ph)$ (**5b**) in the 4-H region.

It is immaterial which ligand, CO or phosphine, enters the axial position, because at that point the plane of symmetry has made Pz*(1) equivalent to Pz*(2). Clearly no such intermediate is possible in the bis(pyrazolyl)borate complex (5a or 5b), so no facile averaging process occurs.

The fluxional processes involved in the $(HBPz^*_3)Rh(CO)(PR_3)$ system can be summarized in the following way. There are two kinds of fluxional processes: i) a high temperature process that averages all Pz* signals at room temperature and can be frozen out in the -40 to -85°C temperature range to 2:1 ratio of Pz* signals; ii) a low temperature process that averages the two equatorial Pz* ligands which are trans to different ligands in the four-coordinate static structure; the latter has not been frozen out.

Particularly interesting results were obtained using PMe_2Ph as the ligand. It is convenient to discuss at this point the ^1H NMR spectrum of the bis(pyrazolyl)borate complex $(H_2BPz^*_2)Rh(CO)(PMe_2Ph)$, **5b**, the synthesis of which will be described later. The complex $(H_2BPz^*_2)Rh(CO)(PMe_2Ph)$ (**5b**) is considered to have four-coordinate square planar geometry. The ^1H NMR spectrum of **5b** showed the two methyl groups bound to phosphorus as diastereotopic, having different chemical shifts. This is because of the chirality of the fragment to which PMe_2Ph is attached as shown below.

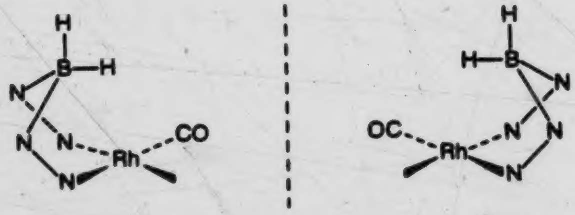

The boat shape of the ring differentiates the top and bottom of the planar N_2RhCO fragment. This is in contrast to (acac)Rh(CO)(PMe_2Ph), where the acac ligand, Rh and CO lie in a symmetry plane of the molecule.

Returning to the trispyrazolylborate complex 4b, a moment's consideration will show that the ($HBPz*_3$)Rh(CO) fragment is also chiral as shown below.

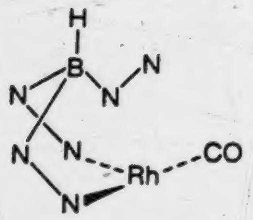

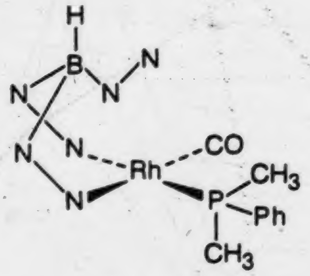

Hence in the PMe_2Ph complex (4b) diastereotopic methyls are expected. However, experimentally a single methyl resonance is observed down to -85°C.

An explanation for this is provided by the same trigonal bipyramidal intermediate invoked in the low temperature processes to account for the equivalence of the two equatorially bonded Pz* rings. The trigonal bipyramidal fragments to which PMe_2Ph is bound as shown below have a plane of symmetry, they are achiral groups. As a result the equatorial Pz* ligands and the two methyl groups on phosphorus are equivalent.

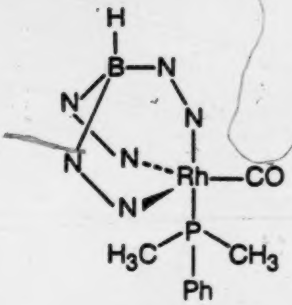
H
B
N
N
N
N
N
N
Rh
CO
P
H3C
CH3
Ph

4b (axial phosphine)

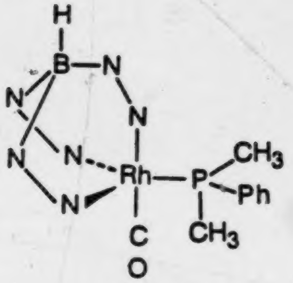
H
B
N
N
N
N
N
N
Rh
P
CH3
Ph
CH3
C
O

4b (equatorial phosphine)

It is therefore concluded that the instantaneous plane of symmetry in the five-coordinate trigonal bipyramidal intermediate averages the two equatorial Pz* ligands and also the two methyls on phosphorus.

The foregoing considerations can be taken one step further by the use of a chiral phosphine. In such a case, even formation of the proposed trigonal bipyramidal intermediate would not generate a plane of symmetry in the complex. The two equatorially bonded Pz* ligands would not become equivalent; in effect, they would be rendered diastereotopic by the chiral phosphine.

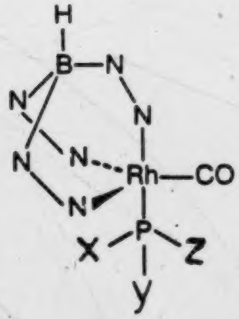
H
B
N
N
N
N
N
N
Rh
CO
P
X
Z
Y

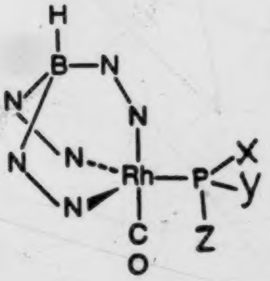
H
B
N
N
N
N
N
N
Rh
P
X
Y
Z
C
O

The above drawings illustrate diastereotopic character of the equatorially bonded Pz* ligands (here represented by N) when a chiral phosphine PXYZ is coordinated, regardless of whether the phosphine is axial or equatorial.

Accordingly, a chiral monophosphine derivative $(HBPz^*_3)Rh(CO)(PEtMePh)$ (**4e**) was synthesized and fully characterized. The ^1H NMR spectrum of 4e at ambient temperature indicated three equivalent Pz* rings as one would expect. The variable temperature NMR studies showed three sets of Pz* resonances in a ratio of 1:1:1 at -60°C, which became sharp at -85°C. The six methyl resonances of the Pz* rings are a definitive indication of three nonequivalent Pz* rings. This result is consistent with the proposed low temperature fluxional process.

Energy barrier of the fluxional process

In continuation of the investigations on fluxional behaviour of monophosphine derivatives, it was of interest to measure the energy barrier of the exchange process which can be frozen into two sets of Pz* signals in 2:1 ratio on cooling. This has been referred to as the high temperature averaging process. Exchange process which occur too slowly to cause NMR line broadening can sometimes be studied by the NMR double resonance technique known as spin saturation transfer (SST).[19]

Spin saturation transfer can be applied in cases where the rate of exchange is comparable to the rate of longitudinal relaxation of the nucleus used for observation (spin lattice relaxation time T_1). The two sites linked by an exchange process can be identified by saturation of one site and observation of an intensity decrease at the site with which it is exchanging. The observed decrease in intensity results from the partial transfer of saturation to the new site effected by the exchange process.

A spin saturation transfer experiment was performed on $(HBPz^*_3)Rh(CO)(PMe_2Ph)$ (**4b**). It has already been mentioned that the low temperature ^1H NMR indicted two sets of Pz* resonances with an intensity ratio of 2:1. Confirmation of the site exchange is obtained by saturating the resonance due to 4-H (δ 5.92 (1H)) of the unique Pz* ring. The intensity of the 4-H (δ 5.79 (2H)) resonance due to the two equivalent Pz* rings decreases indicating that the two equivalent Pz* rings are exchanging with the third. The decrease in signal intensity at the δ 5.79 (2H) site can be quantitatively measured, most readily by means of a difference spectrum. In this procedure, a normal spectrum of **4b** is taken with saturating field on, but not centered on δ 5.92 (1H). A spectrum is then taken with saturation of the resonance at δ 5.92 and the two FID's are subtracted to give a difference FID, which is then fourier transformed to give a difference spectrum. This allows the intensity decrease to be quantitatively determined by integration against an internal standard. The normal, saturated and difference spectra of **4b** are shown in Fig. II.4.

Rate constants are derived from the size of the decrease in signal intensity and a knowledge of T_1 values for each proton involved in the process. The SST experiment was carried out in the temperature range of -48 to -75°C. The spin saturation transfer data along with the rate constants are summarized in Table 2.II.

Activation parameters for the exchange process were obtained from an Eyring plot of the data in Table 2.II. The Eyring plot is shown in

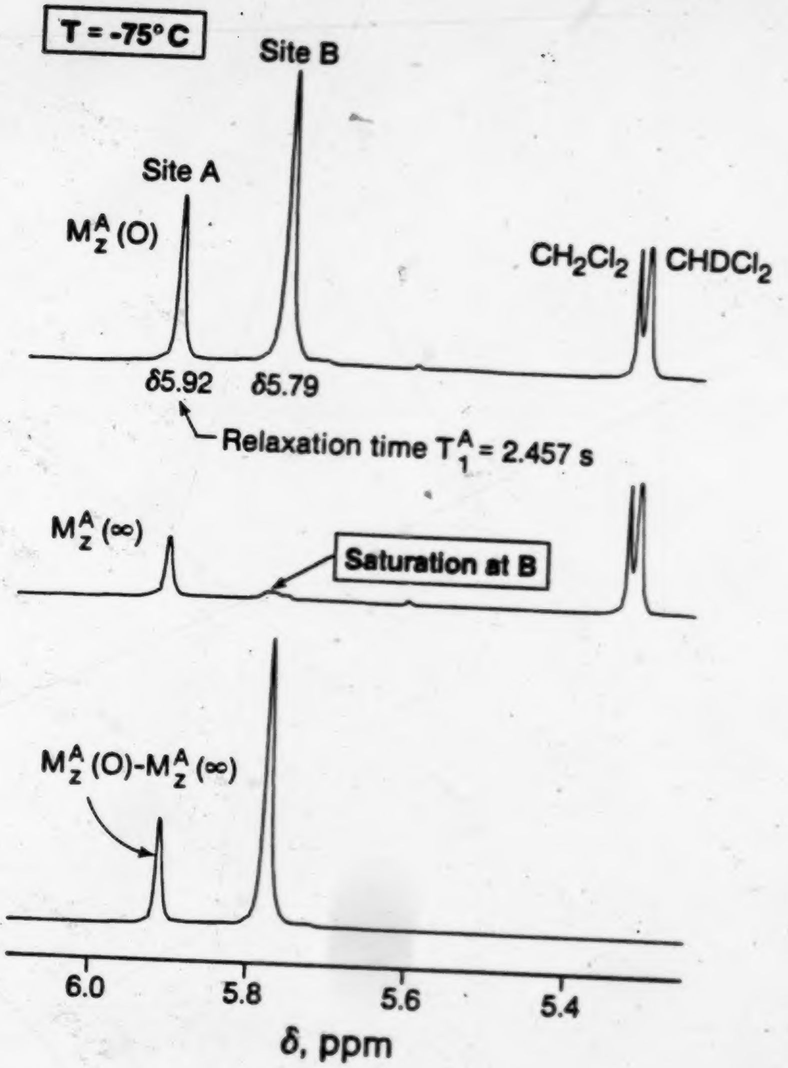

Figure II.4a ^1H SST experiment on $(HBPz^*_3)Rh(CO)(PMe_2Ph)$ (4b).
Top: normal spectrum (4-H region).
Middle: saturation at 2H site (indicated as B).
Bottom: difference spectrum.

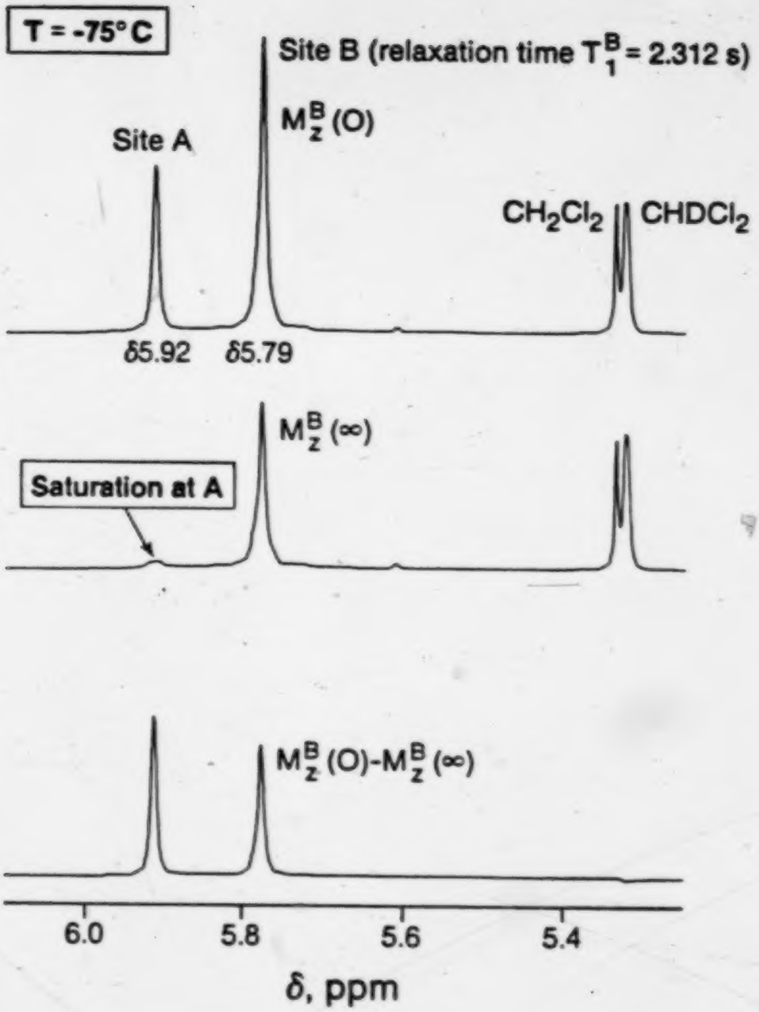

Figure II.4b ^1H SST experiment on $(HBPz^*_3)Rh(CO)(PMe_2Ph)$ (4b).
Top: normal spectrum (4-H region).
Middle: saturation at 1 H site (indicated as A).
Bottom: difference spectrum.

Table 2.II Spin Saturation Transfer Data for 4b

Temp (K)	Saturation at δ 5.92		Saturation at δ 5.79		T_1 (s) 2H site δ 5.79	T_1 (s) 1H site δ 5.92	k[c] (s^{-1}) 2H site	k (s^{-1})[d] 1H site
	M_z^{∞}[a]	M_z^{o}[b]$-M_z^{\infty}$	M_z^{∞}	$M_z^{o}-M_z^{\infty}$				
198	14.876	12.358	4.858	8.523	2.312	2.457	0.359	0.357
207	9.133	18.710	3.135	10.885	2.397	2.444	0.855	0.710
214	3.637	13.419	1.008	7.483	2.418	2.443	1.526	1.519
225	1.385	15.005	0.355	7.752	2.697	2.658	4.016	4.102

[a] M_z^{∞} is the equilibrium magnetization with saturation at other site.

[b] M_z^{o} is the normal magnetization without saturation.

[c] $k = \frac{1}{T_1}\left[\frac{M_z^{o} - M_z^{\infty}}{M_z^{\infty}}\right]$ where T_1 is the relaxation time for the nucleus.

[d] Calculated k dividing by 2 to express as rate for transfer to one of other sites.

Fig. II.5. Values obtained were $\Delta H^{\ddagger}$=7.5±0.1 kcal mol^{-1}, $\Delta S^{\ddagger}$=-22.1±0.6 eu and $\Delta G^{\ddagger}{}_{298}$=14.1±0.2 kcal mol^{-1}. These values were calculated using data for 2H site. Using data for 1H site, values obtained were $\Delta H^{\ddagger}$=7.7±0.5 kcal mol^{-1}, $\Delta S^{\ddagger}$=-22.1±2.38 eu, $\Delta G^{\ddagger}{}_{298}$=14.0±0.8 kcal mol^{-1}. Activation parameters obtained from 2H and 1H sites are in remarkably good agreement.

The exchange rates of Pz* rings were also determined by the line broadening technique. The rate constants were calculated according to eq. 2-1 from the excess line width due to exchange. Excess widths Δ were

$$k = \pi \times \Delta \qquad (2\text{-}1)$$

obtained by subtracting the line widths of the internal standard peaks from the measured line widths of the peaks (at half height) of interest. Hexamethyldisiloxane was used as an internal standard. The resonance due to the 4-H of pyrazole ring was the peak of interest. The exchange rate constants were determined in the temperature range -40 to -55°C. Beyond this temperature range, no significant change in line width of resonances due to 4-H of pyrazole ring was observed. The line widths of the resonance at δ 5.79 (2H site) along with the rate constants at different temperatures are presented in Table 2.III. The resonance at δ 5.92 (1H site) was not well resolved, particularly at -40°C, so it was not used for determination of rate constants.

Activation parameters were obtained from an Eyring plot (Fig. II.5), using data of Table 2.III. Values obtained were $\Delta H^{\ddagger}$=7.4±0.7 kcal mol^{-1}, $\Delta S^{\ddagger}$=-20±3 eu, $\Delta G^{\ddagger}{}_{298}$=13.5±1.2 kcal mol^{-1}.

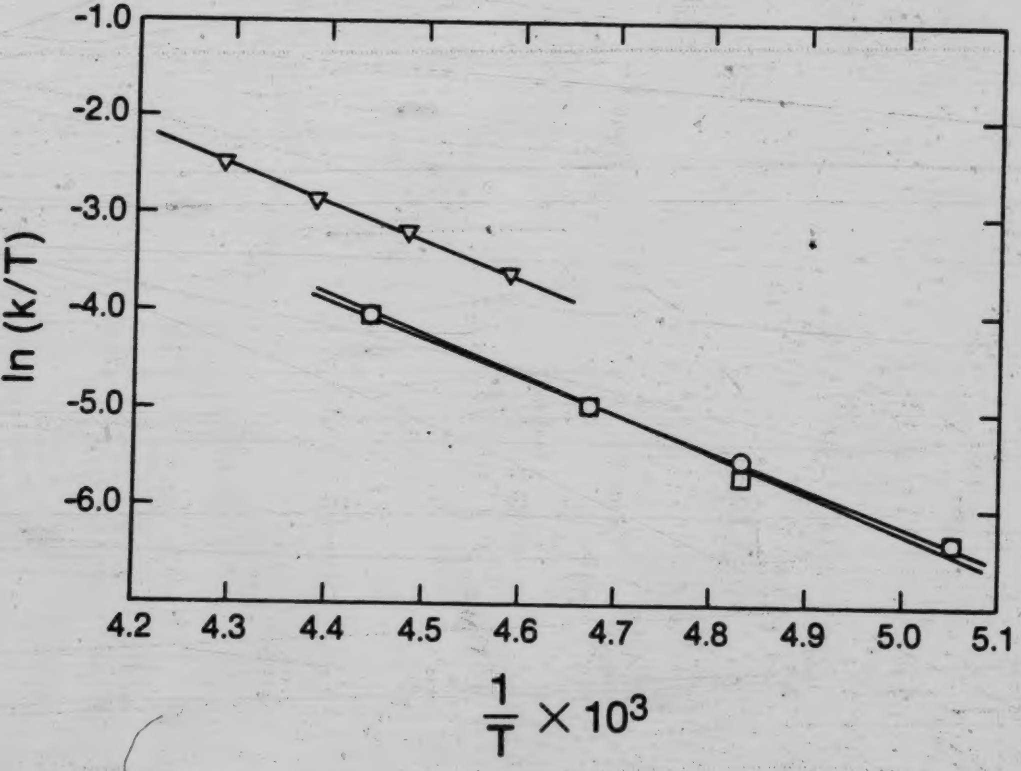

Figure II.5 Eyring plot of ^1H rate constant data for $(HBPz^*_3)Rh(CO)(PMe_2Ph)$ (**4b**). O, 2H site (SST); □, 1H site (SST); Δ, 2H site (line broadening).

Table 2.III Line Broadening Data for 4b

Temp (K)	Line width (Hz) Int. std.	Line width (Hz) 2H site	Excess line width Δ	k (s^{-1})
218	1.12	3.00	1.88	5.89
223	0.70	3.90	3.20	10.05
228	1.02	5.10	4.08	12.80
233	0.75	7.05	6.30	19.79

The activation parameters obtained by both spin saturation transfer and line broadening analysis are in reasonably good agreement.

$(H_2BPz^*_2)Rh(CO)(PR_3)$ complexes

$(H_2BPz^*_2)Rh(CO)_2$ (2) reacted readily with one equivalent of tertiary phosphines affording the corresponding monophosphine derivatives $(H_2BPz^*_2)Rh(CO)(PR_3)$ (eq. 2-2) as light yellow solids, characterized by elemental analysis and spectroscopic methods.

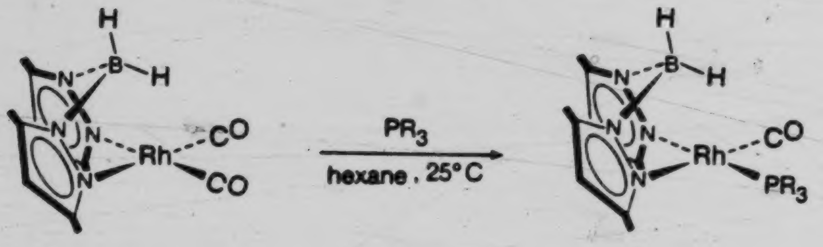

(2-2)

2

5a : R = Me

5b : PR_3 = PMe_2Ph

Addition of more than one equivalent of phosphine yielded an unidentified compound (ν_{CO} (n-hexane): 1964 cm^{-1}; R_3 = Me_3) in addition to the above mentioned desired compound. The unidentified compound can be isolated by fractional crystallization but in insufficient quantity for characterization.

As mentioned earlier, the ^1H NMR spectra of these complexes indicated two different Pz* environments as expected for square planar geometry. The six membered B-N-N-Rh-N-N is expected, on the basis of reported structural data, to have a boat configuration. Thus, Storr et al.[20] have reported the crystal structure of $(Me_2GaPz_2)Rh(COD)$, which is related to the $(H_2BPz^*_2)Rh(CO)(PR_3)$ system, and the boat conformation was confirmed.

As noted earlier, an interesting consequence of the boat conformation is observed in the ^1H NMR spectrum of 5b. The two methyl groups on phosphorus are found to be diastereotopic at ambient temperature. The nonequivalency of two methyl groups requires that the boat is not rapidly inverting at room temperature. The boat conformation of 5b is shown below.

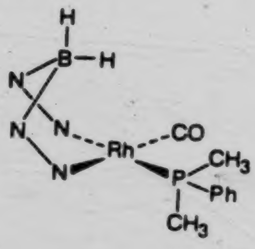

Boat conformation of 5b

It is worth noting that this is different from the $(HBPz^*_3)Rh$ system, where only one methyl resonance was found even at -95°C. In the case of 5b, the PMe_2 groups are not equivalent since it is attached to a chiral fragment. There is not a plane of symmetry in the boat conformation. An early example of nonequivalent methyls was found in $[RhCl_2Et(CO)(PMe_2Ph)_2]$.[21]

Interestingly, the ^1H NMR spectrum of $[Me_2GaPz_2]Rh(CO)(PPh_3)$ has been reported by Storr et al.[20] who observed a single "GaMe" resonance at ambient temperature. On cooling, two singlets were observed as inversion of the boat form slowed. In contrast, the PMe_2 groups are nonequivalent in the ^{1}H NMR spectrum of ($H_2BPz^*_2$)Rh(CO)(PMe_2Ph) (**5b**) at room temperature. This direct comparison suggests that the barrier for the boat inversion in the $H_2BPz^*_2$ system is higher than that in the Me_2GaPz_2 system. However, to our knowledge, no prior report on the magnitude of the barrier for the inversion of boat in a pyrazolylborate complex has appeared in the literature.

To determine the magnitude of the barrier for the boat inversion, an SST experiment was carried out on **5b**. Saturation of one of the methyl resonances of PMe_2 at room temperature indicated a significant decrease in intensity to the other methyl resonance. This result clearly indicated that there is transfer of spin between the two methyls on phosphorus. Rate constants for the exchange process were calculated from the size of the decrease in signal intensity and magnitude of T_1 value (1.17 s) (using the equation in Table 2.II). The rate constant k was 1.15 s^{-1} which converts to $\Delta G^{\ddagger}_{299} \cong 16.6$ kcal mol^{-1}.

An alternate approach to determine the free energy barrier is from the coalescence temperature of the two methyl resonances bound to phosphorus. The two methyl resonances coalesce at 80°C (toluene-d_8) and the rate constant is derived from eq. 2-2.

$$k = \pi/\sqrt{2} \times \Delta\nu \qquad (2-2)$$

where $\Delta\nu$ is the difference in frequency at coalescence temperature. The rate constant k was calculated as 31.9 s^{-1}, ($\Delta\nu$=14.4 Hz) which led to $\Delta G^{\ddagger}_{353} \cong 18.3$ kcal mol^{-1}. The value of $\Delta G^{\ddagger}$ indicates a substantial kinetic barrier for the inversion of boat. From the published[20] variable temperature NMR spectra of [Me_2GaPz_2]Rh(CO)(PPh_3), we estimated

$\Delta G^{\ddagger}_{238} \cong 11.8$ kcal mol^{-1}. This value is lower than that in the $H_2BPz^*_2$ system. This is consistent with the observed single methyl resonance for $GaMe_2$ and the two methyl resonances for PMe_2 in case of 5b at ambient temperature.

Section 4

EXPERIMENTAL

The published procedure[22] was utilized for preparation of $[Rh(CO)_2Cl]_2$. Potassium dihydrobis- and hydrotris-(3,5-dimethylpyrazolyl)borates were purchased from Columbia Organic Chemical Co., Inc. All tertiary phosphines except PEtMePh were purchased from Sterm Chemical Inc. and used as obtained. PEtMePh was obtained from Alfa Products Division of Morton Thiokol Inc.

General Techniques

All reactions and manipulations were carried out under an atmosphere of purified nitrogen using standard Schlenk techniques. Reactions were carried out at room temperature unless otherwise stated. Linde commercial nitrogen was purified by passing through a heated column (*ca*. 50°C) of BASF Cu-based catalyst (R3-11) to remove oxygen and a column of Molecular Sieves (Type 3A) to remove water.

Solvents were distilled under nitrogen immediately prior to use from the following drying agents: pentane, hexane and benzene from CaH_2; dichloromethane from P_2O_5; THF and toluene potassium/benzophenone.

Infared spectra were recorded using a Nicolet MX-1 FT IR spectrometer in 0.5 mm KCl cells unless otherwise noted. Mass spectra were measured using an Associated Electronics Industries MS-12 mass spectrometer coupled with a Nova-3 computer employing D5-50 software. All NMR spectra were recorded using Bruker WH-200, AM-300 and WH-400 FT NMR instruments. NMR samples for all monophosphine derivatives for regular runs and also for SST experiments were prepared by vacuum transfer of dried, degassed solvents into 5 mm NMR tubes. After three or four cycles of freeze-thaw degassing, the tubes were sealed off under vacuum. CD_2Cl_2 was used as the NMR solvent unless otherwise noted. For NMR line broadening experiments, hexamethyldisiloxane was used as an internal standard and a twenty second relaxation delay was applied.

Melting points were determined using a microscope equipped with a Kofler hot stage. Microanalyses were performed by the microanalytical laboratory of this department.

Preparation of $(HBPz^*_3)Rh(CO)_2$ (1)

A suspension of $K[HBPz^*_3]$ (800 mg, 2.38 mmol) in toluene (70 mL) was stirred for 15 minutes. To the suspension $[Rh(CO)_2Cl]_2$ (400 mg, 1.03 mmol) was added and the reaction mixture stirred in the dark for ca. 2.5 h at room temperature. The solution was then filtered to remove KCl and unreacted starting materials and the filtrate was cooled to -20°C for ca. 24 h, at which time orange-yellow crystals of 1 had formed in the flask. The supernatant was syringed from the crystals which were then dried in vacuo (520 mg). The supernatant was concentrated to ca. 40 mL and cooled to -20°C for 48 h, giving a further 127 mg of 1 (total yield 647 mg, 69%). MP decomposes above 210°C.

Characterization: IR (n-hexane) 2055, 1981 cm^{-1} (s, ν_{CO}). MS (200°C, 16 eV) M^+ (456), M^+-CO, M^+-2CO, M^+-2CO-$C_5H_7N_2$. UV (n-hexane) 221 (ε 17600), 353 (ε 1820) nm (λ_{max}). ^1H NMR (CD_2Cl_2, 200 MHz, ambient) δ 5.56 (s, 3H), 2.36 (s, 9H), 2.16 (s, 9H). ^{13}C NMR (CD_2Cl_2, 100.6 MHz, ambient) δ 189.68 (d, J_{Rh-C}=69.1 Hz), 149.48 (s), 144.71 (s), 105.36 (s), 14.89 (s), 12.44 (s). Anal. Calcd for $C_{15}H_{22}BN_6O_2Rh$: C, 44.74; H, 4.82; N, 18.42. Found: C, 44.92; H, 4.90; N, 18.12.

Preparation of $(H_2BPz^*_2)Rh(CO)_2$ (2)

To a stirred suspension of $K[H_2BPz^*_2]$ (400 mg, 1.65 mmol) in toluene (50 mL) was added $[Rh(CO)_2Cl]_2$ (300 mg, 0.771 mmol). A black precipitate formed immediately. The solution was filtered and evaporated to dryness. The residue was then extracted with hexane (5 x 10 mL) and evaporated to dryness which was sublimed immediately at 75°C (0.1 mm Hg) overnight to give pale yellow solid (255 mg, 46%).

Characterization: IR (n-hexane) 2079, 2013 cm^{-1} (s, ν_{CO}). MS (60°C, 16 eV) M^+-H (361), M^+-H-CO, M^+-H-2CO. ^1H NMR (CD_2Cl_2, 200 MHz, ambient) δ 5.8 (s, 2H), 2.35 (s, 6H), 2.27 (s, 6H). Anal. Calcd for $C_{12}H_{16}BN_4O_2Rh$: C, 39.82; H, 4.45; N, 15.48. Found: C, 40.03; H, 4.40; N, 15.44.

Preparation of $(HBPz^*_3)(Pz^*_2)Rh_2(CO)_2H$ (3)

Dicarbonyl 1 (150 mg, 0.329 mmol) was taken in two 0.5 mm NMR tubes and heated at 220°C for ca. 15 minutes in a silicone oil bath. During heating the color of the solid changed from original orange-yellow to dark brown. The combined dark brown solid was extracted with CH_2Cl_2 (5 mL) and chromatographed on a Florisil column (8 x 1.5 cm) with n-hexane eluent. Removal of the solvent yielded yellow solid, which was further purified by crystallization from n-hexane at -20°C over a period of couple of days affording light yellow crystals (20 mg, 25%).

Characterization: IR (n-hexane) 2067, 2000 cm^{-1} (s, ν_{CO}) MS (175°C) M^+

(750), M^+-H-CO, M^+-H-2CO. ^{1}H NMR (CD_2Cl_2, 200 MHz, ambient) δ 5.79 (s, 1H), 5.71 (s, 2H), 5.67 (s, 2H), 2.51 (s, 3H), 2.41 (s, 6H), 2.37 (s, 3H), 1.65 (s, 6H), 1.47 (s, 3H), 0.94 (s, 6H), -12.31 (dd, J_{Rh_1-H}=15.6 Hz, J_{Rh_2-H}=6.1 Hz, 1H). Anal. Calcd for $C_{27}H_{37}BN_{10}O_2Rh_2$: C, 43.20; H, 4.93; N, 18.67. Found: C, 43.09; H, 4.96; N, 18.22.

Preparation of ($HBPz^*_3$)Rh(CO)(PMe_3) (4a)

Addition of PMe_3 (18 μL, 0.177 mmol) to a solution of 1 (80.0 mg, 0.175 mmol) in CH_2Cl_2 (30 mL) gave compound **4a** instantly. The solvent was then removed under reduced pressure and the solid was washed with ice-cold hexane (2 x 2 mL) and dried under vacuum (0.1 mm Hg) for ca. 48 h affording the product as an extremely air sensitive analytically pure yellow solid (84.8 mg, 96%). MP darkens above 140°C.

Characterization: IR (n-hexane) 1973 cm^{-1} (s, ν_{CO}) MS (135°C, 16 eV) M^+ (504), M^+-CO, M^+-CO-PMe_3. ^{1}H NMR (CD_2Cl_2, 200 MHz, ambient) δ 5.83 (br, 3H), 2.26 (br, 12H), 2.00 (br, 6H), 1.24 (dd, $^2J_{P-H}$=9.8 Hz, $^3J_{Rh-H}$=1.3 Hz, 9H). -40°C: δ 5.88 (s, 1H), 5.80 (s, 2H), 2.34 (s, 3H), 2.32 (s, 3H), 2.21 (s, 6H), 1.94 (s, 6H) (PMe_3 signal remains unchanged. ^{31}P NMR (CD_2Cl_2) δ 2.36 (d, J_{P-Rh}=147.7 Hz). Anal. Calcd for $C_{19}H_{31}BN_6OPRh$: C, 45.24; H, 6.15; N, 16.67. Found: C, 43.90; H, 6.09; N, 15.65.

Preparation of ($HBPz^*_3$)Rh(CO)(PMe_2Ph) (4b)

To a solution of 1 (130 mg, 0.285 mmol) in CH_2Cl_2 (40 mL) was added PMe_2Ph (41 μL, 0.287 mmol) resulting in the color of the solution changing instantaneously from bright-yellow to greenish-yellow. The solvent was removed under reduced pressure to give a solid which was then washed with *n*-hexane (2 x 2 mL) and dried under vacuum (0.1 mm Hg) at 48°C for *ca*. 48 h yielding the moderately air sensitive product (152 mg, 94%). MP decomposes above 120°C.

Characterization: IR (*n*-hexane) 1978 cm^{-1} (s, ν_{CO}). MS (130°C, 16 eV) M^+ (566), M^+-CO, M^+-CO-C_6H_5-CH_3. ^1H NMR (CD_2Cl_2, 200 MHz, ambient) δ 7.86 (m, 2H), 7.45 (m, 3H), 5.83 (br, 3H), 2.20 (br, 9H), 2.14 (br, 9H), 1.42 (dd, $^2J_{P-H}$=9.8 Hz, $^3J_{Rh-H}$=1.5 Hz, 6H). -75°C (CD_2Cl_2) δ 5.92 (s, 1H), 5.79 (s, 2H), 2.39 (s, 3H), 2.33 (s, 3H), 2.06 (s, 6H), 1.94 (s, 6H) (phenyl proton and PMe_2 signal remains unchanged). ^{31}P NMR (CD_2Cl_2) δ 15.71 (d, J_{P-Rh}=154.1 Hz). Anal. Calcd for $C_{24}H_{33}BN_6OPRh$: C, 50.88; H, 5.83; N, 14.84. Found: C, 50.78; H, 5.88; N, 14.84.

Preparation of (HBPz*$_3$)Rh(CO)(PMePh$_2$) (4c)

Addition of $PMePh_2$ (42 μL, 0.223 mmol) to a solution of 1 (100 mg, 0.219 mmol) in CH_2Cl_2 (40 mL) gave a light yellow solution immediately. Removal of the solvent under reduced pressure gave a pale yellow solid which was then washed with *n*-hexane (2 x 4 mL) and dried in vacuo (0.1 mm Hg) at 70°C for *ca*. 48 h affording compound **4c** (128 mg, 93%). MP darkens above 150°C.

Characterization: IR (*n*-hexane) 1983 cm^{-1} (s, ν_{CO}). MS (135°C, 16 eV) M^+ (597), M^+-CO, M^+-CO-C_6H_5-CH_3. UV (*n*-hexane) 213.3 (ε 33711), 359.6 (ε 2407) nm (λ_{max}). ^1H NMR (CD_2Cl_2, 200 MHz, ambient) δ 7.42 (m, 10H), 5.86 (br, 3H), 2.16 (br, 9H), 2.10 (br, 9H), 1.70 (dd, $^2J_{P-H}$=9.8 Hz, $^3J_{Rh-H}$=1.4 Hz, 3H). -85°C (CD_2Cl_2) δ 5.94 (s, 1H), 5.78 (s, 2H), 2.38 (s, 3H), 2.34 (s, 3H), 1.96 (s, 6H), 1.90 (s, 6H) (the rest of the signals remain unchanged). ^{31}P NMR (CD_2Cl_2) δ 27.45 (d, J_{P-Rh}=156.5 Hz). Anal. Calcd for $C_{29}H_{35}BN_6OPRh$: C, 55.41; H, 5.57; N, 13.38. Found: C, 55.43; H, 5.50; N, 12.73.

Preparation of ($HBPz^*_3$)Rh(CO)(PPh_3) (4d)

To a solution of 1 (228.3 mg, 0.5 mmol) in CH_2Cl_2 (50 mL) was added PPh_3 (131.2 mg, 0.5 mmol) and this was stirred for ca. one and a half hour. IR indicated complete conversion. The solvent was removed under reduced pressure and the resulting solid was washed with n-hexane (3 x 5 mL) and dried in vacuo (0.1 mm Hg) for ca. 24 h affording the product as a bright yellow solid (330 mg, 96%). MP darkens above 175°C.

Characterization: IR (n-hexane) 1983 cm^{-1} (s, ν_{CO}). MS (155°C, 16 eV) M^+ (690), M^+-CO. ^{1}H NMR (CD_2Cl_2, 200 MHz, ambient) δ 7.40 (m, 15H), 5.68 (s, 3H), 2.20 (s, 9H), 1.86 (s, 9H). -105°C (CD_2Cl_2) δ 5.88 (s, 1H), 5.52 (s, 2H), 2.30 (br, 6H), 1.96 (br, 6H), 1.30 (br, 6H) (phenyl proton resonance remains unchanged). ^{31}P NMR (CD_2Cl_2) δ 42.46 (d, J_{P-Rh}=160.5 Hz). Anal. Calcd for $C_{34}H_{37}BN_6OPRh$: C, 59.13; H, 5.36; N, 12.17. Found: C, 59.09; H, 5.39; N, 12.22.

Preparation of ($HBPz^*_3$)Rh(CO)(PEtMePh) (4e)

To a stirred solution of 1 (150 mg, 0.329 mmol) in CH_2Cl_2 (50 mL) was added PEtMePh (50 μL). The original yellow solution became pale yellow immediately. IR indicated complete conversion. The solvent was then removed under reduced pressure to give a yellow solid which was dissolved in a minimum volume of CH_2Cl_2 and n-hexane was added to this solution. Cooling the solution to -20°C over a period of couple of days afforded the compound 4e as a yellow crystalline solid (162 mg, 85%).

Characterization: IR (n-hexane) 1973 cm^{-1} (s, ν_{CO}). MS (150°C, 16 eV) M$^+$ (580), M$^+$-CO, M$^+$-CO-P(C_6H_5)$_3$. ^{1}H NMR (CD_2Cl_2, 200 MHz, ambient) δ 7.68 (m, 2H), 7.40 (m, 3H), 5.79 (br, 3H), 2.14 (br, 18H), 1.66 (m, 2H), 1.44 (dd, $^2J_{P-H}$=9.7 Hz, $^3J_{Rh-H}$=1.2 Hz, 3H), 0.76 (m, 3H). -85°C (CD_2Cl_2) δ 7.64 (m, 2H), 7.42 (m, 3H), 5.89 (s, 1H), 5.76 (s, 2H), 2.36 (s, 3H), 2.30 (s, 3H), 2.16 (s, 3H), 2.10 (s, 3H), 1.84 (s, 3H), 1.66 (s, 3H), 1.54 (m, 2H), 1.37 (d, 3H), J_{Rh-H} was not observed at (low temperature), 0.66 (m, 3H). Anal. Calcd for $C_{25}H_{35}BN_6OPRh$: C, 51.72; H, 6.03; N, 14.48. Found: C, 51.34; H, 6.16; N, 14.27.

Preparation of ($H_2BPz^*_2$)Rh(CO)(PMe_3) (5a)

To a stirred solution of ($H_2BPz^*_2$)Rh(CO)$_2$ (**2**) (63 mg, 0.174 mmol) in n-hexane (25 mL) was added PMe_3 (18 µL, 0.177 mmol) resulting in the color of the solution changing immediately from light yellow to bright yellow. The solvent was removed under reduced pressure and the residue extracted with n-hexane (2 x 10 mL), filtered and cooled to -20°C for ca. three days affording the yellow crystalline product (30 mg, 73%).

Characterization: IR (n-hexane) 1975 cm^{-1} (s, ν_{CO}). MS (70°C, 16 eV) M$^+$ (410), M$^+$-CO, M$^+$-CO-PMe_3. ^{1}H NMR (200 MHz, ambient) δ 5.72 (s, 1H), 5.70 (s, 1H), 2.28 (s, 3H), 2.25 (s, 3H), 2.21 (s, 3H), 2.20 (s, 3H), 1.44 (dd, $^2J_{P-H}$=9.7 Hz, $^3J_{Rh-H}$=1.3 Hz, 9H). Anal. Calcd for $C_{14}H_{25}BN_4OPRh$: C, 40.97; H, 6.09; N, 13.66. Found: C, 40.60; H, 6.16; N, 12.80.

Preparation of $(H_2BPz^*_2)Rh(CO)(PMe_2Ph)$ (5b)

To a stirred solution of 2 (70 mg, 0.193 mmol) in n-hexane (50 mL) was added PMe_2Ph (28 µL, 0.196 mmol). After five minutes IR indicated complete conversion to the product. Removal of the solvent under reduced pressure afforded the analytical pure compound **5b** (87 mg, 95%).

Characterization: IR (n-hexane) 1979 cm^{-1} (s, ν_{CO}). MS (120°C, 16 eV) M^+ (472), M^+-CO. ^1H NMR (CD_2Cl_2, 200 MHz, ambient) δ 8.86 (m, 2H), 8.43 (m, 3H), 5.76 (s, 1H), 5.58 (s, 1H), 2.33 (s, 3H), 2.26 (s, 3H), 2.21 (s, 3H), 1.93 (s, 3H), 1.71 (dd, $^2J_{P-H}$=9.2 Hz, $^3J_{Rh-H}$=1.5 Hz, 3H), 1.64 (dd, $^2J_{P-H}$=9.5 Hz, $^3J_{Rh-H}$=1.1 Hz, 3H). Anal. Calcd for $C_{19}H_{27}BN_4OPRh$: C, 48.31; H, 5.72; N, 11.68. Found: C, 48.72; H, 5.90; N, 11.55.

References for Chapter II

1. S. Trofimenko, J. Am. Chem. Soc., 89 (1967) 3170.
2. S. Trofimenko, J. Am. Chem. Soc., 89 (1967) 3904.
3. S. Trofimenko, Acc. Chem. Res., 4 (1971) 17.
4. S. Trofimenko, J. Am. Chem. Soc., 91 (1969) 588.
5. R. Cramer, J. Am. Chem. Soc., 86 (1964) 217.
6. R. Cramer, J.B. Kline and J.D. Roberts, J. Am. Chem. Soc., 91 (1969) 2519.
7. M. Herberhold, C.G. Kreiter and G.O. Wiedersatz, J. Organomet. Chem., 120 (1976) 103.
8. R. Cramer and J.J. Mrowca, Inorg. Chim. Acta., 5 (1971) 528.
9. R. Cramer, J. Am. Chem. Soc., 94 (1972) 5681.
10. R. Cramer and L.P. Seiwell, J. Organomet. Chem., 92 (1975) 245.
11. D.J. O'Sullivan and F.J. Lalor, J. Organomet. Chem., 65 (1974) C47.
12. (a) M. Cocivera, G. Ferguson, B. Kaitner, F.J.Lalor, D.J. O'Sullivan, M. Parvez and B. Ruhl, Organometallics, 1 (1982) 1132.
    (b) M. Cocivera, G. Ferguson, F.J. Lalor and P. Szczecinski, Organometallics, 1 (1982) 1139.
13. S. Trofimenko, Inorg. Chem., 10 (1971) 1372.
14. S. May, P. Reinsalu and J. Powell, Inorg. Chem., 19 (1980) 1582.
15. F. Bonati and G. Wilkinson, J. Chem. Soc. (1964) 3156.
16. H.C. Clark and S. Goel, J. Organomet. Chem., 165 (1979) 383.
17. F. Bonati, G. Minghetti and G. Banditelli, J. Organomet. Chem., 87 (1975) 365.
18. A.D. McMaster, Personal communication.

19. J.W. Faller, in "Determination of Organic Structures by Physical Methods", Vol. 5, F.C. Nachod and J.J. Zuckerman, Eds., Academic Press, New York, 1973, Chapter 2.

20. B.M. Louie, S.J. Rettig, A. Storr and J. Trotter, Can. J. Chem., 62 (1984) 1057.

21. J. Powell and B.L. Shaw, J. Chem. Soc., (A) (1968) 211.

22. J.A. McCleverty and G. Wilkinson, Inorg. Synth., 8 (1966) 211.

CHAPTER III

ARENE C-H ACTIVATION

Section 1

INTRODUCTION

One of the ways in which carbon-hydrogen bonds may be activated involves interaction with a transition metal complex in such a way that the C-H bond is cleaved and metal-carbon and metal-hydrogen bonds are formed. The process is shown schematically below, and may also be described as an oxidative addition reaction.

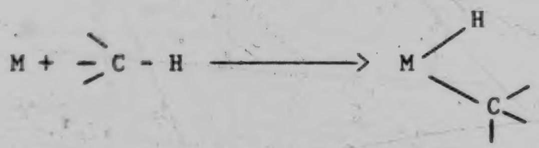

The activation of C-H bonds by soluble transition metal complexes has received considerable attention and significant progress has been made in this area over the past 25 years.[1] Major interest in this field arises from its potential application in synthetic organic chemistry and in industrial processes as a method of functionalizing C-H bonds. The discussions in this Chapter will be limited to arene C-H activation reactions.

Electrophilic aromatic metallation reactions have been known for many years and have been demonstrated for mercury,[2] thallium,[3] lead,[4] platinum,[5] palladium,[6] and rhodium.[7]

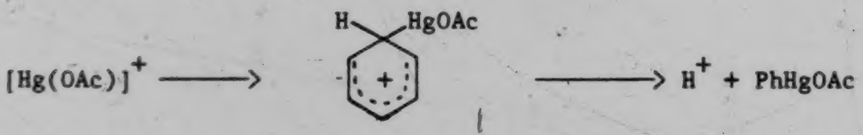

One of the problems of electrophilic aromatic metallation is that it is unselective and reactions with substituted arenes generally result in metallation at most of the positions on the arene ring.

The recently emerging field of intermolecular activation of C-H bonds by oxidative addition may enable greater control of selectivity by varying the nature of metal complexes.

The activation of C-H bonds by oxidative addition remained elusive until the discovery of cyclometallation. This is simply an intramolecular addition of a ligand C-H bond to the metal.

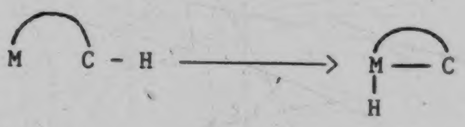

There are many examples of cyclometallations,[8] termed orthometallations when an ortho aromatic C-H bond is activated. An early example of a reaction[9] that must involve aromatic C-H bond cleavage is the catalytic synthesis of indazolones from azobenzene and carbon monoxide (eq. 3-1).

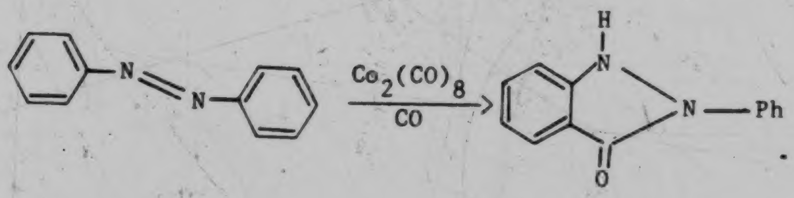

(3-1)

The first isolated cyclometallation product was reported by Kleiman[10] in 1963, an explicit example of intramolecular aromatic C-H bond activation (eq. 3-2).

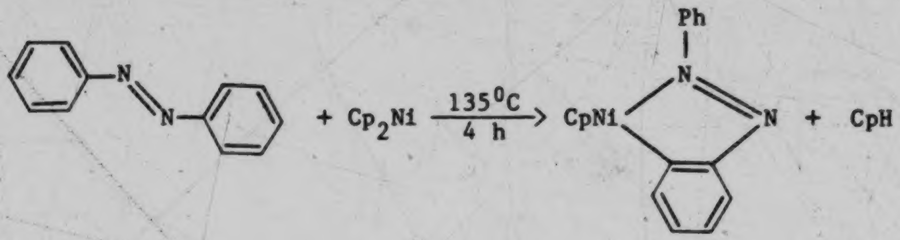

(3-2)

Perhaps the most common intramolecular C-H oxidative addition is the orthometallation reaction of aryl groups. A typical example[11] is provided in eq. 3-3.

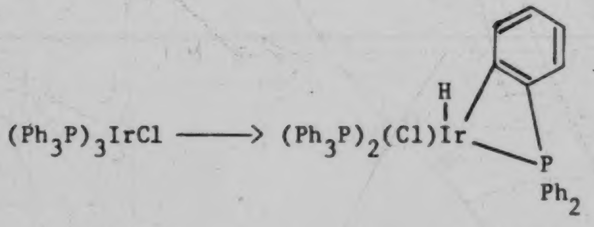

(3-3)

Clearly, proximity of the reacting C-H bond to the metal center is a critical factor favouring such cyclometallation processes. The more common occurrence of intramolecular C-H activation led chemists earlier to speculate that entropy played a major role in the difference between intra and intermolecular oxidative addition reactions.

Recently Jones and Feher carried out the first systematic study of intramolecular versus solvent C-H oxidative addition reactions.[12] Their studies on Cp*Rh(PMe$_2$CH$_2$Ph)(H)(C$_6$H$_5$) showed that there was only a very slight *kinetic* preference for solvent activation; on the other hand, there was a moderately high *thermodynamic* preference for intramolecular aromatic C-H activation in this system.

The first example of intermolecular oxidative addition of arene C-H bonds was reported by Chatt and Davidson[13] in 1965. They observed that a reduction product of RuCl$_2$(dmpe)$_2$ interacted with benzene, naphthalene, and other aromatic hydrocarbons to give arylruthenium hydride complexes (eq. 3-4).

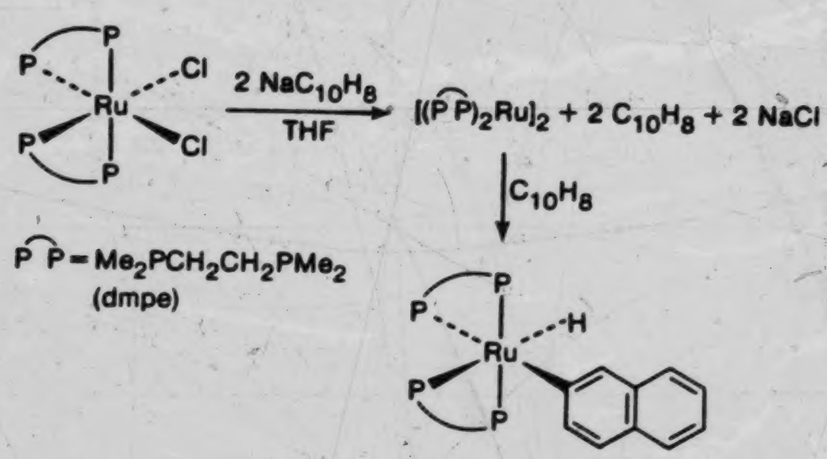
P
Cl
Ru
2 NaC10H8
THF
[(P P)2Ru]2 + 2 C10H8 + 2 NaCl
C10H8
P P = Me2PCH2CH2PMe2
(dmpe)
H

(3-4)

Following this report, numerous other examples of intermolecular arene C-H oxidative addition reactions have appeared in the literature. Green et al.[14] have reported activation of arene C-H bonds by photochemically or thermally generated "tungstenocene", $(\eta^5\text{-}C_5H_5)_2W$ (eq. 3-5).

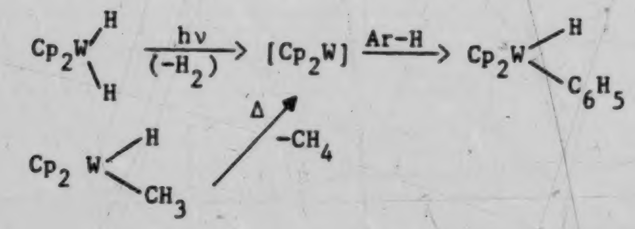
Cp2W
H
hν
(-H2)
[Cp2W]
Ar-H
C6H5
Δ
-CH4
CH3

(3-5)

Rausch et al.[15] found evidence of formation of $(\eta^5\text{-}C_5H_5)Ir(CO)(H)(C_6H_5)$ during photolysis of $(\eta^5\text{-}C_5H_5)Ir(CO)_2$ in benzene, although they were unable to isolate the former compound. More recently, Hoyano and Graham[16] reported the formation of

Cp*Ir(CO)(H)(C_6H_5) during irradiation of Cp*Ir$(CO)_2$ in benzene solution (eq. 3-6).

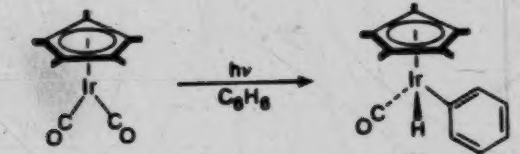

(3-6)

The unstable Cp*Ir(CO)(H)(C_6H_5) was converted to the more stable chloro derivative Cp*Ir(CO)(Cl)(C_6H_5) for characterization. Aromatic C-H oxidative addition by a relatively electron-rich complex was also demonstrated by Janowicz and Bergman[17] (eq. 3-7)

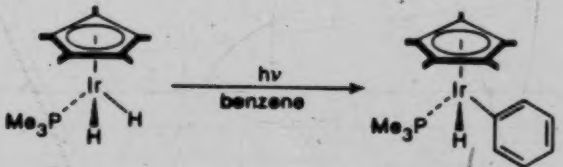

(3-7)

The more widespread occurrence and earlier observation of arene C-H activation has led to the view that sp^2-hybridized aromatic C-H bonds are more easily activated than are sp^3-hybridized C-H bonds by transition metal complexes. This may seem surprising in the light of the difference in C-H bond strengths involved (110 kcal mol^{-1} for benzene against 95 kcal mol^{-1} for a typical alkane). Parshall[8] suggested that the arene may precoordinate to the metal in an η^2-fashion prior to activation, a formulation that was postulated as early as 1965 by Chatt.[13]

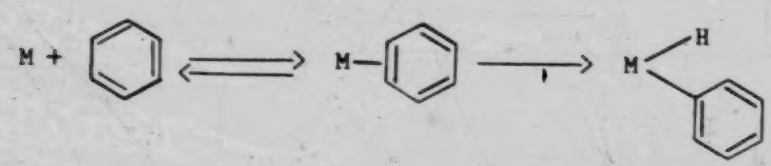

It is suggested that prior η^2-arene coordination can provide a lower energy pathway for the oxidative addition of the C-H bonds, a route which is not available to alkanes. However, the strength of M-Ar bonds exceeds that of M-R bonds by a greater margin than that (ca. 15 kcal mol^{-1}) by which the strength of H-Ar bonds exceeds that of H-R bonds.[18] Fuller discussions of M-C and M-H bond energies will be found in Chapter IV and Chapter VI.

Until recently, no experimental evidence was available for the widely accepted hypothesis of η^2-arene intermediate. Jones and Feher[19] have made a strong case that η^2-arene coordination is required before C-H bond activation in eq. 3-8.

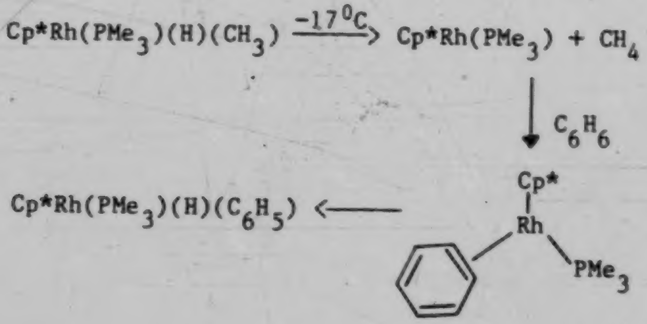
$Cp^*Rh(PMe_3)(H)(CH_3) \xrightarrow{-17^0C} Cp^*Rh(PMe_3) + CH_4$
C_6H_6
$Cp^*Rh(PMe_3)(H)(C_6H_5)$
Cp*
Rh
PMe_3

(3-8)

In the photochemical oxidative addition reactions the reactive intermediates were presumed to be 16-electron coordinatively unsaturated species.[16,20] For example, the photochemical reaction of $Cp^*Ir(CO)_2$ with benzene is considered to proceed via loss of CO to give $[Cp^*Ir(CO)]$, a coordinatively unsaturated 16-electron intermediate, which can then oxidatively add C-H bonds.[16] Evidence in favour of the postulated intermediate $[Cp^*Ir(CO)]$ was found in N_2 and Ar matrix at 12 K, though only small amounts were generated[21] and the interpretation was far from unambiguous. Jones and Feher[19] reported that irradiation of $Cp^*Rh(PMe_3)(H)_2$ in C_6D_6 resulted in the rapid formation of $Cp^*Rh(PMe_3)(D)(C_6D_5)$, presumably through the formation of a coordinatively unsaturated $[Cp^*Rh(PMe_3)]$ intermediate (eq. 3-9).

$$Cp^*Rh(PMe_3)(H)_2 \xrightarrow{h\nu\ (-H_2)} [Cp^*Rh(PMe_3)] \xrightarrow{C_6D_6} Cp^*Rh(PMe_3)(D)(C_6D_5) \qquad (3\text{-}9)$$

A reactive intermediate can also be formed by thermally induced reductive elimination. Thus thermolysis of $Cp^*Ir(PMe_3)(H)(C_6H_{11})$ in benzene yielded $Cp^*Ir(PMe_3)(H)(C_6H_5)$.[22] The rate of thermolysis was retarded by added cyclohexane but unaffected by the concentration of benzene or PMe_3. On the basis of these results Bergman et al.[22] proposed the mechanism (eq. 3-10) in which $[Cp^*Ir(PMe_3)]$ was postulated as an intermediate formed by reversible loss of cyclohexane.

$$\begin{tikzcd} Cp^{*}Ir(PMe_3)(H)(Cy) \arrow[r, shift left] & \left[Cp^{*}Ir(PMe_3)\right] + H\text{-}Cy \arrow[l, shift left] \arrow[d, "C_6H_6"] \\ & Cp^{*}Ir(PMe_3)(H)(C_6H_5) \end{tikzcd} \qquad (3\text{-}10)$$

The intermediate in the photochemical and thermal reactions appears to be the same. Its relative reactivity toward benzene and cyclohexane is similar whether it is generated from photolysis of $Cp^{*}Ir(PMe_3)(H)_2$ or from thermolysis of $Cp^{*}Ir(PMe_3)(H)(C_6H_{11})$.[22]

Previous studies related to arene C-H activation were centered on transition-metal complexes containing Cp, Cp* and phosphine ligands. Pyrazolylborate transition-metal chemistry has developed extensively over 20 years[23] but the area of carbon-hydrogen activation by such complexes has not been previously investigated. The analogy between Cp and $HBPz_3$, and between Cp* and $HBPz^{*}_3$ ligands has been discussed in Chapter II. It seemed that the facile tridentate-bidentate interconversion of the tris(pyrazolyl)borate ligand (Chapter II) might be interesting from the point of view of C-H activation. The unavailability of $(HBPz_3)Rh(CO)_2$, which forms an insoluble carbonyl-bridged species led to the choice of the 3,5-dimethyl compound $(HBPz^{*}_3)Rh(CO)_2$ (1). The interaction of 1 with a variety of aromatic hydrocarbons will be discussed in this Chapter. Some kinetic and mechanistic aspects of arene C-H activation will also be described.

Section 2

BENZENE ACTIVATION AND THE PROPERTIES OF THE HYDRIDOPHENYL PRODUCT

The tris(dimethylpyrazolyl)borato complex $(HBPz^*{}_3)Rh(CO)_2$ (1) photochemically activates[24] aromatic hydrocarbons with great efficiency at room temperature (eq. 3-11).

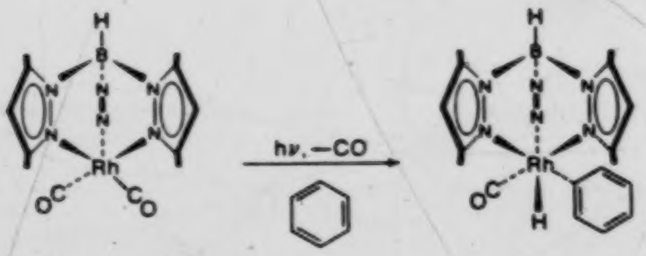

(3-11)

1 6

Unlike previously reported photochemical systems, activation proceeds under daylight or tungsten illumination as well as with use of a mercury arc.

When a pale yellow solution of 1 (*ca*. 2 m*M*) in a closed, evacuated Pyrex Schlenk tube was irradiated under standard conditions (Experimental Section) for five minutes by means of a 450-W Hanovia medium pressure mercury lamp, the solution became colorless, and the conversion to the hydridophenyl rhodium (III) complex according to eq. 3-11 was complete. It is important to note that under the same conditions, conversion of $(\eta^5\text{-}C_5Me_5)Ir(CO)_2$ to the hydridophenyl complex was only *ca*. 60% after six hours irradiation, and there was a general degradation at longer times.[16] Activations using $(\eta^5\text{-}C_5Me_5)Ir(PMe_3)(H)_2$ also require long irradiation with a powerful UV source and do not proceed to completion.[17,20,22b] On the other hand, a benzene solution of 1 (ca. 2.9 mM) was >95% converted to hydridophenyl complex (6) even when irradiated with an ordinary 75-W incandescent reflector flood light at a distance of 2-3 cm for only two hours.

The hydridophenylrhodium (III) complex 6 is a moderately air stable colorless crystalline solid, although it is quite air sensitive in solution. It was characterized by elemental analysis and spectroscopic methods. The low resolution electron impact mass spectrum did not show the molecular ion M^+, and the observed heaviest fragment corresponded to $[(HBPz^*_3)Rh(CO)]_2$; this species is probably formed as the solid sample is heated. However, fast atom bombardment MS (Cleland matrix) indicated M^+ and $(M\text{-}CO)^+$. The IR spectrum (n-hexane) showed a single ν_{CO} at 2049 cm^{-1} and a weak broad absorption peak at ca. 2060 cm^{-1}, assigned as the Rh-H stretching vibration. A high field resonance at δ-12.31 (1H, d, J_{Rh-H}=21.3 HZ) in the ^1H NMR spectrum is a definitive indication of the rhodium-hydrogen bond. The six methyl and three 4-H resonances in the ^1H NMR spectrum of 6 (Fig. III.1) are consistent with the three nonequivalent pyrazole rings in the octahedral structure. The phenyl protons are broad (Fig. III.1) at ambient temperature suggesting a somewhat slowed rotation of the phenyl ring about rhodium-phenyl bond. This is confirmed by the ^1H NMR spectrum at -20°C, (Fig. III.2) which shows five sharp sets of multiplets as rotation about the rhodium-phenyl bond becomes slow on the NMR timescale. The two edges of the phenyl ring are nonequivalent. In the aromatic region, the resonance at δ 6.95 appears as a triplet at ambient temperature and remains as such on

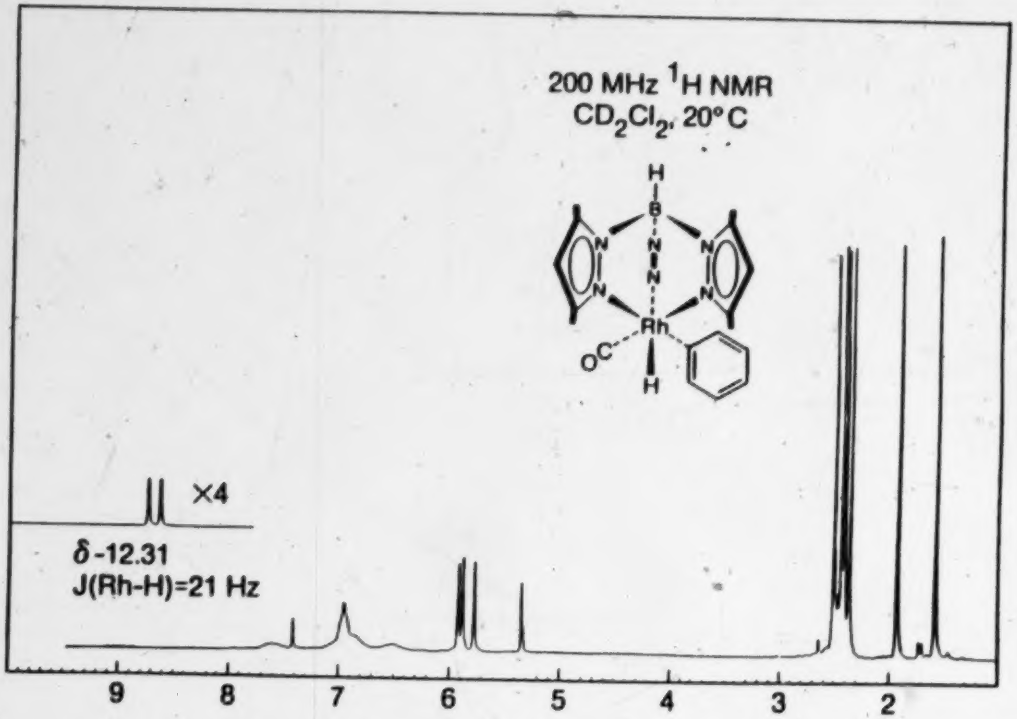

Figure III.1 ^{1}H NMR spectrum of (HBPz*$_3$)Rh(CO)(H)(C_6H_5) (6) at ambient temperature.

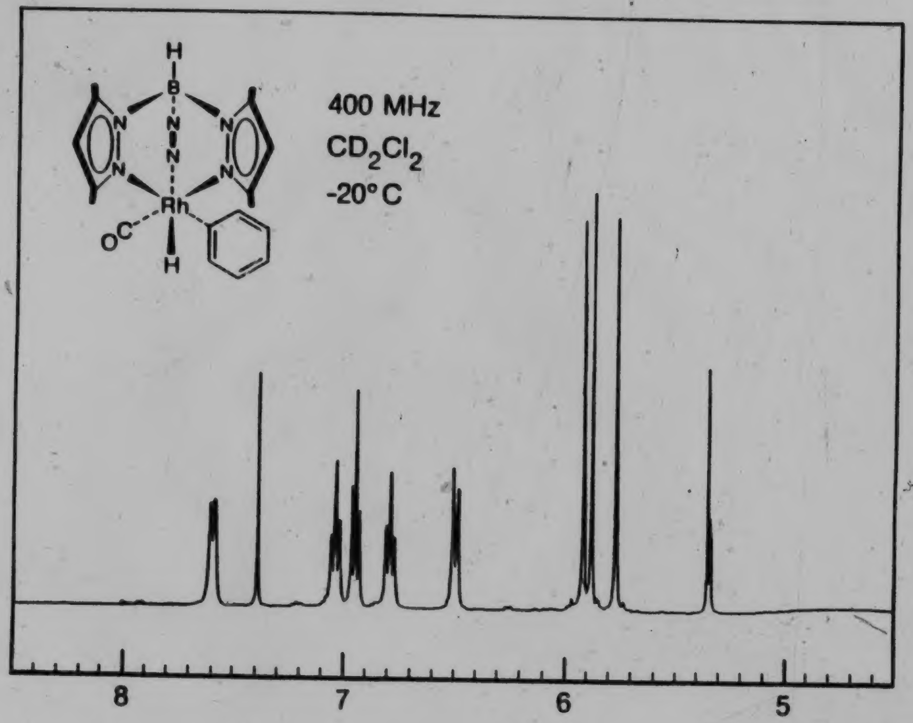

Figure III.2 ^{1}H NMR spectrum of (HBPz*$_3$)Rh(CO)(H)(C_6H_5) at -20°C (phenyl region).

cooling, and is accordingly assigned to the *para* proton. The *para* proton is expected to be a triplet even at ambient temperature, since for a proton at the para position, no site is available for exchange upon rotation. However the *ortho* and *meta* protons have sites available for exchange. In the low temperature ^1H NMR spectrum (Fig. III.2), selective decoupling experiments confirm that the resonances at δ 7.59 and at δ 6.49 are due to the *ortho* and *ortho*' protons respectively, while the resonance at δ 7.30 and δ 6.79 are due to the *meta* and *meta*' protons respectively.

Assignment of the $\{^1H\}$ ^{13}C NMR of complex **6** at -20°C is given in Experimental Section but this spectrum alone does not identify the phenyl carbons as *ortho*, *meta* and *para*. The two dimensional (2-D) NMR spectrum was taken in the aromatic region to correlate carbons with the hydrogens, resonances due to the hydrogens having already been assigned in the ^1H NMR spectrum. Such a 2-D NMR spectrum, shown in Fig. III.3, allows assignments of the phenyl carbons as indicated.

Kinetics of C_6H_6 exchange of $(HBPz^*_3)Rh(CO)(H)(C_6H_5)$ (6) with C_6D_6 solvent

The hydridophenyl complex (**6**) is quite stable thermally and does not eliminate benzene at an appreciable rate at room temperature. When a solution of **6** in C_6D_6 is heated above 40°C, a smooth first order reductive elimination occurs to produce C_6H_6 and $(HBPz^*_3)Rh(CO)(D)(C_6D_5)$. The formation of $(HBPz^*_3)Rh(CO)(D)(C_6D_5)$ (**8a**) is presumed to occur via the coordinatively unsaturated $[(HBPz^*_3)Rh(CO)]$ intermediate (eq. 3-12).

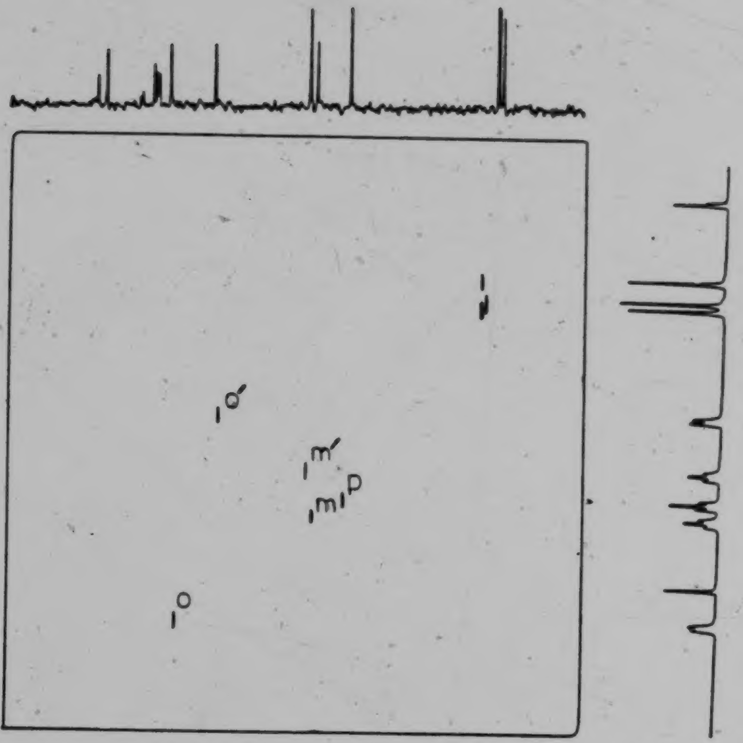

Figure III.3 2-D NMR ^1H-^{13}C correlation spectrum of $(HBPz^*_3)Rh(CO)(H)(C_6H_5)$ in the phenyl region. Horizontal axis, ^{13}C; vertical axis, ^1H.

$$(HBPz^{*}_{3})Rh(CO)(H)(C_6H_5) \underset{k_{-1}}{\overset{k_1}{\rightleftharpoons}} [(HBPz^{*}_{3})Rh(CO)] + C_6H_6$$

6

(3-12)

$$[(HBPz^{*}_{3})Rh(CO)] + C_6D_6 \underset{k_{-2}}{\overset{k_2}{\rightleftharpoons}} (HBPz^{*}_{3})Rh(CO)(D)(C_6D_5)$$

8a

The rate of disappearance of **6** was followed by heating the complex **6** in C_6D_6 solvent and monitoring the rate of disappearance of rhodium hydride resonance against an internal standard (hexamethyldisiloxane). The reaction was pseudo first order under these conditions. A logarithmic plot of the ratio (hydride resonance/internal standard) versus time yielded a straight line with slope equal to -k (rate constant). The rate of the exchange was determined at several different temperatures, a typical plot is shown in Fig. III.4. At each temperature, the rate was followed for at least two to three half lives. The rate constants at various temperatures are listed in Table 3.I.

From an Eyring plot of the data in Table 3.I (Fig. III.5) the activation parameters for the rate of disappearance of **6** were found to be $\Delta H^{\ddagger}=29.6\pm0.4$ kcal mol^{-1} and $\Delta S^{\ddagger}=12.2\pm1.2$ eu. Jones and Feher[19] reported the activation parameters for exchange of $Cp^{*}Rh(PMe_3)(H)(C_6H_5)$ with C_6D_6 as $\Delta H^{\ddagger}=30.5\pm0.8$ kcal mol^{-1} and $\Delta S^{\ddagger}=14.9\pm2.5$ eu. The similarity of activation parameters in the two systems is so striking that the mechanisms for exchange are likely very similar in the two systems. Jones et al.[19] expressed surprise regarding the large positive

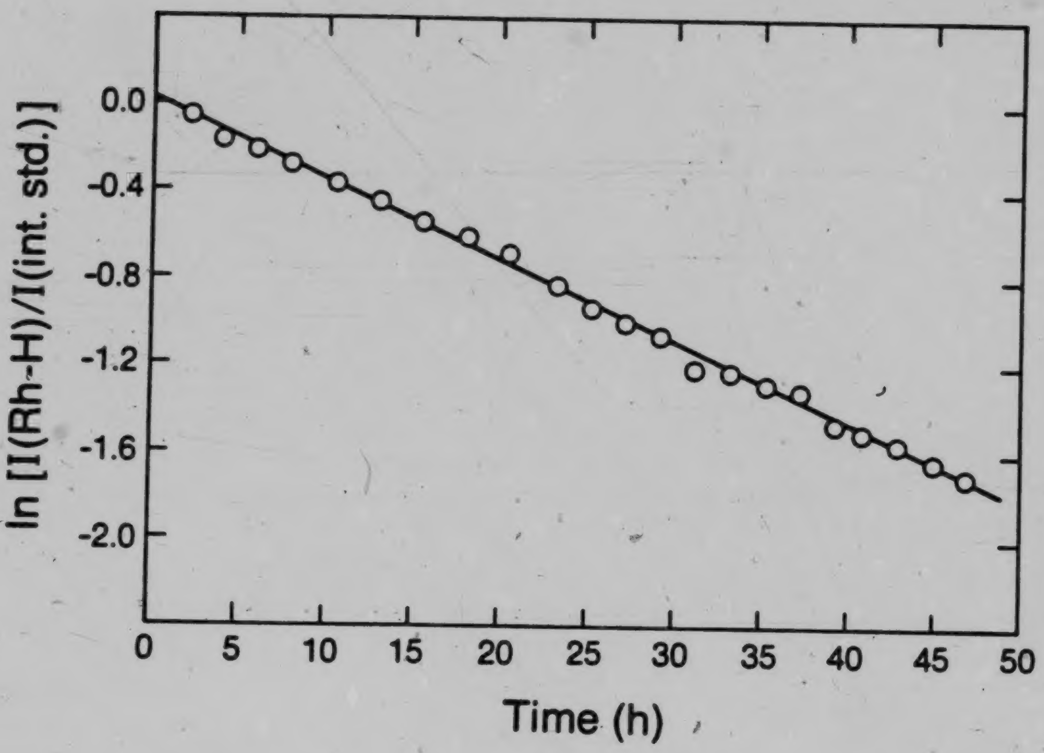

Figure III.4 First order plot of benzene exchange data for $(HBPz^*_3)Rh(CO)(H)(C_6H_5)$ (6) in C_6D_6 at 42°C

Table 3.I Rate Constants for Exchange of Benzene-d_6 with 6

Temp (K)	k (s^{-1})
315	$(1.01 \pm 0.01) \times 10^{-5}$
323	$(2.92 \pm 0.05) \times 10^{-5}$
333	$(1.25 \pm 0.04) \times 10^{-4}$
343	$(5.14 \pm 0.08) \times 10^{-4}$

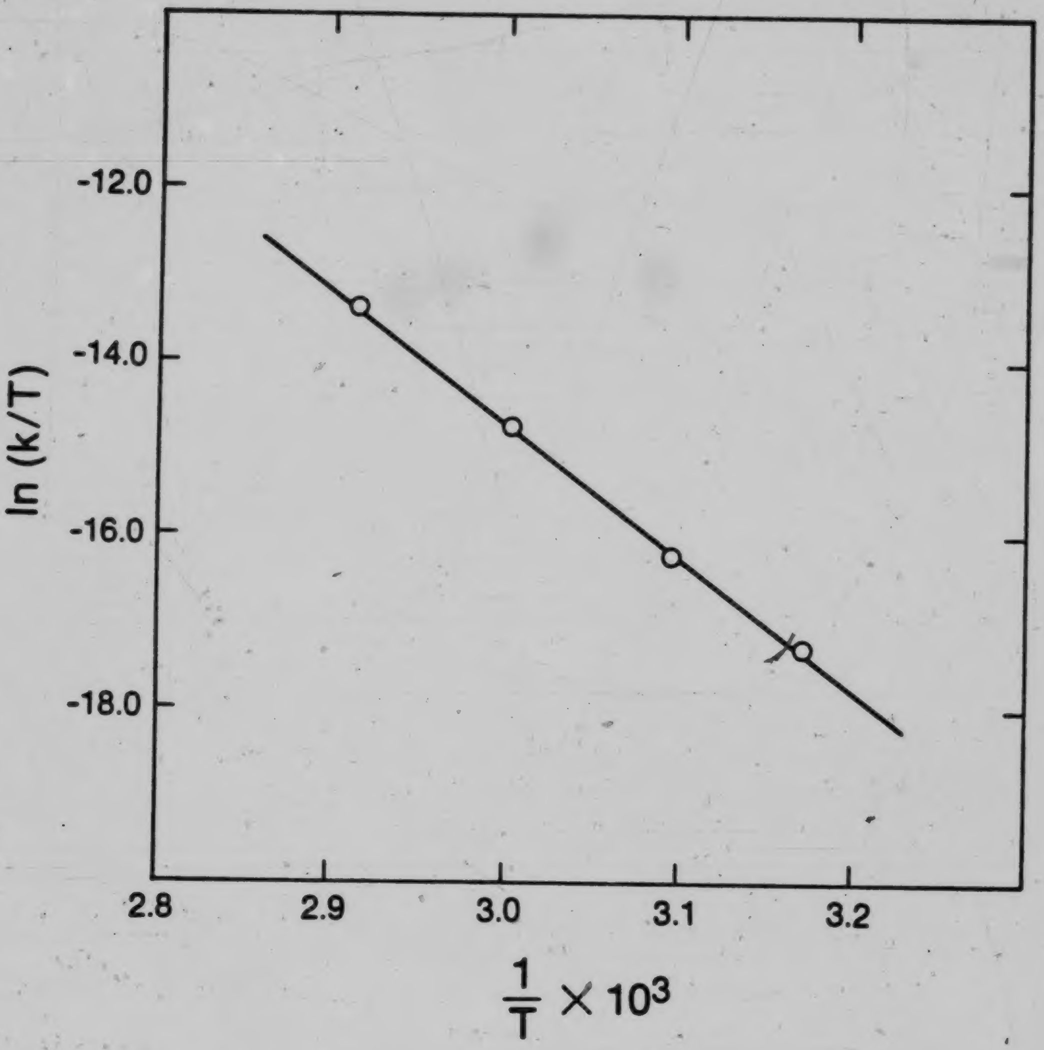

Figure III.5 Eyring plot for the exchange of $(HBPz^*_3)Rh(CO)(H)(C_6H_5)$ (6) with C_6D_6.

$\Delta S^{\ddagger}$ value for reductive elimination which presumably involves a highly ordered three-center transition state.

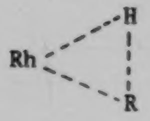

Negative or slightly positive $\Delta S^{\ddagger}$ values have been found for previously studied reductive elimination reactions.[25]

In view of the similarity of kinetic parameters of complex **6** to those of Cp*Rh(PMe_3)(H)(C_6H_5),[19] one would expect precoordination of benzene to rhodium in an η^2-fashion prior to C-H activation in the HBPz*$_3$ system as was found for the Cp*Rh system. Evidence for the η^2-benzene intermediate could in principle be found by irradiation of the hydride resonance of (HBPz*$_3$)Rh(CO)(H)(C_6H_5) (**6**). One would expect spin saturation transfer between the hydride resonance and the ring proton signals (eq. 3-13).

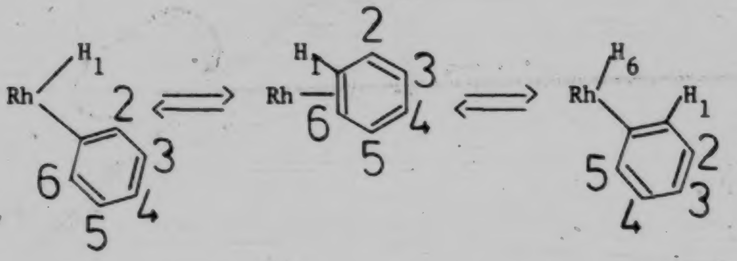

etc. (3-13)

Such an experiment was carried out on **6** by irradiating the high field hydride resonance in the temperature range -20°C to ambient temperature. Under the experimental conditions, no appreciable transfer of spin was observed. This negative result suggests either that an η^2

intermediate is not involved or that there is an η^2-benzene intermediate but the rate of η^1-η^2 interconversion is too slow relative to relaxation times to detect in this experiment.

In an attempt to resolve this question, an alternative approach was to synthesize $(HBPz^*_3)Rh(CO)(D)(C_6H_5)$ (**8b**) and to examine its ^1H NMR spectra from time to time to observe whether any deuterium scrambling over the phenyl ring takes place on the laboratory time scale. If the expected η^2-benzene intermediate is involved, the ^1H NMR spectrum of **8b** would show gradual formation of a hydride resonance with time and consequently, there would be a decrease in intensity of the phenyl proton resonances due to scrambling of deuterium over the phenyl ring. In accordance with this view, complex **8b** was prepared (eq. 3-14) by reducing $(HBPz^*_3)Rh(CO)(Cl)(C_6H_5)$ (**7**) with zinc dust and acetic acid-d_4 in methanol-d_4. The synthesis and properties of **7** will be discussed later in this Section.

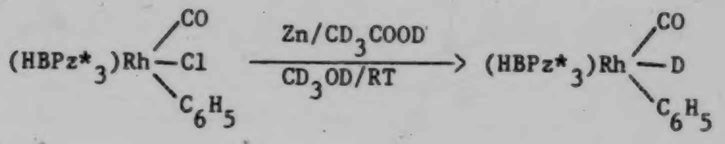

$$(HBPz^*_3)Rh(CO)(Cl)(C_6H_5) \xrightarrow[CD_3OD/RT]{Zn/CD_3COOD} (HBPz^*_3)Rh(CO)(D)(C_6H_5) \qquad (3\text{-}14)$$

7 **8b**

The ν_{CO} of **8b** is identical to the corresponding protio complex **6**. The ^1H NMR spectrum of **8b** recorded approximately two hours after the synthesis showed a high field resonance, the integration of which corresponded to ca. 5/6 protons, as expected statistically for complete deuterium scrambling over the phenyl ring. This result provides some evidence for the intermediacy of the η^2-benzene complex for oxidative addition of benzene C-H bonds. This is consistent with the observation of η^2-benzene intermediate by Jones et al.[19] in the Cp*ML system. It is of interest that an η^2-C_6H_6 rhenium complex has recently been crystallographically characterized.[26]

The rate of deuterium scrambling in **8b** was too fast to determine under the experimental conditions. Low temperature synthesis of **8b** and low temperature ^1H NMR studies might allow determination of the rate of scrambling, but were not pursued in this work in view of Jones' persuasive results.

Reactions of $(HBPz^*_3)Rh(CO)(H)(C_6H_5)$ (6)

Reaction with CCl_4

Complex **6** reacted quite readily with an excess of CCl_4 to give $(HBPz^*_3)Rh(CO)(Cl)(C_6H_5)$ (**7**) (eq. 3-15) in ca. 80% isolated yield.

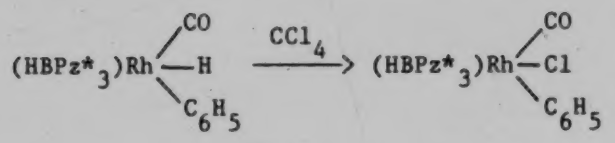

$$(HBPz^*_3)Rh(CO)(H)(C_6H_5) \xrightarrow{CCl_4} (HBPz^*_3)Rh(CO)(Cl)(C_6H_5) \qquad (3\text{-}15)$$

6 **7**

During the reaction of **6** with CCl_4, a small amount of new species formed, presumed on the basis of ν_{CO} at 2116 cm^{-1} (n-hexane) to be $(HBPz^*_3)Rh(CO)(Cl)_2$. However, this product could not be isolated; it is unstable in solution, losing CO slowly at room temperature.

The compound **7** was isolated as yellow, air stable crystals and was characterized by IR, MS, ^{1}H NMR and elemental analysis. In contrast to $(HBPz^*_3)Rh(CO)(H)(C_6H_5)$ (**6**), the ^{1}H NMR spectrum of $(HBPz^*_3)Rh(CO)(Cl)(C_6H_5)$ (**7**) at ambient temperature showed five sharp sets of multiplets in the aromatic region. This is considered to be due to the higher barrier to phenyl rotation in 7 (as compared to 6) due to the greater bulk of the chloride ligand. This kind of hindered rotation has been observed about rhodium-phosphorus and rhodium-carbon bonds in the $(C_5Me_5)Rh(PR_3')(R)(X)$ system (R' = tertiary phosphines, RX = aromatic halides).[27]

Decoupling experiments indicated that the pair of doublets at δ 7.87 and 6.18 are due to the ortho and ortho' protons, and the pair of triplets at δ 7.15 and 6.79 are due to the meta and meta' protons. The triplet at δ 7.01 was assigned as the para proton.

Reaction with CO

The complex **6** in n-hexane reacted slowly at room temperature under one atm pressure of CO to give $(HBPz^*_3)Rh(CO)_2$ (**1**). IR monitoring indicated ca. 70% conversion in 40 hours of reaction, corresponding to a half life of about 23 hours. The IR gave no indication of the formation of formyl or benzoyl intermediates or of benzaldehyde as a product.

Regarding the mechanism of formation of $(HBPz^*_3)Rh(CO)_2$ (**1**), the most obvious possibility is perhaps a reversible first order reductive elimination of benzene as the rate determining step (eq. 3-16).

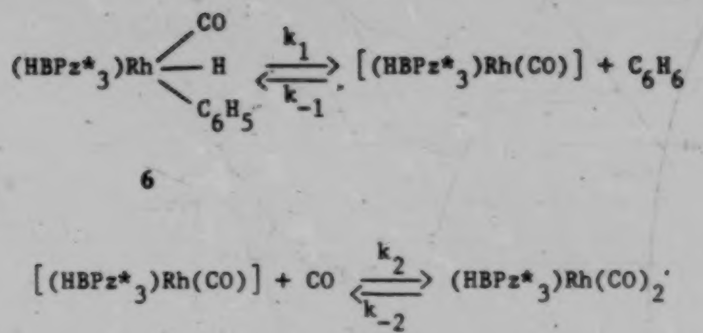

6

$$[(HBPz^{*}_{3})Rh(CO)] + CO \underset{k_{-2}}{\overset{k_{2}}{\rightleftharpoons}} (HBPz^{*}_{3})Rh(CO)_{2}$$

1

(3-16)

If k_1 in eq. 3-16 is the rate determining step, then an upper limit for the rate of reaction of 6 with CO may be computed from the activation parameters for the C_6D_6 exchange reaction of 6 (eq. 3-12). Using the activation parameters for eq. 3-12, the value of k at room temperature is calculated as $5.62 \times 10^{-7}\ s^{-1}$, which translates to a half life of 343 hours as a lower limit. The half life for the reaction of 6 with one atm. CO pressure was approximately 23 hours. This comparison excludes the "obvious" mechanistic possibility of eq. 3-16.

An important observation concerned the reaction of 6 with four atm CO pressure in n-hexane at room temperature. The rate of disappearance of 6 was monitored qualitatively by IR, and it was clear that complex 6 reacted relatively faster at four atm. CO pressure than it did at one atm. CO. This pressure dependency suggests an associative mechanism for the formation of 1. To account for the observed CO pressure dependency the following mechanism is proposed (eq. 3-17).

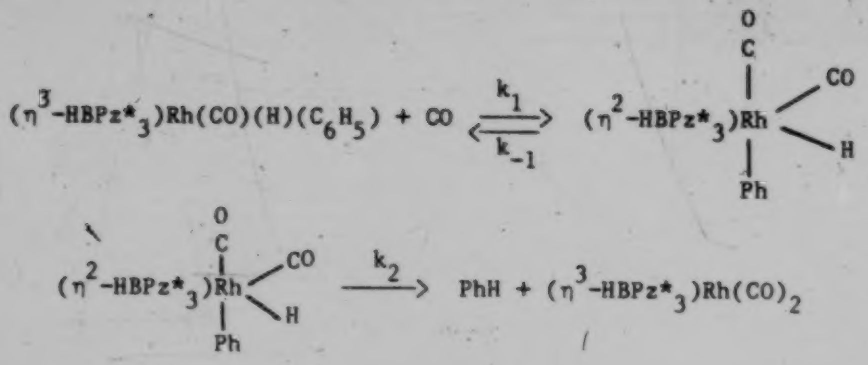

(3-17)

A process such as eq. 3-17 would be CO pressure dependent if k_1 were the rate determining step. Further studies of the reactions of **6** with donor ligands would be of considerable interest and importance.

Since functionalization of benzene by reaction of $(HBPz^*_3)Rh(CO)(H)(C_6H_5)$ (**6**) with CO was not accomplished, an alternative approach was to prepare derivatives of the hydridophenyl complex that would reductively eliminate less readily. One such compound is $(HBPz^*_3)Rh(CO)(CH_3)(C_6H_5)$, discussed in the following section.

Reaction with CH_2N_2

Complex **6** reacted at a moderate rate with CH_2N_2 at 0°C to give cleanly $(HBPz^*_3)Rh(CO)(CH_3)(C_6H_5)$ (**9**) (eq. 3-18).

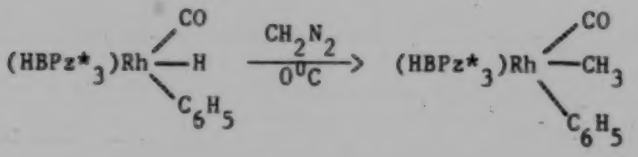

(3-18)

6 **9**

The compound 9 was isolated as colorless crystals in ca. 70% yield. The formulation of the compound was confirmed by IR, MS, ^{1}H NMR and elemental analysis. The IR spectrum showed a single ν_{CO} at 2045 cm^{-1}; this is 4 cm^{-1} lower than that of the hydrido complex 6, a reasonable shift for the more electron-releasing methyl group. The ^{1}H NMR spectrum indicated a doublet at δ 1.20 (d, $^2J_{Rh-H}$=2.1 Hz), characteristic for methyl bound to a rhodium center. Two sets of doublets and three sets of triplets were found in the aromatic region, as was the case for $(HBPz^*_3)Rh(CO)(Cl)(C_6H_5)$ (7). This is another example of hindered rotation of the phenyl ring about the rhodium-carbon bond. The CO insertion reaction of this compound will be discussed in Chapter VI along with the other CO insertion reactions.

Section 3

ACTIVATION OF OTHER AROMATIC HYDROCARBONS

As it does benzene, the tris(dimethylpyrazolyl)borato complex $(HBPz^*_3)Rh(CO)_2$ (**1**) also photochemically activates other aromatic hydrocarbons with great efficiency.

Toluene as substrate

Complex **1** activates toluene sp^2 C-H bonds efficiently at ambient temperature. Irradiation of a yellow solution of **1** (*ca*. 7.8 *mM*) in a closed Pyrex Schlenk tube for 15 minutes afforded a colorless solution. IR indicated quantitative conversion to the hydridotolyl rhodium (III) complex (**10**) according to eq. 3-19.

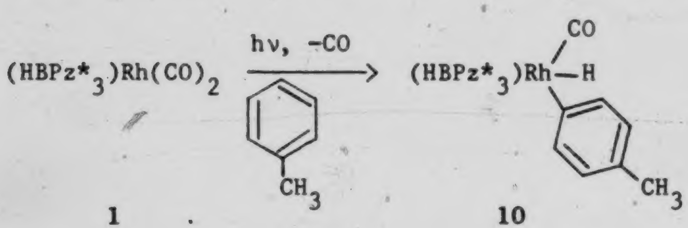

1 **10** (3-19)

Conversion of $Cp^*Rh(PMe_3)(H)_2$ to the hydridotolyl complex[19] was only *ca*. 20% after 43 minutes of irradiation at -45°C. Complex **10** was characterized by spectroscopic methods and elemental analysis.

The IR spectrum (*n*-hexane) showed a single ν_{CO} at 2048 cm^{-1} and a weak broad band at 2060 cm^{-1}, assigned as the Rh-H stretching vibration. The ^1H NMR spectrum of **10** at ambient temperature indicated two sets of doublets in 2:1 ratio in the high field region. On cooling to -80°C, three sets of hydride resonances in 21:46:33 ratio were found in the ^1H NMR spectrum. The three pairs of Rh-H resonances are presumably due to para and two meta conformers as shown in eq. 3-20.

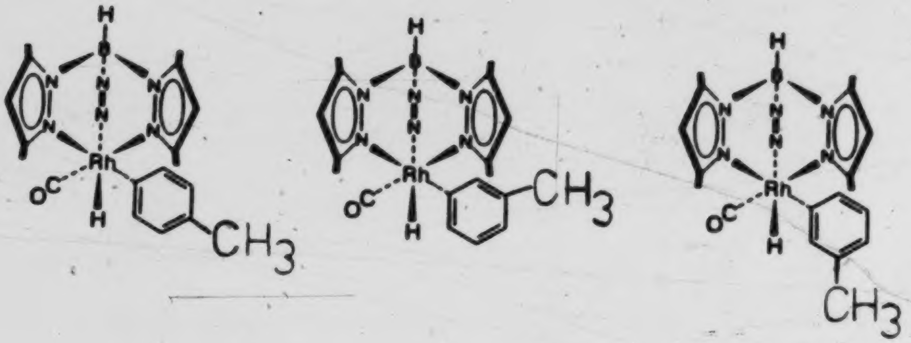

(3-20)

para meta meta

Presumably the meta conformers interconvert rapidly at ambient temperature on the NMR timescale, but only slowly at -80°C.

Although the foregoing interpretation of the isomers of 10 appears most reasonable, there is an alternative explanation that cannot be excluded without further experimentation. That alternative is that the three hydride resonances at -80°C are due to ortho, meta and para tolyl isomers. Thus in the photochemical reaction of $Cp^*Rh(PMe_3)(H)_2$ with toluene at -45°C, Jones et al.[19] found an isomeric distribution of 56% meta, 36% para, 7.6% ortho and less than 1% benzyl isomer. Present toluene experiments using 1 were carried out at ambient temperature, and so are not directly comparable to those of Jones.[19] In view of the lower stability of the p-xylyl derivative of 1 (see below) it is possible that an initially formed ortho-tolyl isomer would be unstable at room temperature with respect to reductive elimination, leading to *meta* or *para* isomers. Certainly, this would be the likely fate of any benzyl isomer at room temperature, in view of the lability of hydridoalkyl derivatives of 1, to be discussed in a later Chapter. Prentice-Hall (PH) models suggest that the *para* isomer would be the most favoured sterically, then *meta*, while the *ortho* isomer would be the least favoured.

The resonances due to the aromatic protons are broad at room temperature while a number of sharp sets of multiplets are found on cooling. Overlap of resonances does not allow assignments of the aromatic protons.

P-xylene as substrate

Irradiation of 1 in p-xylene (*ca*. 3.3 *mM*) at room temperature in an evacuated Pyrex Schlenk tube for *ca*. 25 minutes resulted in *ca*. 90% conversion to complex 11. IR showed complete conversion of 1 to 11 within seven minutes when a N_2 or Ar purge was used during photolysis to prevent the back reaction with released CO (eq. 3-21).

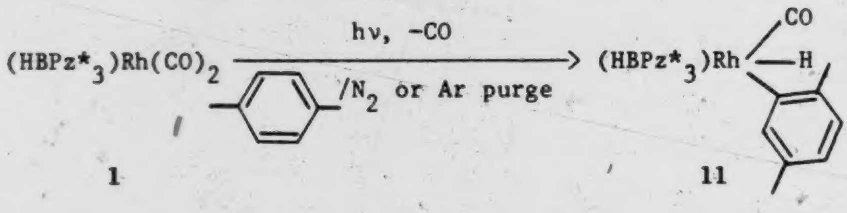

1 11 (3-21)

This is unlike $(HBPz^*_3)Rh(CO)(H)(C_6H_5)$ (**6**), where no appreciable back reaction with released CO was observed and indicates qualitatively the greater lability of the p-xylyl hydride (**11**). In view of its limited stability, the complex 11 was not isolated but converted by reaction with CCl_4 to the stable chloride $(HBPz^*_3)Rh(CO)(Cl)(2,5\text{-}C_6H_3Me_2)$ (12) for characterization.

Compound 12 was isolated as yellow crystalline solid. The IR in n-hexane showed a weak ν_{CO} at 2085 cm^{-1} and a strong ν_{CO} at 2079 cm^{-1}. The ^1H NMR indicated eight methyl resonances, six of them due to the methyls of three nonequivalent pyrazole rings and two due to the methyl groups on the aromatic ring. Two doublets at δ 6.95, 6.73 and a singlet at δ 5.91 were found in the aromatic region.

Additional weak peaks in the ^1H NMR spectrum of 12 clearly indicate the presence of a minor isomer, which by integration of xylyl methyl signals represents ca. 13% of the product. This is consistent with the presence of two ν_{CO} bands in the IR spectrum. The two isomers presumably result from the two different orientations of methyl groups bound to the benzene ring. Sketches of the two conformers are shown in eq. 3-22.

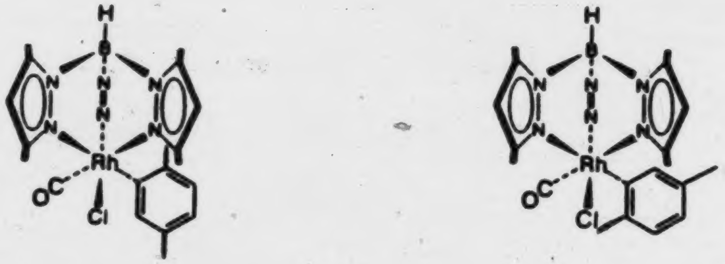

(3-22)

The X-ray crystal structure of $(HBPz^*_3)Rh(CO)(C_2H_5)(C_6H_5)$ (Chapter VI) suggests that the orientation of the phenyl ring would be such as to align it with one of the "grooves" between the pyrazolyl groups. PH models show the crowded surroundings if the _ortho_ methyl on aromatic ring is directed towards the pyrazolylborate ligand. From this it is suggested that the major isomer has the _ortho_ methyl directed away from the pyrazolylborate ligand, while the minor isomer has the other orientation. From the elemental analysis and also from ^{1}H NMR it appears that **12** contains 0.5 mol CH_2Cl_2 as solvent of crystallization. Hydridoaryl complex with methyl substituents close to the metal center appear to be less stable than $(HBPz^*{}_3)Rh(CO)(H)(C_6H_5)$ (**6**), as might be expected.

Para-difluorobenzene as substrate

Irradiation of **1** in para-difluorobenzene (_ca_. 3.3 _mM_) in an evacuated Pyrex Schlenk tube for seven minutes afforded complex **13** according to eq. 3-23 in quantitative yield.

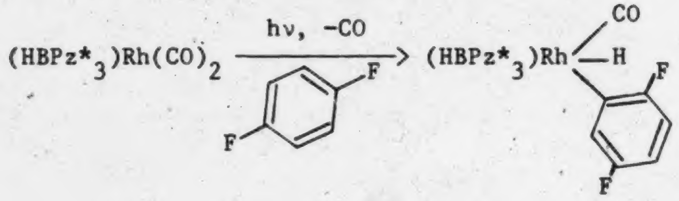

(3-23)

1 **13**

Compound **13** was isolated after chromatography on a Florisil column as colorless crystals, and characterized by the usual spectroscopic methods and elemental analysis. The IR (_n_-hexane) showed a strong ν_{CO} at 2065 cm^{-1} and a weak broad band _ca_. 2080 cm^{-1} assigned as ν_{Rh-H}. The observed IR band positions for this complex are much higher than those of the corresponding hydridophenyl complex (6) (2049 cm^{-1}, 2060 cm^{-1}).

The ^1H NMR of 13 showed the high field resonance at δ-12.31 (dd, $^1J_{Rh-H}$=19.0 Hz, $^3J_{F-H}$=13.0 Hz, 1H), characteristic of rhodium hydride. Three complex multiplets were found in the aromatic region. The six methyl resonances are consistent with the three nonequivalent pyrazole rings in the octahedral geometry. The $\{^1H\}$ ^{19}F NMR indicated two nonequivalent fluorines which appeared as a doublet and a triplet.

Compound 13 is more robust than the unsubstituted phenyl hydride 6; for example, 13 is readily chromatographed. A more detailed study of the stability of 13, such as the barrier to reductive elimination of p-$C_6H_4F_2$, has not yet been carried out, although it would certainly be of interest.

Section 4

MECHANISM OF C-H ACTIVATION - SOME SPECULATION

Judging from carbonyl stretching frequencies, the electron richness of 1 (ν_{CO} 2055, 1981 cm^{-1} in n-hexane) is similar to that of (η^5-C_5H_5)Rh$(CO)_2$ (ν_{CO} 2049, 1986 cm^{-1} in n-hexane); the averages of the band pairs are identical. In this context, it will be interesting to compare ultraviolet-visible (UV-VIS) spectral data of 1 with those of other compounds which have been known previously to activate C-H bonds. Such a comparison is shown in Table 3.II.

Table 3.II UV-VIS spectral data

Compound	Solvent	λ_{max}, nm (ε)
(HBPz*$_3$)Rh$(CO)_2$	n-hexane	221 (17600), 353 (1820)
(η^5-C_5Me_5)Ir$(CO)_2$	n-hexane	220 (13000), 290 (5500)
(η^5-C_5Me_5)Ir$(PMe_3)(H)_2$	cyclohexane	259 (1600)[17]

The ability of (HBPz*$_3$)Rh$(CO)_2$ (**1**) to function with near UV light presumably results from the position of its lowest energy electronic absorption band at 353 nm. High quantum efficiency is also necessary for response to the much less intense incandescent and daylight sources. Surprisingly, there is some flux from an incandescent tungsten lamp even at 350 nm.[28] Although the origin of this efficiency is not yet clear, it is tempting to speculate that it may involve facile tridentate-bidentate interconversions of the tris(pyrazolyl)borate ligand.

The previously reported examples of intermolecular C-H activation reactions cited in the introductory section of this Chapter have usually been considered to result from the oxidative addition of the 16-electron coordinatively unsaturated metal fragments $[ML_n]$, generated by the photochemically induced loss of H_2 or CO, into C-H bonds of hydrocarbons as shown below.

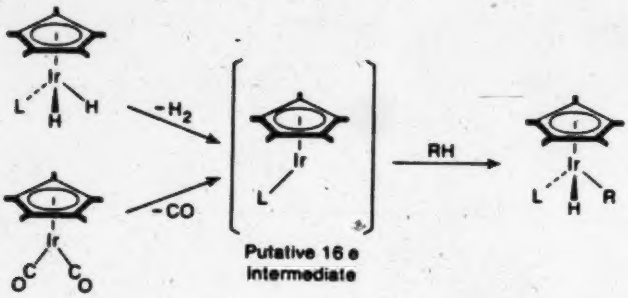

This point has not been settled however. Recent results of Marx and Lees[35] on $(\eta^5-C_5H_5)Ir(CO)_2$ appear to favor $\eta^5 \rightarrow \eta^3$ ring slippage, rather than CO dissociation, as the initial photochemical step. Also very recently, Bloyce et al.[29,36] reported work on C-H activation by $(\eta^5-C_5H_5)Ir(CO)(D)_2$ which were difficult to reconcile with D_2 loss as the only photochemical process.

Similarly, the photochemical process for $(HBPz^*_3)Rh(CO)_2$ could involve either CO ejection or "slippage" of the trispyrazolylborate ligand. If it is the latter, $\eta^3 \rightarrow \eta^1$ is more attractive than $\eta^3 \rightarrow \eta^2$, because ground state $(\eta^2-HBPz^*_3)Rh(CO)(L)$ complexes (Chapters II and VI) are not reactive to hydrocarbons at 25°C without irradiation. A reaction scheme based on a 14-electron $(\eta^1-HBPz^*_3)$ intermediate is shown in eq. 3-24.

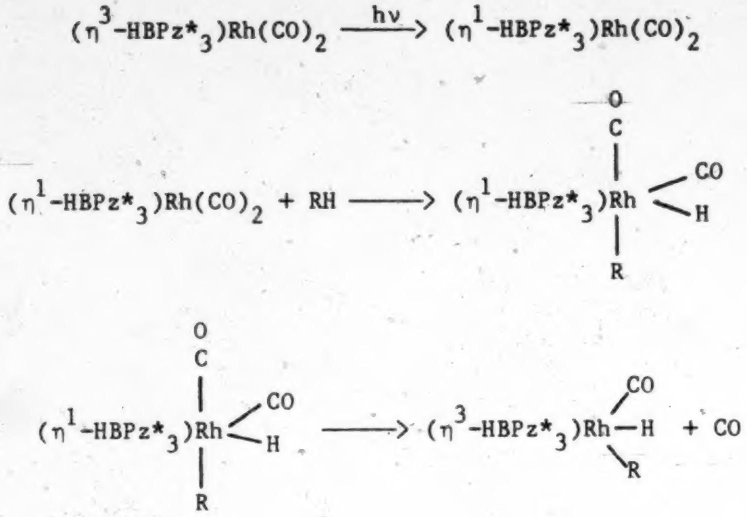

$$(\eta^3\text{-HBPz}^{*}_3)\text{Rh(CO)}_2 \xrightarrow{h\nu} (\eta^1\text{-HBPz}^{*}_3)\text{Rh(CO)}_2$$

$$(\eta^1\text{-HBPz}^{*}_3)\text{Rh(CO)}_2 + \text{RH} \longrightarrow (\eta^1\text{-HBPz}^{*}_3)\underset{\text{R}}{\overset{\text{OC}}{\text{Rh}}}{<}^{\text{CO}}_{\text{H}}$$

$$(\eta^1\text{-HBPz}^{*}_3)\underset{\text{R}}{\overset{\text{OC}}{\text{Rh}}}{<}^{\text{CO}}_{\text{H}} \longrightarrow (\eta^3\text{-HBPz}^{*}_3)\text{Rh}(\text{CO})(\text{H})(\text{R}) + \text{CO}$$

(3-24)

Section 5

CHEMICALLY ASSISTED C-H ACTIVATION

Introduction

As discussed at the beginning of this Chapter, ultraviolet or visible light has been utilized in most cases for intermolecular C-H activation. The role of the photon (hν) is to generate a coordinatively unsaturated, highly reactive intermediate. Carbon-hydrogen activation products are considered to result from insertion of this reactive intermediate into the C-H bonds of hydrocarbons.

From the standpoint of large scale industrial applications, it would be desirable to find alternatives to photochemistry in C-H activation. One approach would be to use a chemical reagent to remove a ligand by converting it to a new and weakly binding species. Hawthorne et al.[30] introduced the use of arylnitrile oxides, $Ar\overset{+}{C}{=}N{-}O^{-}$ (one of the class of 1,3-dipolar reagents[31]) to remove a CO ligand from a relatively electron rich complex. They recently[32,33] applied these reagents to chemically and thermally induce benzene activation by $Cp^{*}Ir(CO)_2$ as shown in eq. 3-25.

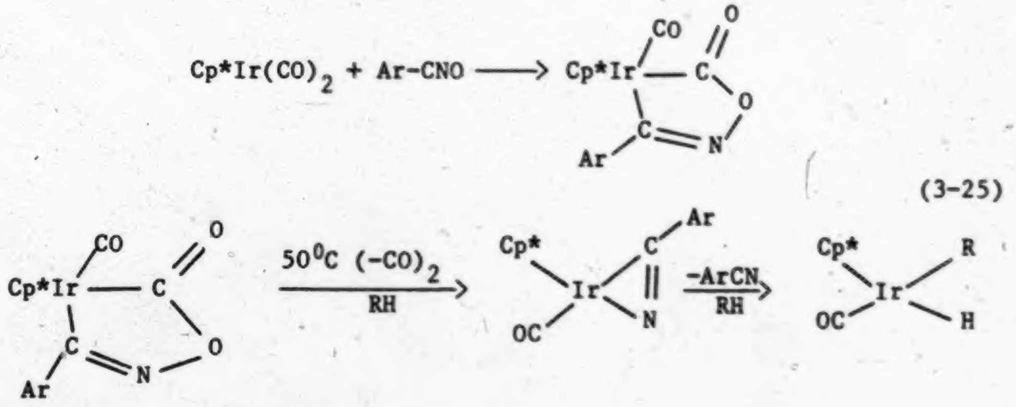

(3-25)

Following the initial report on the use of arylnitrile oxides for CO removal, Dr. C.F. Barrientos in this Laboratory also explored their use with $Cp^*Ir(CO)_2$ to achieve C-H activation.[34] He also successfully used a readily available 1,3-dipolar reagent, nitrous oxide, $:\overset{+}{N} = \ddot{N} - \underset{\cdot\cdot}{\ddot{O}}:^{-}$ in the 60-80°C temperature range to induce benzene activation by $Cp^*Ir(CO)_2$.[34]

It was accordingly of interest to explore N_2O as a reagent in inducing C-H activation in the pyrazolylborate system. The results are described in this section.

Nitrous oxide induced benzene activation

Chemically induced arene C-H activation was achieved when a benzene solution of $(HBPz^*_3)Rh(CO)_2$ (**1**) (2.19 m$\underline{M}$) was purged with nitrous oxide at room temperature in the dark as shown in eq. 3-27.

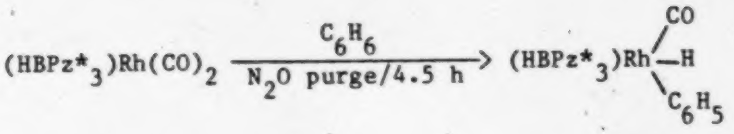

$$(HBPz^*_3)Rh(CO)_2 \xrightarrow[N_2O\ purge/4.5\ h]{C_6H_6} (HBPz^*_3)Rh\begin{smallmatrix}CO\\ -H\\ C_6H_5\end{smallmatrix} \qquad (3\text{-}27)$$

1 **6**

The conversion of 1 to hydridophenyl complex (**6**) was complete in 4.5 h. Judging from the IR carbonyl stretching frequency intensities of 1 and 6 and assuming that the extinction coefficient of ν_{CO} in the compounds are similar, it appeared that the conversion of 1 to 6 was quantitative. This is the first example of chemically induced C-H activation at room temperature. For comparison it is worth noting that $(\eta^5\text{-}C_5Me_5)Ir(CO)(\eta^2\text{-}NCC_6H_4Cl)$ activated benzene at 50°C in 90% yield after five weeks.[32]

Cyclohexane activation using nitrous oxide

After nitrous oxide induced benzene activation, it was of interest to attempt activation of sp^3 C-H bonds. Thus a cyclohexane (Ultrapure) solution of 1 (ca. 2.0 mM) was purged with N_2O at room temperature in the dark. At an early stage of the reaction, the IR showed ν_{CO} at 2028 cm^{-1} presumed to be due to $(HBPz*_3)Rh(CO)(H)(C_6H_{11})$ (**17**), although the short-lived **17** (Chapter III) converted to the hydridophenyl complex (**6** with the progress of the reaction. After seven hours of N_2O purge, no starting material was left. Judging from the IR band intensities, the yield of **6** was ca. 30%. The conversion of **17** to **6** is an interesting but a complicated phenomenon, which will be discussed in Chapter III. The presence of **17**, at the initial stage of reaction, and of **6** indicated N_2O induced cyclohexane activation.

Possible mechanism

The anticipated reaction with nitrous oxide is shown in eq. 3-28.

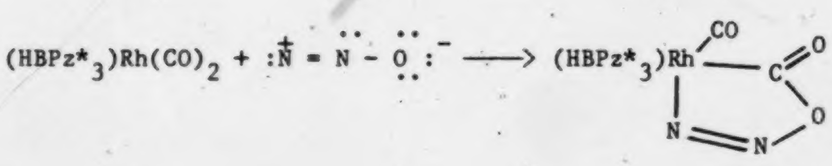

(3-28a)

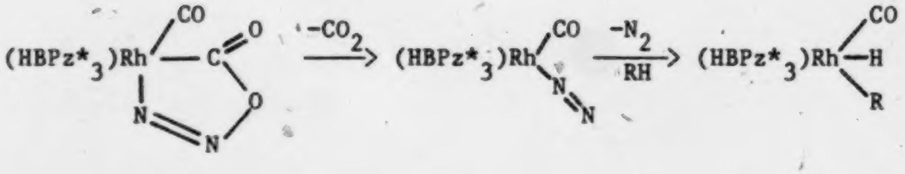

(3-28b)

The metallacycle in eq. (3-28a) is not expected to be stable because of the formation of two very stable products, CO_2 and N_2 on decomposition. The CO_2 by-product was detected by passing the effluent gases during the reaction through $Ba(OH)_2$ solution. This observation supports the formation of the intermediate metallacycle (eq. 3-28a). The intermediate dinitrogen complex (eq. 3-28b), if formed at all, is expected to lose N_2 readily to generate the reactive intermediate for C-H activation.

Section 6

EXPERIMENTAL

General

In irradiation experiments, degassed solutions in closed Pyrex Schlenk tubes were placed approximately 2 cm from a Hanovia 450-W medium pressure mercury lamp fitted with a cylindrical Pyrex filter and a water-cooled quartz jacket.

Preparation of $(HBPz^*_3)Rh(CO)(H)(C_6H_5)$ (6)

When a yellow degassed solution of 1 (120 mg, 0.263 mmol) in benzene (50 mL) was irradiated for 12 min, the solution had become colorless and the IR indicated complete conversion to the hydridophenyl complex **6**. Removal of solvent under reduced pressure afforded an analytically pure off-white solid (125 mg, 94%). A trace amount of free benzene was found in the ^{1}H NMR spectrum of **6**. Cooling the *n*-hexane solution of **6** at -20°C under a nitrogen atmosphere yielded colorless crystalline material (99.7 mg, 75%).

Characterization: IR (*n*-hexane) 2060 cm^{-1} (w, br, ν_{Rh-H}), 2049 cm^{-1} (s, ν_{CO}). MS (FAB, Cleland matrix) M^+ (506), M^+-CO. ^{1}H NMR (CD_2Cl_2, ambient, 200 MHz) δ 7.6-6.4 (br, 5H), 5.90 (s, 1H), 5.86 (s, 1H), 5.76 (s, 1H), 2.50 (s, 3H), 2.44 (s, 3H), 2.41 (s, 3H), 2.36 (s, 3H), 1.92 (s, 3H), 1.57 (s, 3H), -12.31 (d, J_{Rh-H}=21.3 Hz, 1H); Phenyl region (-20°C, 400 MHz) δ 7.59 (d, *o*-H), 7.04 (t, *m*-H), 6.94 (t, *p*-H), 6.79 (t, *m'*-H, 6.49 (d, *o'*-H).

$\{^1H\}$ ^{13}C NMR (CD_2Cl_2, -20°C, 100.6 MHz)

CO (δ)	3,5-C of Pz (δ)	4-C of Pz (δ)	Ar-C (δ)	MeC of Pz (δ)
189.7 (d,	150.58	105.88	145.94	14.64
J=66.4 Hz)	149.74	105.77	(d,J=26.5 Hz)	13.87
	149.63	105.34	142.61	12.76
	144.58		137.46	12.36
	144.22		127.06	
	143.97		126.30	
			122.56	

Anal. Calcd for $C_{22}H_{28}BN_6ORh$: C, 52.17; H, 5.58; N, 16.61. Found: C, 52.55; H, 5.97; N, 15.73.

Arene exchange reactions

A solution of 6 (20 mg, 0.040 mmol) in benzene-d_6 (0.5 mL) along with hexamethyldisiloxane (1 μL, 0.005 mmol) was transferred to an NMR tube fitted with a vacuum adaptor. After three cycles of freeze-thaw, degassing, the NMR tube was sealed off under vacuum. A ^1H NMR spectrum was recorded to determine the relative intensity of hexamethyldisiloxane and hydride resonance of 6. A relaxation delay of 20 sec. was used.

The NMR tube was immersed in a bath (Lauda RK 20) at a specified temperature and periodically removed to record ^1H NMR spectra. The rate of disappearance of 6 was followed by monitoring the rate of disappearance of the hydride resonance against the internal standard (hexamethyldisiloxane).

Preparation of (HBPz*$_3$)Rh(CO)(Cl)(C_6H_5) (7)

To a stirred solution of **6** (80 mg, 0.158 mmol) in CH_2Cl_2 (30 mL), CCl_4 (4 mL) was added. The initially pale yellow solution became greenish-yellow. After 1.5 h of stirring IR indicated complete conversion of **6**. Solvent was removed under reduced pressure, the resulting light yellow solid dissolved in CH_2Cl_2 and was chromatographed on a Florisil column (10 x 2.5 cm) eluting with CH_2Cl_2. Solvent was removed, solid was dissolved in a minimum volume of dichloromethane and _n_-hexane added to it. Cooling the solution to -20°C afforded yellow crystals of 7 (68.5 mg, 80%).

Characterization: IR (_n_-hexane) 2086 cm^{-1} (s, ν_{CO}). MS (110°C, 70 eV) M^+ (540), $M^+-C_6H_5Cl$, $M^+-C_6H_5Cl-CO$. ^1H NMR (CD_2Cl_2, ambient, 200 MHz) δ 7.88 (d, _o_-H), 7.17 (t, _m_-H), 7.03 (t, _p_-H), 6.81 (t, _m_'-H), 6.20 (d, o'-H), 5.91 (s, 1H), 5.83 (s, 1H), 5.79 (s, 1H), 2.59 (s, 3H), 2.44 (s, 3H), 2.43 (s, 3H), 2.42 (s, 3H), 1.66 (s, 3H), 1.65 (s, 3H). Anal. Calcd for $C_{22}H_{27}BClN_6ORh$: C, 48.49; H, 5.00; N, 15.56. Found: C, 48.07; H, 5.03; N, 14.77.

Preparation of (HBPz*$_3$)Rh(CO)(C_6H_5)(D) (8b)

To a stirred solution of 7 (20 mg, 0.037 mmol) in methanol-d_4 (20 mL) at room temperature was added zinc dust (200 mg, 3.06 mmol) and glacial acetic acid-d_4 (0.20 mL, 0.210 mg, 3.50 mmol). The solution was stirred for 0.5 h and filtered. Hexane (10 mL) was added, followed by slow addition of water (ca. 100 mL). The mixture was shaken vigorously and after settling, the lower aqueous layer was removed. The remaining hexane solution was washed with water (3 x 100 mL) and then dried over anhydrous sodium sulfate for 0.5 h. Removal of solvent under reduced pressure yielded colorless solid (**8b**).

Reaction of $(HBPz^*_3)Rh(CO)(H)(C_6H_5)$ (6) with CO

Compound **6** (40 mg, 0.079 mmol) was taken up n-hexane (40 mL) and divided into two parts. One part (ca. 20 mL) of the above stock solution was saturated with one atm. CO pressure in a pop bottle and stirred at room temperature. The rate of disappearance of **6** was monitored qualitatively by IR. The second part (ca. 20 mL) of the stock solution was pressurized with 4 atm. CO in another pop bottle and stirred at room temperature. The progress of the reaction was monitored qualitatively by IR.

At room temperature and 1 atm. CO pressure, the absorbance of the 2049 cm^{-1} band (ν_{CO} of **6**) varied as follows: start, 1.04; 5h, 0.79; 16.5 h, 0.58; 24 h, 0.48; 30 h, 0.43; 40 h, 0.25.

At room temperature and 4 atm. CO pressure, the absorbance of the 2049 cm^{-1} varied as follows: 5h, 0.54; 16.5 h, 0.32; 24 h, 0.18.

Preparation of $(HBPz^*_3)Rh(CO)(CH_3)(C_6H_5)$ (9)

Excess ethereal CH_2N_2 was added to a stirred solution of **6** (150 mg, 0.296 mmol) in n-hexane (100 mL) at 0°C. Reaction was complete in 45 min. Removal of solvent yielded a pale yellow solid which was dissolved in CH_2Cl_2 and chromatographed on a Florisil column (8 x 2.5 cm). Elution with dichloromethane and hexane (1:1) afforded a colorless solid after removal of solvent. Recrystallization from CH_2Cl_2-hexane at -20°C afforded a colorless crystalline solid (120 mg, 78%) of **9**.

Characterization: IR (*n*-hexane) 2045 cm^{-1} (ν_{CO}). MS (130°C, 16 eV) M^+ (520), M^+-CH_3, $M^+-CH_3-C_6H_5$, $M^+-CH_3-C_6H_5-CO$. ^1H NMR (CD_2Cl_2, ambient, 200 MHz), δ 7.40 (d, *o*-H), 7.10 (t, *m*-H), 6.94 (t, *p*-H), 6.74 (t, *m*'-H), 6.51 (d, *o*'-H), 5.86 (s, 1H), 5.79 (s, 1H), 5.75 (s, 1H), 2.44 (s, 6H *coincidental* overlap), 2.42 (s, 3H), 2.40 (s, 3H), 1.72 (s, 3H), 1.52 (s, 3H), 1.29 (d, $^2J_{Rh-H}$=2.1 Hz, 3H). Anal. Calcd for $C_{23}H_{30}BN_6ORh$: C, 53.07; H, 5.77; N, 16.15. Found: C, 53.54; H, 6.01; N, 15.78.

Preparation of $(HBPz^*_3)Rh(CO)(H)[p-C_6H_4(CH_3)]$ (10)

Photolysis of 1 (127.2 mg, 0.279 mmol) in toluene (35 mL) in an evacuated Pyrex vessel for 15 min. yielded cleanly hydridotolyl complex (**10**). Removal of solvent under reduced pressure resulted in an analytically pure colorless solid.

Characterization: IR (*n*-hexane) 2060 cm^{-1} (w, br, ν_{Rh-H}), 2048 cm^{-1} (s, ν_{CO}). MS (195°, 16 eV) 856, assigned as $[(HBPz^*_3)Rh(CO)]_2^+$; M^+ not observed. ^1H NMR (CD_2Cl_2, ambient, 200 MHz) δ 7.5-6.2 (br, 4H), 5.86 (s, 1H), 5.82 (s, 1H), 5.72 (s, 1H), 2.48 (s, 3H), 2.42 (s, 3H), 2.38 (s, 6H *coincidental* overlap), 2.34 (s, 3H), 1.91 (s, 3H), 1.54 (s, 3H), -12.41 (d, J_{Rh-H}=21.2 Hz), -12.44 (d, J_{Rh-H}=21.2 Hz) [Two sets of hydride resonance integrate to 1H], phenyl region (CD_2Cl_2, -80°C, 400 MHz), δ 7.4-6.2 sharp sets of complex multiplets, hydride region: δ -12.39 (d, J_{Rh-H}=21.4 Hz), -12.40 (d, J_{Rh-H}=21.4 Hz), -12.43 (d, J_{Rh-H}=21.4 Hz). Anal. Calcd for $C_{23}H_{30}BN_6ORh$: C, 53.08; H, 5.77; N, 16.15. Found: C, 53.26; H, 5.82; N, 15.09.

Preparation of (HBPz*$_3$)Rh(CO)(2,5-$C_6H_3Me_2$)(Cl) (12)

Compound 1 (60 mg, 0.132 mmol) in p-xylene (40 mL) was irradiated for 7 min under a nitrogen purge. The solution became colorless, indicating formation of the Rh(III) complex was complete. The lamp was extinguished, and excess CCl_4 (3 mL) was added and allowed to react for ca. 1 h. Solvent was removed under reduced pressure and the resulting yellow solid dissolved in CH_2Cl_2 and was chromatographed on a neutral-alumina column (8 x 2.5 cm) with CH_2Cl_2 elution. Recrystallization from a minimum volume of CH_2Cl_2 and hexane at -20°C over five days afforded the product as a yellow crystalline solid (55 mg, 74%).

Characterization: IR (n-hexane) 2085 cm^{-1} (w, ν_{CO}), 2079 cm^{-1} (s, ν_{CO}). MS (130°C, 70 eV) M^+ (568), M^+-Cl, M^+-Cl-2CH_3, M^+-Cl-2CH_3-C_6H_3, M^+-Cl-2CH_3-C_6H_3-CO. ^1H NMR (CD_2Cl_2, ambient, 200 MHz) major isomer: δ 6.95 (d, 1H), 6.73 (d, 1H), 5.91 (s, 1H), 5.83 (s, 1H), 5.80 (s, 2H, coincidental overlap), 2.93 (s, 3H), 2.64 (s, 3H), 2.49 (s, 3H), 2.46 (s, 3H), 2.44 (s, 3H), 1.87 (s, 3H), 1.74 (s, 3H), 1.59 (s, 3H); minor isomer: most peaks of the minor isomer were not resolved, but methyl signals at δ 1.82 and δ 1.76 integrating ca. 13% of products are assigned to it. Anal. Calcd for $C_{24}H_{31}BClN_6ORh \cdot 0.5\ CH_2Cl_2$: C, 48.11; H, 5.24; N, 13.75. Found: C, 48.10; H, 5.78; N, 13.37.

Preparation of (HBPz*$_3$)Rh(CO)(H)($C_6H_3F_2$) (13)

Irradiation of 1 (15 mg, 0.033 mmol) in paradifluorobenzene (10 mL) in an evacuated Pyrex Schlenk tube for 7 min produced a colorless solution of 13. The IR indicated a quantitative conversion. Solvent was removed under reduced pressure and the resulting colorless solid dissolved in CH_2Cl_2 and chromatographed on a Florisil column (8 x 2.5 cm). Elution with 1:1 CH_2Cl_2-hexane and crystallization from the minimum volume of hexane, maintaining the solution at -20°C over a period of two days, afforded 13 as colorless crystals (14 mg, 79%).

Characterization: IR (n-hexane) 2080 (w, br, ν_{Rh-H}), 2065 cm^{-1} (s, ν_{CO}). MS (180°C, 16 eV) m/e 556, 527, 513, 428, 400 etc. The MS of 13 was anomalous, not showing the anticipated molecular ion (at 542). A puzzling feature was a significant peak at 556. ^1H NMR (CD_2Cl_2, ambient, 200 MHz) δ 6.72 (m, 1H), 6.54 (m, 1H), 6.05 (m, 1H), 5.78 (s, 1H), 5.75 (s, 1H), 5.64 (s, 1H), 2.38 (s, 3H), 2.31 (s, 3H), 2.28 (s, 3H), 2.27 (s, 3H), 1.76 (s, 3H), 1.42 (s, 3H), -12.31 (dd, J=19.0 Hz, J=13.0 Hz, 1H). ^{19}F NMR (CD_2Cl_2) δ 65.52 (t, 1F), 36.31 (d, 1F). Anal. Calcd for $C_{22}H_{26}BF_2N_6ORh$: C, 48.71; H, 4.80; N, 15.50. Found: C, 48.71; H, 4.98; N, 14.60.

Nitrous oxide induced activations

Benzene activation

Dicarbonyl 1 (20 mg, 0.044 mmol) was dissolved in benzene (20 mL). The IR spectrum was recorded and the solution placed in a Pyrex purged vessel which was wrapped with Al-foil and a continuous purge of nitrous oxide from the tank (Matheson) was maintained. The reaction was monitored by taking IR. After 4.5 h the IR showed disappearance of 1 and indicated the formation of $(HBPz*_3)Rh(CO)(H)(C_6H_5)$ (**6**).

Cyclohexane activation

A sample of 1 (30 mg, 0.066 mmol) was taken up in ultrapure cyclohexane (30 mL). The IR of the resulting solution was recorded. The solution was placed in a foil-wrapped purged vessel and purged with N_2O at room temperature. After 20 min. the IR examination of the reaction mixture exhibited a new ν_{CO} band at 2028 cm^{-1} presumed to be due to $(HBPz^*_3)Rh(CO)(H)(C_6H_{11})$ (**17**). With time, the band at 2028 cm^{-1} slowly disappeared and at the same time a new band at 2048 cm^{-1} started growing, which is assigned to $(HBPz^*_3)Rh(CO)(H)(C_6H_5)$ (**6**). The IR indicated complete disappearance of 1 in 7 h. At the end of the reaction the IR showed mostly **6** and a small amount of $(HBPz^*_3)Rh(CO)(H)_2$ (**14**).

Detection of CO_2

Nitrous oxide was bubbled through solvent benzene at room temperature in the dark and the effluent gas was allowed to pass through $Ba(OH)_2$ solution for 4.5 h. No significant change in the $Ba(OH)_2$ solution was observed.

A solution of 1 (25 mg, 0.055 mmol) in benzene (20 mL) was purged with N_2O in a foil-wrapped Pyrex vessel and the effluent gases were passed through $Ba(OH)_2$ solution. The $Ba(OH)_2$ solution had become cloudy with the progress of reaction. At the end, white precipitate in the $Ba(OH)_2$ solution was observed. This suggests the presence of CO_2 in the effluent gases.

References for Chaper III

1. (a) R.H. Crabtree, Chem. Rev., 85 (1985) 245.
   (b) M.L.H. Green and D. O'Hare, Pure and Appl. Chem., 57 (1985) 1897.
2. (a) A.J. Kresge, M. Dubeck and H.C. Brown, J. Org. Chem., 32 (1967) 745.
   (b) H.C. Brown and C.W. McGary Jr., J. Am. Chem. Soc., 77 (1955) 2300.
   (c) H.C. Brown and R.A. Wirkkala, J. Am. Chem. Soc., 88 (1966) 1447.
3. A. McKillop and E.C. Taylor, Adv. Organomet. Chem., 11 (1973) 147.
4. D.R. Harvey and R.O.C. Norman, J. Chem. Soc., (1964) 4860.
5. (a) J.L. Garnett and W.A. Sollich-Baumgartner, Adv. Catal., 16 (1966) 95.
   (b) D.E. Webster, Adv. Organomet. Chem., 15 (1977) 147.
6. F.R.S. Clark, R.O.C. Norman, C.B. Thomas and J.S. Willson, J. Chem. Soc., Perkin Trans., 1 (1974) 1289.
7. Y. Aoyama, T. Yoshida, K. Sakurai and H. Ogoshi, Organometallics, 5 (1986) 168.
8. (a) G.W. Parshall, Catalysis (London) 1 (1977) 335.
   (b) G.M. Parshall, "Homogeneous Catalysis", Wiley Interscience, New York, 1980.
9. S. Horiie and S. Murahashi, Bull. Chem. Soc., 33 (1960) 247.
10. J.P. Kleiman and M. Dubeck, J. Am. Chem. Soc., 85 (1963) 1544.
11. M.A. Bennett and D.L. Milner, J. Am. Chem. Soc., 91 (1969) 6983.
12. (a) W.D. Jones and F.J. Feher, J. Am. Chem. Soc., 104 (1982) 4240.
    (b) W.D. Jones and F.J. Feher, J. Am. Chem. Soc., 107 (1985) 620.

13. J. Chatt and J.M. Davidson, J. Chem. Soc., (1965) 843.

14. (a) C. Giannotti and M.L.H. Green, J. Chem. Soc., Chem. Commun., (1972) 1114.

    (b) M. Berry, K. Elmitt and M.L.H. Green, J. Chem. Soc., Dalton Trans., (1979) 1950.

15. M.D. Rausch, R.G. Gastinger, S.A. Gardner, R.K. Brown and J.S. Wood, J. Am. Chem. Soc., 99 (1977) 7870.

16. J.K. Hoyano and W.A.G. Graham, J. Am. Chem. Soc., 104 (1982) 3723.

17. A.H. Janowicz and R.G. Bergman, J. Am. Chem. Soc., 105 (1983) 3929.

18. J.P. Collman, L.S. Hegedus, J.R. Norton and R.G. Finke, "Principles and Applications of Organotransition Metal Chemistry", Univ. Science Books, California, (1987) P300.

19. W.D. Jones and F.J. Feher, J. Am. Chem. Soc., 106 (1984) 1650.

20. A.H. Janowicz and R.G. Bergman, J. Am. Chem. Soc., 104 (1982) 352.

21. A.J. Rest, I. Whitwell, W.A.G. Graham, J.K. Hoyano and A.D. McMaster, J. Chem. Soc., Chem. Commun., (1984) 624.

22. (a) A.H. Janowicz, R.A. Periana, J.M. Buchanan, C.A. Kovac, J.M. Stryker, M. J. Wax and R.G. Bergman, Pure and Appl. Chem., 56 (1984) 13.

    (b) J.M. Buchanan, J.M. Stryker and R.G. Bergman, J. Am. Chem. Soc., 108 (1986) 1537.

23. S. Trofimenko, Prog. Inorg. Chem., 34 (1986) 115.

24. C.K. Ghosh and W.A.G. Graham, J. Am. Chem. Soc., 109 (1987) 4726.

25. (a) R.A. Michelin, S. Faglia, P. Uguagliati, Inorg. Chem., 22 (1983) 1831.

    (b) S.J. Okrasinski and J.R. Norton, J. Am. Chem. Soc., 99 (1977) 295.

(c) S.D. Ittel, C.A. Tolman, A.D. English and J.P. Jesson, ibid, 100 (1978) 7577.

26. H. van der Heijden, A.G. Orpen and P. Pasman, J. Chem. Soc., Chem. Commun., (1985) 1576.

27. W.D. Jones and F.J. Feher, Inorg. Chem., 23 (1984) 2376.

28. L.R. Koller, Ultraviolet Radiation, 2nd Ed., Wiley, New York, (1965) P99.

29. P.E. Bloyce, Ph.D. Thesis, University of Southampton, Chapter 3 (1988).

30. J.A. Walker, C.B. Knobler, M.F. Hawthorne, J. Am. Chem. Soc., 105 (1983) 3370.

31. R. Huisgen, Angew. Chem. Int. Ed. Eng., 2 (1963) 565.

32. P.A. Chetcuti and M.F. Hawthorne, J. Am. Chem. Soc., 109 (1987) 942.

33. P.A. Chetcuti, C.B. Knobler and M.F. Hawthorne, Organometallics, 7 (1988) 650.

34. W.A.G. Graham, Final Report to Alberta Energy Co. Ltd. on Contract Research, University of Alberta, April, 1987.

35. D.E. Marx and A.G. Lees, Inorg. Chem., 27 (1988) 1121.

36. P.E. Bloyce, A.J. Rest, I. Whitwell, W.A.G. Graham and R. Holmes-Smith, J. Chem. Soc., Chem. Commun., (1988) 846.

CHAPTER IV

ALKANE C-H ACTIVATION

Section 1

INTRODUCTION

General

Saturated hydrocarbons are potentially attractive feed-stocks for the synthesis of organic compounds. They are major constituents of natural gas, petroleum, and coal liquefaction processes. A major problem lies in the chemical inertness of alkanes. Thus activation of carbon-hydrogen bonds homogeneously and under mild conditions by transition metal catalysts would be of great interest to the petrochemical industries.

The unreactive character of alkanes is attributed to the unavailability of both lone pairs and empty orbitals at accessible energies. Carbon and hydrogen both have a number of valence electrons equal to the number of valence orbitals available. The strong bonding between carbon and hydrogen (90-100 kcal mol^{-1}) is consistent with the fact that the HOMO's are deep lying σ bonding orbitals and the LUMO's are high lying σ^* antibonding orbitals.[1] Neither of them is easily accessible to an attacking reagent.

In this respect, the problem of activation of C-H bonds in saturated hydrocarbons is similar to that of activation of hydrogen, where the cleavage of the strong H-H σ bond is required. However, many metal complexes are known to activate H_2. Formation of M-H (M stands for metal) bonds is considered as an intermediate step in the process of activation of hydrogen with metal complexes.[2] Shilov and co-workers[3] in 1977 suggested that the strength of M-C bonds was only slightly lower than that of M-H bonds,[4] so that activation of C-H bonds by oxidative addition should be thermodynamically possible. More recently, Halpern[5] has stressed that the relative weakness of metal-alkyl bonds may place a thermodynamic constraint upon the process. From the comparison of physico-chemical properties of alkanes and molecular hydrogen it was proposed[3] that saturated hydrocarbons are "less vulnerable" to a chemical attack than H_2. It is presumed that the latter refers to kinetic barriers.

Since 1982 there have been tremendous advances in the stoichiometric activation of alkanes by oxidative addition reactions. These include the first *direct* observations of R-H (R stands for alkyl) oxidative addition and activation of methane.

Historical

During 1960's the oxidative addition reaction in which low-valent metal complexes were shown to insert into a variety of X-Y bonds (XY = H_2, HCl, MeI, R_3Si-H, Cl_2 etc.) (eq. 4-1), prompted interest in the alkane activation problem.

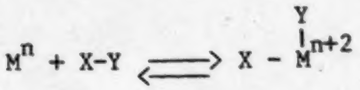

$$M^{n} + X\text{-}Y \rightleftharpoons X - \overset{\overset{\displaystyle Y}{|}}{M}{}^{n+2} \qquad (4\text{-}1)$$

The widespread occurrence of cyclometallation (discussed in Chapter III) raised the possibility that alkane activation might be possible. The first example of cyclometallation of sp^3 C-H bond was reported in 1965 by Chatt and Davidson[6] (eq. 4-2).

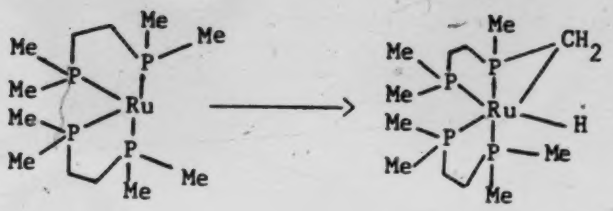
Me
Me
Me
Me
Me
Me
Me
Me
P
P
P
P
Ru
CH2
H

(4-2)

Cotton[7] later showed crystallographically that the cyclometallated form of Ru(dmpe)$_2$ is a dimer of the type shown in eq. 4-3.

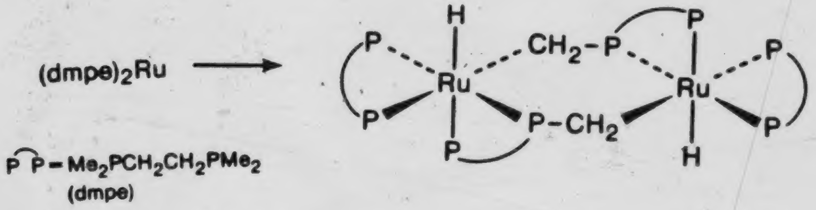
(dmpe)2Ru
P P = Me2PCH2CH2PMe2
(dmpe)
H
P
P
P
Ru
CH2-P
P-CH2
Ru
P
P
P
H

(4-3)

In the late 1960's and early 1970's it was demonstrated that certain platinum salts, in the presence of acids, could be used to effect H-D exchange (eq. 4-4), first in aromatic compounds and then in alkanes.[8]

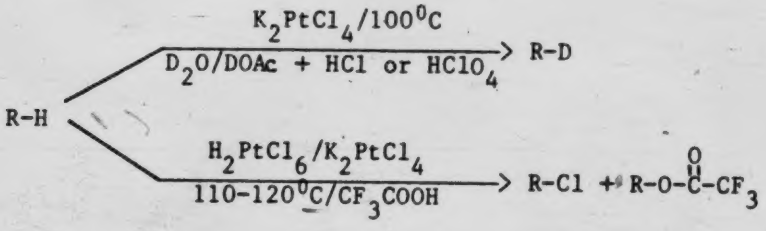
K2PtCl4/100°C
D2O/DOAc + HCl or HClO4
R-D
R-H
H2PtCl6/K2PtCl4
110-120°C/CF3COOH
R-Cl + R-O-C(=O)-CF3

(4-4)

This result is not straightforward, and some considered that it might involve heterogeneous catalysis by platinum metal particles.

Following the report by Chatt and Davidson, a number of examples of intramolecular alkane C-H activation appeared.[9] For example Foley and Whitesides[9a] reported the cleavage of a C-H bond in dineopentyl bis(triphenylphosphine) platinum (II) (eq. 4-5). Shaw et al.[9b] observed intramolecular C-H activation during reaction of $IrCl_3$ with $(t\text{-}Bu)_2P\text{-}(CH_2)_5\text{-}P(t\text{-}Bu)_2$ eq. (4-6).

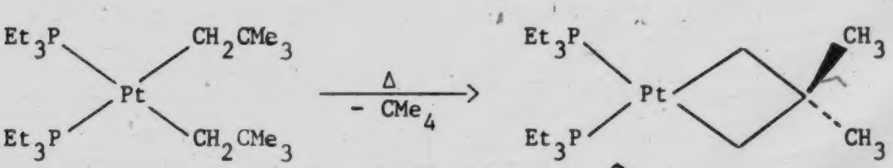
Et_3P
Et_3P
Pt
CH_2CMe_3
CH_2CMe_3
Δ
- CMe_4
Et_3P
Et_3P
Pt
CH_3
CH_3

(4-5)

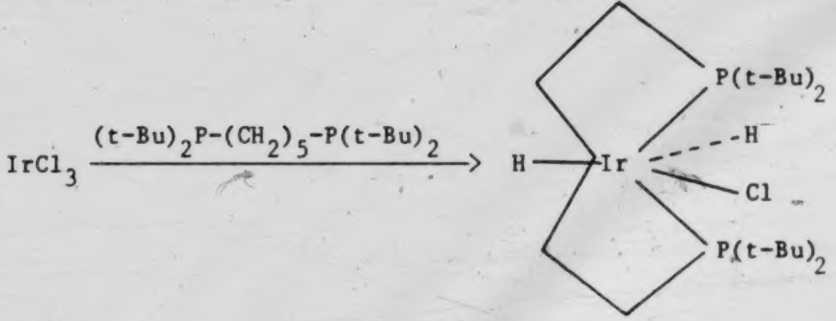
$IrCl_3$
$(t\text{-}Bu)_2P\text{-}(CH_2)_5\text{-}P(t\text{-}Bu)_2$
H
Ir
H
Cl
$P(t\text{-}Bu)_2$
$P(t\text{-}Bu)_2$

(4-6)

The incidence of examples of intramolecular C-H activation led to the suggestion that entropy played a major role in the difference between intra- and intermolecular oxidative addition reactions.[9a]

The search for direct intermolecular C-H oxidative addition had been frustrating. A few relatively electron-rich complexes were known to undergo insertion into C-H bonds activated by adjacent functional groups (eq. 4-7 and 4-9). The metal centers in these complexes reacted more readily with the C-H bonds in their own ligands (eq. 4-8) than with alkanes.[10]

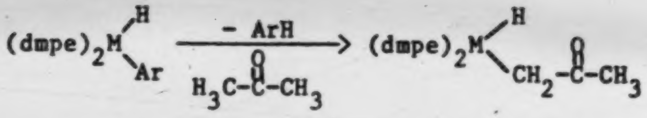
- ArH
$H_3C-\overset{O}{\overset{\|}{C}}-CH_3$

(M = Fe, Ru)

(4-7)

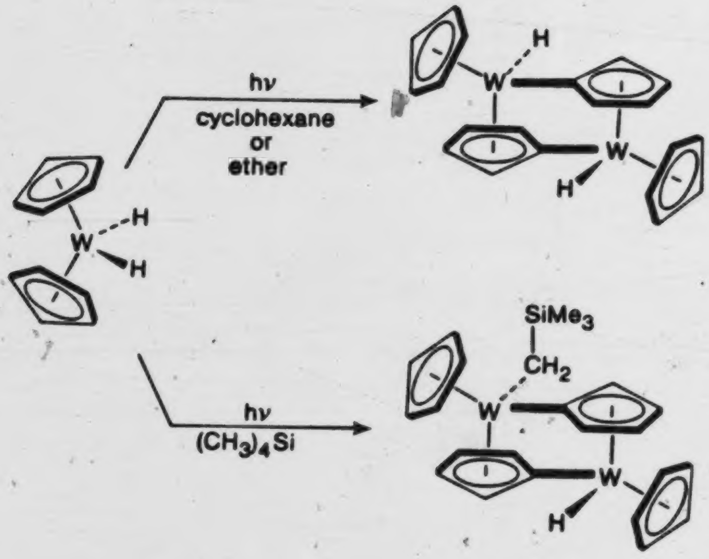
hν
cyclohexane
or
ether
hν
$(CH_3)_4Si$
SiMe$_3$
CH$_2$
W
H

(4-8)

(4-9)

The first observation that seemed mechanistically to require oxidative addition of a saturated hydrocarbon to a metal center was made by Crabtree and co-workers[11] in 1979. They observed the dehydrogenation of cycloalkanes by an iridium complex in chlorinated solvents in the presence of t-butyl ethylene. The olefin was required as an H_2 acceptor to make the reaction thermodynamically feasible (eq. 4-10).

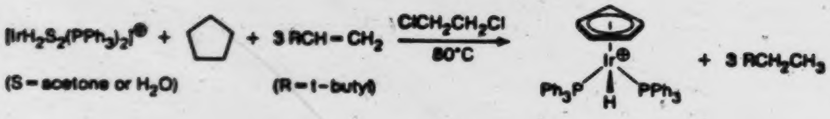
[IrH2S2(PPh3)2]⊕ + ⬠ + 3 RCH=CH2
(S = acetone or H2O)
(R = t-butyl)
ClCH2CH2Cl
80°C
Ir⊕
Ph3P
PPh3
H
+ 3 RCH2CH3

(4-10)

A similar reaction involving L_2ReH_7 has been described by Felkin and coworkers[12] (eq. 4-11).

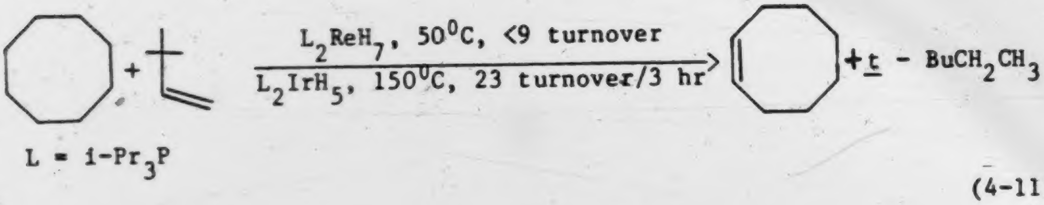
L_2ReH_7, 50°C, <9 turnover
L_2IrH_5, 150°C, 23 turnover/3 hr
+ t - $BuCH_2CH_3$
L = i-Pr_3P

(4-11)

The direct observation of oxidative addition of a saturated hydrocarbon C-H bond to a transition metal center was independently reported in 1982 by two groups. Janowicz and Bergman[13] found that irradiation of $(C_5Me_5)(PMe_3)Ir(H)(H)$ in saturated hydrocarbon media, e.g., cyclohexane and neopentane, led to hydrogen elimination and formation of the corresponding hydridoalkyliridium complex $(C_5Me_5)(PMe_3)Ir(H)(R)$ (eq. 4-12).

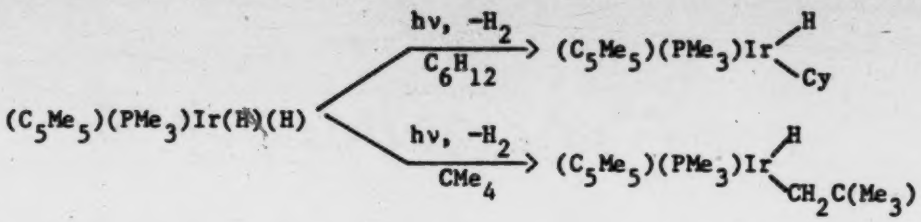

$$(C_5Me_5)(PMe_3)Ir(H)(H) \xrightarrow[C_6H_{12}]{h\nu,\ -H_2} (C_5Me_5)(PMe_3)Ir(H)(Cy)$$

$$(C_5Me_5)(PMe_3)Ir(H)(H) \xrightarrow[CMe_4]{h\nu,\ -H_2} (C_5Me_5)(PMe_3)Ir(H)(CH_2C(Me_3))$$

(4-12)

It is worth noting that the competitive internal oxidative addition was not observed with this particular system. Hoyano and Graham[14] demonstrated that photolysis of a solution of $(C_5Me_5)Ir(CO)_2$ in neopentane at room temperature yielded a new hydridoneopentyliridium compound. A similar compound was generated by the iridium complex in cyclohexane (eq. 4-13).

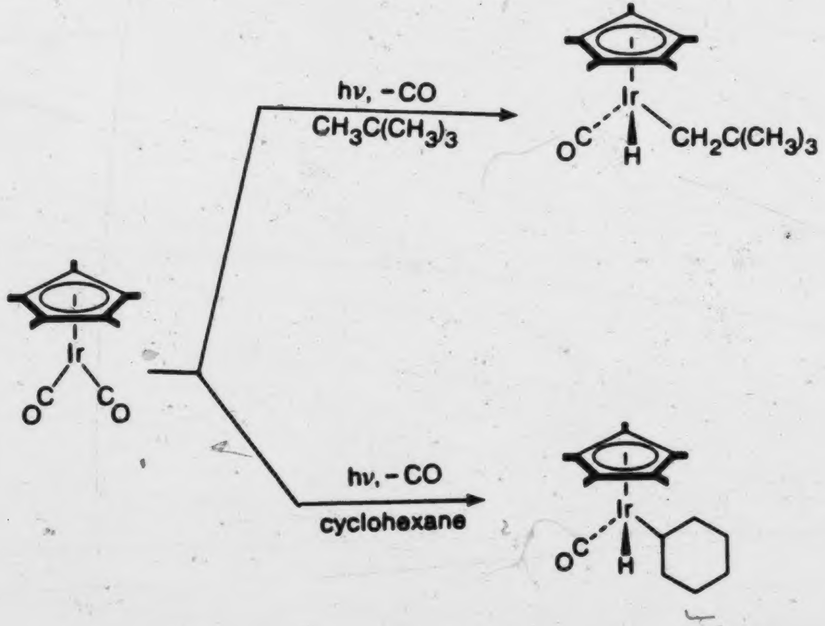

(4-13)

Both groups extended their results to methane showing that even such strong (105 kcal mol^{-1}) C-H bonds can be attacked. Methane was shown to react in the first instance by using eight atm of CH_4 over a perfluorohexane solution of dicarbonyl.[16] Recently, Graham, Rest et al.[17] have reported CH_4 activation at 12 K by irradiation of Cp*Ir(CO)$_2$ in a CH_4 matrix. This demonstrates how low the kinetic barrier to alkane activation by the photochemically generated intermediate must be in this system. The activation of methane C-H bonds was also demonstrated by Watson[18] with a lutetium complex (eq. 4-14); the mechanism of this exchange reaction is entirely different, since oxidative addition to lutetium (III) is not possible.

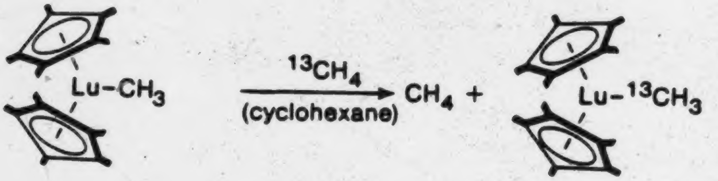

(4-14)

Activation by scandium and the lanthanides and actinides[19,20] will not be considered further here.

Jones and Feher[21] studied $(C_5Me_5)(PMe_3)Rh(H)(H)$, an analogue of Bergman's iridium complex. They reported that irradiation of this rhodium dihydride in liquid propane at -55°C produced hydridopropyl derivative, which decomposed at -15°C unless converted to the corresponding stable bromide with bromoform (eq. 4-15). Generalizing this result would suggest that more stable alkane oxidative addition products be formed with metals from the third row of the periodic table.

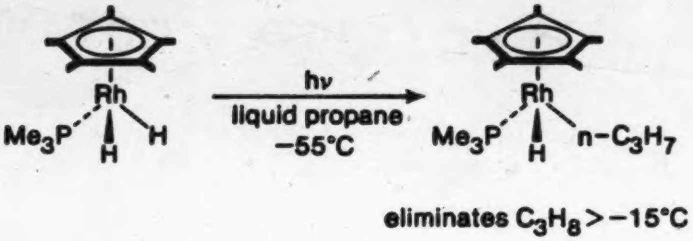
Rh
Me3P
H
H
hν
liquid propane
−55°C
Rh
Me3P
H
n−C3H7
eliminates C3H8 > −15°C

(4-15)

The same rhodium system was also studied by Bergman et al., who found greater selectivity between different types of C-H bonds with the rhodium complex than for the iridium analogue.[13,22]

More recently, Baker and Field[23] reported alkane activation by a first-row transition metal complex at -90°C (eq. 4-16).

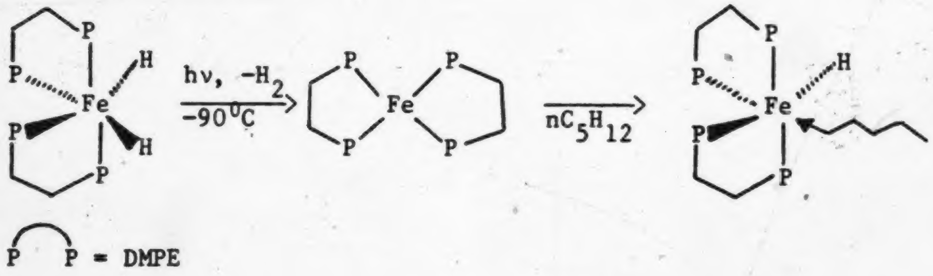
P
P
P
P
Fe
H
H
hν, −H2
−90°C
P
P
Fe
P
P
nC5H12
P
P
P
P
Fe
H
P
P = DMPE

(4-16)

Mechanism

The intermediates in the C-H activation process are presumably the coordinatively unsaturated 16-electron Cp*ML (M = Rh,[21,22] Ir, L = CO,[14,16,17]) species. Bergman et al. [13] suggested that a "σ-complex" is involved in R-H oxidative addition (eq. 4-17).

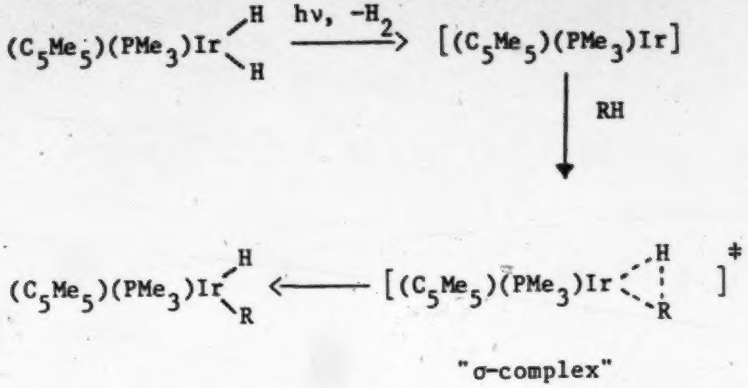

(4-17)

The proposed "σ-complex" is also in line with the Hoffmann predictions and calculations.[24]

Initial formation of weak molecular alkane complexes may help explain the kinetic selectivity observed in C-H oxidative addition by Cp*Ir(PMe_3). In general the rate of attack on C-H bonds is in the order primary > secondary >> tertiary. This is also the order of thermodynamic stability of alkyl complexes.[25,26]

Present work

It is clear from the foregoing that only in recent years has significant progress been made toward intermolecular alkane C-H activation. The previous studies have mainly involved phosphine, Cp and Cp* systems. The small number of systems in which the photochemical activation processes were observed were not very efficient; only partial conversion to hydridoalkyl complexes was obtained. It appeared that useful new information could be derived from the study of other, more varied systems.

As stated in Chapter III, the tris(dimethylpyrazolyl)borato complex (HBPz*$_3$)Rh($CO)_2$ (1) photochemically activates aromatic C-H bonds with high efficiency. Accordingly photochemical activation of saturated hydrocarbons using complex 1 toward molecular hydrogen, cyclohexane, and a variety of acyclic alkanes will be reported in this Chapter. Relative Rh-C bond strengths in some of the alkyl and aryl complexes will also be discussed.

Section 2

ACTIVATION OF DIHYDROGEN AND CYCLOHEXANE

Activation of dihydrogen

The addition of hydrogen to a transition metal complex is a key step in many catalytic cycles. Dihydrogen is the simplest two-atom nonpolar substrate. The reaction of $(HBPz^*_3)Rh(CO)_2$ (1) with H_2 was considered to be a good starting point for the investigations of alkane C-H activation with compound 1.

Complex 1 reacted slowly but smoothly with 42 psig of H_2 pressure in the laboratory light at room temperature with complete conversion after three days to give dihydride 14 as an isolable stable compound (eq. 4-18).

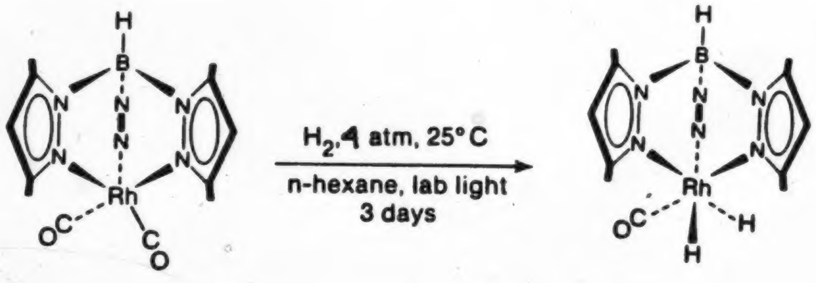

(4-18)

1 14

If the reaction in eq. 4-18 is allowed to continue after complete conversion of 1 to 14, the product slowly decomposes to an unidentified species which shows no carbonyl stretching bands in its IR spectrum and is insoluble in n-hexane. Under similar conditions, the reaction of 1 with H_2 did not take place in the dark. Compound **14** was fully characterized by elemental analysis and spectroscopic methods.

The MS of **14** did not show the molecular ion. The observed heaviest fragment corresponded to $M^{+}-H_2$ (428); simulation and fitting using the program "HLOSS"[27] suggested that loss of hydrogen ligands occurred in pairs. The contribution due to $M^{+}-H$ was not significant. The IR in n-hexane exhibited ν_{CO} at 2041 cm^{-1} and a weak broad band at 2060 cm^{-1} assigned to ν_{Rh-H}. To support the ν_{Rh-H} assignment, the compound (HBPz*$_3$)Rh(CO)(D)(D) (**15**) was prepared by reacting **1** with D_2. The ν_{CO} for **15** was found at 2042 cm^{-1} in n-hexane. The ν_{Rh-D} for **15** was perhaps obscured by the solvent absorption peak in the solution IR spectrum. The solid state IR of **15** (KBr disc) showed a weak band at 1468 cm^{-1}, presumably due to ν_{Rh-D}. The band at 1468 cm^{-1} was not present in the IR spectrum (KBr disc) of a sample of (HBPz*$_3$)Rh(CO)(H)(H) (**14**). The observed ν_{Rh-H}/ν_{Rh-D} ratio is 1.40, which is close to the calculated value of 1.41($\sqrt{2}$). The ^1H NMR spectrum showed the high field hydride resonance at δ -13.55 (d, J_{Rh-H}=18.0 Hz, 2H) and the two sets of pyrazole resonances in a 2:1 ratio. The NMR data is consistent with an octahedral rhodium (III)d^6, 18-electron complex.

Reaction of 14 with CH_2N_2

Complex **14** reacted slowly with an excess of ethereal CH_2N_2 at 0°C to yield (HBPz*$_3$)Rh(CO)(CH_3)(CH_3) (**16**) (eq. 4.19). This reaction was not very satisfactory as a synthetic method.

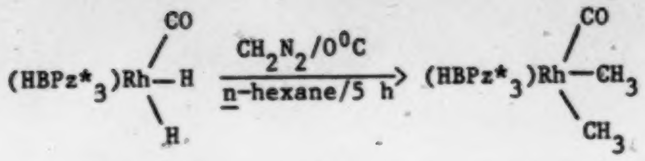

$$(\mathrm{HBPz^*_3})\mathrm{Rh(CO)(H)_2} \xrightarrow[\underline{n}\text{-hexane}/5\ \mathrm{h}]{\mathrm{CH_2N_2}/0^{\circ}\mathrm{C}} (\mathrm{HBPz^*_3})\mathrm{Rh(CO)(CH_3)_2} \quad (4\text{-}19)$$

14 **16**

There appeared to be some decomposition of the starting dihydride (**14**) under the reaction conditions. After chromatography and crystallization complex **16** was isolated as colorless crystals in 20% yield. The IR showed ν_{CO} at 2032 cm^{-1} in n-hexane. The ^{1}H NMR indicated two sets of pyrazole resonances in a 2:1 ratio as one would expect for **16**. The methyl group bound to rhodium appeared as a doublet at δ 1.00 (d, J_{Rh-H}=2.0 Hz, 6H). Compound **16** is a potential candidate for the CO insertion reactions described in Chapter VI, but this was not investigated.

Activation of cyclohexane

Irradiation of (HBPz$^*_3$)Rh(CO)$_2$ (**1**) (ca. 1.8 mM) at room temperature in rigorously purified cyclohexane[28] in an evacuated Pyrex vessel resulted in partial conversion to the hydridocyclohexyl complex (HBPz$^*_3$)Rh(CO)(H)(C$_6$H$_{11}$) (**17**) (eq. 4-20).

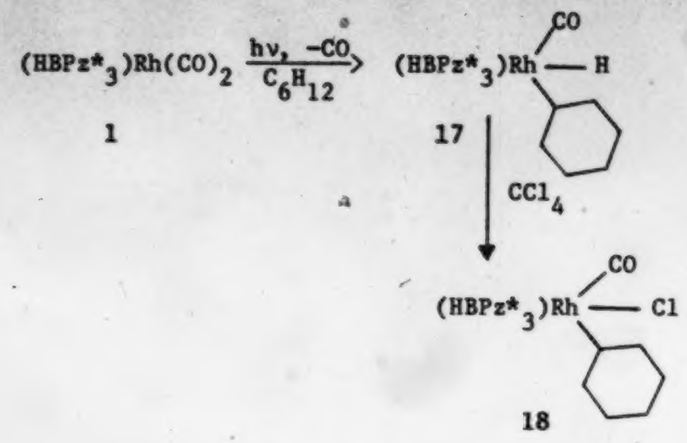

(4-20)

ν_{CO} of 17 in cyclohexane is 2028 cm^{-1}. Compound 17 was present as the major product immediately after irradiation. However, approximately 60% of it was converted fairly rapidly (within minutes) back to the dicarbonyl (1) by released CO in solution. The reversal of the reaction was dramatically shown by the color changes. The initial yellow solution of 1 was colorless when the UV lamp was switched off. It began within minutes to take on the yellow color again as 17 was converted back to 1.

When a N_2 purge was used during photolysis to prevent the back reaction with released CO the IR showed complete conversion of 1 to 17 within five minutes. As soon as the IR spectrum could be taken at the end of the five minute purged photolysis, small peaks (each estimated to be 5% of the intensity of the main band) were observed at 2048 and 2040 cm^{-1}. These are assigned to phenyl hydride (6) and dihydride (14) on the basis of known bands of those compounds. This unusual decomposition reaction of 17 will be discussed in a later section.

In view of complex 17's lability and limited stability, it was not isolated but converted with minimum delay by reaction with CCl_4 to the chloro derivative (HBPz*$_3$)Rh(CO)(Cl)(C_6H_{11}) (**18**) (eq. 4-20) for full characterization.

The reaction of **17** with CCl_4 was fast and compound **18** was isolated after chromatographic purification and crystallization as light yellow solid in *ca*. 70-75% yield. ν_{CO} for **18** was found at 2067 cm^{-1} in *n*-hexane. The six methyl resonances in the ^1H NMR spectrum suggested three nonequivalent pyrazole rings in a octahedral rhodium (III) structure. The Rh-C$\underline{H}$ resonance appeared at δ 4.65, rather far downfield. In the analogous Cp and Cp* iridium complexes, the position of α-cyclohexyl protons is δ 3.1-3.3.[14,29]

The complete characterization of the chloro derivative **18** establishes that in the evacuated and therefore unpurged vessel the complex **17** was present as the major product immediately after photolysis; it was rapidly but not completely converted back to the starting dicarbonyl (**1**) by released CO in solution. It is presumed that this happens by a dissociative equilibrium (eq. 4-21), from which the 16-electron species is scavenged by CO to give **1**.

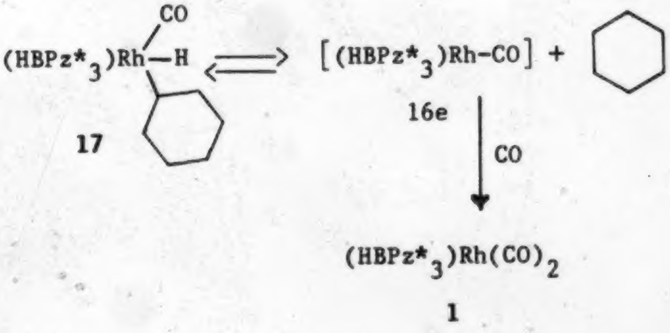

(4-21)

This is in contrast with $CpRh(CO)_2$, which upon irradiation in hexane at room temperature gave $Cp_2Rh_2(CO)_3$ and $[CpRh(CO)]_3$.[30] Formation of binuclear or trinuclear species is not favoured in the

$HBPz^*_3$ system, perhaps for steric reasons.

Since reasonably pure $(HBPz^*_3)Rh(CO)(H)(C_6H_{11})$ (17) could be obtained in ultrapure cyclohexane by using a purge, it appeared that this solution would provide what amounted to a thermal source of the reactive intermediate $[(HBPz^*_3)Rh(CO)]$ for activation of other molecules, such as C_6H_6, CH_4, H_2, C_2H_4, C_3H_6, etc. In effect, cyclohexane provides a quasi-inert solvent for studying reactions of 1, within the short times before significant irreversible thermal decomposition of 17 occurs.

Reactions of $(HBPz^*_3)Rh(CO)(H)(C_6H_{11})$ (17)

Reaction with C_6H_6

Addition of a slight excess of benzene to a freshly prepared cyclohexane solution of 17 at 25°C resulted in its quantitative conversion to $(HBPz^*_3)Rh(CO)(H)(C_6H_5)$ (6) within ten minutes (eq. 4-22).

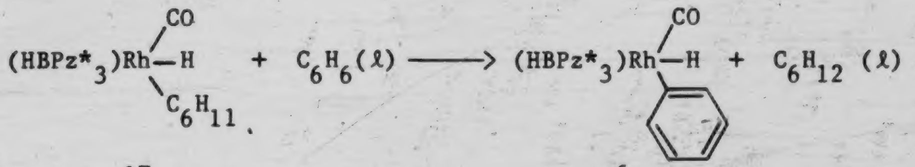

(4-22)

17

6

This transformation underlines the lability of 17 and relative stabilities in the system. It also explains the need for rigorously purified cyclohexane in the preparation of 17, since benzene is a persistent impurity. Displacement of alkane by arene in $(C_5Me_5)M(PMe_3)(H)(R)$ complexes appears general. Rates are significant at -17°C for M=Rh[31] but only above 100°C for M=Ir[26]. Compound 17 is a remarkably efficient scavenger for aromatic hydrocarbons.

Kinetics of the reaction of 17 with C_6H_6

The reaction in eq. 4-22 was too fast for accurate kinetic studies and temperature control was based on room temperature. The reaction of **17** with C_6H_6 at 25°C follows pseudo-first-order kinetics. Kinetics were measured by following the decrease in absorbance of the band at 2028 cm^{-1} of **17**. A pseudo-first-order condition was obtained using a 50 fold excess of benzene. A straight line was observed for plot of ln absorbance against time (Fig. IV.1). The rate constant was evaluated in the usual way from the negative gradient of the straight line. The observed rate constant for eq. 4-22 is $k = (8.8 \pm 0.4) \times 10^{-3} s^{-1}$ at 25°C. As mentioned earlier, this reaction was rather fast, with half-life 79 seconds, so k is certainly not very accurate.

It is reasonable to assume that the reaction in eq. 4-22 involves the 16-electron intermediate $[(HBPz^*_3)Rh(CO)]$. The proposed overall reaction scheme is shown in eq. 4-23.

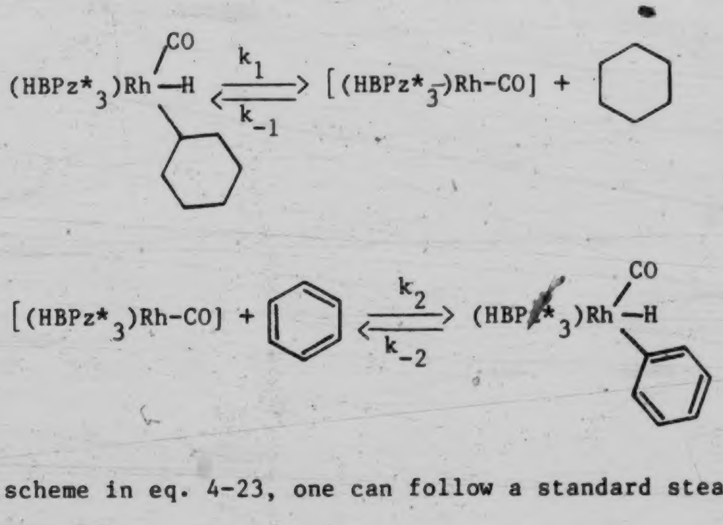

(4-23)

Now for the scheme in eq. 4-23, one can follow a standard steady state

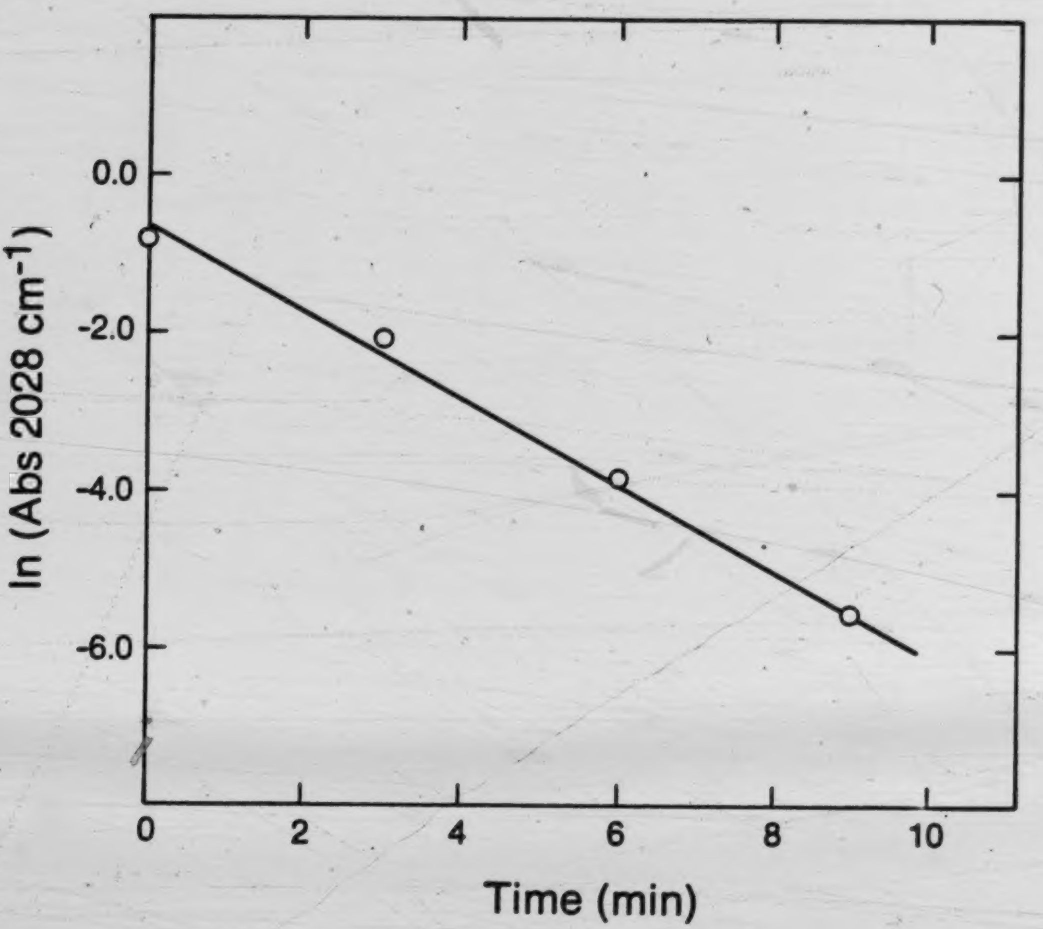

Figure IV.1 Pseudo first-order plot for the reaction of (HBPz*$_3$)Rh(CO)(H)(Cy) (17) with C_6H_6 in cyclohexane at 25°C with 50-fold excess of C_6H_6.

method[32] to obtain the ratio k_2/k_{-1}. k_{-2} is negligible at 25°C. The ratio k_2/k_{-1} gives the relative rates at which an intermediate [$(HBPz^*_3)Rh(CO)$] reacts with substrates benzene and cyclohexane. Application of the steady-state approximation to [$(HBPz^*_3)Rh(CO)$] leads to eq. 4-24.

$$\frac{1}{k_{obsd}} = \frac{1}{k_1} + \frac{k_{-1}\,[C_6H_{12}]}{k_1 k_2 [C_6H_6]} \qquad (4\text{-}24)$$

The observed rate constants at different ratios of $[C_6H_{12}]/[C_6H_6]$ are shown in Table 4.I.

A plot of $1/k_{obsd}$ against $[C_6H_{12}]/[C_6H_6]$ was linear (Fig. IV.2) with a slope of k_{-1}/k_1k_2, and intercept of $1/k_1$; from these the ratio k_2/k_{-1} is calculated as 99.0. This means that benzene reacts with the intermediate [$(HBPz^*_3)Rh(CO)$] about 100 times faster than does cyclohexane, an impressive selectivity. In this context, a 5.4:1 selectivity for benzene over cyclopentane was observed at −35°C in $Cp^*Rh(PMe_3)$ system.[31] In a related $Cp^*Ir(PMe_3)$ system[13b] a 4:1 selectivity for benzene over cyclohexane was found at room temperature.

The kinetic results, even though approximate, plus assumptions about the reaction coordinate enable a reasonable estimate of $\Delta G^{\ddagger}_{298}$ for the reaction to be made. This can in turn be used to estimate $\Delta G°$ for eq. 4-22; this is shown in Fig. IV.3. All $\Delta G^{\ddagger}$ values are given at 25°C. The value of k for eq. 4-22 is $(8.8\pm0.4) \times 10^{-3} s^{-1}$ at 25°C which converts to $\Delta G^{\ddagger}_{298}$=20.3 kcal mol^{-1}. The activation parameters for eq. 3-12 are given in Chapter III, from which $\Delta G^{\ddagger}$ is calculated as 25.7

Table 4.I

Rate constants of the reaction of 17 at different $[C_6H_{12}]/[C_6H_6]$ ratios

Cyclohexane (M)	Benzene (M x 10^2)	Ratio $[C_6H_{12}]/[C_6H_6]$	k_{obsd} x 10^3 (s^{-1})
9.20	2.19	420	3.01
9.20	6.58	140	6.62
9.20	10.96	84	8.77

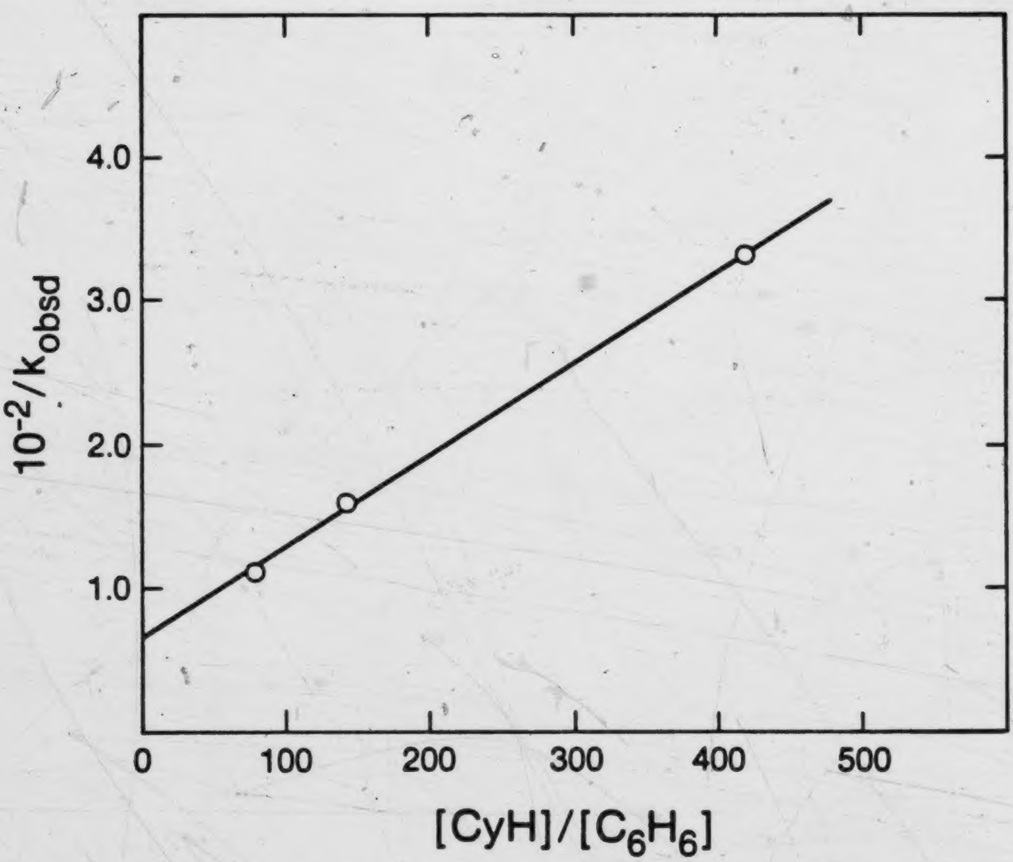

Figure IV.2 Plot of $1/k_{obsd}$ versus $[CyH]/[C_6H_6]$ ratios for the reaction of $(HBPz^*_3)Rh(CO)(H)(Cy)$ (17) with benzene at 25°C.

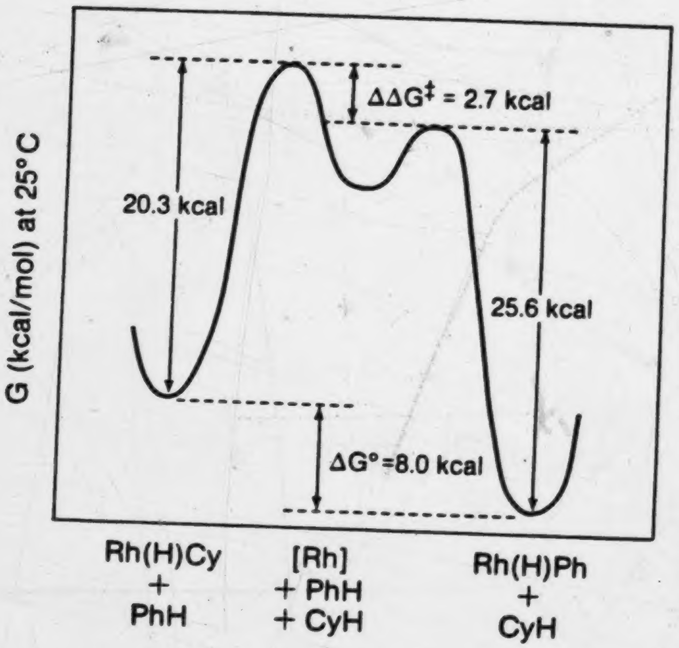
G (kcal/mol) at 25°C
ΔΔG‡ = 2.7 kcal
20.3 kcal
25.6 kcal
ΔG°=8.0 kcal
Rh(H)Cy + PhH
[Rh] + PhH + CyH
Rh(H)Ph + CyH

Figure IV.3 Energy profile for the reaction of $(HBPz^*_3)Rh(CO)(H)(Cy)$ with C_6H_6 (not to scale).

kcal mol^{-1} at 25°C.

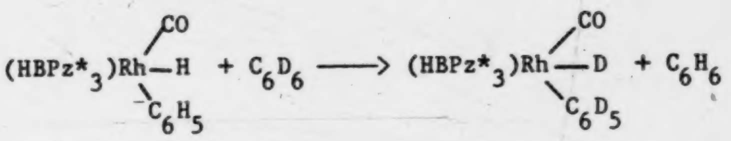

$$(HBPz^*_3)Rh(CO)(H)(C_6H_5) + C_6D_6 \longrightarrow (HBPz^*_3)Rh(CO)(D)(C_6D_5) + C_6H_6 \qquad (3\text{-}12)$$

Now, the ratio k_2/k_{-1} when combined with the Eyring equation (at 25°C), leads to $\Delta G^{\ddagger}_{-1}-\Delta G^{\ddagger}_{2}=2.7$ kcal as the difference in activation energies

$$\ln k = \ln \text{constant} - (\Delta G^{\ddagger}/RT)$$

for reaction of the intermediate with cyclohexane on the one hand and benzene on the other. The diagram in Fig. IV.3 is then complete. $\Delta G°$, the free energy change at 25°C for eq. 4-22, is approximately -8 kcal. Making the assumption that $\Delta S° \cong 0$ for eq. 4-22, $\Delta H° \cong -8$ kcal. Applying Hess's law to the bond dissociation energies[33] involved in eq. 4-22,

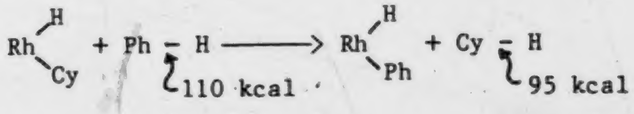

$$Rh(H)(Cy) + \underbrace{Ph-H}_{110\ kcal} \longrightarrow Rh(H)(Ph) + \underbrace{Cy-H}_{95\ kcal}$$

one calculates:

$$D[Rh\text{-}Ph] - D[Rh\text{-}Cy] \cong 23\ \text{kcal}$$

This means that the Rh-Ph bond is approximately 23 kcal stronger than the Rh-Cy bond. This is not unreasonable, given sp^2 versus sp^3

carbon, and the very important steric factor in this complex.

For the Cp*(PMe_3)Ir system, Bergman and co-workers[26] estimated that D{[Ir-Ph] - [Ir-Cy]} > 25 kcal mol^{-1}. More recent thermochemical studies[34] in the same system lead to the conclusion that Ir-Ph bond is 30 kcal mol^{-1} stronger than the Ir-Cy bond.

Reaction with CH_4

Methane is one of the most interesting hydrocarbons because of its abundance, availability and also because of its C-H bond strength (105 kcal mol^{-1}).

A cyclohexane solution of 1 (ca. 2.0 mM) was irradiated under CH_4 purge for eight minutes. The IR spectrum in cyclohexane (Fig. IV.4) then exhibited ν_{CO} at 2035 cm^{-1}, assigned to ($HBPz*_3$)Rh(CO)(H)(CH_3) (**19**) and at 2028 cm^{-1}, due to ($HBPz*_3$)Rh(CO)(H)(C_6H_{11}) (**17**). Weaker ν_{CO} bands (<10%) appearing at 2048 and 2040 cm^{-1} are assigned to ($HBPz*_3$)Rh(CO)(H)(C_6H_5) (**6**) and ($HBPz*_3$)Rh(CO)(H)(H) (**14**) respectively.

In a variation of this procedure, a fresh cyclohexane solution of **17** (ca. 2.2 mM) was prepared with N_2 purge. The lamp was extinguished, and the purge was immediately changed to CH_4. After 17 minutes, the solution exhibited IR bands at 2035 cm^{-1} (**19**) and 2028 cm^{-1} (**17**) and two other weaker bands as already mentioned. The dark reaction of CH_4 with **17** indicates thermal equilibrium between **17** and **19** (eq. 4-25) at room temperature.

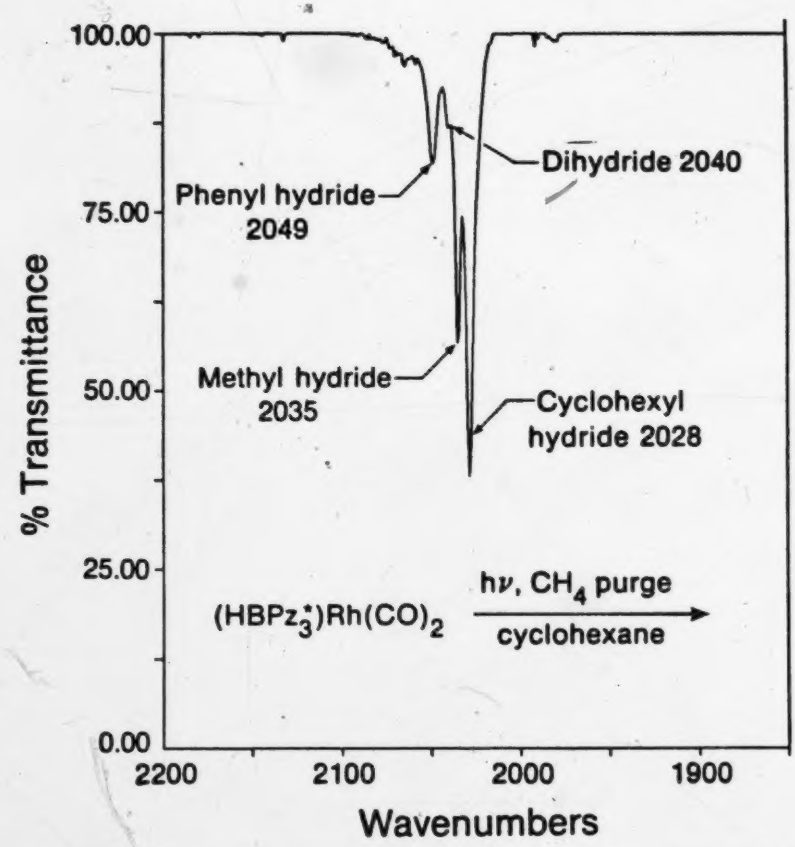

Figure IV.4 IR spectrum showing the equilibrium between $(HBPz^*_3)Rh(CO)(H)(Cy)$ (17) and $(HBPz^*_3)Rh(CO)(H)(CH_3)$ (19) at 25°C.

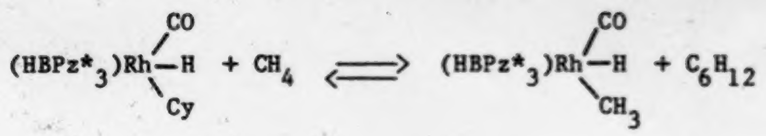

$$(HBPz^*_3)Rh(CO)(H)(Cy) + CH_4 \rightleftharpoons (HBPz^*_3)Rh(CO)(H)(CH_3) + C_6H_{12} \qquad (4\text{-}25)$$

17 **19**

$$K_{eq} = \frac{[C_6H_{12}]}{[CH_4]} \cdot \frac{[19]}{[17]}$$

The ratio of absorbances of the 2035 and 2038 cm^{-1} bands was 0.60; this would represent the molar ratio if extinction coefficients of **19** and **17** were the same. Another estimate of the molar ratio **19**:**17** was 0.63, obtained from the ^1H NMR of the mixture of stable chloro derivatives $(HBPz^*_3)Rh(CO)(Cl)(CH_3)$ (**20**) and **18** resulting from reaction with excess CCl_4. At 25°C and 1 atm the solubility of CH_4 is 0.0302 M,[35] [cyclohexane] is 9.20 M, and thus $K_{eq} \cong 190$ for eq. 4-25. This indicates a reasonably high equilibrium selectivity favouring the primary rhodium-methyl bond.

For $K_{eq} = 190$, $\Delta G°$ is calculated as -3.0 kcal mol^{-1}. Taking $\Delta G° \cong \Delta H° = -3.0$ kcal (i.e., the assumption $\Delta S° = 0$) for eq. 4-25, using the known values[33] of $D[H\text{-}CH_3]$ and $D[H\text{-}C_6H_{11}]$, one can

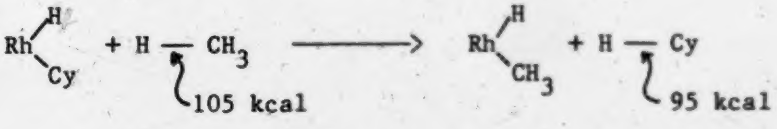

estimate

$$D[Rh\text{-}CH_3] - D[Rh\text{-}Cy] \cong 13 \text{ kcal mol}^{-1}.$$

This of course implies, with the previous result, that D[Rh-Ph] - D[Rh-CH_3] $\cong$ 10 kcal mol^{-1}. Interestingly Jones and Feher[31] made an estimate of the same quantity by kinetic methods in the Cp*Rh(PMe_3)(H)(R) system and found 12.6 kcal mol^{-1}. Considering the uncertainties involved this is indistinguishable from the ($HBPz^*_3$)Rh difference.

Repeated attempts to separate ($HBPz^*_3$)Rh(CO)(H)(Cl)(CH_3) (**20**) from the mixture of **18** and **20** were unsuccessful. However **20** was independently synthesized from ($HBPz^*_3$)Rh(CO)(I)(CH_3) (**21**) according to the eq. 4-26.

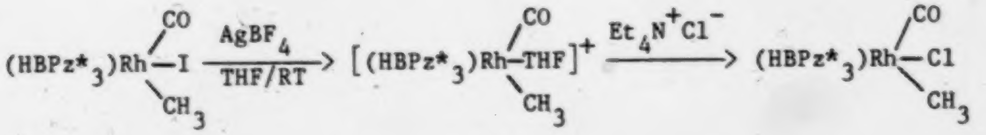

$$(HBPz^*_3)Rh(CO)(I)(CH_3) \xrightarrow[THF/RT]{AgBF_4} [(HBPz^*_3)Rh(CO)(THF)(CH_3)]^+ \xrightarrow{Et_4N^+Cl^-} (HBPz^*_3)Rh(CO)(Cl)(CH_3)$$

21 **20**

(4-26)

The intermediate cation (eq. 4-26) was not isolated. Compound **20** was isolated after chromatographic purification as a light yellow solid. The IR (n-hexane) showed ν_{CO} at 2075 cm^{-1}, 11 cm^{-1} higher than the corresponding iodo compound (**21**). The methyl group on rhodium appeared as a doublet in the ^1H NMR (δ 1.94, d, $^2J_{Rh-H}$=1.9 Hz, 3H).

The complex ($HBPz^*_3$)Rh(CO)(I)(CH_3) (**21**) was synthesized by reacting **1** with CH_3I. Dicarbonyl (**1**) reacted quite rapidly and smoothly with CH_3I at room temperature to yield **21**. Compound **21** was isolated as orange crystals after chromatography and crystallization and fully characterized by the usual spectroscopic and analytical techniques.

Reaction with H_2

Irradiation of 1 (2.19 mM) in cyclohexane for half an hour under a H_2 purge afforded mostly $(HBPz^*_3)Rh(CO)(H)(H)$ (14) (eq. 4-27).

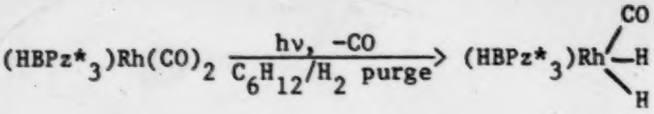

$$(HBPz^*_3)Rh(CO)_2 \xrightarrow[C_6H_{12}/H_2\ purge]{h\nu,\ -CO} (HBPz^*_3)Rh(CO)(H)(H) \qquad (4\text{-}27)$$

1 14

Weaker bands estimated to be less than 5% of the intensity of the ν_{CO} of 14 were observed at 2048 and at 2028 cm^{-1}. As discussed earlier, the band at 2048 cm^{-1} is assigned to $(HBPz^*_3)Rh(CO)(H)(C_6H_5)$ (6); the band at 2028 cm^{-1} is due to $(HBPz^*_3)Rh(CO)(H)(C_6H_{11})$ (17). Based on ν_{CO} band intensities it appeared that conversion of 1 to 14 was approximately 90%. This method of synthesis of 14 is faster than that of the H_2 pressurized reaction of 1, discussed at the beginning of this section.

Reaction with C_2H_4

A cyclohexane solution of 1 (1.8 mM) was saturated by means of a C_2H_4 purge and then irradiated for 15 minutes under a continuous purge of ethylene. The IR showed two new ν_{CO} bands at 2048 and 2012 cm^{-1} in a 1:1 ratio. As the solution stood for a few hours at 25°C, the band at 2048 cm^{-1} disappeared and at the same time the band at 2012 cm^{-1} showed a relative increase in intensity. The ν_{CO} band at 2048 cm^{-1} is presumed to be due to the vinyl hydride $(HBPz^*_3)Rh(CO)(H)(CH{=}CH_2)$. The peak at 2012 cm^{-1} is assigned to $(HBPz^*_3)Rh(CO)(\eta^2\text{-}C_2H_4)$ (34a). The η^2-ethylene complex was isolated as a yellow solid after chromatography. An alternate synthesis, characterization and properties of 34a will be discussed in Chapter VI.

Bergman et al.[36] observed $Cp^*(PMe_3)(H)(CH{=}CH_2)$ and $Cp^*(PMe_3)Ir(\eta^2$-$C_2H_4)$ in a 2:1 ratio when a cyclohexane solution of $Cp^*Ir(PMe_3)(H)(C_6H_{11})$ was heated at 130-160°C under 20 atm of C_2H_4, which on further heating above 170°C yielded exclusively $Cp^*(PMe_3)Ir(\eta^2$-$C_2H_4)$. From the IR observations, in conjunction with the results of related $Cp^*(PMe_3)Ir$ system, it is suggested that η^2-C_2H_4 complex (**34a**) formed via the intermediate vinyl hydride $(HBPz^*_3)Rh(CO)(H)(CH{=}CH_2)$, as shown in eq. 4-28.

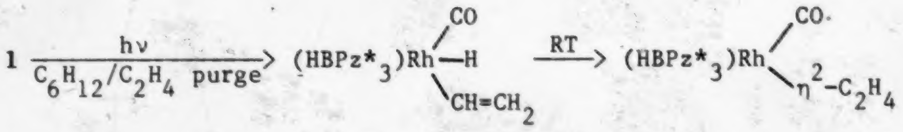

$$1 \xrightarrow[C_6H_{12}/C_2H_4\ \text{purge}]{h\nu} (HBPz^*_3)Rh(CO)(H)(CH{=}CH_2) \xrightarrow{RT} (HBPz^*_3)Rh(CO)(\eta^2\text{-}C_2H_4) \qquad (4\text{-}28)$$

34a

34a is considered to be the thermodynamic product. The presumed vinyl hydride intermediate was not isolated.

Reaction with CH_3OH

The methanol reaction was examined only in a cursory fashion. A slight excess of CH_3OH was added to a freshly generated cyclohexane solution of **17**. After four minutes, the IR examination of the reaction mixture showed ν_{CO} at 2038 cm^{-1} and at 2028 cm^{-1} in approximately a 1:1 ratio. On the basis of ν_{CO} band positions in other well characterized hydrido species, the band at 2038 cm^{-1} is presumed to be due to $(HBPz^*_3)Rh(CO)(H)(CH_2OH)$, and the band at 2028 cm^{-1} is assigned to **17**.

After the solution stood for 15 minutes, the IR indicatd a gradual disappearance of ν_{CO} band at 2038 cm^{-1}, and at the same time a band at

2040 cm^{-1} was growing. The ν_{CO} band at 2040 cm^{-1} is assigned to $(HBPz^*_3)Rh(CO)(H)(H)$ (14). As judged from the IR carbonyl stretching frequencies, it appeared that the converstion of the presumed $(HBPz^*_3)Rh(CO)(H)(CH_2OH)$ to 14 was complete in about 40 minutes. The overall reaction is shown by eq. 4-29.

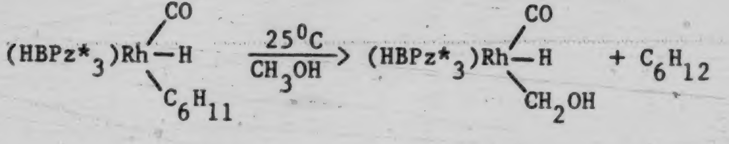

$$(HBPz^*_3)\underset{C_6H_{11}}{\overset{CO}{Rh}}-H \xrightarrow[CH_3OH]{25^0C} (HBPz^*_3)\underset{CH_2OH}{\overset{CO}{Rh}}-H + C_6H_{12} \qquad (4\text{-}29a)$$

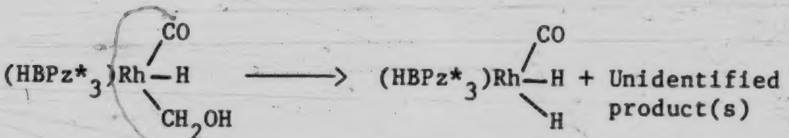

$$(HBPz^*_3)\underset{CH_2OH}{\overset{CO}{Rh}}-H \longrightarrow (HBPz^*_3)\underset{H}{\overset{CO}{Rh}}-H + \text{Unidentified product(s)} \qquad (4\text{-}29b)$$

The unidentified product(s) in eq. 4-29b could be either HCHO or CO and H_2. The analysis of unidentified product(s) was not pursued. May and Graham[37] reported conversion of $(C_5Me_5)Os(CO)_2CH_2OH$ to $(C_5Me_5)Os(CO)_2H$, CO and H_2 either photochemically or at elevated temperatures.

Reaction with cyclopropane

Irradiation of a cyclohexane solution of 1 for nine minutes under a cyclopropane purge afforded stable isolable rhodacyclobutane $(HBPz^*_3)(CO)\overline{Rh-CH_2CH_2CH_2}$. A fuller discussion of this reaction will be found in Chapter VII.

Decomposition of $(HBPz^*_3)Rh(CO)(H)(C_6H_{11})$ (17)

IR monitoring of a cyclohexane solution of a freshly prepared sample of 17 at room temperature indicated disappearance of its ν_{CO} band.

(2028 cm^{-1}) with time. At the same time it showed the growth of two peaks at 2048 and 2040 cm^{-1}. The disappearance of ν_{CO} band at 2028 cm^{-1} (**17**) was complete in about three hours. The peaks at 2048 and 2040 cm^{-1} were estimated to be 30% and 10% respectively of the intensity of 2028 cm^{-1} band (**17**) initially present. The bands at 2048 and 2040 cm^{-1} are assigned to $(HBPz^*_3)Rh(CO)(H)(C_6H_5)$ (**6**) and $(HBPz^*_3)Rh(CO)(H)(H)$ (**14**) respectively on the basis of known bands of those compounds. The estimated combined yield of **6** and **14** (eq. 4-30) was substantially less than the amount of **17** initially used.

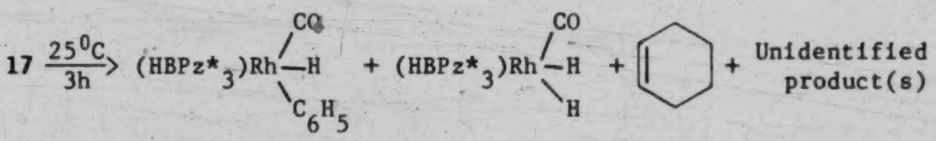

6 **14** (4-30)

Another estimate of the yields of **6** and **14** was obtained from ^1H NMR of the mixture of methyl derivatives $(HBPz^*_3)Rh(CO)(CH_3)(C_6H_5)$ (**9**) and $(HBPz^*_3)Rh(CO)(CH_3)(CH_3)$ (**16**) resulting from treating the reaction products with excess CH_2N_2 at 0°C. The values were 33 and 8% respectively. Hexamethyldisiloxane was used as an internal standard for the ^1H NMR run.

Cyclohexene was detected as the major organic product in the decomposition reaction of eq. 4-30 by gas chromatography and estimated to be ca. 9% of **17**. The details of GC work will be found in the Experimental Section. As mentioned earlier, the yield of $(HBPz^*_3)Rh(CO)(H)(H)$ (**14**) in eq. 4-30 was about 10% of **17**. These observations led to the speculation that dihydride **14** may result from β-elimination of **17**.

Phenyl hydride **6** may be the result of a thermal reaction superimposed on the photochemical reaction. When a cyclohexane solution of **17** was irradiated for about half an hour it gave mostly dihydride (**14**) (30% of **17** initially present) and only ca. 5% phenyl hydride (**6**). On the other hand the dark reaction of **17** yielded ca. 30% phenyl hydride (**6**).

One might presume that **6** is formed from **17** by dehydrogenation of cyclohexane as shown in eq. 4-31.

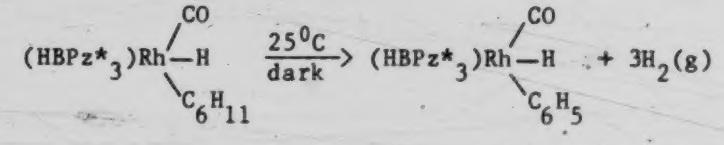

$$(HBPz^*_3)Rh(CO)(H)(C_6H_{11}) \xrightarrow[\text{dark}]{25^0C} (HBPz^*_3)Rh(CO)(H)(C_6H_5) + 3H_2(g) \qquad (4\text{-}31)$$

17 **6**

If ΔG° for eq. 4-31 is estimated and indicates that the process is unfavourable, then it is likely the overall eq. 4-31 is wrong even though one of the products is correct. Such an estimate is possible by noting that eq. 4-31 is the sum of eq. 4-22 and eq. 4-32:

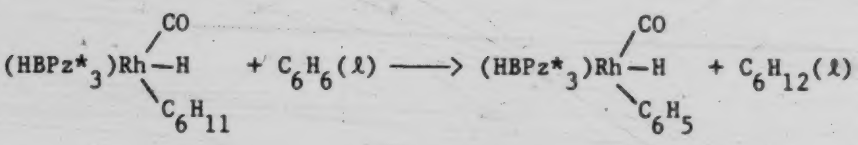

$$(HBPz^*_3)Rh(CO)(H)(C_6H_{11}) + C_6H_6(\ell) \longrightarrow (HBPz^*_3)Rh(CO)(H)(C_6H_5) + C_6H_{12}(\ell) \qquad (4\text{-}22)$$

17 **6**

$$C_6H_{12}(\ell) \longrightarrow C_6H_6(\ell) + 3H_2(g) \qquad (4\text{-}32)$$

$\Delta G° = 23.35$ kcal

$\Delta H° = 49.06$ kcal

$\Delta S° = 86.20$ eu

If $\Delta G°$ for eq. 4-31 is to be negative, then $\Delta G°$ for eq. 4-22 must be negative to the extent of 23.4 kcal or more to drive it along. As discussed earlier in this section, $\Delta G°$ for eq. 4-22 is estimated to be -8 kcal, not nearly favourable enough to offset eq. 4-32. In fact it leads to an equilibrium constant for eq. 4-31 of ca. 5×10^{-12}. This suggests that eq. 4-31 is incomplete in some important way, most likely in terms of unidentified products that play an essential part. Considering that the yield of phenyl hydride (**6**) is only 30%, this is likely. Identification of the other rhodium-containing product(s) will be required to reach an understanding of the interesting decomposition of 17.

The preceding thermodynamic argument is not exact owing to the use of different standard states for benzene and hydrogen. Equations 4-31 and 4-22 involve cyclohexane solutions of benzene and hydrogen, whereas eq. 4-3 refers to pure liquid benzene and hydrogen gas at 25°C and 1 atm. The assumption has been made that correction terms for standard states will be small in comparison with the other quantities involved.

Section 3

ACYCLIC ALKANE ACTIVATION

Activation of n-hexane

When a yellow solution of $(HBPz^*_3)Rh(CO)_2$ (1) (ca. 2.5 mM) in hexane was irradiated for five minutes under a purge of nitrogen, it became colorless and from IR spectra the conversion to $(HBPz^*_3)Rh(CO)(H)(C_6H_{13})$ (**22**) according to eq. 4-33 was complete. The IR (n-hexane) showed ν_{CO} at 2030 cm^{-1} and a weak broad band at 2060 cm^{-1}, assigned to ν_{Rh-H}. In some experiments, a trace amount of $(HBPz^*_3)Rh(CO)(H)(H)$ (**14**), recognized by its IR bands, formed along with **22** during photolysis.

Complex **22** in n-hexane was not stable with time and it appeared that isolation was not feasible. Observations on the decomposition are described at the end of this Section. Immediately after photolysis an excess of CCl_4 was added to the n-hexane solution of **22** to make the more stable chloro derivative for characterization.

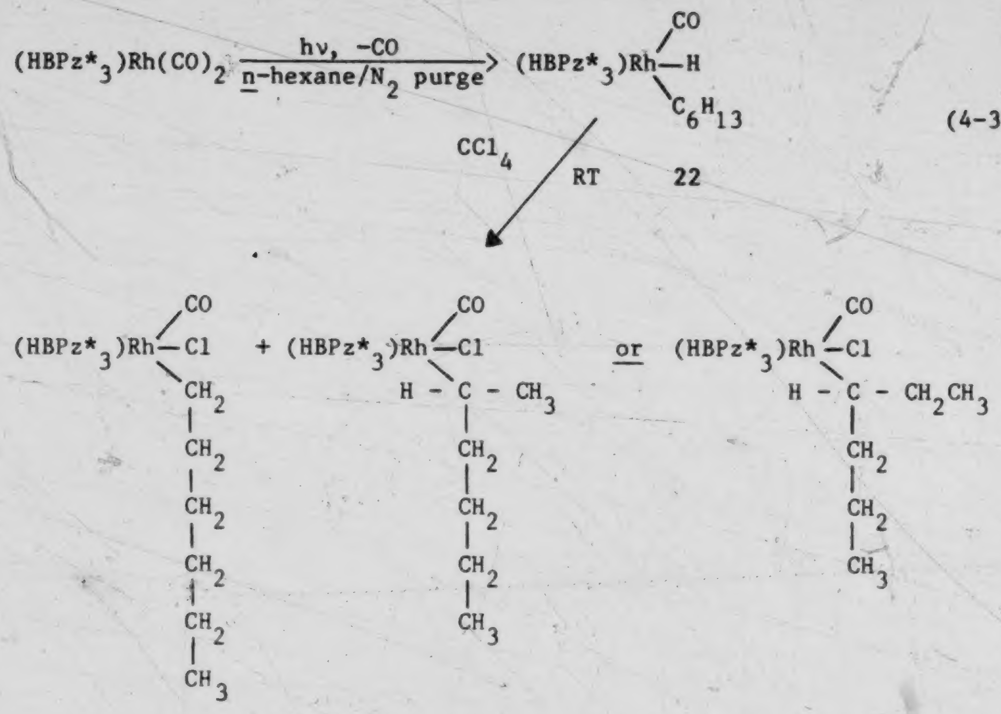
(HBPz*3)Rh(CO)2
hν, -CO
n-hexane/N2 purge
(HBPz*3)Rh—H
CO
C6H13
CCl4
RT
(HBPz*3)Rh—Cl
CO
CH2
CH2
CH2
CH2
CH2
CH3
+
(HBPz*3)Rh—Cl
CO
H - C - CH3
CH2
CH2
CH2
CH3
or
(HBPz*3)Rh—Cl
CO
H - C - CH2CH3
CH2
CH2
CH3

(4-33)

22

23a (87%) **23b** (13%) **23c**

The reaction of **22** with CCl_4 was fast and the colorless solution became yellow during the reaction. After chromatography and crystallization the chloro derivative of **22** was isolated as yellow crystals in 81% yield. The IR in n-hexane exhibited ν_{CO} at 2070 cm^{-1} with a small shoulder; the shoulder suggested that more than one isomer of **23** might be present. There was an indication of the presence of a minor isomer in the ^1H NMR but it was not well resolved due to complex nature of resonances in the hexyl region. Six methyl and three 4-H resonances of pyrazole rings were recognized clearly.

The attached proton test (APT) ^{13}C NMR enabled the isomers of **23** to be recognized and identified. Compound **23a** appeared as the major isomer (87%). For **23a**, seven methyl carbon resonances (six from three nonequivalent pyrazole rings and one from n-hexyl) were found. Of the methylene carbons, four appeared as singlets and the one bound to rhodium as doublet (δ 23.46, d, J_{Rh-C}=17.2 Hz) as one would expect.

In addition to these resonances, APT ^{13}C NMR showed the presence of a carbon bound to rhodium (δ 38.11, d, J_{Rh-C}=6.7 Hz) having an odd number of hydrogens. Three singlet resonances in the methylene carbon region and eight singlet resonances in the methyl carbon region were also found. These data are consistent with structure **23b** or **23c**. The APT ^{13}C NMR cannot distinguish between the two possibilities. The minor isomer accounts for about 13% of the stable chloro derivative. The primary insertion appears to be preferred over secondary.

In the foregoing, it has been assumed that isomer ratios initially present are not altered by the CCl_4 reaction. This may not be correct, and the conclusions regarding primary versus secondary C-H activation must for the present be regarded as tentative.

As the hexane solution of **22** stood at room temperature for approximately two hours the intensity of the 2030 cm^{-1} band decreased (ultimately disappearing in eight hours) as a new band at 2049 cm^{-1} grew in. The 2049 cm^{-1} band then began to disappear and after a day or two no ν_{CO} were observed in the solution. Some precipitate was noted. it was initially thought that the 2049 cm^{-1} band was due to a vinylic hydride, but this would have been expected to isomerize to an η^2-olefin complex, which it did not.

Pertinent to this problem is the reaction of **17** with hexene-1, which, by IR monitoring, passed through a vinylic hydride stage (ν_{CO} 2040 cm^{-1}) to an η^2-olefin complex (ν_{CO} 2006 cm^{-1}), which suffered little decomposition over two hours in solution.

Activation of _n_-pentane

In continuation of the investigation of acylic hydrocarbons, photolysis of **1** in _n_-pentane was examined to see whether both primary and secondary C-H insertion products would also be obtained. Thus, irradiation of **1** (_ca_. 1.46 m_M_) in _n_-pentane with a N_2 purge for six minutes at room temperature gave a colorless solution. The IR of the solution at this stage exhibited ν_{Rh-H} at 2060 cm^{-1} and ν_{CO} at 2031 cm^{-1}, which are assigned to the pentyl hydride **24** (eq. 4-34). The conversion of **1** to **24** was quantitative on the basis of IR. Complex **24** was converted to its stable chloro derivative by reaction with CCl_4 with minimum delay (eq. 4-34). The chloro derivative of **24** was isolated as a yellow crystalline solid after chromatography.

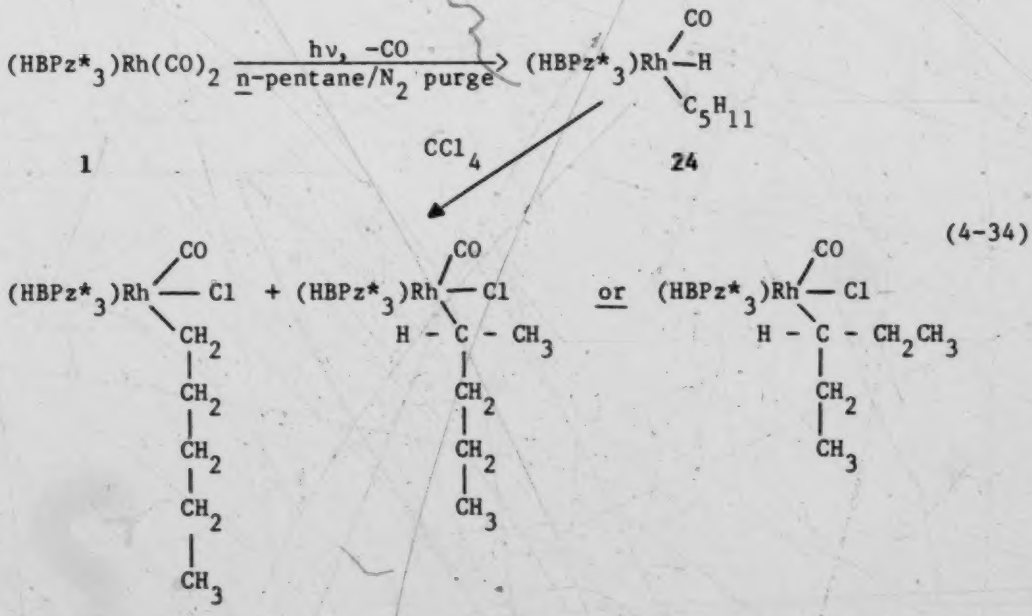
(HBPz*$_3$)Rh(CO)$_2$
hν, -CO
_n_-pentane/N_2 purge
(HBPz*$_3$)Rh
CO
H
C_5H_{11}
CCl_4
(HBPz*$_3$)Rh
CO
Cl
CH_2
CH_2
CH_2
CH_2
CH_3
+
(HBPz*$_3$)Rh
CO
Cl
H - C - CH_3
CH_2
CH_2
CH_3
or
(HBPz*$_3$)Rh
CO
Cl
H - C - CH_2CH_3
CH_2
CH_3

1 **24**

(4-34)

25a (90%) **25b** (10%) **25c**

The IR of the stable chloro derivative in n-hexane showed ν_{CO} at 2070 cm^{-1} with a small shoulder. This again suggested the presence of more than one isomer in the product. The ^1H NMR is consistent with the structure as shown for **25a**. However the APT ^{13}C NMR suggested **25a** as the major isomer (90%), while the minor isomer (10%) could be either **25b** or **25c**.

Interestingly, Bergman et al.[13b] observed a number of different secondary insertion products in addition to the primary C-H insertion product during photolysis of $Cp^*(PMe_3)Ir(H)(H)$ in n-pentane at 6°C. Heating the mixture of four products formed from n-pentane to 110°C for 17 h converted them completely into the primary product, which was thermodynamically the most stable. It is worth noting that in Cp*Ir system, the alkyl hydrides were much more stable to β-elimination or other degradation reactions.

Activation of neohexane

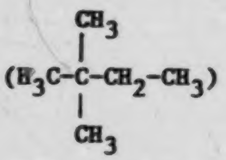

$(H_3C-\overset{CH_3}{\underset{CH_3}{C}}-CH_2-CH_3)$

The dicarbonyl (1) apparently does not activate C-H bond of neopentane, which is perhaps due to steric factors. In the $Cp^*(PMe_3)Ir$ system, Bergman and co-workers[26] reported that neopentyl hydride was less stable than cyclohexyl hydride. Neohexane was considered as a convenient alternative to neopentane, in which only the methylene bonded methyl group would be a likely candidate for activation.

Irradiation of a yellow solution of 1 (ca. 2.0 mM) in neohexane for eight minutes using N_2 as a purge afforded a colorless solution indicating complete conversion of the starting material. The IR spectrum of the neohexane solution showed ν_{Rh-H} at 2060 cm^{-1} (w, br) and ν_{CO} assigned to **26** at 2030 cm^{-1} (s). Addition of excess of CCl_4 to the hydridoneohexyl complex (**26**) gave cleanly the stable chloro derivative (**27**) (eq. 4-35).

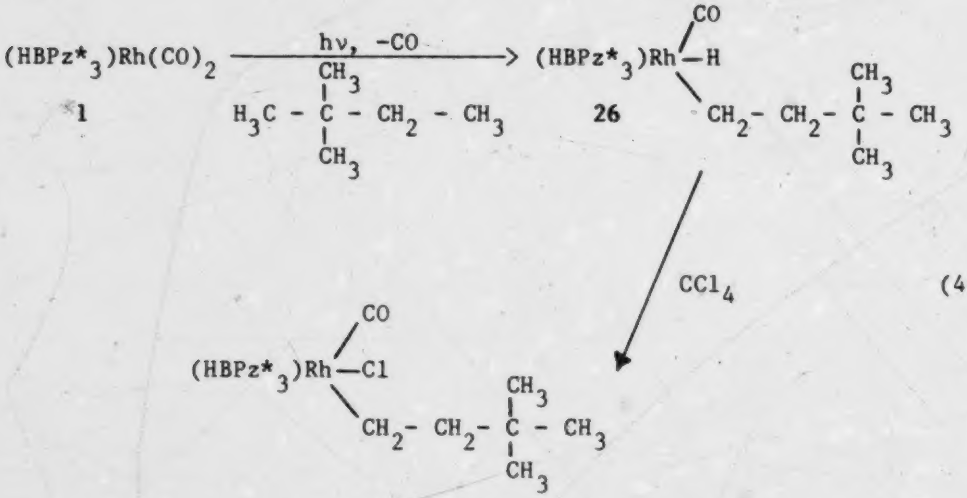
$(HBPz^*_3)Rh(CO)_2$
1
hν, -CO
$H_3C-C(CH_3)_2-CH_2-CH_3$
$(HBPz^*_3)Rh(CO)(H)$
26
$CH_2-CH_2-C(CH_3)_2-CH_3$
CCl_4
$(HBPz^*_3)Rh(CO)(Cl)$
$CH_2-CH_2-C(CH_3)_2-CH_3$

27

(4-35)

The reaction of CCl_4 with **26** was complete within half an hour. Complex **27** was isolated as yellow crystalline solid and fully characterized. The IR in n-hexane showed a single ν_{CO} at 2085 cm^{-1}, suggesting one isomer. A single resonance was found for the t-butyl group in the ^1H NMR. The methylene protons for the α and β carbons are diastereotopic. The ^{13}C NMR suggested only one isomer in agreement with the IR. This demonstrates high selectivity for primary C-H insertion product.

For comparison it is noted that a 1:1 mixture of $Cp^*(PMe_3)Ir$ 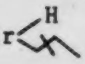 and $Cp^*(PMe_3)Ir$ 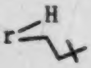 formed during photolysis of $Cp^*(PMe_3)Ir(H)(H)$ in neohexane,[26] which on heating at 140°C converted completely to the least sterically hindered $Cp^*(PMe_3)Ir$ 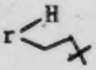.

Activation of *t*-butyl methyl ether

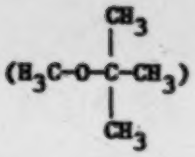

$(H_3C{-}O{-}C(CH_3)_2{-}CH_3)$

Tertiary butyl methyl ether, $H_3C{-}\underline{O}{-}C(CH_3)_3$ is a little like $H_3C{-}\underline{C}H_2{-}C(CH_3)_3$ sterically. Based on the results for neohexane one might expect that $H_3C{-}O{-}C(CH_3)_3$ to be activated at the $O{-}\underline{CH_3}$ group to form $(HBPz^*_3)Rh(CO)(H)(CH_2OC(CH_3)_3)$. The electronegative oxygen might raise the stability of the hydrido species.

Photolysis of dicarbonyl (**1**) (*ca*. 2.7 m*M*) in *t*-butyl methyl ether for eight minutes using N_2 as a purge gave **28** in quantitative yield (eq. 4-36) by IR. Compound **28** showed reasonable thermal stability, although it did not survive chromatography. Removal of solvent under reduced pressure afforded a pale yellow solid that was characterized by elemental analysis and spectroscopic methods.

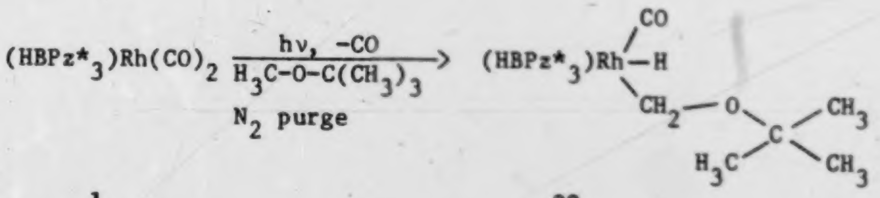

(4-36)

1 **28**

The IR in *n*-hexane showed ν_{Rh-H} at 2070 cm^{-1} (w, br) which is a little higher than other Rh-H complexes; ν_{CO} at 2050 cm^{-1} (s, br), very close to the ν_{CO} of $(HBPz^*_3)Rh(CO)(H)(C_6H_5)$ (**6**). The high field resonance in the ^1H NMR spectrum was found at δ -13.02 (d, J_{Rh-H}=22.0 Hz) indicative of hydride. The methylene protons appeared as two broad resonances, while a single resonance was observed for the *t*-butyl group. The ^{13}C NMR showed only one isomer which is consistent with the

IR observation. This is another example of selective C-H activation.

It is worth noting that complex **28** reacted with a tenfold excess of PPh_3 at room temperature in hexane to give $(HBPz*_3)Rh(CO)(PPh_3)$. The reaction appeared to follow pseudo first order kinetics with a half life of about 10 hours.

Reaction with CCl_4

Compound **28** reacted with an excess of CCl_4 to give the corresponding chloro derivative $(HBPz*_3)Rh(CO)(Cl)(CH_2\text{-}O\text{-}C(CH_3)_3)$ (**29**). Complex **29** was isolated as a yellow crystalline solid and fully characterized in the usual fashions. The methylene protons appeared as two widely separated doublets at δ 6.03 (d, J=3.0 Hz) and 4.02 (d, J=3.0 Hz) in the ^1H NMR spectrum.

Section 4

EXPERIMENTAL

General

Prior to use in photolysis experiment, cyclohexane was purified by passing through a $AgNO_3$-Al_2O_3 column.[28] Tertiary butyl methyl ether was purified in the same way.

Preparation of ($HBPz^*_3$)Rh(CO)(H)(H) (14)

Dicarbonyl (1) (70 mg, 0.153 mmol) and n-hexane (60 mL) were placed in a pressure bottle which was closed with a rubber septum and a bottle cap that contained a stir bar. The resulting yellow solution was then pressurized with hydrogen (42 psig) and stirred at room temperature in the laboratory light (fluorescent and daylight). The IR indicated complete disappearance of the starting material after three days. At this stage, the solvent was removed in vacuo, and the residue was taken up in a minimal amount of CH_2Cl_2 and chromatographed on a Florisil column (10 x 2.5 cm) with 1:1 CH_2Cl_2:hexane eluent. Removal of the solvent under reduced pressure afforded compound **14** as a colorless solid (40 mg, 61%).

Characterization: IR (n-hexane) 2060 cm^{-1} (w, br, ν_{Rh-H}), 2041 cm^{-1} (s, ν_{CO}). MS (180°C, 16 eV) M^+-H_2 (428), M^+-H_2-CO. ^1H NMR (CD_2Cl_2, ambient, 200 MHz) δ 5.83 (s, 2H), 5.82 (s, 1H), 3.24 (s, 6H), 3.21 (s, 3H), 2.37 (s, 6H), 2.33 (s, 3H), -13.55 (d, J_{Rh-H}=18.0 Hz, 2H), Anal. Calcd for $C_{16}H_{24}BN_6ORh$: C, 44.65; H, 5.58; N, 19.53. Found: C, 45.10; H, 5.64; N, 18.88.

Preparation of $(HBPz^*_3)Rh(CO)(CH_3)(CH_3)$ (16)

To a stirred solution of 14 (60 mg, 0.136 mmol) in hexane (40 mL) at 0°C, an excess of ethereal CH_2N_2 was added. The reaction was followed by IR. After 4 h no starting material remained. Solvent was removed under reduced pressure. The resulting pale yellow solid was taken up in a minimum amount of CH_2Cl_2 and chromatographed on a small alumina column (10 x 1 cm) with 1:1 CH_2Cl_2-hexane as eluent. Removal of solvent under vacuum left a colorless solid which was recrystallized from CH_2Cl_2-hexane at -20°C over one week to afford colorless crystals (13 mg, 20%).

Characterization: IR (n-hexane) 2032 cm^{-1} (s, ν_{CO}). MS (150°C, 16 eV) M^+ (458), M^+-CH_3, M^+-$2CH_3$-CO. ^1H NMR (CD_2Cl_2, ambient, 200 MHz) δ 5.86 (s, 1H), 5.80 (s, 2H), 2.37 (s, 3H), 2.35 (s, 6H), 2.32 (s, 3H), 2.30 (s, 6H), 1.00 (d, $^2J_{Rh-H}$=2.0 Hz, 6H). Anal. Calcd for $C_{18}H_{28}BN_6ORh$: C, 47.16; H, 6.11; N, 18.42. Found: C, 46.17; H, 6.30; N, 16.75.

Preparation of $(HBPz^*_3)Rh(CO)(Cl)(C_6H_{11})$ (18)

Complex 17 [$(HBPz^*_3)Rh(CO)(H)(C_6H_{11})$] was generated by irradiation of 1 (70 mg, 0.154 mmol) in ultrapure cyclohexane (85 mL) for 5 min in a Pyrex photolysis vessel using N_2 as purge. An excess CCl_4 (5 mL) was added immediately after photolysis to the above mentioned solution and the reaction was allowed to continue for 0.5 h. Solvent and excess CCl_4 were removed in vacuo. The IR of a hexane extract of the resulting yellow solid showed ν_{CO} at 2067 cm^{-1}, assigned to 18 and two weaker bands at 2116 and 2049 cm^{-1}, presumed to be due to

(HBPz*$_3$)Rh(CO)(Cl)(Cl) and (HBPz*$_3$)Rh(CO)(Cl)(C_6H_5) (7) respectively. The yellow solid was dissolved in the minimun amount of CH_2Cl_2 and chromatographed on a Florisil column (8 x 2.5 cm) with CH_2Cl_2 eluent. After chromatography, a small amount of 7 was still present (by IR) along with the major product (18). Crystallization from CH_2Cl_2-hexane afforded yellow crystals (58.7 mg, 70%).

Characterization: IR (n-hexane) 2067 (s, ν_{CO}). MS (125°C, 16 eV) m/e 750, 722, 692, 654, 598, 464, 428, 400 etc. The MS of **18** was anomalous, not showing the anticipated molecular ion (at 547). A puzzling feature was a significant peak at 750. Peaks at higher masses may be present, but the mass limit of MS-12 was 750 in this particular case. The MS of **18** was not recorded at higher masses using the MS-9 instrument. ^1H NMR (CD_2Cl_2, ambient, 200 MHz) δ 5.88 (s, 1H), 5.86 (s, 1H), 5.78 (s, 1H), 4.65 (br, RhCH), 2.74 (s, 3H), 2.52 (s, 3H), 2.44 (s, 3H), 2.39 (s, 3H), 2.37 (s, 3H), 2.32 (s, 3H), 1.5 (br, m, 10H). Anal. Calcd for $C_{22}H_{33}BClN_6ORh$: C, 48.31; H, 6.09; N, 15.38; Cl, 6.49. Found: C, 47.61; H, 6.45; N, 15.56; Cl, 6.53.

Preparation of (HBPz*$_3$)Rh(CO)(I)(CH_3) (21)

Complex 21 was prepared by the addition of methyl iodide (0.03 mL, 0.478 mmol) to a CH_2Cl_2 solution (40 mL) of 1 (150 mg, 0.329 mmol). The reaction was complete in ca. 2 h. Solvent was removed under vacuum to leave an orange solid. The residue was dissolved in CH_2Cl_2 and chromtographed on an alumina column (8 x 2.5 cm) with CH_2Cl_2 as eluent. Crystallization from CH_2Cl_2-hexane at 0°C afforded orange crystals (140 mg, 75%).

Characterization: IR (n-hexane) 2064 (s, ν_{CO}). MS (90°C, 16 eV) M^+ (570), M^+-CH_3I, M^+-CH_3I-CO. ^1H NMR (CD_2Cl_2, ambient, 200 MHz) δ 5.95 (s, 1H), 5.88 (s, 2H, coincidental overlap), 2.68 (s, 3H), 2.57 (s, 3H), 2.44 (s, 3H), 2.42 (s, 3H), 2.37 (s, 3H), 2.36 (s, 3H), 1.93 (d, $^2J_{Rh-H}$=2.0 Hz, 3H). Anal. Calcd for $C_{17}H_{25}BIN_6ORh$: C, 35.78; H, 4.38; N, 14.74. Found: C, 35.60; H, 4.30; N, 14.44.

Preparation of $(HBPz^*_3)Rh(CO)(Cl)(CH_3)$ (20)

To a stirred THF solution (40 mL) of 21 (60 mg, 0.105 mmol) was added $AgBF_4$ (20.5 mg, 0.105 mmol). After 40 min of stirring at room temperature, the solution was filtered to remove the white precipitate of AgI. To the filtrate was added solid Et_4NCl (64.5 mg, 0.390 mmol) and the mixture was stirred for a further 8 h. The resulting solution was filtered and evaporation of solvent afforded a pale yellow solid. The solid was taken up in CH_2Cl_2 and chromatographed on a small Florisil column (8 x 1 cm) with 1:1 CH_2Cl_2-hexane as eluent. The residue after removal of solvent was dissolved in a minimal volume of CH_2Cl_2 and hexane added. Crystallization at room temperature afforded pale yellow crystals of **20** (15 mg, 30%).

Characterization: IR (n-hexane) 2075 cm^{-1} (ν_{CO}), MS (210°C, 16 eV) M^+ (478), M^+-CH_3, M^+-CH_3-CO. ^1H NMR (CD_2Cl_2, ambient, 200 MHz) δ 5.86 (s, 3H, accidental degeneracy of pyrazole 4-H groups), 2.56 (s, 3H), 2.48 (s, 3H), 2.37 (s, ~6H), 2.36 (s, ~3H), 2.32 (s, 3H), 1.94 (d, $^2J_{Rh-H}$=1.9 Hz, Rh-$\underline{CH_3}$). Anal. Calcd for $C_{17}H_{25}BClN_6ORh$: C, 42.63; H, 5.22; N, 17.55. Found, C, 43.06; H, 5.79; N, 16.07.

Detection and estimation of cyclohexene

Gas chromatography (GC) analyses of the decomposed products of **17** were performed by using a Hewlett-Packard Model 5890 gas chromatograph using a 30 ft x 0.13 in. stainless steel column packed with 23% sp-1700/chromosorb PAW at 105°C. Helium was used as a carrier gas and a flow rate of 25 mL/min was maintained.

In a typical run, 1 µL cyclohexane solution of the decomposed products of **17** was injected into the column. Cyclohexene was detected in the injected sample by matching the retention time of an authentic sample. The retention time of cyclohexene was recorded as 31 min. The GC integrator could not pick up the area of cyclohexene peak produced from the unknown sample, perhaps because of the fact that the peak was weak and broad. To estimate the amount of cyclohexene produced, a series of standard solutions of cyclohexene in cyclohexane (0.001, 0.002, 0.004, 0.01% cyclohexene) were made and their GC traces were recorded. By comparing the peak areas of these standard solutions with the peak area of the unknown sample, it appeared that the amount of cyclohexene produced was approximately 0.002% by volume. Mmol Rh used: 4.38×10^{-2}; mmol cyclohexene produced: 0.4×10^{-2}, % cyclohexene ≅ 9.

Preparation of $(HBPz^*_3)Rh(CO)(Cl)(C_6H_{13})$ (23)

Dicarbonyl **1** (80 mg, 0.175 mmol) in n-hexane (70 mL) was irradiated for 7 min under a N_2 purge in a purged photolysis vessel. The solution became colorless and the IR indicated a single ν_{CO} band at 2030 cm^{-1} assigned to $(HBPz^*_3)Rh(CO)(H)(C_6H_{13})$ (**22**). An excess CCl_4 (5 mL) was added to the photolyzed solution and the reaction was allowed to continue for ca. 1 h. The solvent and excess CCl_4 were removed in vacuo and the light yellow solid was taken up in CH_2Cl_2 and chromatographed on a Florisil column (10 x 2.5 cm) with CH_2Cl_2 as eluent. Removal of solvent under reduced pressure yielded a solid which was dissolved in the minimum amount of CH_2Cl_2 and hexane added to it. Cooling the solution to 0°C gave yellow crystals (79.6 mg, 82%).

Characterization: IR (n-hexane) 2070 cm^{-1} (s, ν_{CO}) MS (150°C, 16 eV) M^+ (548), $M^+-C_6H_{13}$, $M^+-C_6H_{13}-Cl$, $M^+-C_6H_{13}-Cl-CO$. ^1H NMR (CD_2Cl_2, ambient, 200 MHz), δ 5.82 (s, 1H), 5.80 (s, 1H), 5.75 (s, 1H), 2.90 (m, 2H), 2.58 (s, 3H), 2.42 (s, 3H), 2.34 (s, 3H), 2.32 (s, 3H), 2.30 (s, 3H), 2.28 (s, 3H), 1.74 (m, 1H), 1.53 (m, 1H), 1.25 (m, 6H), 0.82 (5, 3H). Attached proton test (APT) ^{13}C NMR (see text) indicated the presence of two isomers; **23a**: (CD_2Cl_2, ambient, 75.5 MHz) δ 184.47 (d, J_{Rh-C}=61.5 Hz), 153.09, 151.63, 151.45, 145.98, 144.58, 144.36, 109.03, 108.54, 106.93, 34.14, 32.31, 31.95, 23.46 (d, J_{Rh-C}=17.2 Hz, $Rh-\underline{C}H_2$), 23.01, 14.69, 14.42, 14.24, 13.86, 13.23, 12.97, 12.36. **23b** or **23c**: δ 41.11 ($\underline{C}H_2$), 38.11 (d, J_{Rh-C}=6.7 Hz, $Rh-\underline{C}(H)(CH_3)$ or $Rh-\underline{C}H(CH_2(CH_3)$, 29.82 ($\underline{C}H_2$), 23.06 ($\underline{C}H_2$), 19.35, 15.09, 14.79, 14.62, 12.89, 12.62, 11.89, 11.75. Anal. Calcd for $C_{22}H_{35}BClN_6ORh$: C, 48.13; H, 6.38; N, 15.31; Cl, 6.47. Found: C, 47.04; H, 6.31; N, 15.03; Cl, 6.01.

Preparation of $(HBPz^*_3)Rh(CO)(Cl)(C_5H_{11})$ (25)

An n-pentane solution (90 mL) of 1 (60 mg, 0.132 mmol) in a Pyrex photolysis vessel was irradiated for 6 min using N_2 as purge. The IR indicated complete disappearance of 1 and formation of hydridopentyl complex (**24**). An excess CCl_4 (4 mL) was added quickly with a syringe to the colorless solution and conversion to **25** was complete within 1 h. Solvent was removed under reduced pressure and the resulting yellow residue was dissolved in CH_2Cl_2 and chromatographed on an alumina column (8 x 2.5 cm) with CH_2Cl_2 as eluent. The solid after evaporation of solvent was taken up in a minimal amount of CH_2Cl_2, and *n*-hexane added. The solution afforded yellow crystals (52.7 mg, 75%) after cooling to 0°C over a period of a few days.

Characterization: IR (*n*-hexane) 2070 cm^{-1} (s, ν_{CO}). MS (145°C, 16 eV) M^+ (534), $M^+-C_5H_{11}$, $M^+-C_5H_{11}-Cl$, $M^+-C_5H_{11}-Cl-CO$. ^1H NMR (CD_2Cl_2, ambient, 200 MHz) δ 5.90 (s, 1H), 5.87 (s, 1H), 5.82 (s, 1H), 2.95 (m, 2H), 2.63 (s, 3H), 2.47 (s, 3H), 2.40 (s, ~3H), 2.39 (s, ~3H), 2.38 (s, 3H), 2.36 (s, 3H), 1.78 (m, 1H), 1.54 (m, 1H), 1.29 (m, 4H), 0.90 (t, 3H). ^{13}C NMR (75.5 MHz) **25a**: δ 184.46 (d, J_{Rh-C}=60.7 Hz), 153.09, 151.63, 151.45, 145.99, 144.59, 144.37, 109.03, 108.53, 106.93, 34.91, 33.89, 23.42 (d, J_{Rh-C}=17.2 Hz), 22.78, 14.69, 14.41 (accidental overlap of two pyrazole methyl carbons), 13.88, 13.22, 12.97, 12.35, **25b** or **25c**: δ 31.88 ($\underline{C}H_2$), 27.5 (d, J_{Rh-C}=6.7 Hz, Rh-$\underline{C}$H), 23.03 ($\underline{C}H_2$); resonances in the methyl region were difficult to read, but on the expanded scale eight methyl carbon signals were found. Anal. Calcd for $C_{21}H_{33}BClN_6ORh$: C, 47.14; H, 5.98; N, 15.71. Found: C, 46.18; H, 6.10; N, 14.47.

Preparation of $(HBPz^*_3)Rh(CO)(Cl)(CH_2CH_2C(CH_3)_3)$ (27)

A yellow solution of 1 (70 mg, 0.154 mmol) in neohexane (80 mL) was placed in a Photolysis vessel and irradiated for 8 min using N_2 purge.

At the end of this period, the solution had become colorless and excess CCl_4 (8 mL) was added to it without any delay. The conversion to **27** was complete within 0.5 h. Removal of the solvent under reduced pressure yielded a yellow solid that was dissolved in CH_2Cl_2 and chromatographed on a Florisil column (10 x 2.5 cm) with CH_2Cl_2 as eluent. The residue after removal of solvent was taken up in a minimum amount of hexane and cooling the hexane solution at 0°C gave yellow crystals of **27** (64.8 mg, 77%).

Characterization: IR (n-hexane) 2069 cm^{-1} (s, ν_{CO}). MS (170°C, 16 eV) M^+ (549), $M^+-CH_2CH_2C(CH_3)_3$), $M^+-CH_2-CH_2-C(CH_3)_3-Cl$, $M^+-CH_2CH_2C(CH_3)_3-Cl-CO$. ^1H NMR (CD_2Cl_2, ambient, 200 MHz), δ 5.92 (s, 1H), 5.90 (s, 1H), 5.84 (s, 1H), 3.15 (m, 1H), 2.86 (m, 1H), 2.67 (s, 3H), 2.48 (s, 3H), 2.40 (s, 3H), 2.39 (s, ~6H), 2.36 (s, 3H), 2.10 (dt 1H), 1.73 (dt, 1H), 0.97 (s, 9H). ^{13}C NMR (75.5 MHz) δ 185.91 (d, J_{Rh-C}=66.0 Hz), 154.52, 153.05, 152.90, 147.52, 146.15, 110.56, 110.01, 108.39, 49.96, 31.51, 31.04, 21.76 (d, J_{Rh-C}=17.3 Hz, Rh-$\underline{CH}_2$), 16.27, 15.68, 15.28, 14.63, 14.39, 13.78. Anal. Calcd for $C_{22}H_{35}BClN_6ORh$: C, 48.13; H, 6.36; N, 15.31. Found: C, 47.77; H, 6.62; N, 14.75.

Preparation of $(HBPz^*_3)Rh(CO)(H)(CH_2-O-C(CH_3)_3)$ (28)

Dicarbonyl 1 (50 mg, 0.109 mmol) taken in purified t- butyl methyl ether (40 mL) and was photolyzed for 8 min using N_2 as purge. The IR indicated quantitative conversion to **28**. The solvent was removed under vacuum (25°C, 10^{-2} mm Hg) affording pale yellow solid (53 mg, 94%).

Characterization: IR (n-hexane) 2070 cm^{-1} (w, br, ν_{Rh-H}), 2050 cm^{-1} (s, br, ν_{CO}). MS (110°C, 70 eV) $M^+-CH_3-O-C(CH_3)_3$ (428), $M^+-CH_3OC(CH_3)_3-CO$. ^1H NMR (C_6D_{12}, ambient, 200 MHz) δ 5.70 (s, 1H), 5.64 (s, 1h), 5.54 (s, 1H), 4.66 (t, br, 1H), 4.54 (t, br, 1H), 2.49 (s, 3H), 2.43 (s, 3H) 2.36 (s, 3H), 2.30 (s, 3H), 2.26 (s, 3H), 2.17 (s, 3H), 1.19 (s, 9H), -13.02 (d, J_{Rh-H}=22.0 Hz, 1H). A trace amount of free t-butyl methyl ether was found in the ^1H NMR spectrum. ^{13}C NMR (75.5 MHz) δ 191.11 (d, J_{Rh-C}=70.9 Hz), 150.64, 150.54, 149.24, 143.99, 143.39, 143.12, 106.66 (accidental overlap of two Pz* 4-C resonances), 105.61, 74.15, 56.0 (d, J_{Rh-C}=23.4 Hz, Rh-O-$\underline{C}H_2$) 27.73, 15.40, 14.83, 14.35, 12.85, 12.58, 12.50. Anal. Calcd for $C_{21}H_{34}BN_6O_2Rh$: C, 48.84; H, 6.59; N, 16.28. Found: C, 48.65, H, 6.79; N, 15.71.

Preparation of $(HBPz^*_3)Rh(CO)(Cl)(CH_2-O-C(CH_3)_3)$ (29)

A yellow solution of 1 (64 mg, 0.140 mmol) was irradiated in purified t-butyl methyl ether (50 mL) for 8 min using N_2 purge. Excess CCl_4 (6 mL) was added to the irradiated sample and the reaction was allowed to continue for 1 h. The solvent was removed, the resulting yellow solid dissolved in CH_2Cl_2 and chromatographed on an alumina column (8 x 2.5 cm) with CH_2Cl_2 as eluent. Solvent was evaporated and the solid was taken up in a minimal amount of hexane. At -20°C, the hexane solution afforded yellow crystal (57 mg, 74%).

Characterization: IR (n-hexane) 2088 cm^{-1} (s, ν_{CO}). MS (150°C, 16 eV) M^+ (550), $M^+-CH_2-O-C(CH_3)_3$, $M^+-CH_2-O-C(CH_3)_3-Cl$, $M^+-CH_2-O-C(CH_3)_3-Cl-CO$. ^1H NMR (CD_2Cl_2, ambient, 200 MHz) δ 6.03 (d, J=3.0 Hz, 1H), 5.90 (s, 1H), 5.82 (s, 2H), 4.02 (d, J=3.0 Hz, 1H), 2.63 (s, 3H), 2.56 (s, 3H), 2.44 (s, 3H), 2.34 (s, 9H, accidental overlap of three methyl resonances), 1.28 (s, 9H, t-butyl). Anal. Calcd for $C_{21}H_{33}BClN_6O_2Rh$: C, 45.77; H, 5.99; N, 5.26. Found: C, 45.21; H, 6.37; N, 13.81.

References for Chapter IV

1. R.H. Crabtree, Chem. Rev., 85 (1985) 245.
2. J. Halpern, Advan. Catal., 9 (1959) 301.
3. A.E. Shilov and A.A. Shteinman, Coordination Chem. Rev., 24 (1977) 97.
4. P.J. Davidson, M.F. Lappert and R. Pearce, Acc. Chem. Res., 7 (1974) 209.
5. J. Halpern, Inorg. Chim. Acta., 100 (1985) 41.
6. J. Chatt and J.M. Davidson, J. Chem. Soc., (1965) 843.
7. F.A. Cotton, D.L. Hunter and B.A. Frenz, Inorg. Chim. Acta., 15 (1975) 155.
8. (a) N.F. Gol'dshleger, M.B. Tyabin, A.E. Shilov and A.A. Shteinman, Zh. Fiz, Khim, 43 (1969) 2174.
   (b) R.J. Hodges, D.E. Webster and P.B. Wells, J. Chem. Soc., Chem. Commun., (1971) 462.
9. (a) P. Foley and G.M. Whitesides, J. Am. Chem. Soc., 101 (1979) 2732.
   (b) H.D. Empsall, E.M. Hyde, R. Markham, W.S. McDonald, M.C. Norton, B.L. Shaw and B. Weeks, J. Chem. Soc., Chem. Commun., (1977) 589.
   (c) T.H. Tulip and D.L. Thorn, J. Am. Chem. Soc., 103 (1981) 2448.
   (d) S.J. Simpson, H.W. Turner and R.A. Andersen, J. Am. Chem. Soc., 101 (1979) 7728.
10. (a) G.M. Parshall, Acc. Chem. Res., 8 (1975) 113.
    (b) M. Berry, K. Elmitt and M.L.H. Green, J. Chem. Soc., Dalton Trans., (1979) 1950.

(c) M.L.H. Green, M. Berry, C. Couldwell and K. Prout, Nouv. J. Chim., 1 (1977) 187.

(d) S.D. Ittel, C.A. Tolman, A.D English and J.P. Jesson, J. Am. Chem. Soc., 98 (1976) 6073; 100 (1978) 7577.

11. (a) R.H. Crabtree, J.M. Mihelcic and J.M. Quirk, J. Am. Chem. Soc., 101 (1979) 7738.

(b) R.H. Crabtree, M.F. Mellea, J.M. Mihelcic and J.M. Quirk, J. Am. Chem. Soc., 104 (1982) 107.

(c) R.H. Crabtree and C.P. Parnell, Organometallics, 3 (1984) 1727.

(d) R.H. Crabtree, E.M. Holt, M. Lavin and S.M. Morehouse, Inorg. Chem., 24 (1985) 1986.

12. (a) D. Baudry, M. Ephritikhine, H. Felkin and J. Zakrzewski, Tetrahedron Lett., 25 (1984) 1283.

(b) J.W. Faller and H. Felkin, Organometallics, 4 (1985) 1488.

13. (a) A.H. Janowicz and R.G. Bergman, J. Am. Chem. Soc., 104 (1982) 352.

(b) A.H. Janowicz and R.G. Bergman, J. Am. Chem. Soc., 105 (1983) 3929.

14. J.K. Hoyano and W.A.G. Graham, J. Am. Chem. Soc., 104 (1982) 3723.

15. M.J. Wax, J.M. Stryker, J.M. Buchanan, C.A. Kovac and R.G. Bergman, J. Am. Chem. Soc., 106 (1984) 1121.

16. J.K. Hoyano, A.D. McMaster and W.A.G. Graham, J. Am. Chem. Soc., 105 (1983) 7190.

17. A.J. Rest, I. Whitwell, W.A.G. Graham, J.K. Hoyano and A.D. McMaster, J. Chem. Soc., Chem. Commun., (1984) 624.

18. (a) P.L. Watson, J. Chem. Soc., Chem. Commun., (1983) 276.

(b) P.L. Watson, J. Am. Chem. Soc., 105 (1983) 6491.

19. I.P. Rothwell, Polyhedron, 4 (1985) 177.

20. H. Rabaâ, J.-Y. Saillard and R. Hoffmann, J. Am. Chem. Soc., 108 (1986) 4327.

21. W.D. Jones and F.J. Feher, J. Am. Chem. Soc., 104 (1982) 4240.

22. R.A. Periana and R.G. Bergman, Organometallics, 3 (1984) 508.

23. M.V. Baker and L.D. Field, J. Am. Chem. Soc., 109 (1987) 2825.

24. J.-Y. Saillard and R. Hoffmann, J. Am. Chem. Soc., 106 (1984) 2006.

25. A.H. Janowicz, R.A. Periana, J.M. Buchanan, C.A. Kovac, J.M. Stryker, M.J. Wax and R.G. Bergman, Pure and Appl. Chem., 56 (1984) 13.

26. J.M. Buchanan, J.M. Stryker and R.G. Bergman, J. Am. Chem. Soc., 108 (1986) 1537.

27. L. Vancea, Univ. of Alberta "Little Blue Book of Computer Programs", locally printed, 1976.

28. E.C. Murray and R.N. Keller, J. Org. Chem., 34 (1969) 2234.

29. J.K. Hoyano, Personal communication.

30. (a) O.S. Mills and E.F. Paulus, J. Organomet. Chem., 10 (1967) 331.
    (b) E.F. Paulus, E.O. Fischer, H.P. Fritz, H. Schuster-Woldan, J. Organomet. Chem., 10 (1967) P3.

31. W.D. Jones and F.J. Feher, J. Am. Chem. Soc., 106 (1984) 1650.

32. A.J. Hart-Davis and W.A.G. Graham, J. Am. Chem. Soc., 93 (1971) 4388.

33. D.F. McMillen and D.M. Golden, Ann. Rev. Phys. Chem., 33 (1982) 493.

34. S.P. Nolan, C.D. Hoff, P.O. Stoutland, L.J. Newman, J.M. Buchanan, R.G. Bergman, G.K. Yang and K.S. Peters, J. Am. Chem. Soc., 109 (1987) 3143.

35. E. Wilhelm and R. Battino, Chem. Rev., 73 (1973) 1.

36. P.O. Stoutland and R.G. Bergman, J. Am. Chem. Soc., 107 (1985) 4581.

37. C.J. May and W.A.G. Graham, J. Organomet. Chem. 234 (1982) C49.

CHAPTER V

C-H ACTIVATION BY MONOPHOSPHINE DERIVATIVES

Section 1

INTRODUCTION

As shown in Chapter III and IV, dicarbonyl **1** efficiently activates C-H bonds under irradiation. Accordingly it was of interest to examine the potential of the new class of monophosphine derivatives $(HBPz^*_3)Rh(CO)(PR_3)$ (**4**) described in Chapter II, particularly $(HBPz^*_3)Rh(CO)(PMe_2Ph)$ (**4b**), for C-H activation.

Metallations of phenyl-substituted phosphine ligands have been frequently described and termed orthometallations. A few examples of orthometallation of complexes containing phenylphosphine[1,2] and phosphite[3,4,5] ligands are represented in eq. 5-1 and 5-2 respectively.

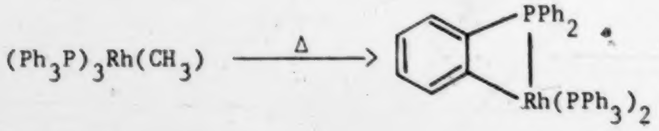

(5-1)

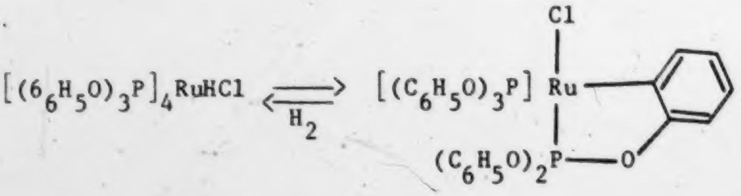

(5-2)

Metallation of sp^3-hybridized C-H bonds of alkyl groups attached to phosphines has also been observed. For instance, Werner[6] reported intramolecular cyclometallation of a phosphine isopropyl group by a ruthenium complex (eq. 5-3). However, the intermolecular C-H activation was observed only in the case of benzene by this ruthenium compound.

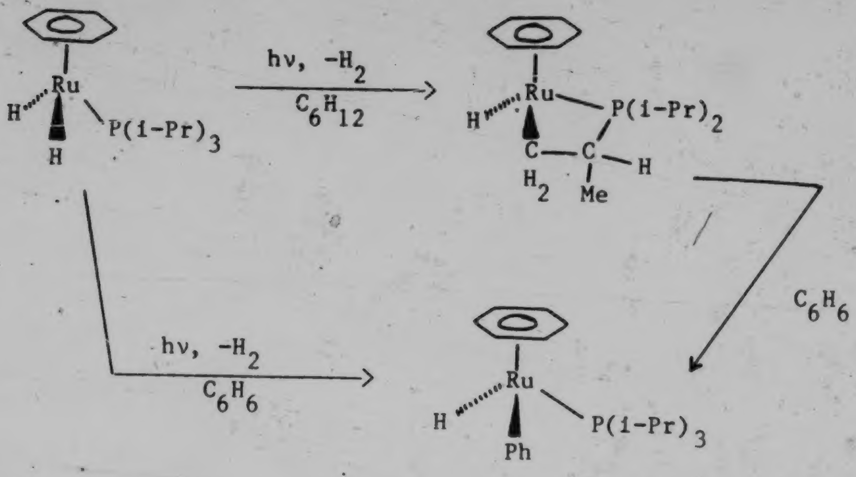

(5-3)

The absence of intermolecular alkane activation indicated this particular process was kinetically or thermodynamically unfavourable. On the other hand, intermolecular arene and alkane C-H activation were observed during irradiation of $(\eta^5\text{-}C_5Me_5)Ir(PMe_3)(H)_2$ in aromatic and saturated hydrocarbons respectively; no evidence for any intramolecular reaction was reported.[7] Prior to that report, there were no clearly defined examples of intermolecular alkane C-H activation.

Irradiation of complexes containing phenyl-substituted phosphine ligands in aromatic hydrocarbons have been reported to give both intra- and intermolecular C-H activation products. For example, irradiation of $(\eta^5\text{-}C_5Me_5)(PPh_3)Ir(H)_2$[7] in benzene yielded intermolecular and orthometallated products (eq. 5-4).

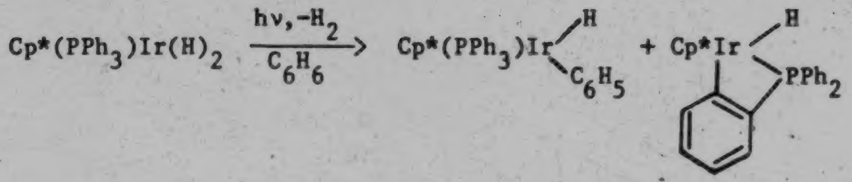
(5-4)

However, irradiation in other solvents (e.g. acetonitrile and cyclohexane) gave either all or mostly orthometallated product.

In the context of intra- versus intermolecular C-H activation, Halpern[8] suggested that the greater ease of intramolecular C-H oxidative addition has its origin in thermodynamic rather than kinetic differences. Jones and Feher[9] have studied the thermolysis of $Cp^*Rh(PMe_2CH_2Ph)(C_6H_5)(H)$ in cyclohexane-d_{12} solution, and observed a clean first-order reductive elimination of benzene with the formation of orthometallated species $Cp^*\overline{Rh(PMe_2CH_2C}_6H_4)H$. A similar thermolysis in benzene also resulted in a first-order elimination of benzene, but it did not go to completion. Instead an equilibrium mixture of $Cp^*\overline{Rh(PMe_2CH_2C}_6H_4)H$ and $Cp^*Rh(PMe_2CH_2Ph)(C_6H_5)(H)$ was formed. From the kinetic results it was concluded that there is little kinetic selectivity between intra- and intermolecular reactions involving neat solvent, but that there is moderate thermodynamic preference for the intramolecular activation.

The aim of the present work was to investigate the potential of the new monophosphine derivative $(HBPz^*_3)Rh(CO)(PMe_2Ph)$ (**4b**) toward carbon-hydrogen activation. The results of irradiation of **4b** in aromatic and also in saturated hydrocarbons will be described in this Chapter. Irradiation of **4b** in benzene afforded mainly $(HBPz^*_3)Rh(H)(C_6H_5)(PMe_2Ph)$, while in cyclohexane, orthometallation of the phenyl group occurred. The x-ray structure of a derivative of the latter will be described.

Section 2

C-H ACTIVATION BY (HBPz$^*_3$)Rh(CO)(PMe$_2$Ph) (4b)

Activation of benzene

Irradiation of **4b** (3.53 mM) in benzene in a Pyrex photolysis vessel under a N_2 purge afforded two products (**6**, **30**) and the reaction according to eq. 5-5 was complete in ca. 40 minutes.

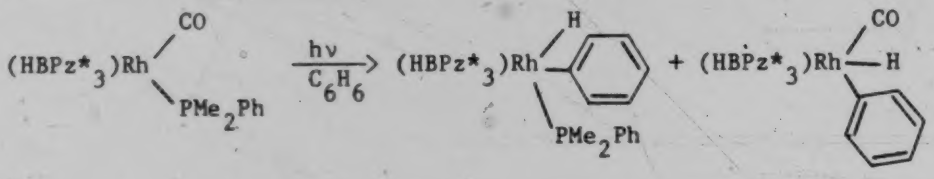

(5-5)

4b **30** **6**

Judging from the intensity of ν_{CO} of **4b** and **6** and assuming, as usual, that the extinction coefficients of ν_{CO} in the compounds are not very different, it appeared that conversion of **4b** to **6** only ca. 15-20%. However, the relatively strong ν_{Rh-H} in the IR suggested the presence of a major hydrido species in addition to **6**. Considering the probable difficulties of separating the mixture of hydrido species by chromatography, they were instead converted to the more stable chloro derivatives (eq. 5-6) by reaction with excess CCl_4 for separation and characterization.

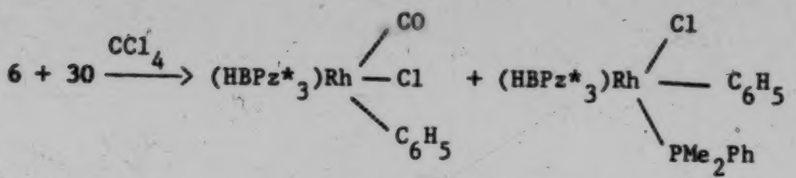

$$6 + 30 \xrightarrow{CCl_4} (HBPz^*_3)Rh(CO)(Cl)(C_6H_5) + (HBPz^*_3)Rh(Cl)(C_6H_5)(PMe_2Ph) \quad (5\text{-}6)$$

7 **31**

The chloro derivatives (**7** and **31**) were separated by careful chromatography on a Florisil column. The identity of **31** was established by MS, ^1H NMR and elemental analysis.

The MS indicated the molecular ion, and subsequent loss of C_6H_5, Cl, etc. The ^1H NMR of **31** is shown in Fig. V.1. The resonances at δ 7.92 (d, 1H), 6.68 (t, 1H) and 6.30 (d, 1H) are due to the phenyl group bound to rhodium center. The resonance at δ 7.02 (m, 7H) accounts for the five protons of the phenyl group attached to phosphorus and also for the remaining two protons of the rhodium-bound phenyl group. The two methyl groups on phosphorus are diastereotopic (δ 2.04, d, $^2J_{P-H}$=10.2 Hz); δ 1.75, d, $^2J_{P-H}$=9.5 Hz) as expected. The six methyl resonances of the three non-equivalent pyrazole rings are consistent with octahedral geometry for **31**. The ^1H NMR and elemental analysis suggested that **31** contains one mole of CH_2Cl_2 as solvent of crystallization.

The formation of $(HBPz^*_3)Rh(H)(C_6H_5)(PMe_2Ph)$ (**30**) is considered to occur via loss of CO from **4b**, while loss of phosphine ligand would account for **6**. No evidence for any intramolecular reaction was observed during photolysis of **4b** in benzene.

Photolysis of 4b in cyclohexane

Irradiation of **4b** (*ca*. 2.0 *mM*) in "ultrapure" cyclohexane at room

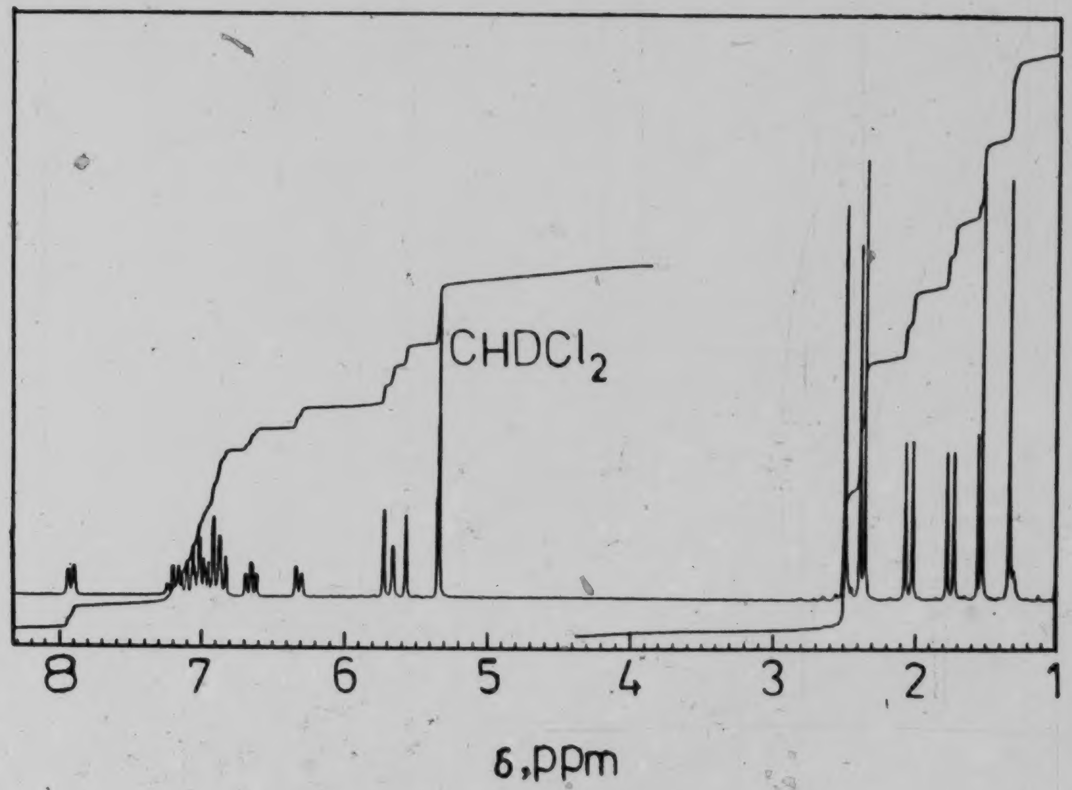

Figure V.1 ^1H NMR spectrum (200 MHz, CD_2Cl_2) of $(HBPz^*_3)Rh(Ph)(Cl)(PMe_2Ph)$ (31).

temperature using N_2 purge afforded one product as shown in eq. 5-7. The reaction was complete in *ca.* 45 minutes.

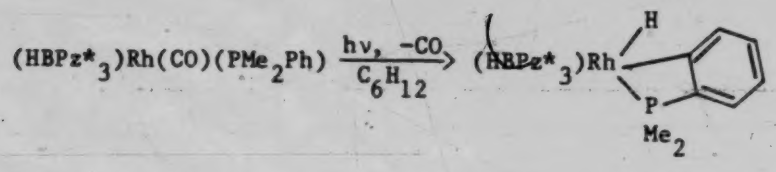

(5-7)

4b 32

The presence of ν_{Rh-H} in the IR suggested the formation of a hydrido species of rhodium. In view of anticipated limited stability of 32, it was converted to the more stable chloro derivative (33) for characterization (eq. 5-8). Compound 33 was isolated as yellow crystals in 75% yield after chromatographic purification and crystallization.

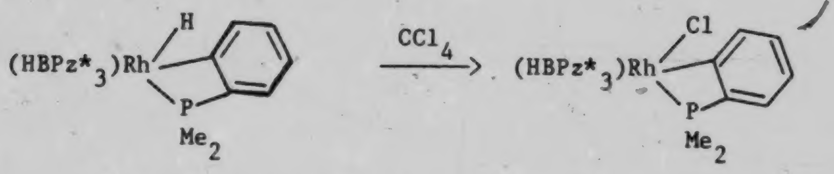

(5-8)

32 33

Complex 33 was characterized by the usual spectroscopic methods and elemental analysis. The evidence of orthometallation of phenyl group was first provided by the ^1H NMR spectrum. In the phenyl region, the resonances at δ 6.32 (m, 1H), 6.22 (m, 1H) and 6.14 (m, 2H) account only for four protons of the phenyl ring, suggesting loss of a hydrogen from the aromatic ring with the concomitant formation of a metal-carbon bond, making the four-membered metallacycle. The diastereotopic phosphorus-bound methyl groups appeared as two doublets (δ 2.90, d, $^2J_{P-H}$=12.0 Hz,

δ 1.49, d, $^2J_{P-H}$=12.0 Hz) in the ^{1}H NMR spectrum. The ^{1}H NMR spectrum and microanalysis suggested the presence of 0.5 mol CH_2Cl_2 in compound **33** as solvent of crystallization.

The spectroscopically deduced structure of **33** was confirmed by an X-ray crystal structure determination carried out by Dr. Richard Ball of this Department. Details of the data collection and refinement procedure as well as tables of structural parameters, bond lengths and bond angles will be found in the Experimental Section. The structure of **33** in the solid state is shown in Fig. V.2. It shows approximately octahedral geometry around rhodium; the three pyrazole rings occupy one face of the octahedron, and the other face is occupied by P, Cl and C_{19}. The dimensions of the four membered metallacyclic ring are (A°): Rh-P=2.282; P-C_{18}=1.793; C_{18}-C_{19}=1.388; Rh-C_{19}=2.004.

The absence of any intermolecular C-H activation product in cyclohexane is likely due to thermodynamic factors. As shown in Chapter IV, Rh-R bonds are much stronger when R=aryl than when R=alkyl. Moreover, as demonstrated earlier, cyclohexyl hydride (**17**) is very labile, and reacts with benzene to form the phenyl hydride (**6**) quantitatively. The implication for all these factors is that $(HBPz^*_3)Rh(CO)(PMe_2Ph)$ (**4b**) may also activate cyclohexane C-H bonds intermolecularly but that the product may have been missed due to its lability and lack of thermal stability. This means that the equilibrum in eq. 5.9 favours **32** and CyH.

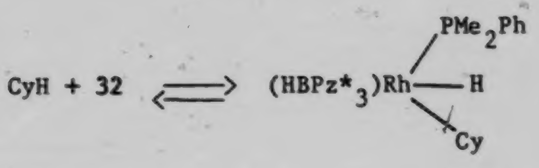

$$CyH + 32 \rightleftharpoons (HBPz^*_3)Rh(PMe_2Ph)(H)(Cy) \qquad (5\text{-}9)$$

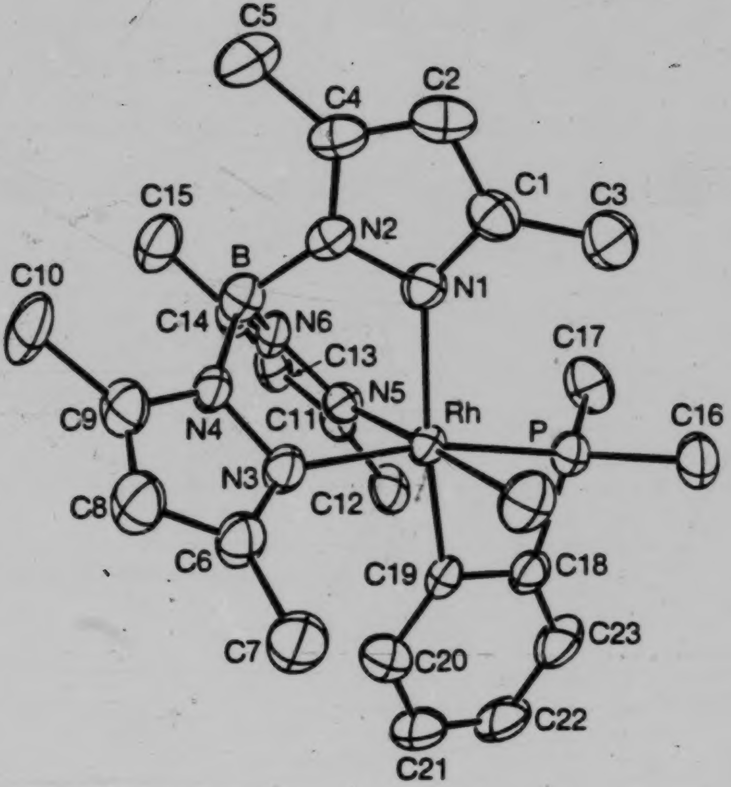
C5
C4
C2
C1
C3
C15
B
N2
N1
C10
C14
N6
C13
N5
Rh
C17
C9
N4
C11
P
C16
N3
C8
C12
C6
C19
C18
C23
C7
C20
C22
C21

Figure V.2 Molecular structure of $(HBPz^*_3)\overline{Rh(Cl)(PMe_2C}_6H_4)$ (33).

Section 3

EXPERIMENTAL

Preparation of (HBPz*$_3$)Rh(Cl)(C_6H_5)(PMe$_2$Ph) (31)

Compound **4b** (100 mg, 0.177 mmol) was irradiated in benzene (50 mL) for ca. 40 min using N_2 purge. The initial pale yellow solution was colorless at the end of irradiation. The IR indicated the presence of (HBPz*$_3$)Rh(CO)(H)(C_6H_5) (**6**) ($\nu_{CO(hexane)}$:2049 cm^{-1}) and a relatively strong ν_{Rh-H}. Excess CCl_4 (10 mL) was added to the photolyzed solution. After 1h, solvent and excess CCl_4 were removed under reduced pressure. The resulting solid was taken up in a minimum volume of CH_2Cl_2 and chromatographed on a Florisil column (10 x 2.5 cm) with 1:4 CH_2Cl_2-n-hexane eluent. Removal of solvent from this fraction afforded light yellow solid of 7 (14 mg, 15%). The remaining pale yellow band was eluted with CH_2Cl_2. The yellow solid after removal of the solvent in vacuo was dissolved in a minimum amount of CH_2Cl_2 and n-hexane was added. Slow evaporation of the solvent at room temperature yielded light yellow crystals of 31 (69 mg, 60%).

Characterization: MS (145°C, 70 eV) M^+ (650), M^+-C_6H_5, M^+-C_6H_5-Cl. ^1H NMR (CD_2Cl_2, ambient, 200 MHz) δ 7.92 (d, 1H), 7.02 (m, 7H), 6.68 (s, 1H), 6.30 (d, 1H), 5.72 (s, 1H), 5.66 (s, 1H), 5.56 (s, 1H), 2.50 (s, 3H), 2.48 (s, 3H), 2.38 (s, 3H), 2.34 (s, 3H), 2.04 (d, $^2J_{P-H}$=10.2 Hz, 3H), 1.75 (d, $^2J_{P-H}$=9.5 Hz, 3H), 1.52 (s, 3H), 1.32 (s, 3H). Anal. Calcd for $C_{29}H_{38}BClN_6PRh$.1.0 CH_2Cl_2: C, 48.95; H, 5.44; N, 11.42. Found: C, 49.01; H, 5.47; N, 11.59.

Preparation of $(HBPz^*_3)\overline{Rh(Cl)\{P(CH_3)_2C}_6H_4\}$ (33)

Compound **4b** (80 mg, 0.141 mmol) was photolyzed in "ultrapure" cyclohexane (70 mL) for _ca_. 40 min under N_2 purge. The IR indicated complete disappearance of **4b**. Excess CCl_4 (5 mL) was added to the photolyzed solution and the mixture was stirred for 1 h. Solvent and excess CCl_4 were removed under vacuum and the resulting light-yellow solid was taken up in CH_2Cl_2 and chromatographed on a Florisil column (8 x 2.5 cm) with CH_2Cl_2 as eluent. Solvent was removed _in vacuo_, and pure 33 was obtained as yellow crystals (60.7 mg, 75%) from CH_2Cl_2-_n_-hexane by slow evaporation of solvent.

Characterization: MS (110°C, 16 eV) M^+ (572), M^+-Cl, M^+-Cl-PMe_2. ^1H NMR (CD_2Cl_2, ambient, 200 MHz) δ 6.32 (m, 1H), 6.22 (m, 1H), 6.14 (m, 2H), 5.96 (s, 1H), 5.89 (s, 1H), 5.62 (s, 1H), 2.54 (s, 3H), 2.46 (s, 6H, accidental degeneracy), 2.43 (s, 6H), 2.38 (s, 3H), 2.90 (d, J_{P-H}=12.0 Hz, 3H), 1.50 d, J_{P-H}=12.0 Hz, 3H), 1.10 (s, 3H). Anal. Calcd for $C_{23}H_{32}BClN_6PRh\cdot 0.5\ CH_2Cl_2$: C, 45.85; H, 5.37; N, 13.65. Found: C, 45.48; H, 5.38; N, 13.52.

X-ray structure of 33

The X-ray crystallographic study was carried out by Dr. R.G. Ball in the Structure Determination Laboratory of this Department. This section and the Tables are adapted from his report. The computer programs used in the data analysis include the Enraf-Nonius structure determination package. Version 3 (1985, Delft, The Netherlands) rewritten for a Sun Microsystems computer and several locally written or modified programs.

A yellow crystal with approximate dimensions of 0.21 x 0.21 x 0.06 mm was used for data collection. Crystals were grown by slow evaporation of 1,2-dichloroethane and n-butyl ether at room temperature. Details of data collection are listed in Table 5.I.

The structure was solved using a three dimensional Patterson synthesis which gave the positional parameters for the Rh atom. The remaining nonhydrogen atoms were located by the usual combination of least squares refinement and difference fourier synthesis.

Refinement of atomic parameters was carried out using full-matrix least-squares techniques on F_o minimizing the function

$$\Sigma W \left(|F_o| - |F_c|\right)$$

where $|F_o|$ and $|F_c|$ are the observed and calculated structure factor amplitudes respectively, and the weighting factor W is given by

$$W = 4F_o/\sigma(F_o)$$

All hydrogen atoms were included at their idealized calculated positions, assuming C-H and B-H of 0.95A° and appropriate sp^2 and sp^3 geometries. The methyl H's were fitted by least-squares to peaks observed in a difference Fourier. These atoms were then included in the calculations with fixed, isotropic thermal parameters 1.2 times that of the attached atom and constrained to 'ride' with this atom.

In the final cycle 298 parameters wree refined using 3314 observations having $I > 3\sigma(I)$. The final agreement factors were:

$$R_1 = \Sigma \, |F_o| - |F_c| \, / \, \Sigma \, |F_o| = 0.061$$

$$R_2 = [\Sigma W \, (|F_o| - |F_c|) \, / \, \Sigma W F_o]^{1/2} = 0.071$$

The largest shift in any parameter was 0.05 times its estimated standard deviation and the error in an observation of unit weight was 1.90e. An analysis of R_2 in terms of F_o, λ^{-1} $\sin\theta$, and various combinations of Miller indices showed no unusual trends. The highest peak in the final difference fourier has a density of 2.0(1)$eA°^{-3}$, is located near the Rh atom and is without chemical significance. The structure of 33 is depicted in Fig. V.2. Relevant bond lengths and bond angles are tabulated in Tables 5.II and 5.III. Positional and thermal parameters are available in the detailed report from Structure Determination Laboratory.[10]

Table 5.I. Experimental Details

A. Crystal Data

$C_{23}H_{32}BClN_6PRh$; FW = 572.69

Crystal dimensions: 0.21 x 0.21 x 0.06 mm

monoclinic space group $P2_1/n$

a = 14.207 (5), b = 12.870 (5), c = 14.319 (4) Å

β = 101.84 (3)°

V = 2562 $Å^3$; Z = 4; D_c = 1.484 g cm^{-3}; μ = 8.44 cm^{-1}

B. Data Collection and Refinement Conditions

Radiation:	MoK_α (λ = 0.71073 Å)
Monochromator:	incident beam, graphite crystal
Take-off angle:	3.0°
Detector aperture:	2.40 mm horiz x 4.0 mm vert
Crystal-to-detector distance:	205 mm
Scan type:	ω-2θ
Scan rate:	5.0 - 1.6° min^{-1}
Scan width:	0.70 + 0.35tan(θ)°
Data collection 2θ limit:	55°
Data collection index range:	h, k, ±l
Reflections measured:	6153 unique, 3314 with I > 3σ(I)
Observations: variables ratio:	3314: 298
Agreement factors R_1, R_2, GOF:	0.061, 0.071, 1.90

Table 5.II Selected Interatomic Distances[a]

Atom1	Atom2	Distance	Atom1	Atom2	Distance	Atom1	Atom2	Distance
Rh	C1	2.341 (2)	N3	N4	1.388 (6)	C6	C8	1.385 (9)
Rh	P	2.282 (2)	N3	C6	1.343 (7)	C8	C9	1.347 (9)
Rh	N1	2.190 (5)	N4	C9	1.348 (7)	C9	C10	1.522 (9)
Rh	N3	2.131 (5)	N4	B	1.523 (8)	C11	C12	1.501 (8)
Rh	N5	2.095 (4)	N5	N6	1.388 (6)	C11	C13	1.391 (8)
Rh	C19	2.004 (6)	N5	C11	1.344 (7)	C13	C14	1.372 (8)
P	C16	1.823 (6)	N6	C14	1.341 (7)	C14	C15	1.512 (9)
P	C17	1.807 (6)	N6	B	1.543 (8)	C18	C19	1.388 (8)
P	C18	1.793 (6)	C1	C2	1.389 (9)	C18	C23	1.394 (8)
N1	N2	1.367 (6)	C1	C3	1.501 (9)	C19	C20	1.385 (8)
N1	C1	1.337 (7)	C2	C4	1.38 (1)	C20	C21	1.39 (1)
N2	C4	1.346 (8)	C4	C5	1.493 (9)	C21	C22	1.38 (1)
N2	B	1.523 (8)	C6	C7	1.480 (9)	C22	C23	1.39 (1)

[a] In angstroms. Numbers in parentheses are estimated standard deviations in the least significant digits.

Table 5.III Selected Interatomic Angles[a]

Atom1	Atom2	Atom3	Angle
Cl	Rh	P	85.67 (6)
Cl	Rh	N1	91.3 (1)
Cl	Rh	N3	90.6 (1)
Cl	Rh	N5	176.9 (1)
Cl	Rh	C19	89.8 (2)
P	Rh	N1	103.7 (1)
P	Rh	N3	168.5 (1)
P	Rh	N5	97.2 (1)
P	Rh	C19	69.4 (2)
N1	Rh	N3	87.3 (2)
N1	Rh	N5	89.1 (2)
N1	Rh	C19	172.9 (2)
N3	Rh	N5	86.3 (2)
N3	Rh	C19	99.7 (2)
N5	Rh	C19	90.2 (2)
Rh	P	C16	125.4 (2)
Rh	P	C17	123.5 (2)
Rh	P	C18	83.8 (2)
C16	P	C17	100.2 (3)
C16	P	C18	108.7 (3)
C17	P	C18	113.8 (3)
Rh	N1	N2	116.8 (4)
Rh	N1	C1	136.5 (4)
N2	N1	C1	106.7 (5)
N1	N2	C4	110.1 (5)
N1	N2	B	118.3 (5)
C4	N2	B	131.5 (5)
Rh	N3	N4	115.8 (3)
Rh	N3	C6	136.9 (4)
N4	N3	C6	106.4 (4)
N3	N4	C9	108.2 (4)
N3	N4	B	120.2 (4)
C9	N4	B	131.1 (5)
Rh	N5	N6	114.7 (3)
Rh	N5	C11	139.4 (4)
N6	N5	C11	105.8 (4)
N5	N6	C14	109.5 (4)
N5	N6	B	121.7 (4)
C14	N6	B	128.5 (5)
N1	C1	C2	109.7 (6)
N1	C1	C3	121.8 (6)
C2	C1	C3	128.4 (6)
C1	C2	C4	106.1 (6)
N2	C4	C2	107.4 (6)
N2	C4	C5	124.2 (7)
C2	C4	C5	128.4 (6)
N3	C6	C7	123.6 (6)
N3	C6	C8	109.6 (6)
C7	C6	C8	126.7 (6)
C6	C8	C9	106.5 (5)

C

Table 5.III Contd ...

Atom1	Atom2	Atom3	Angle
N4	C9	C8	109.3 (5)
N4	C9	C10	120.5 (6)
C8	C9	C10	130.1 (6)
N5	C11	C12	126.7 (5)
N5	C11	C13	110.3 (5)
C12	C11	C13	122.9 (5)
C11	C13	C14	105.6 (5)
N6	C14	C13	108.8 (5)
N6	C14	C15	123.4 (6)
C13	C14	C15	127.8 (6)
P	C18	C19	100.0 (4)
P	C18	C23	136.4 (5)
C19	C18	C23	123.5 (6)
Rh	C19	C18	106.7 (4)
Rh	C19	C20	134.8 (4)
C18	C19	C20	118.2 (5)
C19	C20	C21	119.3 (6)
C20	C21	C22	121.6 (7)
C21	C22	C23	120.2 (6)
C18	C23	C22	117.2 (6)
N2	B	N4	109.5 (5)
N2	B	N6	110.1 (5)
N4	B	N6	109.8 (5)

---

[a] In degrees. Numbers in parentheses are estimated standard deviations in the least significant digits.

References for Chapter V

1. M.A. Bennett and D.L. Milner, Chem. Commun., (1967) 581.
2. W. Keim, J. Organomet. Chem., 14 (1968) 179.
3. W.H. Knoth and R.A. Schunn, J. Am. Chem. Soc., 91 (1969) 2400.
4. J.J. Levison and S.D. Robinson, J. Chem. Soc., (A) (1970) 639.
5. E.W. Ainscough, S.D. Robinson and J.J. Levison, J. Chem. Soc. (A) (1971) 3413.
6. H. Kletzin and H. Werner, Agnew. Chem., Int. Ed. Eng., 22 (1983) 873.
7. A.H. Janowicz and R.G. Bergman, J. Am. Chem. Soc., 105 (1983) 3929.
8. J. Halpern, Inorg. Chim. Acta. 100 (1985) 41.
9. W.D. Jones and F.J. Feher, J. Am. Chem. Soc., 107 (1985) 620.
10. R.G. Ball, University of Alberta, Structure Determination Laboratory, Report No. SR: 07801-13-87 (8 Oct. 1987).

CHAPTER VI

OLEFIN COMPLEXES

Section 1

INTRODUCTION

Olefins are ligands in numerous transition metal compounds. Olefin complexes are involved in many reactions which are promoted or catalyzed by transition metal compounds. These include alkene hydrogenation, dimerization, polymerization, cyclization, hydrocarbonylation, hydrocyanation etc.

The two major classes of bis(olefin) rhodium(I) complexes are: i) the four-coordinate, 16-electron 2,4-pentanedionato derivative (acac)Rh$(C_2H_4)_2$, and (ii) five-coordinate, 18-electron, η-cyclopentadienyl complex $(\eta^5-C_5H_5)Rh(C_2H_4)_2$. The hydrotris (pyrazol-1-yl)borato bis(ethylene)rhodium(I), $(HBPz_3)Rh(C_2H_4)_2$ is a bridge between the above two groups. It might exist as a four-coordinate, 16-electron square planar rhodium(I) complex, or as a trigonal bipyramidal five-coordinate 18-electron species. However, a four-coordinate 16-electron structure was favoured by Trofimenko[1a] (as has been discussed in Chapter II). Similarly, a four-coordinate square planar geometry was preferred for hydrotris (3,5-dimethylpyrazol-1-yl)borato bis(cyclooctadiene) rhodium(I), $(HBPz^*_3)Rh(COD)$.[1b]

More recently, Cocivera et al.[2,3,4] have studied Rh(I) complexes of the type (BPz_4)Rh(diene) where BPz_4 signifies tetrakis (1-pyrazolyl) borate ion and diene signifies duroquinone (dq), 1,5 cyclooctadiene (cod), or norbornadiene (nbd). The x-ray crystal structures[3] showed that the dq complex is pentacoordinate whereas the cod and nbd complexes are four-coordinate. The question of coordination number in solution was studied by means of ^1H NMR[4] and it was suggested that the dq and cod complexes were pentacoordinate; i.e, three pyrazolyl groups of BPz_4 are bound to rhodium via nitrogen.

From the point of view of carbon-hydrogen activation by olefin complexes, an interesting report of deuterium exchange between benzene-d_6 and $(\eta^5\text{-}C_5H_5)Rh(C_2H_4)_2$ appeared in 1974.[5] A phenyl hydride intermediate formed by ethylene loss was proposed to account for the exchange. The proposed mechanism is illustrated in Fig. VI.1.

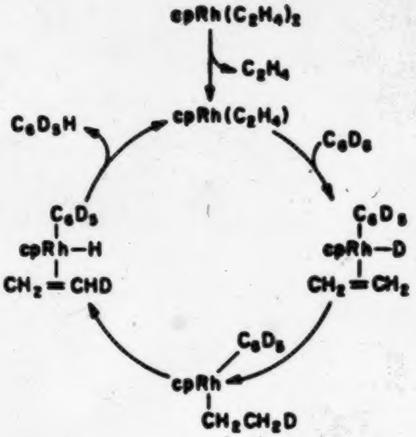

Figure VI.1 Mechanism for exchange betwen benzene-d_6 and coordinated ethylene in $(\eta\text{-}C_5H_5)Rh(C_2H_4)_2$.

Since then no report on C-H activation using olefin complexes has appeared in the literature.

Mixed carbonyl-olefin complexes containing pyrazolylborate ligands have not been reported. Thus synthesis of carbonyl-olefin complexes, $(HBPz^*_3)Rh(CO)(olefin)$ was of interest. Synthesis, properties and fluxional behaviour of these complexes will be discussed in this Chapter. In addition, novel photochemical and thermal reactions of the mixed carbonyl-olefin complexes with hydrocarbons leading to C-H activation will be described. Finally, as an extension of the investigation, functionalization of C-H activation products has been explored.

Section 2

SYNTHESIS AND PROPERTIES OF OLEFIN COMPLEXES

η^2-ethylene complex

The mixed carbonyl-ethylene complex, $(HBPz^*_3)Rh(CO)(\eta^2\text{-}C_2H_4)$ (**34a**) was prepared by reacting $K[HBPz^*_3]$ with the known binuclear mixed complex $[(\mu\text{-}Cl)Rh(CO)(\eta^2\text{-}C_2H_4)]_2$ in the dark (eq. 6-1).

$$K[HBPz^*_3] + [(\mu\text{-}Cl)Rh(CO)(C_2H_4)]_2 \xrightarrow[\text{Toluene}]{\text{RT}} \underset{\textbf{34a}}{(HBPz^*_3)Rh(CO)(\eta^2\text{-}C_2H_4)} \qquad (6\text{-}1)$$

During reaction (eq. 6-1), a small amount of $(HBPz^*_3)Rh(CO)_2$ (1) formed along with the desired product **34a**. **34a** was isolated as a pale yellow crystalline solid in 64% yield after chromatographic purification and characterized by MS, IR, NMR spectroscopy and microanalysis.

As expected, the IR exhibited a single ν_{CO} at 2013 cm^{-1} in n-hexane. The ^1H NMR spectrum at room temperature indicated three equivalent Pz* rings, suggesting that one or more fluxional processes averages all three Pz* resonances. The resonance due to 4-H of the Pz* rings appeared as a broad singlet at δ 5.83(3H). At the same time a broad singlet was found at δ 2.36 due to the 3-CH_3 and 5-CH_3 ring protons. Two resonances were observed for olefinic protons, one as a broad singlet at δ 3.24 and the other ($\delta \sim 2.47$) overlapping the pyrazolyl methyl resonances.

On cooling to -60°C, the 4-H resonance splits into signals at δ 5.90 and 5.60 in a 2:1 ratio. At the same time the peak at δ 2.36 splits into four signals of intensity ratio 6:6:3:3. The olefinic resonance at δ 3.24 appeared as a doublet (J=8.5 Hz), while the resonance at ~δ 2.47 remains partly obscured by the methyl resonances of the ring. Thus at -60°C, two Pz* rings are equivalent and one is unique on the NMR timescale. This result is similar to that observed in the low temperature ^1H NMR spectrum of $(HBPz^*_3)Rh(CO)(PMe_2Ph)$ (**4b**) in Chapter II, and the interpretation is similar.

A distinction between η^2 and η^3 coordination in **34a** is not readily made by ^1H NMR, partly owing to this fluxional behaviour. The best approach is to compare the ν_{CO} of **34a** with that of the related $(H_2BPz^*_2)Rh(CO)(C_2H_4)$, which is necessarily 16-electron square planar. Accordingly, the bis-pyrazolylborate complex, $(H_2BPz^*_2)Rh(CO)(C_2H_4)$ was prepared by reacting $K[H_2BPz^*_2]$ with $[(\mu\text{-}Cl)Rh(CO)(\eta^2\text{-}C_2H_4)]_2$ in n-hexane at room temperature. The hexane solution immediately after the reaction (no purification was attempted) exhibited ν_{CO} at 2012 cm^{-1}, which is almost identical to ν_{CO} of **34a** (2013 cm^{-1}). Unfortunately $(H_2BPz^*_2)Rh(CO)(C_2H_4)$ could not be fully characterized owing to its fairly rapid disproportionation to $(H_2BPz^*_2)Rh(CO)_2$ in solution at room temperature. The comparison of ν_{CO} shows that η^2-ethylene complex (**34a** is four-coordinate in solution.

The ^1H NMR spectrum corresponding to a static, square planar structure with an η^2-$HBPz^*_3$ ligand should exhibit three nonequivalent Pz* rings (barring accidental degeneracies). As was the case for the monophosphine derivatives, this low temperature limiting spectrum was not observed down to -90°C.

The variable temperature spectra can similarly be explained on the basis of two kinds of fluxional process. The high temperature process that averages all Pz* resonances at ambient temperature can be frozen at

-60°C to 2:1 ratio of Pz* signals. The low temperature process, which averages the two equatorial Pz* rings which are trans to different ligands has not been frozen out even at -90°C. To account for the observed equivalence of the two equatorially bonded Pz* rings in the low temperature fluxional process, a trigonal bipyramidal intermediate having a plane of symmetry is again proposed. It does not matter which ligand, CO or C_2H_4, enters the axial position, because at that point the plane of symmetry has made Pz*(1) equivalent to Pz*(2).

For the carbonyl-phosphine complexes, evidence consistent with the postulated trigonal bipyramidal intermediate for the low temperature fluxional process came from NMR studies of the chiral monophosphine derivative (**4e**), which showed three nonequivalent Pz* rings in the low temperature ^1H NMR spectrum.

A similar reasoning can be applied to an olefin ligand, recognizing that a chiral center is generated when one face of an olefin such as propylene is coordinated to a transition metal.[6] Such a chiral center would not produce a plane of symmetry in the proposed trigonal bipyramidal intermediate; the equatorial pyrazoles would be rendered diastereotropic by the chiral center.

Accordingly, the synthesis of the propylene complex $(HBPz^*_3)Rh(CO)(CH_2{=}CHCH_3)$ was of interest. It appeared that **34b** would possess a chiral center and at the same time represent only a slight perturbation on the original molecule (**34a**). Moreover, it would still have an uncluttered NMR spectrum. In the $(acac)Rh(olefin)_2$ system, substituted ethylenes are 100-1000 times less stable (in terms of equilibrium constant) than ethylene itself.[7] From the viewpoint of this reduced binding energy, **34b** was also considered to be a candidate for thermal carbon-hydrogen activation.

η^2-propylene complex

The complex $(HBPz^*_3)Rh(CO)(\eta^2\text{-}CH_2CHCH_3)$ (**34b**) was prepared by photolysis using a propylene purge of a cyclohexane solution of $(HBPz^*_3)Rh(CO)_2$ (**1**). Immediately after irradiation, the IR in cyclohexane exhibited ν_{CO} at 2040 cm^{-1} (with a small shoulder). As the cyclohexane solution stood in the dark at room temperature, a new ν_{CO} appeared at 2006 cm^{-1}, while the band at 2040 cm^{-1} slowly disappeared. The 2040 cm^{-1} band had completely disappeared in ca 48 hours. The band at 2040 cm^{-1} is assigned to the allylic hydride $(HBPz^*_3)Rh(CO)(H)(H_2CCH{=}CH_2)$ (**35**), while **34b** accounts for ν_{CO} at 2006 cm^{-1}. The IR indicated a quantitative conversion of $(HBPz^*_3)Rh(CO)_2$ (**1**). A plausible mechanism for the formation of **34b** is shown below.

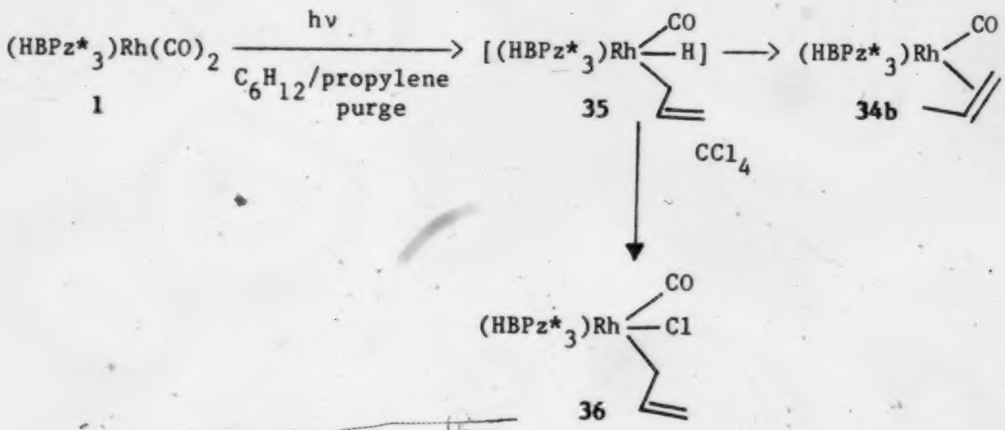

The proposed intermediate (**35**) was converted by reacting with CCl_4 to the stable chloro derivative (**36**) for characterization. Carbon tetrachloride was added to the photolyzed solution with minimum delay and the reaction was complete in an hour. The IR band at 2077 cm^{-1} (n-hexane) suggested **36** as the major product. A minor band at 2117 cm^{-1} (n-hexane) was presumed to be due to $(HBPz*_3)Rh(CO)(Cl)_2$. Compound **36** was isolated as a yellow crystalline solid after chromatography and crystallization.

The identity of **36** was confirmed by MS, IR, NMR methods and elemental analysis. As expected the ^1H NMR spectrum showed three nonequivalent Pz* rings. In the allylic region, H_a

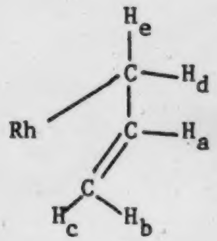

appeared as a multiplet at δ 6.40; two doublets of doublets were found for H_b and H_c at δ 5.36 (J_{bc}=10.0 Hz, J_{ba}=2.2 Hz) and 5.00; two triplets were observed for H_d and H_e at δ 3.85 and 3.55.

The intermediate **35** is somewhat surprising. One might have expected the vinyllic isomer $(HBPz*_3)Rh(CO)(H)(CH=CHCH_3)$ as the intermediate since the sp^2C-Rh bond would be stronger. Moreover, one cannot rule out the possibility of rearrangement in the CCl_4 reaction.

The rate of isomerization of **35** to **34b** was studied at room temperature (ca. 25°C). It appeared most convenient to monitor the rate of growth of ν_{CO} band (2006 cm^{-1}) of the product being formed (**34b**). It followed first order kinetics over three half lives. The rate constant was found to be $k = (1.4\pm0.1) \times 10^{-4}\ s^{-1}$, which gives the half life of the isomerization as $t_{1/2}$ = 84 min at 25°C.

Addition of a slight excess of benzene to a freshly prepared cyclohexane solution of 35 did not produce any detectable amount of $(HBPz^*_3)Rh(CO)(H)(C_6H_5)$ (**6**), instead **35** was converted to **34b** in the usual fashion. This suggests that conversion of 35 to **34b** is intramolecular. If **35** had the η^1-allyl hydride structure, it might have been expected to react with benzene (cf. the reaction of the cyclohexyl hydride 17). This observation may indicate an η^3-allyl structure.

The η^2-propylene complex **34b** was isolated as a pale yellow solid in ca. 90% yield. It does not survive chromatography, but the synthesis was clean enough that pure product was obtained by removing cyclohexane under vacuum. Solid **34b** is quite stable, and was fully characterized. The ^1H NMR at ambient temperature showed three equivalent Pz* rings indicating fluxional behaviour. The methyl resonance of propylene was found at δ 1.70 (dd J=6.2 Hz and J=2.0 Hz). The resonance due to the $C\underline{H}$ proton appeared as a multiplet at δ 4.05. The $C\underline{H_2}$ resonances overlapped with the Pz* methyl resonances. The ^1H NMR spectrum at -60°C indicated three nonequivalent Pz* rings as expected from the foregoing discussion. This NMR result is also consistent with the trigonal bipyramidal intermediate previously invoked to explain the low temperature fluxional process observed for **34a**.

Energy barrier of the fluxional process in 34a

The energy barrier of the fluxional process that can be slowed at -60°C was of interest. This has been referred to as the high temperature averaging process.

A spin saturation transfer (SST) experiment was carried out on the ethylene complex **34a**. A brief description of SST experiment has been provided in Chapter II. As pointed out earlier, two sets of Pz* resonances with an intensity ratio 2:1 were found in the low temperature ^1H NMR spectrum of **34a**. Confirmation of site exchange was obtained by saturating the resonance due to 4-H of the unique Pz* ring (δ 5.58(1H)) in the temperature range -40 to -60°C. The intensity of the 4-H signal due to the two equivalent Pz* ring (δ 5.88(2H)) decreased significantly, indicating that the two equivalent Pz* rings were exchanging with the unique one. Similarly, saturation of the resonance at δ 5.88 resulted in a decrease in intensity of the resonance at δ 5.58.

The decrease in signal intensity due to partial spin transfer was quantitatively measured by integration of a difference spectrum against an internal standard. The experiments were carried out at -40°C, -50°C and -60°C. Rate constants were derived from the decrease in signal intensity of the proton to which spin saturation is transferred, and a knowledge of its T_1 value. The SST data along with the derived rate constants are summarized in Table 6.I.

An Eyring plot of the rate constants from Table 6.I is shown in Fig. VI.2. Using data of 2H site, the activation parameters obtained for the exchange process are $\Delta H^{\ddagger} = 10.7 \pm 0.2$ kcal mol^{-1}, $\Delta S^{\ddagger} = -14.0 \pm 1.0$ eu. Using data of 1H site, the values obtained are $\Delta H^{\ddagger} = 8.70 \pm 0.03$ kcal mol^{-1}, $\Delta S^{\ddagger} = -22.60 \pm 0.13$ eu.

The exchange rate of Pz* rings was also determined in a higher temperature range (0 to -20°C) by measurement of line broadening. The line width of resonance due to 4-H of Pz* ring [δ5.88(2H)], internal standard (hexamethyldisiloxane), excess line width and rate constants at different temperatures are given in Table 6.II.

Table 6.I Spin Saturation Transfer Data for $(HBPz^*_3)Rh(CO)(\eta^2\text{-}C_2H_4)$ (34a)

Temp (K)	Saturation at δ5.88		Saturation at δ5.58		T_1 (s) 2H site δ5.88	T_1 (s) 1H site δ5.58	k (s^{-1})[c] 2H site x 10^2	k (s^{-1})[d] 1H site x 10^2
	M_z^{∞} [a]	$M_z^{o}-M_z^{\infty}$ [b]	M_z^{∞}	$M_z^{o}-M_z^{\infty}$				
213	0.797	0.243	1.781	0.297	3.361	2.836	4.960	5.374
223	0.499	0.498	1.227	0.822	3.943	3.487	16.989	14.308
233	0.252	0.774	0.656	1.365	4.442	4.285	46.838	34.445

[a] M_z^{∞} is the equilibrium magnetization with saturation at other site.

[b] M_z^{o} is the normal magentization without saturation.

[c] $k = \frac{1}{T_1}\left[\frac{M_z^{o} - M_z^{\infty}}{M_z^{\infty}}\right]$ where T_1 is the relaxation time for the nucleus.

[d] Calculated k dividing by 2 to express as rate for transfer to one of the other sites.

Table 6.II

Line Broadening Data for $(HBPz^{*}_{3})Rh(CO)(\eta^{2}-C_{2}H_{4})$ (34a)

Temp (K)	Line width[a] int. std.[c] (Hz)	Line width[a] δ 5.88 (2H) (Hz)	Excess line width (Δ)	k (s^{-1})[b]
253	0.875	3.700	2.825	8.87
258	0.813	4.950	4.135	12.99
263	0.625	7.050	6.425	20.18
268	0.675	10.250	9.575	30.08
273	0.875	15.250	14.375	45.16

[a] Full line width at half height of the peak.

[b] Determined from the equation $k = \pi \times \Delta$.

[c] Internal standard is hexamethyldisiloxane.

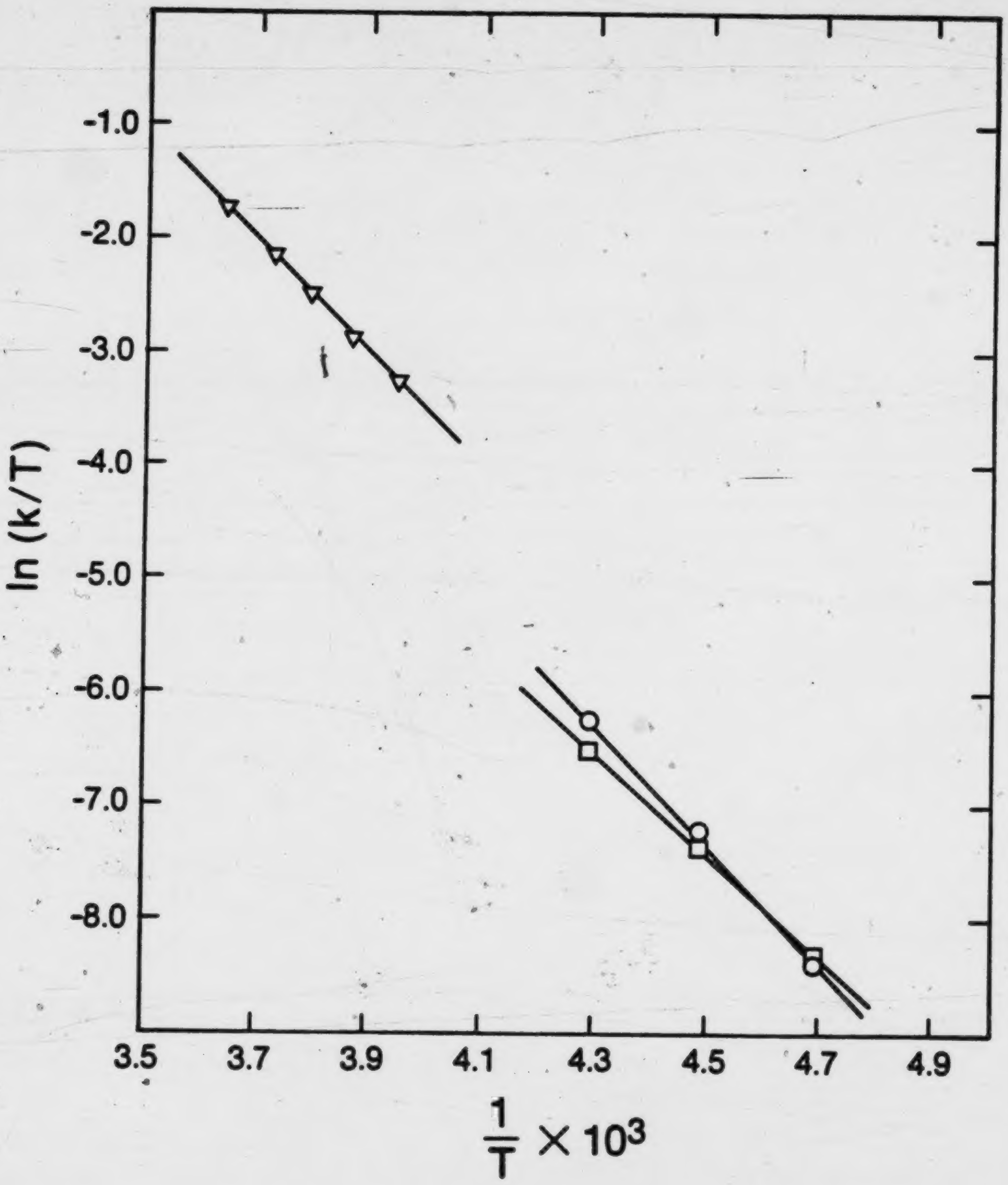

Figure VI.2 Eyring plot of ^{1}H rate constant data for (η^2-HBPz*$_3$)Rh(CO)(η^2-C_2H_4) (34a). O, 2H site (SST); □, 1H site (SST); Δ, 2H site (line broadening).

An Eyring plot of the rate constants is shown in Fig. VI.2. Values of activation parameters obtained $\Delta H^{\ddagger} = 10.70\pm0.2$ kcal mol^{-1}, $\Delta S^{\ddagger} = -12.0\pm1.0$ eu. The values don't compare terribly well, but this may not be surprising considering small temperature range and small number of points.

η^2-cyclohexene complex

Examples of η^2-cyclohexene complexes of transition metals are rare. Angelici and Loewen[8] studied the stability of a series of $(C_5H_5)Mn(CO)_2$(olefin) complexes, and reported that attempted preparations of the cyclohexene complex did not even give spectroscopic evidence for its formation. An interest in weakly bonded ligands that would dissociate thermally and activate C-H bonds at lower temperature led to an investigation of cyclohexene complexes of the pyrazolylborate rhodium system.

In this work, some spectroscopic evidence has been found for the formation of $(HBPz^*_3)Rh(CO)(\eta^2$-cyclohexene) during the reaction of $(HBPz^*_3)Rh(CO)(H)(C_6H_{11})$ (**17**) with cyclohexene. This reaction is interesting but complex in nature.

When a slight excess of cyclohexene was added to a freshly generated cyclohexane solution of cyclohexyl hydride (**17**), the IR exhibited three new ν_{CO} bands at 2043, 2037 and 1996 cm^{-1}. The IR also indicated that a small amount of $(HBPz^*_3)Rh(CO)(H)(C_6H_5)$ (**6**, ν_{CO} 2048 cm^{-1}) was present. The cyclohexane solution was allowed to stand at room temperature for several hours; no noticeable change in the ratio of the three bands was found during this time. Removal of solvent yielded a light yellow solid (**37**).

Elemental analysis (C, H, N) on this yellow solid gave results in fair agreement with the composition $(HBPz*_3)Rh(CO)(C_8H_{14})$. The spectroscopic data discussed below indicate that **37** is a mixture (possibly an equilibrating mixture) of three isomers. No purification was possible, so the sample studied contains a small quantity of **6**, no doubt formed from the cyclohexyl hydride. The IR of **37** in a KBr disc showed ν_{CO} at 2040 (br) and 1990 cm^{-1}, while the IR in n-hexane indicated three bands at 2044, 2039 and 1997 cm^{-1}. The 2044 and 2039 cm^{-1} bands appeared as a doublet with 2039 cm^{-1} a little stronger. Visual estimation suggestd that the combined absorbance of these two bands was about the same as that of the 1997 cm^{-1} band.

The 1997 cm^{-1} band of mixture **37** is close to that of the ethylene and propylene complexes **34a** (2013 cm^{-1}) and **34b** (2007 cm^{-1}) and to that of the well-characterized cyclooctene complex[9] $(HBPz*_3)Rh(CO)(\eta^2$-cyclooctene) at 2001 cm^{-1}. On the IR evidence, it is reasonable to suggest that this component of **37** is in fact the η^2-cyclohexene complex $(HBPz*_3)Rh(CO)(\eta^2$-cyclohexene) which will be referred to as **37a**. ^1H NMR studies discussed below are consistent with this.

The other two IR bands (2044 and 2039 cm^{-1}) are high enough to suggest a rhodium (III) complex; compare, for example the phenyl hydride **6** (ν_{CO} 2049 cm^{-1}) and the proposed intermediate allyl hydride **35** (ν_{CO} 2040 cm^{-1}). ^1H NMR spectroscopy, discussed below is consistent in showing that two hydridorhodium species are present in mixture **37** (in addition to the known impurity **6**). These two hydridorhodium (III) species will be referred to as **37b** and **37c**, but their identity is not clear from the evidence presently available.

The ^1H NMR spectrum of **37** will be discussed next. The regions of interest will be the metal hydride region, the pyrazole 4-H region, and the olefinic region. Spectra were run in toluene-d_8, and samples were kept frozen except during runs to avoid a slow room temperature reaction with the solvent (see below). The hydride region at ambient temperature consisted of a broad resonance centered at δ-12.45, and the sharp doublet of impurity **6** (δ-13.04, J=18.5 Hz in this solvent). At -80°C, three sharp doublets were observed at -12.13 (J=21.3 Hz), -12.45 (J=22.2 Hz) and -12.83 (J=18.8 Hz; **6** with a slight temperature shift). Integrals of these peaks are in a ratio of 9:5:3, respectively. It is clear that the "major" (**37b**) and "minor" (**37c**) unknown hydride species are interconverting, and that the rate is such as to produce coalescence near room temperature.

The room temperature averaging of hydride signals affects the Pz* 4-H region; and the η^2-cyclohexene complex **37a** believed to be present should, like the well characterized η^2-olefin complexes discussed earlier, exhibit a single 4-H signal at ambient temperature which goes to two in a 2:1 ratio at low temperature. In fact, the 4-H region is quite simple at ambient temperature: three peaks at δ 5.65, 5.53 and 5.43 (relative ratio ca. 8:35:7). At -85°C, this region of the spectrum is quite complex, exhibiting no less than 13 peaks; it is reproduced in Fig. VI.3. These signals can be grouped or assigned up to a point, keeping in mind that a complex of the type $(HBPz^*_3)Rh(CO)(H)(R)$ will have three 4-H resonances in its static form.

Assignments are fairly unambiguous for the η^2-cyclohexene complex **37a**, peaks at δ 5.70 and 5.11 (2:1 ratio) are designated "a" in Fig. VI.3. The broader peak at δ 4.55 is likely due to the olefinic protons in **37a**. In the η^2-cyclooctene complex[9] the olefinic protons showed

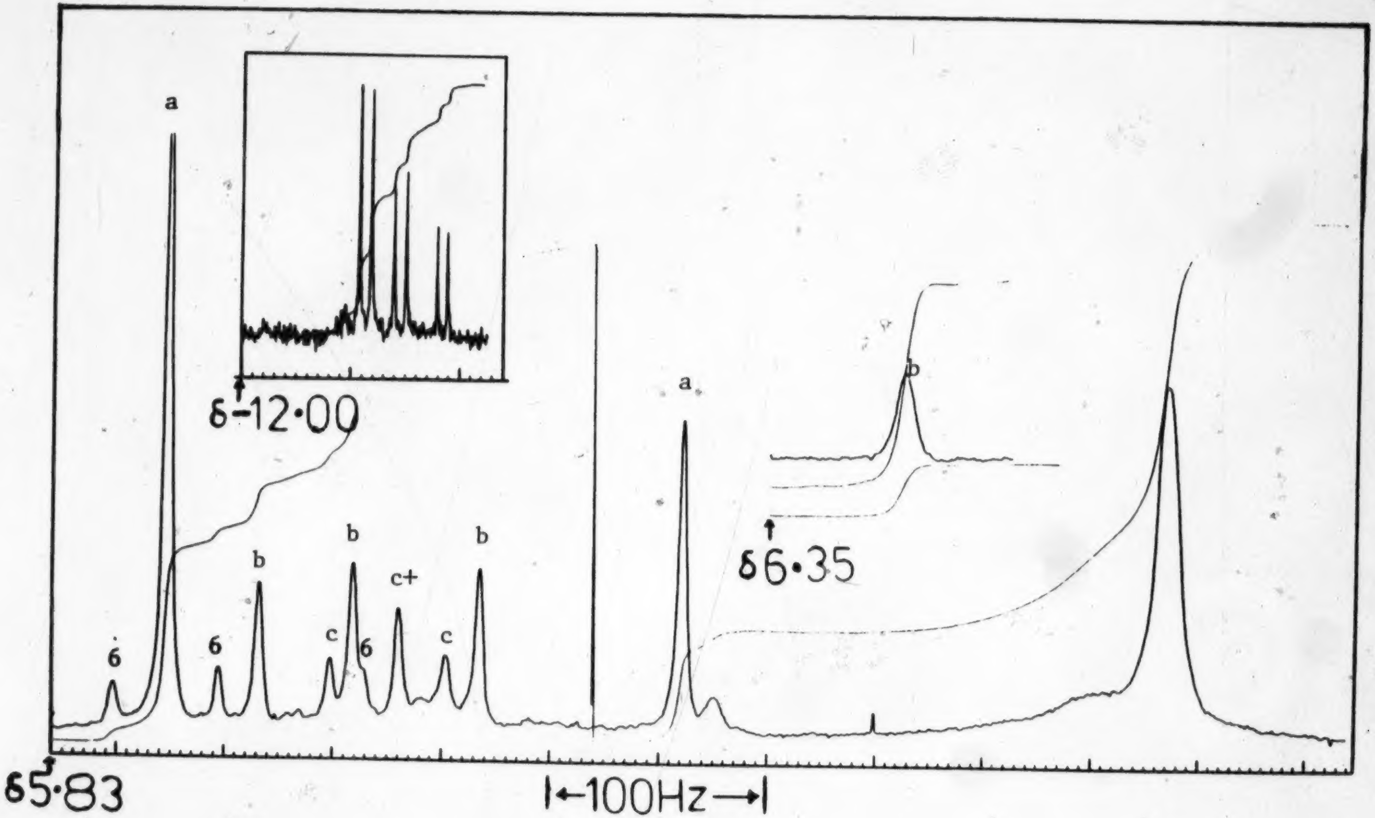

Figure VI.3 ^1H NMR (400 MHz, CD_2Cl_2) spectrum of $(HBPz^*{}_3)Rh(CO)(C_8H_{14})$ (37) at -85°C. Insert shows the hydride resonances.

J=7.7 Hz to rhodium; this coupling is not resolved for **37a** at −85°C. However, at 20°C, the δ 4.51 peak of **37a** is a symmetrical multiplet (quartet or dd) that could involve J_{Rh-H}.

The 4-H protons of **37b** (major hydride) and **37c** (minor hydride) may be assigned, keeping in mind that a complex of the type $(HBPz^*_3)Rh(CO)(H)(R)$ should have three 4-H signals of equal intensity in its static form. These are marked "b" and "c" in Fig. VI.3. 4-H peaks due to impurity **6** are marked as such.

The unsettled question about the two hydride species is the nature of the "R" group. Two possibilities are the cyclohexen-1-yℓ and cyclohexen-3-yl (vinylic and allylic) isomers.

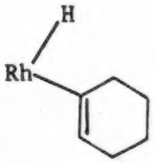

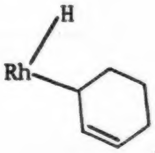

Isomers having rhodium bonded to the cyclohexene 4 (or 5) carbon atom are considered unlikely because cyclohexyl-like instability might be expected.

A distinction between these bonding modes or a clue to other possibilities should be possible on the basis of the olefinic protons in the NMR. Unfortunately, that region is somewhat ambiguous due to possible overlap with the Pz* 4-H region. In the spectrum three signals can be assigned with reasonable confidence to olefinic protons of the hydrido complexes. That at δ 6.19 appears from its intensity to be associated with major isomer **37b**. On the same grounds a peak at δ 5.07 seems to belong with **37c**. Intensity considerations for the δ 5.43 peak suggest it may involve accidental degeneracy of 4-H and an olefinic proton of **37c**. Integrations of these closely spaced resonances are unreliable. This uncertain and possibly incomplete information simply does not permit a decision as to the mode or modes of attachment of the cyclohexenyl group.

Section 3

THERMAL C-H ACTIVATION

Thermolysis in benzene

No example has been reported in which a carbon-hydrogen bond oxidatively adds to a stable coordinatively unsaturated complex (i.e. undergoes activation) in the way that dihydrogen adds to $ClIr(CO)(PPh_3)_2$.[10] The difference can perhaps be rationalized in terms of relative bond energies, although values of D[M-H] and D[M-C] remain for the most part uncertain.[11] The energetics of C-H activation are even less attractive when a metal-ligand bond must be broken, as in eq. 6-2.

$$L_nM + RH \longrightarrow L_{n-1}M(H)(R) + L \qquad (6\text{-}2)$$

Consistent with this view, activations of C-H bonds have generally required photolysis.[12] Two exceptions have very recently been reported. Chetcuti and Hawthorne[13] observed activation of benzene by $(C_5Me_5)Ir(CO)(\eta^2\text{-}NCC_6H_4Cl)$ at 50°C with thermal loss of the side-bonded nitrile ligand. After five weeks reaction the yield was 90%. Another example of thermal benzene activation was by the presumed 14-electron intermediate $IrCl\{P(\underline{i}\text{-}Pr)_3\}_2$ at 80°C in 58% yield.[14]

Investigation of trispyrazolylborate rhodium complexes has shown that $(HBPz^*_3)Rh(CO)(\eta^2\text{-olefin})$ (**34a** and **34b**) activate benzene in the dark in a closed system forming $(HBPz^*_3)Rh(CO)(H)(C_6H_5)$ (**6**) in high yield at temperatures from 75-105°C (eq. 6-3). This provides another example of thermal C-H activation with loss of an electron pair donor ligand. It is the first example where the ligand is an olefin.

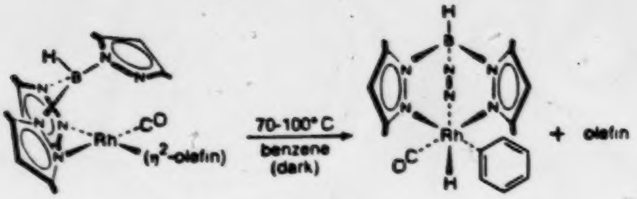

(6-3)

34a: olefin = C_2H_4

34b: olefin = CH_2CHCH_3

For **34a** (13.2 mM), the reaction was complete in five days at 105°C, and the yield of **6** was 89% (NMR). In case of **34b** (29.8 mM), **6** formed in 94% yield (NMR) at 75°C in 45 hours. It appeared that **34b** reacted faster than **34a**, which can be related to the weaker attachment of propylene to rhodium.[7] Free ethylene and propylene were detected in the products by NMR for **34a** and **34b** respectively.

From the discussions in Section 1, it is likely that **34a** and **34b** exist in solution as the four-coordinate, 16-electron Rh(I), sketched in eq. 6-3, while there is little question of the tridentate character of $HBPz^*_3$ ligand in the Rh(III) product (**6**). Thus in the overall energetics, formation of a new Rh-N bond partly offsets the loss of the Rh-olefin bond. This may be a significant factor in the effectiveness of trispyrazolylborate system in C-H activation.

It was surprising in light of the introductory discussion that the activation of eq. 6-3 proceeded thermally to a measureable extent. Initially, the reaction of **34a** with benzene was carried out with intermittent pumping down to monitor progress; this would have removed ethylene and displaced the equilibrium. However, the reaction was nearly complete in about the same time when the container was kept closed so that released ethylene would have accumulated. This means that K_{eq} for the reaction is not very small. The reaction of **34b** in cyclohexane at 75°C with a tenfold molar excess of benzene proceeded nearly to completion but at a slower rate (ca. eight days) than that in pure benzene under similar conditions.

Interestingly, Rodgers[9] determined the equilibrium at 100°C for the reaction (eq. 6-4)

$$(HBPz^*_3)Rh(CO)(\eta^2\text{-cyclooctene}) + C_6H_6 = \mathbf{6} + \text{cyclooctene} \qquad (6\text{-}4)$$

as 0.016. $K_{eq} = 0.016$ implies that $\Delta G°_{373} = 3.1$ kcal. Rodgers[9] has also measured the activation enthalpy for the reaction in eq. 6-4 as 35.4 Kcal, which sets an upper limit for D[Rh-COE]. Assuming that $\Delta S° \cong 0$, $\Delta H° \cong \Delta G°_{373} = 3.1 \text{ kcal} < D[\text{H-Ph}]^{15} + D[\text{Rh-COE}] - D[\text{Rh-H}] - D[\text{Rh-Ph}] = 110 + 35.4 - D[\text{Rh-H}] - D[\text{Rh-Ph}]$, so that

$$D[\text{Rh-H}] + D[\text{Rh-Ph}] < 142 \text{ kcal}$$

This treatment neglects the potentially important formation of the third pyrazole-rhodium linkage in the product, which as noted above would offset to some degree the loss of the olefin-rhodium bond. The larger the contribution of this ligand reorganization, the further

{D[Rh-H] + D[Rh-Ph]} will fall below the stated upper limit. For comparison, the strengths of generic first-row transition metal-hydrogen and - carbon bonds have been estimated at 60 and 30 kcal, respectively;[11] while in the $(C_5Me_5)Ir(PMe_3)(H)(R)$ series, {D[Ir-H] + D[Ir-Ph]} = 154.8 kcal.[16]

Thermolysis in cyclohexane

Thermolysis of **34b** was carried out in pure cyclohexane at 75°C in the dark. After eight days, the reaction was complete and a new binuclear species had formed. In the initial stage of thermolysis a small amount of $(HBPz^*_3)Rh(CO)(H)(C_6H_5)$ (**6**) formed, which slowly disappeared with the progress of reaction. In a separate experiment, a cyclohexane solution of **6** was heated at 75°C and found to be converted to the same binuclear species. As discussed in Chapter IV, **6** is presumed to be formed from the primary solvent activation product $(HBPz^*_3)Rh(CO)(H)(C_6H_{11})$ (**17**). Moreover, the presence of cyclohexene in the products suggested solvent activation.

The binuclear species was isolated as yellow microcrystals after chromatography and crystallization. Its IR in n-hexane indicated a terminal and a bridging ν_{CO} at 2039 and 1860 cm^{-1} respectively. The MS gave the heaviest fragment at m/e 856, which corresponds to $[(HBPz^*_3)Rh(CO)]_2$. Elemental analysis is consistent with the formulation $[(HBPz^*_3)Rh(CO)]_2$. The ^1H NMR showed a high field hydride resonance at δ-18.00, a much higher field than the terminal Rh-H observed in mononuclear pyrazolylborates. This suggested a bridging hydride, and this was confirmed by its sizeable coupling constants to two rhodium centers (J=18.9 Hz and J=14.9 Hz). The ^1H NMR also revealed six 4-H resonances, and eleven 3- and 5-CH_3 resonances (Fig. VI.4) (Twelve 3- and 5-CH_3 signals expected). Interestingly, two additional doublets of doublets were found at δ 2.52 (dd, J_{H-H}=15.0 Hz, J_{Rh-H}=2.2 Hz, 1H) and at δ 2.42 (dd, J_{H-H}=14.6 Hz, J_{Rh-H}=3.2 Hz). These two signals are presumed to be due to the two diastereotopic protons of $\underline{CH_2}$ group. The ^1H NMR results suggested that one of the pyrazole methyl groups has been activated during thermolysis. On the basis of IR, MS and ^1H NMR results structure **38** is proposed for the new binuclear hydrido species.

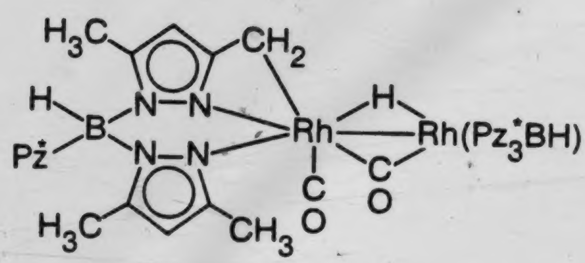

38

Further evidence in support of the proposed structure is provided by the APT ^{13}C NMR. The ^{13}C NMR is shown in Fig. VI.5. It showed the bridging and terminal CO at δ 226.80 (dd, J=51.7 Hz and J=25.3 Hz) and 187.36 (d, J=57.4 Hz) respectively. It indicated twelve 3- and 5-carbon and six 4-C of the Pz* ring as one would expect. Eleven methyl carbons of the rings were also found. More importantly, the $\underline{CH_2}$ appeared at δ 4.78, and is a doublet (J_{Rh-C}=20.3 Hz). Unfortunately, attempts to

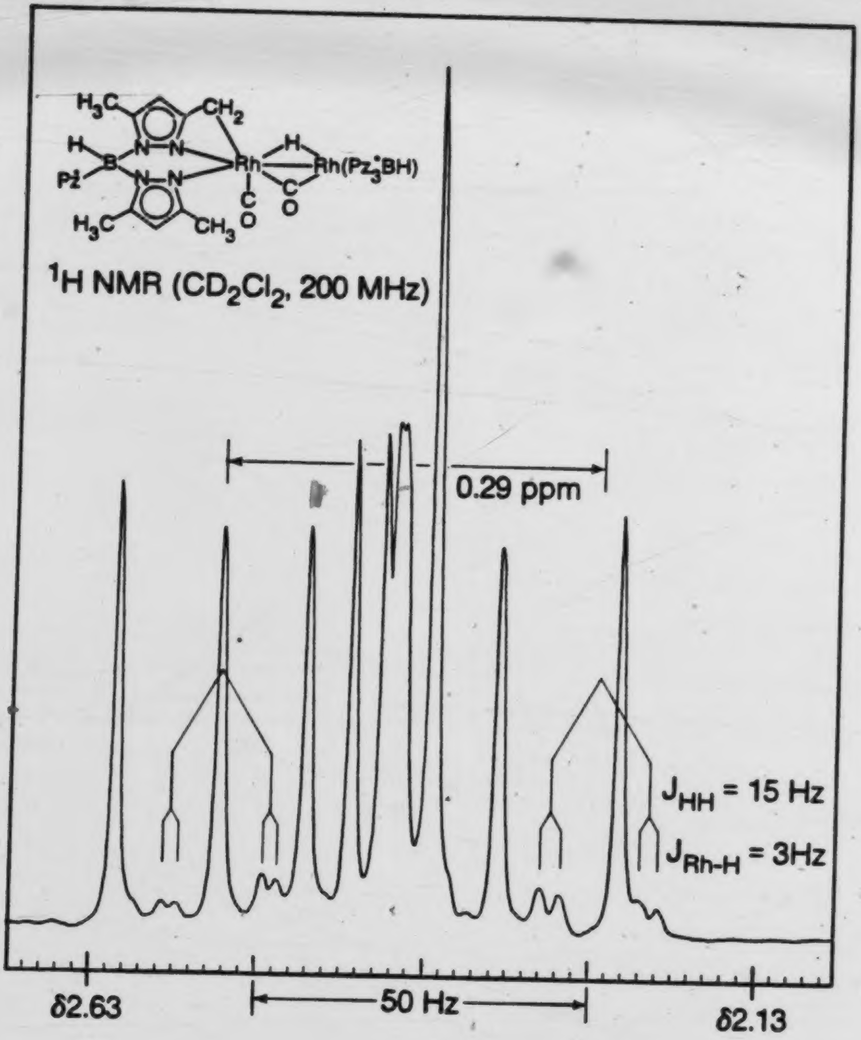

Figure VI.4 ^{1}H NMR spectrum of binuclear hydrido species (38) in Pz-CH$_3$ region; showing eleven methyls and two diastereotopic methylene protons.

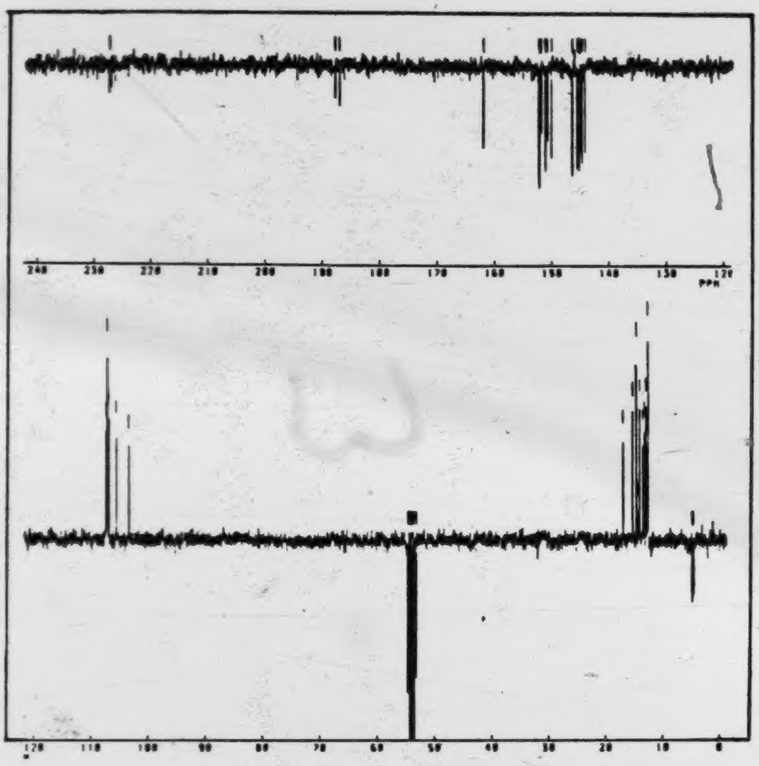

Figure VI.5 ^{13}C NMR spectrum (75.5 MHz, CD_2Cl_2) of binuclear hydride species (**38**).

obtain X-ray quality crystals for structure determination were not successful.

This provides an example of thermal intramolecular sp^3 C-H activation in the trispyrazolylborate rhodium system. **38** can also be prepared by thermolysis of **6** in cyclohexane at 75°C. Thermolysis of ethylene complex (**34a**) in cyclohexane at 105°C also yielded **38**.

It is of interest to contrast the behavior of the 16-electron fragment [Cp*Rh(CO)]. Generation of this fragment apparently leads to the dimer $[Cp^*Rh(\mu\text{-}CO)]_2$.[17] The related intermediate $[(HBPz^*_3)Rh(CO)]$ does not simply dimerize - presumably for steric reasons - but intramolecularly attacks its own methyl group, ultimately forming the hydride-bridged species **38**.

Thermal C-H activation at room temperature

A benzene solution of the cyclohexene complexes **37** (2mM) in a closed foil-wrapped Schlenk vessel at room temperature was converted completely to hydridophenyl complex (**6**) in ca. five days. This provides a rare example of thermal benzene activation at room temperature. In this reaction, the ratio of the IR bands of **37** remained approximately constant, (benzene removed, spectra in hexane) indicating either that all components reacted at the same rate, or that there was an equilibrium.

Complex **37** also activated a C-H bond of the methoxy group of $H_3C\text{-}O\text{-}C(CH_3)_3$ at room temperature in the dark. This ether was selected as solvent because the activation product would be stable in this case. A t-butyl methyl ether solution of **37** (2mM) was stirred in a closed foil-wrapped Schlenk vessel at room temperature for five days.

The conversion to $(HBPz^*_3)Rh(CO)(H)(CH_2OC(CH_3)_3)$ (**28**) was complete.

Section 4

NOVEL PHOTOCHEMICAL REACTION OF THE CARBONYL-ETHYLENE COMPLEX (34a)

Irradiation of $(HBPz^*_3)Rh(CO)(\eta^2\text{-}C_2H_4)$ (**34a**) (2-4 mM) in benzene in a closed, evacuated Pyrex Schlenk tube for eight minutes yielded two products in a 1:1 ratio (eq. 6-5). No starting material was left at this point. One of the products was the familiar $(HBPz^*_3)Rh(CO)(H)(C_6H_5)$ (**6**) and the other was the new and unexpected ethyl phenyl complex (**39**).

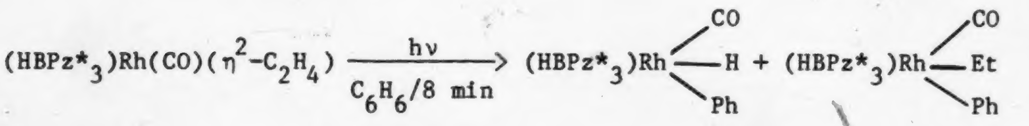

$$(HBPz^*_3)Rh(CO)(\eta^2\text{-}C_2H_4) \xrightarrow[C_6H_6/8\ min]{h\nu} (HBPz^*_3)Rh(CO)(H)(Ph) + (HBPz^*_3)Rh(CO)(Et)(Ph)$$

34a **6** **39**

(6-5)

Complex **39** is air stable even in solution, and is quite robust thermally. Investigation of its reactivity seemed warranted.

Compound **39** was isolated as colorless crystals (39% yield) and characterized by IR, MS, NMR spectroscopy and elemental analysis. Its IR in n-hexane exhibited a single ν_{CO} at 2043 cm^{-1}, which is 6 cm^{-1} lower than that of **6**. The MS showed the molecular ion. Peaks corresponding to successive loss of C_2H_5, CO and C_6H_5 were also observed. The ^1H NMR spectrum indicated three nonequivalent Pz* rings suggesting octahedral geometry. Two doublets and three triplets were found in the aromatic region, indicative of hindered rotation of the phenyl ring about the rhodium carbon bond. This is in contrast to **6**, where five sharp sets of multiplets were found only at temperatures below ca. -20°C. The diastereotopic methylene ($C\underline{H}_2$) protons appeared as multiplets, and the methyl group ($CH_2-C\underline{H}_3$) was a triplet.

The structure of **39** was confirmed by an X-ray crystal structure determination carried out by Dr. R. Ball of this department. Details of the data collection, bond lengths and bond angles will be found in the Experimental Section. The structure is shown in Fig. VI.6, while the Fig. VI.7 shows a view of the complex looking approximately along the B-Rh pseudo three-fold axis. The structure is consistent with the spectroscopically deduced structure. It confirms the η^3-coordination of Pz* groups to rhodium. The phenyl ring is aligned with one of the "grooves" between the pyrazolyl groups. The rhodium atom lies 0.127A° on the boron side of the plane formed by C5, C10, and C15; that is, the rhodium lies in a shallow pocket formed by the methyl groups.

Thermolysis of **34a** in benzene yielded only phenyl hydride (**6**); no ethyl phenyl complex (**39**) was detected in the thermolysis product. The thermal and photochemical reactions are therefore quite different. To optimize the yield of the ethyl phenyl compound (**39**), a number of different irradiation sources were explored. A maximum yield of 55% was obtained using the Oriel focussed beam 500 W lamp.

The relative yields of **39** and **6** for different irradiation sources are summarized in Table 6.III. These results are not easily interpreted, but the product ratio appears sensitive to the wavelength used. The highest ratio **39**/**6** was obtained with a relatively narrow bandpass filter at 360 nm. It appears that longer wavelengths present in the other experiments lowered the ratio. It is not known what

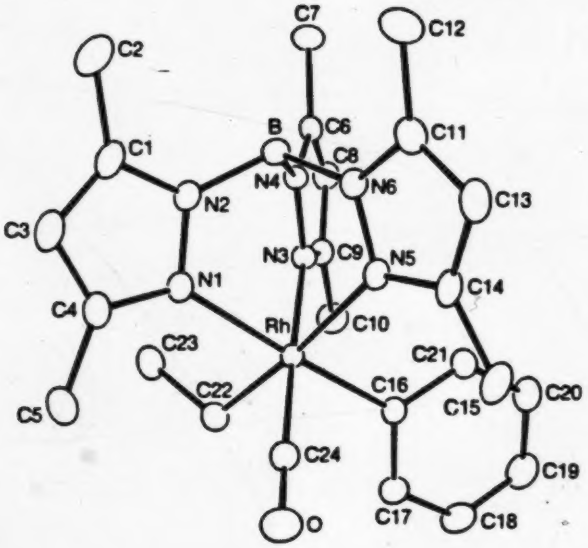
C7
C12
C2
B
C6
C11
C1
C8
N4
N6
N2
C13
C3
N3
C9
N5
N1
C14
C4
Rh
C10
C23
C21
C16
C20
C22
C15
C5
C24
C19
C17
O
C18

Figure VI.6 Molecular structure of $(HBPz^*_3)Rh(CO)(Et)(Ph)$ (**39**).

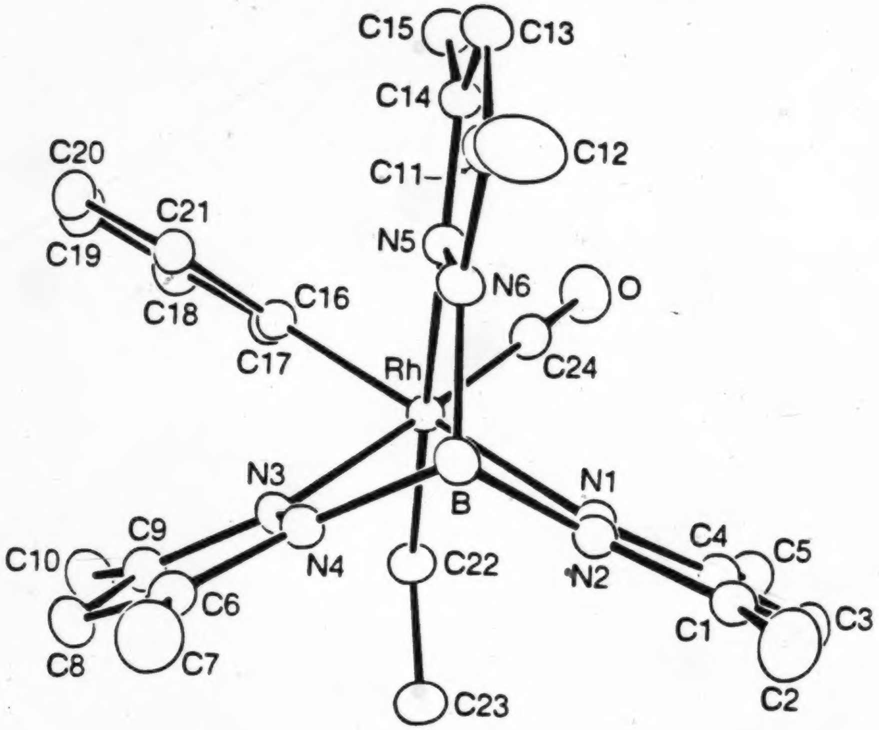
C15
C13
C14
C12
C20
C11
C21
N5
C19
N6
O
C18
C16
C17
Rh
C24
B
N3
N1
C9
C4
C5
C10
N4
C22
N2
C6
C1
C3
C8
C7
C2
C23

Figure VI.7 A view of ethyl phenyl complex (39) along the boron-rhodium pseudo three-fold axis.

Table 6.III

Relative yields of Ethyl phenyl (39) and Phenyl hydride (6)

Irradiation source	Time of** irradiation	log (transmittance)$^{-1}$		Ratio 39/6
		6	39	
Direct sunlight in laboratory	35 min	0.84	0.41	0.49
Tungsten§ lamp	2 h	0.89	0.45	0.51
450 W * mercury lamp (Pyrex filtration)	8 min	0.66	0.66	1.0
Oriel focussed beam 500 W 7-37 filter†	6 min	0.34	0,42	1.24

** Approximate time for disappearance of **34a**, irradiation of 2 mM benzene solution

* $\lambda > 290$ nm; † $340 < \lambda < 380$ with λ_{max} at 360 nm

§ *ca*. 2 cm from 75 W reflector flood light wavelength initiates the reaction, but **34a** shows weak absorption in the 350–400 nm region. Sunlight and even a tungsten lamp have a small output even at 350 nm.

Temperature of the irradiated samples in these experiments was not controlled; it was subsequently shown that sample temperature during irradiation with the tungsten lamp increased from 25°C to nearly 50°C at the end of the irradiation. To ascertain the importance of temperature effects on the product ratio, two additional experiments were performed using the 450 W mercury lamp. Samples were thermostatted at 5°C and 38°C by means of a beaker of water; there was not significant difference in the ratio in these two experiments. Further detailed studies of the wavelength dependence of reaction in eq. 6-5 would clearly be of interest, but were beyond the scope of the present work.

To elucidate the mechanism of the reaction in eq. 6-5, a few reactions were carried out which ruled out some possible reaction pathways. A freshly genenerated benzene solution of $(HBPz^{*}_{3})Rh(CO)(H)(C_6H_5)$ (**6**) was purged with ethylene for about an hour at room temperature in the dark; no appreciable change was found to take place. The solution was then photolyzed for about an hour under ethylene purge. No reaction was observed apart from a slight decomposition of the starting material. This experiment clearly demonstrated that **39** is not formed by reaction of phenyl hydride (**6**) with C_2H_4 released during the reaction. Photolysis of **39** in benzene afforded **6**, but only very slowly. For example, less than 10% conversion was obtained after 30 min irradiation; in contrast, the original photolysis of carbonyl-ethylene (**34a**) in benzene was complete in only eight minutes to give **6** and **39**. This rules out the possibility that **39** is the primary product of the reaction, with **6** formed from it in a subsequent photochemical step. One possible reaction pathway would involve a common intermediate such as $(\eta^2\text{-HBPz*}_3)\text{Rh(CO)}(\eta^2\text{-C}_2\text{H}_4)\text{(H)(Ph)}$; the η^2-η^3 change of the (HBPz*_3) ligand could be accompanied either by ethylene loss (to form **6**) or ethylene insertion into the Rh-H bond (to form **39**). However, there is at present no evidence for such an intermediate.

It is worth noting that irradiation of **34a** in cyclohexane and in n-hexane yielded $(\text{HBPz*}_3)\text{Rh(CO)(H)}(\text{C}_6\text{H}_{11})$ and $(\text{HBPz*}_3)\text{Rh(CO)(H)}(\text{C}_6\text{H}_{13})$ respectively. No ethylene insertion product was observed. Furthermore, irradiation of a benzene solution of the propylene complex **34b** afforded ca. 95% **6**, but an IR band at 2046 cm^{-1} (n-hexane) suggested that ca. 5% of the propyl phenyl complex had formed; the latter complex was not isolated or otherwise characterized. Thus it appears that this interesting combination of C-H activation and olefin insertion is not a general reaction, but imposes fairly definite requirements on both hydrocarbon and olefin.

Section 5

FUNCTIONALIZATION USING CARBON MONOXIDE

Introduction

This section addresses the question of how the compounds formed in the initial C-H activation step can be transformed to useful end products. The objective was to find some process that would convert the C-H activation products to functionalized organic products.

The catalytic incorporation of carbon monoxide into organic compounds has been extensively studied since the early 1940s. One of the most important and fundamental reactions in transition metal organometallic chemistry and in catalysis is the insertion of CO into metal-carbon sigma bonds to form an acyl complex as shown in eq. 6.6.

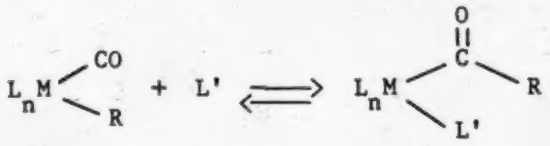

(6-6)

R is an organic group, and L' represents a ligand capable of donating an electron pair. The reaction in eq. 6-6 is referred to as an alkyl migration or a CO insertion or sometimes even as a migratory insertion.

The classical example of an insertion reaction is the carbonylation of alkyl (pentacarbonyl) manganese by carbon monoxide (eq. 6-7).[18]

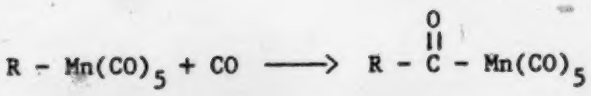

$$R - Mn(CO)_5 + CO \longrightarrow R - \overset{\overset{O}{\|}}{C} - Mn(CO)_5 \qquad (6\text{-}7)$$

A large number of examples are now known of the above type of reaction, in which CO is inserted into a metal-carbon sigma bond, and the area has been reviewed extensively.[19-22]

In most cases it has been established that CO insertion reactions proceed via alkyl (or aryl) migration from the metal to coordinated CO. The alkyl migration mechanism was first confirmed for [$\mathrm{MeMn(CO)_5}$] by a series of classic studies with labelled CO.[23]

The reactions of [$\mathrm{RMn(CO)_5}$][24-29] with various nucleophiles (L) to give the corresponding [$\mathrm{Mn(CO)_4(COR)L}$] complexes have been the subject of many kinetic studies. These have shown that the first step involves an equilibrium between the octahedral alkyl and a five-coordinate acyl (eq. 6-8).

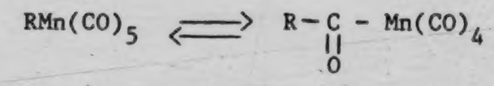

$$\mathrm{RMn(CO)_5} \rightleftharpoons \mathrm{R-\underset{\underset{O}{\|}}{C}-Mn(CO)_4} \qquad (6\text{-}8)$$

The coordinatively unsaturated acyl then adds the incoming ligand L (CO, $\mathrm{PPh_3}$ etc) to reform an octahedral complex (eq. 6-9).

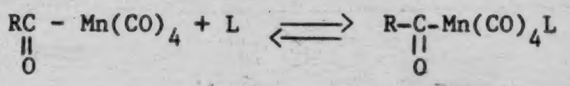

$$\mathrm{R\underset{\underset{O}{\|}}{C}-Mn(CO)_4} + \mathrm{L} \rightleftharpoons \mathrm{R-\underset{\underset{O}{\|}}{C}-Mn(CO)_4L} \qquad (6\text{-}9)$$

Donor solvents can participate in preequilibria and increase the rate by as much as 10^3-10^4 times (eq. 6-10).

$$\mathrm{RMn(CO)_5} \underset{-S}{\overset{+S}{\rightleftharpoons}} \mathrm{RCOMn(CO)_4S} \xrightarrow{+L} \mathrm{RCOMn(CO)_4L} \qquad (6\text{-}10)$$

Such equilibria are well known for complexes of other metals (e.g. for Rh and Ir species), and equilibrium constants and rates have been measured.[30]

One point worth noting is that a hydride ligand has never been observed to migrate to CO to produce a metal formyl complex (eq. 6-11). Instead, the reverse reaction is a general feature of formyl complexes.

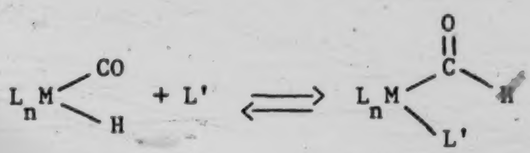

(6-11)

As shown in Chapter III, carbonylation of $(HBPz^*_3)Rh(CO)(H)(C_6H_5)$ (**6**) led to $(HBPz^*_3)Rh(CO)_2$ (**1**). No formyl or benzoyl complex was detected, and it appeared that reductive elimination of benzene was favoured over migration. However, since the kinetic barrier to reductive elimination is higher in dialkyls than in alkyl hydrides, possible migration process in the ethyl phenyl complex **39** were of interest. The likely products would be the propionyl complex $(HBPz^*_3)Rh(CO)(COEt)(Ph)$ or the benzoyl complex $(HBPz^*_3)Rh(CO)(Et)(COPh)$. Finally if alkyl or aryl migration occurs, there would be the interesting possibility of ketone formation in a subsequent reductive elimination process (eq. 6-12).

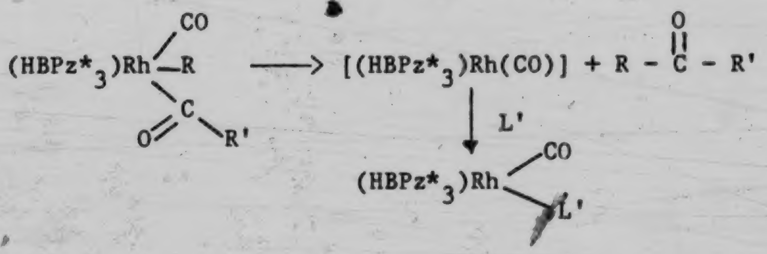

(6-12)

With this in mind, carbonylation of $(HBPz^*_3)Rh(CO)(C_2H_5)(C_6H_5)$ (**39**) and (HBPz*$_3$)Rh(CO)(CH$_3$)(C$_6$H$_5$) (9) have been explored. The results of these reactions will be discussed in this Section.

Carbonylation of (HBPz*$_3$)Rh(CO)(C$_2$H$_5$)(C$_6$H$_5$) (39)

The carbonylation of **39** was carried out in a Parr bench autoclave with 950 psig of CO at 100°C using hexane as a solvent. The IR indicated complete disappearance of **39** in two weeks and suggested formation of two new acyl complexes (eq 6-13).

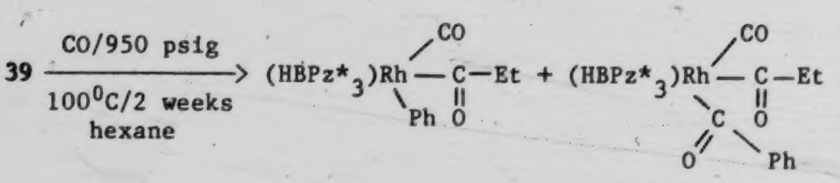

(6-13)

40 **41**

Judging from the ν_{CO} band intensities of **40** and **41** and assuming that the extinction coefficients of ν_{CO} in the compounds are not very different, the ratio of **40** and **41** shortly after the reaction is approximately 2:1. The IR monitoring suggested that the ratio of **40** and **41** remained almost unchanged during the progress of reaction. Propiophenone was not observed in the reaction products.

The propionyl phenyl compound **40** was isolated as colorless crystals in 43% yield after chromatography and crystallization. However, **41** did not survive chromatography under the experimental conditions and has not been obtained pure; its identity will be discussed later.

The IR spectrum of **40** in n-hexane exhibited a terminal ν_{CO} at 2069 cm^{-1} and an acyl ν_{CO} at 1670 cm^{-1}. The MS showed peaks for (M-C$_2$H$_5$),

$(M-C_2H_5-CO)$, $(M-C_2H_5-2CO)$, $(M-C_2H_5-C_6H_5-2CO)$ but the molecular ion was not observed. The ^1H NMR spectrum indicated three nonequivalent Pz* rings. The phenyl protons appeared in the range δ 8.24 to 6.37 as three triplets and two doublets. The methylene protons ($C\underline{H_2}$) in **39** were diastereotopic with a chemical shift separation of 0.45 ppm; in **40**, the methylene protons appeared as a multiplet, resembling a quintet but overlapping Pz* methyl signals to some extent. The methylene protons in **40** are more nearly equivalent than they are in the ethyl phenyl complex **39**; this is reasonable in view of their greater separation from the chiral rhodium center. A triplet (J=7.2 Hz) was found for the methyl protons.

The APT ^{13}C NMR of **40** showed both terminal (δ 187.85, d, $J_{Rh-C}=72.4$ Hz) and acyl (δ 233.42, d, $J_{Rh-C}=27.2$ Hz) carbonyls. The key point is that the ^{13}C NMR indicates that the phenyl group is bound directly to the rhodium center; the value of J_{Rh-C} for the phenyl carbon is 28.7 Hz which is very similar to that found in $(HBPz*_3)Rh(CO)(H)(C_6H_5)$ (**6**) ($J_{Rh-C}=26.6$ Hz). Moreover the $\underline{C}H_2$ resonance of **40** appeared as a singlet (δ 45.58). These NMR results strongly suggest that in **40**, CO has inserted into the $Rh-C_2H_5$ bond.

An important and interesting observation is that the other product of the reaction, formulated as the bis(acyl)complex **41** slowly converted in *n*-hexane solution at room temperature to **40** (eq. 6-14).

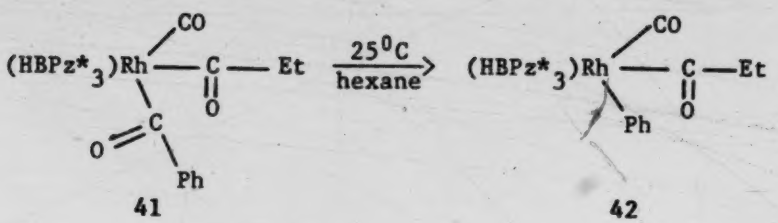

41

42

(6-14)

This conversion was monitored by IR and was complete in about a month at room temperature. An identical result was found by following the ^1H NMR of the mixture of **40** and **41** in CD_2Cl_2 in a sealed NMR tube using an internal standard to monitor the decrease of one and increase of the other.

Recently[31] it was shown that carbonylation of $(C_5Me_5)Rh(CO)(Me)(Ph)$ yielded acetophenone more readily in acetonitrile, than in cyclohexane, no intermediate acyl complex was detected or isolated.

In the light of this report, it was of interest to study the carbonylation of **39** in acetonitrile. Either an enhanced rate of acyl formation or actual ketone $(C_2H_5COC_6H_5)$ elimination was expected. Accordingly, the carbonylation of **39** was carried out in acetonitrile with 1000 psig of CO at 100°C. The reaction was complete in ca. 60 hours, a rate enhancement of roughly five times as compared with cyclohexane.

When acetonitrile was removed in vacuum and replaced by n-hexane, the IR showed mainly **41** with a small quantity of **40** (ca. 5%). As noted earlier, **41** could not be obtained pure. The IR spectrum of this sample of **41** (n-hexane) exhibited the terminal ν_{CO} at 2068 cm^{-1} (1 cm^{-1} lower than **40**; the terminal carbonyl bands of **40** and **41** are not resolved) and the acyl ν_{CO} at 1694 and 1621 cm^{-1}.

The carbonylation in acetonitrile provided the best sample of 41 that has been obtained. As mentioned above, 41 does not survive chromatography and slowly converts to 40 in solution. Hence the identification of 41 is based on studies of a solution of ca. 95% purity.

In contrast with 40 (slow phenyl rotation at ambient temperature, five sharp multiplets), the phenyl region of 41 shows three broad resonances in the ^{1}H NMR spectrum. This implies more rapid rotation of the phenyl ring in 41, consistent with the benzoyl structure, which would place the ring at a greater distance from the bulky (HBPz*$_3$) ligand. The methylene protons in 41 appears as two multiplets at δ 3.63 and δ 2.90 in CD$_3$CN. Although the diastereotopic methylene protons in the phenyl ethyl compound 39 differed by 0.45 ppm, it is extremely surprising to see an even larger chemical shift difference in 41, where the ethyl group is separated by an acyl group from the chiral rhodium center. In the phenyl propionyl complex 40, the methylene proton separation was only 0.093 ppm.

The large chemical shift difference of the methylene protons of 41 (0.73 ppm) initially led to its formulation as a benzoyl ethyl complex, (HBPz*$_3$)Rh(CO)(COPh)(Et). However the ^{13}C NMR of a 40/41 mixture measured by Dr. Glenn Sunley established that the methylene carbon atom of 41 was not directly bonded to rhodium in view of its small (4.6 Hz) coupling constant. Moreover, the two acyl bands in the IR of 41 would seem to indicate that it contains two acyl groups.

The formulation of 41 as a bis(acyl)complex seems the most reasonable interpretation of the results at the present time. The compound has not been isolated in view of its slow conversion to **40**. So the formulation must still be regarded as somewhat tentative; the large diastereotopic shift difference of the methylene protons remains puzzling. Further investigations of 41 and related complexes are currently under way in this laboratory by Dr. Glenn Sunley, to whom we are grateful for stimulating discussions and suggestions.

Elimination of propiophenone from $(HBPz^*_3)Rh(CO)(COEt)(Ph)$ (40)

As just described, reductive elimination of propiophenone during carbonylation of **39** in n-hexane at 100°C did not occur. A further attempt to remove ketone by heating **41** under 1000 psig of CO in acetonitrile at 145°C was also unsuccessful. Under these conditions **41** decomposed to unidentified products.

Bergman et al.[32] demonstrated that treatment of hydrido alkyl complexes $Cp^*Ir(PMe_3)(H)(R)$ with reagents such as $ZnBr_2$, H_2O_2, Br_2, HBF_4 or O_2 resulted in reductive elimination of the hydrocarbons. It therefore appeared reasonable to try the reaction of $(HBPz^*_3)Rh(CO)(COEt)(Ph)$ (**40**) with $ZnBr_2$.

Transformation of **40** into propiophenone occurred readily upon treatment with excess $ZnBr_2$ in dichloromethane at room temperature. The ketone was identified by comparison of its IR and NMR spectra with those of an authentic sample. The yield of propiophenone was ca. 82% by ^1H NMR. Other products of reaction, in particular the fate of the rhodium, are not known.

Carbonylation of $(HBPz^*_3)Rh(CO)(CH_3)(C_6H_5)$ (9)

The carbonylation of **9** was carried out with CO at 1050 psig in n-hexane at 100°C. The reaction proceeded smoothly but very slowly to give $(HBPz*_3)Rh(CO)(COMe)(Ph)$ (**42**) as the major product. The minor product was presumed to be $(HBPz*_3)Rh(CO)(COMe)(COPh)$ (**43**). The ratio of **42** to **43** was about 2:1.

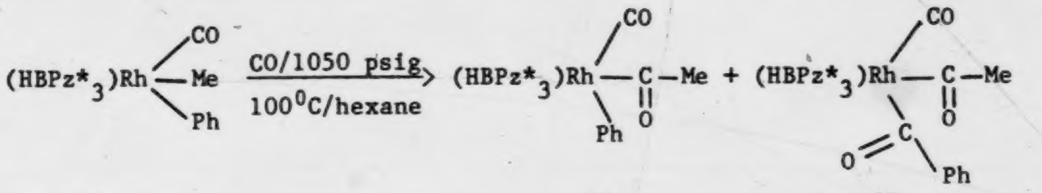

9 **42** **43**

(6-15)

The reaction in eq. 6-15 was almost complete in about three months. Carbonylation of the ethyl phenyl complex (**39**) was faster than that of **9** under similar conditions. This can be related to the presumed weaker attachment of ethyl than that of methyl to rhodium.

Compound **42** was isolated as colorless crystals after chromatography and crystallization. The minor product **43** did not survive chromatography, and was not isolated because of the problem associated with its stability. The IR spectrum of **42** (n-hexane) indicated the terminal ν_{CO} at 2070 cm^{-1} and the acyl ν_{CO} at 1677 cm^{-1}. The MS showed the molecular ion and peaks due to successive loss of CH_3, CO were also observed. The ^1H NMR spectrum showed five sharp multiplets in the aromatic region as expected. The observed six Pz* methyl and three 4-H resonances are consistent with the octahedral geometry of **42**. The methyl group (COMe) appeared as a singlet at δ 1.32. In hexane, **43** exhibited terminal and acyl ν_{CO} bands at 2070, 1697 and 1623 cm^{-1}.

Elmination of acetophenone from (HBPz*$_3$)Rh(CO)(COMe)(Ph) (42)

During carbonylation of **9** in n-hexane at 100°C, no acetophenone was detected, so the reaction of 42 with $ZnBr_2$ was attempted. Compound 42 reacted slowly with excess $ZnBr_2$ in CD_2Cl_2 with the elimination of acetophenone; the ^1H NMR yield was 84%.

Section 6

EXPERIMENTAL

General

Following the procedure reported by Cramer[33] $[(\mu\text{-Cl})Rh(\eta^2\text{-}C_2H_4)]_2$ was prepared. The synthesis of $[(\mu\text{-Cl})Rh(CO)(\eta^2\text{-}C_2H_4)]_2$ was carried out according to the procedure provided by Powell and Shaw.[34] The following compounds were purchased from commercial sources: research grade ethylene, propylene and carbon monoxide.

Preparation of $(HBPz^*_3)Rh(CO)(\eta^2\text{-}C_2H_4)$ (34a)

To a suspension of $K[HBPz^*_3]$ (0.795g, 2.37 mmol) in toluene (100 mL) was added $[(\mu\text{-Cl})Rh(CO)(\eta^2\text{-}C_2H_4)]_2$ (0.402 g, 1.03 mmol). The reaction mixture was stirred for ca. 2.5 h in the dark. Removal of solvent gave a yellow residue which was extracted with CH_2Cl_2 and purification was effected by column chromatography. Neutral alumina column (10 x 2.5 cm) was employed as the stationary phase with CH_2Cl_2 as the eluting solvent. Removal of solvent afforded a pale yellow solid (0.597 g, 64%). MP darkens above 215°C.

Characterization: IR(n-hexane) 2013 cm^{-1} (ν_{CO}). MS (90°C, 16 eV) M^+ (456), M^+ $-CO/C_2H_4$, M^+-CO-C_2H_4. ^1H NMR (CD_2Cl_2, ambient, 200 MHz) δ 5.83 (br, 3H), 3.25 (br, 2H), 2.36 (br, 20H). ^1H NMR (CD_2Cl_2, -60°C, 400 MHz) δ 5.90 (s, 2H), 5.60 (s, 1H), 3.15 (d, 2H, J=8.5 Hz), 2.33 (s, ca. 8H, accidental overlap of ethylene protons and pyrazole methyl protons), 2.32 (s, ca. 6H), 2.20 (s, 3H), 2.16 (s, 3H). ^{13}C NMR (CD_2Cl_2, ambient, 100.6 MHz) δ 190.12 (d, $J_{Rh\text{-}C}$=64.0 Hz), 144.67 (s), 106.84 (br), 24.40 (d, J_{Rh-C}=14.4 Hz), 14.21 (br), 12.88 (s). ^{13}C NMR (CD_2Cl_2, -40°C, 100.6 MHz) δ 189.28 (d, J_{Rh-C}=64.0 Hz), 152.34 (s), 149.89 (s), 144.63 (s), 144.19 (s), 108.70 (s), 105.22 (s), 23.37 (d), 14.62 (s), 13.51 (s), 12.21 (s). Anal. Calcd for $C_{18}H_{26}BN_6ORh$: C, 47.37; H, 5.70; N, 18.42. Found: C, 47.24, H, 5.76; N, 18.28.

Preparation of (H_2BPz*_2)Rh(CO)(η^2-C_2H_4)

To a stirred suspension of K[H_2BPz*_2] (100 mg, 0.409 mmol) in n-hexane (40 mL) was added [(μ-Cl)Rh(CO)(η^2-C_2H_4)]$_2$ (100 mg, 0.257 mmol). The reaction was carried out in the dark at room temperature. After 10 min. the IR showed a new ν_{CO} band at 2012 cm^{-1}; no starting material was left at this stage. The new band is presumed to be due to (H_2BPz*_2)Rh(CO)(η^2-C_2H_4). As the hexane solution of (H_2BPz*_2)Rh(CO)(η^2-C_2H_4) stood for a while at room temperature, a new band at 2079 cm^{-1} was growing without significant decrease in intensity of the band at 2012 cm^{-1}. After 0.5h, two bands of approximately equal intensity were found at 2079 and 2013 cm^{-1}. These bands correspond to the known characterized (H_2BPz*_2)Rh(CO)$_2$ compound. Because of this fairly rapid disproportionation in solution at room temperature (H_2BPz*_2)Rh(CO)(η^2-C_2H_4) was not isolated. Furthermore, a sample of (H_2BPz*_2)Rh(CO)(η^2-C_2H_4) in CD_2Cl_2 in an NMR tube indicated the formation of a new unknown hydrido species (δ-13.52, d, J_{Rh-H}=18.8 Hz). The IR of this latter compound in hexane exhibited ν_{CO} at 2039 cm^{-1}.

Preparation of (H_2BPz*_3)Rh(CO)(η^2-CH_2CHCH_3) (34b)

A solution of ($HBPz*_3$)Rh(CO)$_2$ (1) (50 mg, 0.109 mmol) in purified cyclohexane (50 mL) was irradiated for 10 min. under a continuous purge of propylene. Immediately after photolysis, the IR showed mostly the ν_{CO} band at 2039 cm^{-1}, presumed to be due to (HBPz*$_3$)Rh(CO)(H)($CH_2CH{=}CH_2$) (**35**). Compound **35** in solution at room temperature isomerized to **34b**. The isomerization was complete in 48h. Removal of solvent under reduced pressure afforded light yellow solid (46.3 mg, 90%).

Characterization: IR (n-hexane) 2006 cm^{-1} (ν_{CO}). MS (110°C, 16 eV) M^+ (470), M^+-CH_2CHCH_3, M^+-CH_2CHCH_3-CO. ^1H NMR (CD_2Cl_2, ambient, 200 MHz) δ5.79 (br, 3H), 4.05 (m, 1H), 2.34 (br, 20H), 1.70 (dd J=6.2 Hz and J=2.0 Hz, 3H), ^1H NMR (-60°C) δ 5.89 (s, 1H), 5.87 (s, 1H), 5.59 (s, 1H), 3.94 (m, 1H), 2.37 (s, 3H), 2.36 (s, 3H), 2.34 (s, 3H), 2.31 (s, 3H), ca. 2.28 (ca. 2H, accidental overlap with Pz* methyl resonance), 2.21 (s, 3H), 2.19 (s, 3H), 1.64 (d, 3H). Anal. Calcd for $C_{19}H_{28}BN_6ORh$: C, 48.51; H, 5.96; N, 17.87. Found: C, 47.67, H, 6.18; N, 16.76.

Preparation of (HBPz*$_3$)Rh(CO)(Cl)(CH_2CHCH_2) (36)

Compound 1 (60.0 mg, 0.132 mmol) in purified cyclohexane (60 mL) was irradiated for ca. 10 min under a propylene purge. To the photolyzed solution, CCl_4 (5 mL) was added immediately and the solution was stirred for ca. 1 h at room temperature. Removal of solvent under vacuum gave light yellow solid. The solid was extracted with CH_2Cl_2 and chromatographed on a neutral alumina column (8 x 2.5 cm) eluting with CH_2Cl_2. Removal of solvent gave a yellow residue. Crystallization from a layered CH_2Cl_2/hexane afforded yellow crystalline solid (33.3 mg, 50%).

Characterization: IR (n-hexane) 2077 (ν_{CO}). MS (175°C, 16 eV) M^+ (505), M^+-CO, M^+-CO-C_3H_5, M^+-CO-C_3H_5-Cl. ^1H NMR (CD_2Cl_2, ambient, 200 MHz) δ 6.40 (m, 1H), 5.90 (s, 2H), 5.83 (s, 1H), 5.36 (dd, J=10.0 Hz, J=2.2 Hz, 1H), 5.00 (dd, J=10.0 Hz, J=2.2 Hz, 1H), 3.85 (t, 1H), 3.55 (t, 1H), 2.68 (s, 3H), 2.48 (s, 3H), 2.42 (s, 3H), 2.39 (s, 3H), 2.38 (s, 3H), 2.34 (s, 3H). Anal. Calcd for $C_{19}H_{27}BClN_6ORh$: C, 45.19; H, 5.35; N, 16.65. Found: C, 46.01, H, 5.56; N, 15.43.

Preparation of (HBPz*$_3$)Rh(CO)(η^2-cyclohexene) (37)

Compound 1 (45.0 mg, 0.098 mmol) in purified cyclohexane (45 mL) was irradiated for 6 min using N_2 purge. Cyclohexene (1 mL) was added to the above photolyzed solution with minimum delay. The reaction was allowed to continue for 0.5h. Removal of solvent under vacuum yielded pale yellow solid. Anal. Calcd for $C_{24}H_{36}BN_6ORh$: C, 51.76; H, 6.28; N, 16.47. Found: C, 52.94; H, 6.84; N, 15.67.

Thermolysis of (HBPz*$_3$)Rh(CO)(η^2-C_2H_4) (34a)

A solution of **34a** (13.2 mM) in C_6D_6 along with 1 µL hexamethyldisiloxane as an internal standard was transferred to an NMR tube fused to ground glass joint. The tube was subsequently topped with a vaccuum stopcock. After three cycles of freeze-pump-thaw, the NMR tube was sealed under vacuum. The foil-wrapped NMR tube was heated at 105°C for 5 days. During this period, the NMR tube was taken out of the oil bath occasionally, and was shaken to dissolve the solid that came out of the solution and heated again in the usual way. The ^1H NMR indicated complete conversion of **34a** and the yield of

$(\mathrm{HBPz^*_3})\mathrm{Rh(CO)(D)(C_6D_5)}$ was *ca.* 89%.

The thermolysis experiments were normally carried out in closed foil-wrapped Schlenk vessels (total volume *ca.* 45 mL). Compound **34a** (10 mg, 0.022 mmol) in freshly distilled benzene (20 mL) was heated under the above conditions and the progress of the reaction was monitored by taking IR (*n*-hexane). The reaction was complete in 5 days.

Thermolysis of $(\mathrm{HBPz^*_3})\mathrm{Rh(CO)}(\eta^2\text{-}\mathrm{CH_2CHCH_3})$ (34b)

A solution of **34b** (29.8 m*M*) in $\mathrm{C_6D_6}$ (0.5 mL) along with 1 µL hexamethyldisiloxane was transferred to an NMR tube fused to a ground glass joint. The NMR tube was sealed under vacuum after three cycles of freeze-pump-thaw of the solution. The foil-wrapped NMR tube was heated at 75°C for 45 h. The ^{1}H NMR indicated complete conversion of **34b** and the yield of $(\mathrm{HBPz^*_3})\mathrm{Rh(CO)(D)(C_6D_5)}$ was *ca.* 94%.

In the usual run, **34b** (10 mg, 0.021 mmol) in benzene (10 mL) was heated in a closed evacuated foil-wrapped Schlenk vessel (total volume *ca.* 45 mL) and the reaction was monitored by taking IR. Complete disappearance of the starting material was in *ca.* 43 h.

Preparation of $(\mathrm{HBPz^*_3})\mathrm{Rh(CO)}(\mu\text{-}\mathrm{CO})(\mu\text{-}\mathrm{H})\overline{\mathrm{Rh(C_4H_6C}}\mathrm{H_2N_2})(\mathrm{Pz^*_2BH})$ (38)

Compound **34b** (60.0 mg, 0.127 mmol) in purified cyclohexane (45 mL) was heated in an evacuated closed foil-wrapped Schlenk vessel at 75°C for 8 days. Removal of solvent under reduced pressure yielded yellow solid. The residue was extracted with $\mathrm{CH_2Cl_2}$ and chromatographed on a neutral alumina column (8 x 2.5 cm) with $\mathrm{CH_2Cl_2}$ eluent. Crystallization from a layered $\mathrm{CH_2Cl_2}$/hexane at -20°C afforded yellow microcrystals of **38** (40.5 mg, 74%).

Characterization: IR (n-hexane) 2039, 1806 cm^{-1} (ν_{CO}). MS (250°C, 16 eV) M$^+$ (856), M$^+$-CO. ^{1}H NMR (CD_2Cl_2, ambient, 200 MHz) δ 6.03(s, 1H), 6.00 (s, 1H), 5.85 (s, 1H), 5.81 (s, 1H), 5.75 (s, 1H), 5.61 (s, 1H), 2.61 (s, 3H), 2.52 (dd, J_{H-H}=15.0 Hz, J_{Rh-H}=2.2 Hz, 1H), 2.53 (s, 3H), 2.46 (s, 3H), 2.43 (s, 3H), 2.41 (s, 3H), 2.40 (s, 6H), 2.37 (s, 6H), 2.32 (s, 3H), 2.24 (dd, J_{H-H}=14.6 Hz, J_{Rh-H}=3.2 Hz, 1H), 2.23 (s, 3H), -18.00 (dd, J_{Rh-H}=18.9 and 14.9 Hz, 1H). ^{13}C NMR (CD_2Cl_2, ambient, 75.5 MHz) δ 226.80 (dd, J_{Rh-C}=51.7 and 25.3 Hz), 187.36 (d, J_{Rh-C}=57.3 Hz), 161.81 (s), 152.04 (s), 151.69 (s), 150.98 (s), 150.66 (s), 150.00 (s), 146.36 (s), 145.42 (s), 145.12 (s), 145.03 (s), 144.65 (s), 144.13 (s), 107.22 (s), 107.06 (s, 2C), 106.84 (s), 105.50 (s), 103.30 (s), 16.98 (s), 15.30 (s), 14.61 (s, 2C), 14.05 (s), 13.48 (s), 13.25 (s), 12.96 (s), 12.71 (s), 12.54 (s, 2C), 4.78 (d, J_{Rh-C}=20.3 Hz). Anal. Calcd for $C_{32}H_{44}B_2N_{12}O_2Rh_2$: C, 44.86, H, 5.14; N, 19.33. Found: C, 44.89; H, 5.17; N, 19.33.

Preparation of (HBPz*$_3$)Rh(CO)(C_2H_5)(C_6H_5) (39)

Complex **34a** (100.0 mg, 0.219 mmol) in benzene (60 mL) was degassed and irradiated in a closed Pyrex vessel for 8 min. Solvent was removed under reduced pressure and the resulting colorless solid was extracted with hexane. The hexane extract was left in the air for decomposition of (HBPz*$_3$)Rh(CO)(H)(C_6H_5) (**6**) over night. Solvent was removed under reduced pressure and the residue was extracted with CH_2Cl_2 and chromatographed on a Florisil column (8 x 2.5 cm) eluting with 1:1 CH_2Cl_2/hexane mixture. Crystallization from hexane at room temperature afforded colorless crystals of **39** (48.6 mg, 39%) MP 176-178°C.

Characterization: IR (n-hexane) 2043 cm^{-1} (ν_{CO}). MS (100°C, 16 eV) M^+ (534), $M^+-C_2H_5$, $M^+-C_2H_5-CO$, $M^+-C_2H_5-CO-C_6H_5$. ^1H NMR (CD_2Cl_2, ambient, 200 MHz) δ7.34 (d, 1H), 7.13 (t, 1H), 6.98 (t, 1H), 6.79 (t, 1H), 6.58 (d, 1H), 5.90 (s, 1H), 5.80 (s, 1H), 5.79 (s, 1H), 2.65 (m, 1H), 2.49 (s, 3H), 2.48 (s, 3H), 2.46 (s, 3H), 2.44 (s, 3H), 2.20 (m, 1H), 1.68 (s, 3H), 1.58 (s, 3H), 0.69 (t, 7.0 Hz, 3H). Anal. Calcd for $C_{24}H_{32}BN_6ORh$: C, 53.93; H, 5.99; N, 15.73. Found: C, 53.73; H, 6.02; N, 15.62.

X-ray structure of $(HBPz^*_3)Rh(CO)(C_2H_5)(C_6H_5)$ (39)

The x-ray crystallographic study was carried out by Dr. R.G. Ball at the Structure Determination Laboratory of this department. Details of data collection are listed in Table 6.IV. The structure of **39** is depicted in Fig. VI.6 and VI.7. Relevant bond lengths and bond angles are tabulated in Table 6.V and 6.VI. Positional and thermal parameters are available in the detailed report from the Structure Determination Laboratory.[35]

Preparation of $(HBPz^*_3)Rh(CO)(COC_2H_5)(C_6H_5)$ (40)

A solution of **39** (100.0 mg, 0.187 mmol) in hexane (50 mL) was placed in a 150 mL Parr bench autoclave with a magnetic stirrer and was flushed with carbon monoxide. The solution was then pressurized with 950 psig of CO. The reaction mixture was stirred at 100°C for two weeks. No starting material was left at this point. Removal of solvent resulted in off-white solid. The residue was extracted with CH_2Cl_2 and chromatographed on a Florisil column (8 x 2.5 cm) using CH_2Cl_2 as

Table 6.IV

Experimental Details

A. Crystal Data

$C_{24}H_{32}BN_6ORh$
F.W. = 534.28
Crystal dimensions: 0.14 x 0.22 x 0.40 mm
Monoclinic space group $P2_1/n$
a = 10.753 (3) b = 17.591 (3) c = 13.751 (2) A
β = 104.43 (2)°
V = 2519. A^3 Z = 4
Dc = 1.409 gm/cm^3 μ = 6.93 cm^{-1}

B. Data Collection and Refinement Conditions

Radiation:	Mo Kα (λ = 0.71073 A)
Monochromator:	Incident beam, graphite crystal
Take-off angle:	3.0 deg
Detector aperture:	2.40 mm horizontal 4.0 mm vertical
Crystal-to-detector distance:	205 mm
Scan type:	ω-2θ
Scan rate:	10.1 - 2.2 deg/min
Scan width:	0.80 + 0.35tan(θ) deg
Data collection index range:	h, k, -1
Reflections measured:	5936 unique, 3601 width I>3σ(I)
Observations: variables ratio:	3601:298
Agreement factors R_1, R_2, GOF:	0.035, 0.044, 1.26
Corrections applied:	Absorption correction

Table 6.V Bond Distances in Angstroms

Atom 1	Atom 2	Distance	Atom 1	Atom 2	Distance	Atom 1	Atom 2	Distance
Rh	N1	2.170 (3)	N4	C6	1.350 (4)	C9	C10	1.497 (5)
Rh	N3	2.104 (3)	N4	B	1.544 (5)	C11	C12	1.498 (7)
Rh	N5	2.219 (3)	N5	N6	1.372 (4)	C11	C13	1.367 (6)
Rh	C16	2.053 (4)	N5	C14	1.339 (5)	C13	C14	1.386 (6)
Rh	C22	2.106 (4)	N6	C11	1.349 (5)	C14	C15	1.482 (6)
Rh	C24	1.824 (4)	N6	B	1.527 (5)	C16	C17	1.390 (6)
O	C24	1.133 (5)	C1	C2	1.491 (6)	C16	C21	1.389 (5)
N1	N2	1.371 (4)	C1	C3	1.358 (6)	C17	C18	1.398 (6)
N1	C4	1.349 (5)	C3	C4	1.391 (6)	C18	C19	1.363 (7)
N2	C1	1.349 (5)	C4	C5	1.486 (6)	C19	C20	1.385 (7)
N2	B	1.540 (5)	C6	C7	1.494 (5)	C20	C21	1.385 (5)
N3	N4	1.372 (4)	C6	C8	1.364 (6)	C22	C23	1.529 (6)
N3	C9	1.347 (4)	C8	C9	1.394 (5)			

Numbers in parentheses are estimated standard deviations in the least significant digits.

Table 6.VI Bond Angles in Degrees

Atom 1	Atom 2	Atom 3	Angle	Atom 1	Atom 2	Atom 3	Angles	Atom 1	Atom 2	Atom 3	Angle
N1	Rh	N3	88.0 (1)	N4	N3	C9	106.7 (3)	C8	C9	C10	126.6 (4)
N1	Rh	N5	84.6 (1)	N3	N4	C6	109.6 (3)	N6	C11	C12	121.6 (4)
N1	Rh	C16	176.9 (1)	N3	N4	B	121.9 (3)	N6	C11	C13	107.5 (4)
N1	Rh	C22	91.7 (1)	C6	N4	B	128.4 (3)	C12	C11	C13	131.0 (4)
N1	Rh	C24	95.9 (1)	Rh	N5	N6	116.6 (2)	C11	C13	C14	106.9 (4)
N3	Rh	N5	95.8 (1)	Rh	N5	C14	136.3 (3)	N5	C14	C13	109.3 (4)
N3	Rh	C16	89.7 (1)	N6	N5	C14	106.7 (3)	N5	C14	C15	122.0 (4)
N3	Rh	C22	91.2 (1)	N5	N6	C11	109.7 (3)	C13	C14	C15	128.7 (4)
N3	Rh	C24	175.7 (1)	N5	N6	B	119.6 (3)	Rh	C16	C17	123.5 (3)
N5	Rh	C16	93.1 (1)	C11	N6	B	130.6 (3)	Rh	C16	C21	119.1 (3)
N5	Rh	C22	175.4 (1)	N2	C1	C2	123.4 (4)	C17	C16	C21	117.4 (4)
N5	Rh	C24	96.5 (2)	N2	C1	C3	107.8 (4)	C16	C17	C18	120.8 (4)
C16	Rh	C22	90.4 (2)	C2	C1	C3	128.8 (4)	C17	C18	C19	120.6 (4)
C16	Rh	C24	86.4 (2)	C1	C3	C4	106.9 (3)	C18	C19	C20	119.6 (4)
C22	Rh	C24	86.8 (2)	N1	C4	C3	109.1 (4)	C19	C20	C21	119.7 (4)
Rh	N1	N2	117.8 (2)	N1	C4	C5	123.0 (4)	C16	C21	C20	121.8 (4)
Rh	N1	C4	135.6 (3)	C3	C4	C5	127.8 (4)	Rh	C22	C23	113.9 (3)
N2	N1	C4	106.2 (3)	N4	C6	C7	123.8 (3)	Rh	C24	O	176.8 (4)
N1	N2	C1	109.9 (3)	N4	C6	C8	107.9 (3)	N2	B	N4	110.6 (3)
C1	N2	B	130.3 (3)	C6	C8	C9	106.7 (3)	N4	B	N6	109.0 (3)
Rh	N3	N4	116.9 (2)	N3	C9	C8	109.0 (3)				
Rh	N3	C9	136.3 (2)	N3	C9	C10	124.4 (3)				

Numbers in parentheses are estimated standard deviations in the least significant digits.

eluent. Crystallization by slow evaporation from hexane solution afforded colorless crystals of **40** (46.3 mg, 44%). MP 184-185°C.

Characterization: IR (n-hexane) 2069, 1670 cm^{-1} (ν_{CO}). MS (150°C, 16 eV) $M^{+}-C_2H_5$ (533), $M^{+}-C_2H_5-CO$, $M^{+}-C_2H_5-2CO$. ^{1}H NMR (CD_2Cl_2, ambient, 200 MHz) δ 8.24 (d, 1H), 7.18 (t, 1H), 6.96 (t, 1H), 6.74 (t, 1H), 6.37 (d, 1H), 5.94 (s, 1H), 5.84 (s, 1H), 5.72 (s, 1H), 2.50 (s, 3H), 2.46 (s, 3H), 2.42 (s, 3H), 2.35 (m, 2H, CH_2), 2.25 (s, 3H), 1.59 (s, 3H), 1.29 (s, 3H), 0.82 (t, J=7.0 Hz, 3H). The 400 MHz ^{1}H NMR spectrum established that the 2H multiplet at δ 2.35 was an AB spectrum with added 7 Hz coupling to CH_3; the chemical shift separation of these diastereotopic methylene protons was 0.093 ppm, with J_{AB}=19 Hz. ^{13}C NMR (CD_2Cl_2, 75.5 MHz) δ 233.42 (d, J_{Rh-C}=27.2 Hz), 187.85 (d, J_{Rh-C}=72.5 Hz), 151.52 (s), 150.85 (s), 150.34 (s), 145.91 (d, J_{Rh-C}=28.7 Hz), 145.35 (s), 145.10 (s), 144.44 (s), 139.25 (s), 138.49 (s), 127.39 (s), 126.71 (s), 123.69 (s), 107.95 (s), 107.03 (s), 106.61 (s), 45.58 (s), 15.02 (s), 14.35 (s), 13.66 (s), 13.34 (s) 12.90 (s), 12.60 (s), 10.00 (s). Anal. Calcd for $C_{25}H_{32}BN_6O_2Rh$: C, 53.38; H, 5.69; N, 14.95. Found: C, 53.31; H, 5.90; N, 14.30.

Preparation of ($HBPz^{*}_3$)Rh(CO)(COC_2H_5)(COC_6H_5) (41)

Compound **39** (40 mg, 0.071 mmol) in acetonirile (20 mL) was placed in a 100 mL Parr bench autoclave which contained a magnetic bar. The solution was first flushed with CO and then pressurized with 1050 psig of CO and heated at 100°C for 62 h with stirring. The reaction was complete during this period. Removal of solvent yielded off-white solid (**41**).

Characterization: IR (n-hexane) 2068, 1694, 1621 cm^{-1} (ν_{CO}). ^{1}H NMR (CD_3CN, ambient, 200 MHz), δ 7.20 (br, t, 1H), 6.91 (br, t, 2H), 6.65 (br, d, 2H), 5.84 (s, 1H), 5.78 (s, 1H), 5.65 (s, 1H), 3.63 (m, 1H), 2.90 (m, 1H), 2.48 (s, 3H), 2.46 (s, 3H), 2.40 (s, 3H), 2.07 (s, 3H), 1.88 (s, 3H), 1.24 (s, 3H), 1.00 (t, J=7.0 Hz, 3H).

Preparation of $(HBPz^*_3)Rh(CO)(COCH_3)(C_6H_5)$ (42)

A solution of **9** (50 mg, 0.096 mmol) in hexane (35 mL) was pressurized with 1050 psig of CO in a 150 mL Parr bench autoclave. The reaction mixture was stirred at 100°C for three months. Progress was monitored by IR at approximately two-week intervals. At 8 weeks, the concentration of **9** had decreased to approximately 60% of its inital value. At three months disappearance of **9** was nearly complete. Removal of solvent yielded pale yellow solid. The solid residue was extracted with CH_2Cl_2 and chromatographed on a Florisil column (6 x 2.5 cm). The column was first washed with 200 mL n-hexane to remove the small quantity of unreacted starting material. Elution with CH_2Cl_2 gave **42**. Recrystallization by slow evaporation from hexane afforded colorless crystals of **42** (20 mg, 40%). MP 196-198°C.

Characterization: IR (n-hexane) 2070, 1677 cm^{-1} (ν_{CO}). MS (150°C, 16 eV) M^+ (548), M^+-CH_3, M^+-CH_3-CO, M^+-CH_3-2CO. ^{1}H NMR (CD_2Cl_2, ambient, 200 MHz), δ 8.20 (d, 1H), 7.15 (t, 1H), 6.96 (t, 1H), 6.74 (t, 1H), 6.34 (d, 1H), 5.92 (s, 1H), 5.82 (s, 1H), 5.72 (s, 1H), 2.50 (s, 3H), 2.46 (s, 3H), 2.42 (s, 3H), 2.28 (s, 3H), 1.98 (s, 3H), 1.60 (s, 3H), 1.32 (s, 3H). Anal. Calcd for $C_{24}H_{30}BN_6O_2Rh$: C, 55.55; H, 5.47; N, 15.33.

Found: C, 55.23; H, 5.47; N, 14.76.

Reactions of $(HBPz^*_3)Rh(CO)(COC_2H_5)(C_6H_5)$ (40) and $(HBPz^*_3)Rh(CO)(COCH_3)(C_6H_5)$ (42) with $ZnBr_2$

Compound **40** (8.0 mg, 0.015 mmol) was placed in a vial containing CD_2Cl_2 (0.6 mL). Excess $ZnBr_2$ (20.3 mg, 0.090 mmol) was added to the above solution. The vial was shaken for ca. 4 h. The initial colorless solution became dark yellow. The solution was filtered and transferred to an NMR tube. Hexamethyldisiloxane (1.0 μL) was added to the solution as an internal standard. The ^1H NMR showed propiophenone as the organic product [δ 7.92 (m, 2H), 7.56 (m, 3H), 3.92 (q, 2H), 1.24 (t, 3H)] in 82% yield.

Complex **42** (6.0 mg, 0.011 mmol), CD_2Cl_2 (0.6 mL) and excess $ZnBr_2$ (19.6 mg, 0.087 mmol) were placed in a small vial. The vial was shaken for ca. 36 h. No starting material was left at this point. The solution was filtered and transferred to an NMR tube. Hexamethyldisiloxane (1.0 μL) was added to the NMR solution. The ^1H NMR spectrum showed acetophenone [δ 7.98 (m, 2H), 6.54 (m, 3H), 2.26 (s, 3H)] as the organic product in 84% yield.

References for Chapter VI

1. (a) S. Trofimenko, J. Am. Chem. Soc., 91 (1969) 588.
   (b) S. Trofimenko, Inorg. Chem. 10 (1971) 1372.
2. M. Cocivera, T.J. Desmond, G. Ferguson, B. Kaitner, F.J. Lalor and D.J. O'Sullivan, Organometallics, 1 (1982) 1125.
3. M. Cocivera, G. Ferguson, B. Kaitner, F.J. Lalor, D.J. O'Sullivan, M. Parvez and B. Ruhl, Organometallics, 1 (1982) 1132.
4. M. Cocivera, G. Ferguson, F.J. Lalor and P. Szczecinski, Organometallics, 1 (1982) 1139.
5. L.P. Seiwell, J. Am. Chem. Soc. 96 (1974) 7134.
6. G. Paiaro and A. Panunzi, J. Am. Chem. Soc., 86 (1964) 5148, 88 (1966) 4843.
7. (a) R. Cramer, J. Am. Chem. Soc., 89 (1967) 4621.
   (b) E. Gil-Av and V. Schurig, Anal. Chem., 43 (1971) 2030.
8. R.J. Angelici and W. Loewen, Inorg. Chem., 6 (1967) 682.
9. D.P.S. Rodgers, personal communiation.
10. L. Vaska and J.W. DiLuzio, J. Am. Chem. Soc., 84 (1962) 679.
11. J. Halpern, Inorg. Chim. Acta, 100 (1985) 41, Acc. Chem. Res., 15 (1982) 238.
12. (a) J.K. Hoyano and W.A.G. Graham, J. Am. Chem. Soc., 104 (1982) 3723.
    (b) R.G. Bergman, P.F. Seidler and T.T. Wenzel, J. Am. Chem. Soc., 107 (1985) 4358.
    (c) T.T. Wenzel and R.G. Bergman, J. Am. Chem. Soc., 108 (1986) 4856.
    (d) A.H. Klahn-Oliva, R.D. Singer and D. Sutton, J. Am. Chem. Soc.

108 (1986) 3107.

13. P.A. Chetcuti and M.F. Hawthorne, J. Am. Chem. Soc., 109 (1987) 942.

14. H. Werner, A. Höhn and M. Dziallas, Angew. Chem. Int. Ed. Engl. 25 (1986) 1090.

15. D.F. McMillen and D.M. Golden, Ann. Rev. Phys. Chem., 33 (1982) 493.

16. S.P. Nolan, C.D. Hoff, P.O. Stoutland, L.J. Newman, J.M. Buchanan, R.G. Bergman, G.K. Yang and K.S. Peters, J. Am. Chem. Soc., 109 (1987) 3143.

17. A. Nutton and P.M. Maitlis, J. Organomet. Chem., 166 (1979) C21.

18. T.H. Coffield, J. Kozikowski and R.D. Closson, J. Org. Chem., 22 (1957) 598.

19. F. Calderazzo, Angew. Chem. Int. Ed. Eng., 16 (1977) 299.

20. A Wojcicki, Adv. Organomet. Chem., 11 (1973) 87.

21. A. Yamamoto, "Organotransition Metal Chemisry", John Wiley and Sons, NY (1986) 246.

22. E.J. Kuhlmann and J.J. Alexander, Coord. Chem. Rev., 33 (1980) 195.

23. (a) K. Noack and F. Calderazzo, J. Organomet. Chem., 10 (1967) 101.
    (b) T.C. Flood, J.E. Jensen and J.A. Statler, J. Am. Chem. Soc., 103 (1981) 4410.

24. F. Calderazzo and F.A. Cotton, Inorg. Chem., 1 (1962) 30.

25. F. Calderazzo and K. Noack, Coordination Chem. Rev., 1 (1966) 118.

26. R.J. Mawby, F. Basolo and R.G. Pearson, J. Am. Chem. Soc., 86 (1964) 3994.

27. M. Green, R.I. Hancock and D.C. Wood, J. Chem. Soc., (A) (1968) 2718.

28. J.D. Cotton and R.D. Markwell, Organometallics 4 (1985) 937.

29. T.G. Richmond, F. Basolo and D.F. Shriver, Inorg. Chem., 21 (1982)

1272.

30. D.A. Slack, D.L. Egglestone and M.C. Baird, J. Organomet. Chem, 146 (1978) 71.

31. G.J. Sunley, F.P. Fanizzi, I.M. Saez and P.M. Maitlis, J. Organomet. Chem., 330 (1987) C27.

32. A.J. Janowicz and R.G. Bergman, J. Am. Chem. Soc., 105 (1983) 3929.

33. R. Cramer, Inorg. Chem, 1 (1962) 722.

34. J. Powell and B.L. Shaw, J. Chem. Soc., (A) (1968) 211.

35. R.G. Ball, University of Alberta, Structure Determination Laboratory, Report No. SR:071801-15-86 (8 April 1987).

CHAPTER VII

METALLACYCLES

Section 1

INTRODUCTION

A metallacycle can be defined as a carbocyclic system in which one or more carbon atoms is replaced by a metal. Two examples of platinum metallcycles[1] are shown in eq. 7-1.

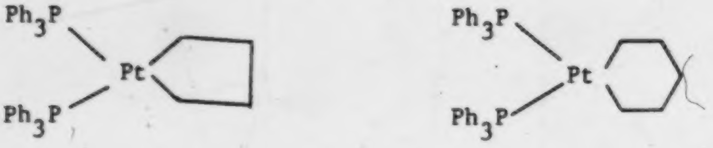

(7-1)

Although metallacycloalkanes can be formally regarded as metal complexes with two alkyl ligands, their chemistry is somewhat different from that of acyclic dialkyl complexes. For example the platinum metallacycles (eq. 7-1) are much more stable thermally than their acyclic counterparts.[2]

During recent years, metallacyclic compounds of the transition metals have drawn considerable attention because of their important role in a number of catalytic reactions, e.g. olefin metathesis,[3-7] isomerization of strained carbocyclic rings,[8-11] cycloaddition of alkenes[12,13] and oligomerization of dienes.[14-17] A general review of metallacycles appeared in 1982.[18]

In 1955, Tipper[19] made the first metallacyclic complex by treating chloroplatinic acid with cyclopropane in acetic anhydride. Its formula was $[PtCl_2(C_3H_6)]_n$, and the compound was later shown[20] to be a chloride bridged tetramer, with a structure analogous to Pt(IV) alkyls in which platinum was inserted into the cyclopropane ring. Platinacyclobutanes are among the most extensively studied metallacyclic compounds, and this area has been reviewed.[21]

Metallacyclobutanes are sometimes prepared by the reaction of 1,3 dimagnesiopropanes with metal dihalides (eq. 7-2).[22]

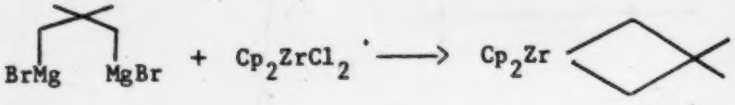
BrMg
MgBr
+
Cp_2ZrCl_2
Cp_2Zr

(7-2)

The product of reaction (7-2) is more stable than the corresponding zirconacyclobutane without methyl substituents. They can also be prepared in certain cases by reduction of appropriate η^3-allyl complexes. Eq. 7-3 illustrates the synthesis of metallacyclobutane derivatives of tungsten[23] from an allylic derivative.

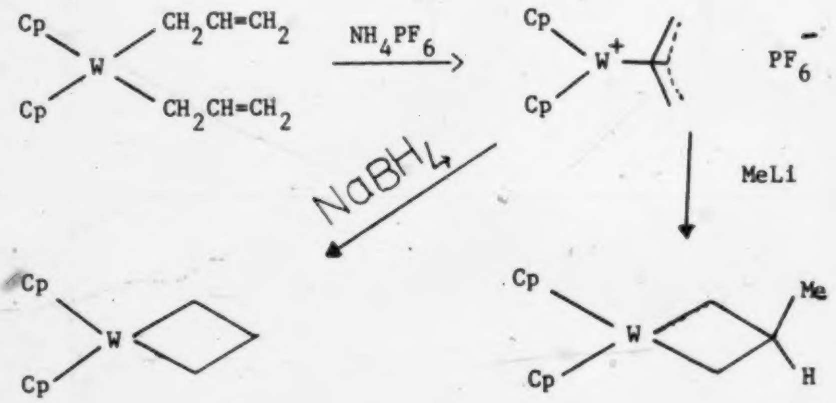
Cp
Cp
W
$CH_2CH=CH_2$
$CH_2CH=CH_2$
NH_4PF_6
Cp
Cp
W^+
PF_6^-
MeLi
NaBH4
Cp
Cp
W
Cp
Cp
W
Me
H

(7-3)

A more recent example[24] is represented by eq. 7-4.

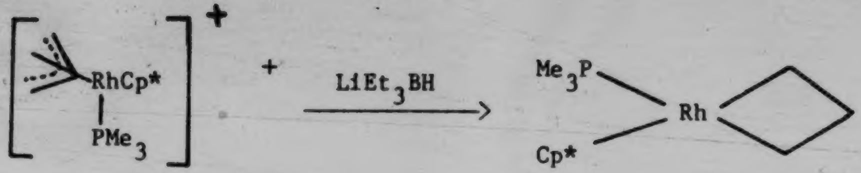
+
RhCp*
PMe3
+
LiEt3BH
Me3P
Rh
Cp*

(7-4)

A number of metallacycles have been prepared via decomposition of alkyl complexes of the transition metals, in which the well known decomposition pathway, β-elimination, is blocked by substitution at the β-carbon atom. Metallacycles have been made by cyclometallation reactions in which a γ_{C-H} bond is attacked.[25,26,27] Eq. 7-5 shows such an example.[25]

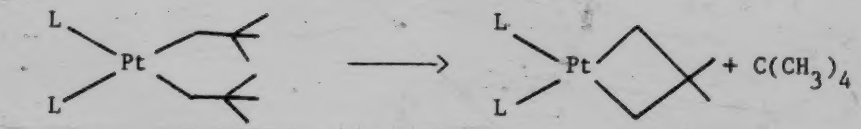
L
Pt
L
L
Pt
L
+ C(CH3)4

(7-5)

(L = PEt_3)

Tulip and Thorn[26] reported the formation of a stable hydridometallacyclobutane (eq. 7-6) from the reaction of $[Ir(PMe_3)_4Cl]$ with $LiCH_2CMe_3$ in hexane or toluene at room temperature. However,

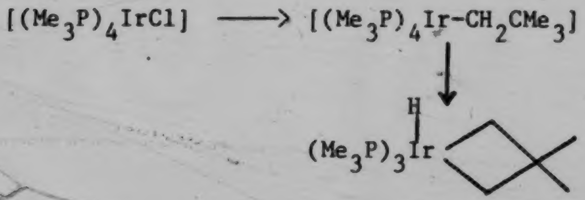
[(Me3P)4IrCl]
[(Me3P)4Ir-CH2CMe3]
H
(Me3P)3Ir

(7-6)

more often the hydrogen is coupled to another alkyl ligand and eliminated as alkane.[25,27] The formation of a thoracyclobutane was reported by Marks et al.[27] and is considered to result from electrophilic attack by a Th-C bond on a C-H bond (eq. 7-7).

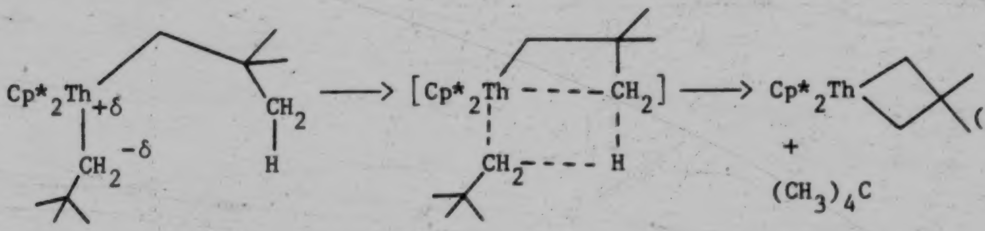
Cp*₂Th
+δ
-δ
CH₂
CH₂
H
[Cp*₂Th
CH₂]
CH₂
H
Cp*₂Th
+
(CH₃)₄C

(7-7)

Periana and Bergman[24,28] reported the formation of hydridocyclopropylrhodium complex (eq. 7-8) by irradiation of $Cp^*(PMe_3)Rh(H)_2$ in liquid cyclopropane at -60°C, which rearranged upon warming to 0°C. The final product (eq. 7-8) was a C-C cleaved metallacycle. It was suggested that completely uncoordinated cyclopropane was not an intermediate, as was shown by the inability of solvent benzene to divert all the rhodium to $Cp^*(PMe_3)Rh(H)(C_6H_5)$ by intercepting $Cp^*(PMe_3)Rh$ during rearrangement.

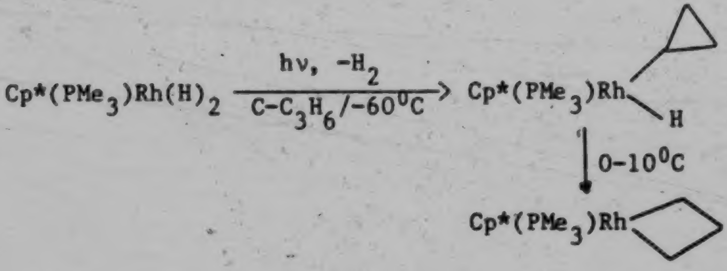
Cp*(PMe₃)Rh(H)₂
hν, -H₂
C-C₃H₆/-60°C
Cp*(PMe₃)Rh
H
0-10°C
Cp*(PMe₃)Rh

(7-8)

In the related iridium system, a stable hydridocyclopropyl complex $[Cp^*(PMe_3)Ir(H)(c\text{-}C_3H_5)]$ was obtained by irradiation of $Cp^*(PMe_3)Ir(H)_2$[29] in liquid cyclopropane. No C-C insertion product was observed in this system.

In continuation of C-H activation studies with $(HBPz^*_3)Rh(CO)_2$ (1), the reaction of cyclopropane was of interest. In view of the results obtained in a related $Cp^*(PMe_3)Rh$ system, one would expect the formation of a rhodacyclobutane in the present system. The reaction of cyclopropane and methylcyclopropane with 1 will be described. The choice of methylcyclopropane raised questions as to the regio- and stereochemistry of the reaction. The kinetic results of thermolysis of rhodacyclobutane in benzene and the mechanism of formation of $(HBPz^*_3)Rh(CO)(H)(C_6H_5)$ in this reaction will be discussed. Finally, carbonylation of the metallacycle to form five and six membered metallacycles has been explored.

Section 2

SYNTHESIS AND CHARACTERIZATION OF METALLACYCLES

Reaction of $(HBPz*_3)Rh(CO)_2$ (1) with cyclopropane

Irradiation of a yellow cyclohexane solution of 1 (2.74 mM) under a cyclopropane purge for nine minutes at room temperature afforded a colorless solution. The IR spectrum of the reaction mixture in cyclohexane immediately after photolysis indicated complete disappearance of 1 and showed new carbonyl bands at 2023 cm^{-1} and 2036 cm^{-1}; the latter was weaker. The IR indicated disappearance of the 2036 cm^{-1} band over a few minutes with a simultaneous increase in intensity of the 2023 cm^{-1} band. The observed ν_{CO} band at 2036 cm^{-1} is presumed to be due to hydridocyclopropyl complex (**44**); while the band at 2023 cm^{-1} is assigned to rhodacyclobutane (**45**) (eq. 7-9).

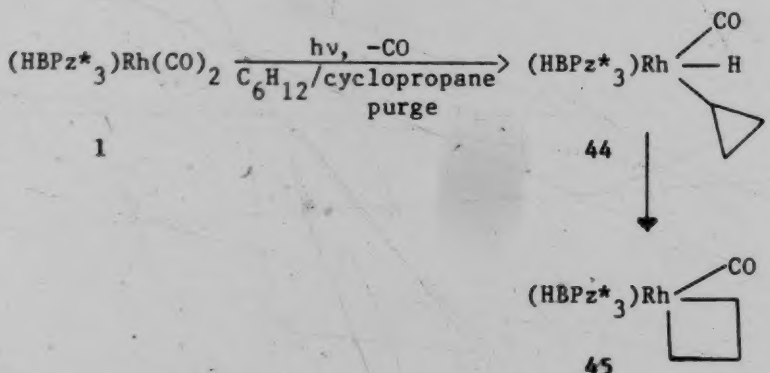

(7-9)

Compound **45** was isolated as colorless crystals in 75% yield after chromatographic purification. It is quite stable thermally and not particularly air sensitive. It was fully characterized by spectral and analytical techniques. The IR spectrum of **45** in n-hexane showed a single ν_{CO} at 2024 cm^{-1}. The MS did not show the molecular ion; the highest observed m/e corresponded to $M^{+}-C_3H_6$. A peak due to loss of CO was observed. The ^1H NMR spectrum exhibited two singlets in the 4-H region of the Pz* ring in a 2:1 ratio, and pairs of signals in the 3- and 5-CH_3 region in 6:3 ratio. This NMR result suggests that the metallacyclobutane ring is symmetric about the Rh-C_β axis as one would expect. The crystal structure[24] of the related $Cp^*(PMe_3)\overline{Rh-CH_2CH_2CH_2}$ showed that the metallacyclobutane ring was essentially symmetric and planar.

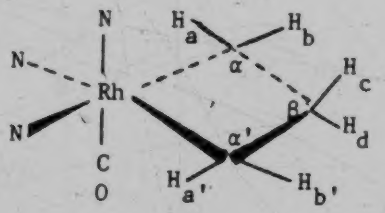

45 (atom labelling for NMR)

In 45, H_a and $H_{a'}$ were equivalent and appeared as a multiplet (δ 1.65) in the ^1H NMR spectrum. A complex multiplet was found for H_b and $H_{b'}$ (δ 1.40). H_c and H_d appear as multiplets at δ 3.15 and 2.82 respectively.

The $\{^1H\}$ ^{13}C NMR spectrum of 45 is informative. The Rh-C_α and Rh-C_β of the metallacycle were found at δ -13.31 (d, J_{Rh-C}=15.0 Hz) and 35.5 (d, J_{Rh-C}=3.8 Hz) respectively. Details of ^{13}C NMR data will be found in the Experimental Section.

Attempts to isolate the presumed hydridocyclopropyl intermediate (44) (eq. 7-9) were not successful. A cyclohexane solution of 1 was irradiated at -15°C using a cyclopropane purge for 15 minutes. Excess

CCl_4 was added to the photolyzed solution at -15°C and the reaction was allowed to continue for 1.5 h. The IR spectrum (hexane) exhibited ν_{CO} at 2077 and 2024 cm^{-1} in an absorbance ratio of 2.5:1. Based on the positions of ν_{CO} bands of some well characterized alkylrhodium chlorides, the band at 2077 cm^{-1} is presumed to be due to the chloro derivative of **44**. Unfortunately, attempts to separate the mixture by chromatography on alumina or by crystallization were not successful.

Based on the IR evidence and also from the results of the related $Cp^*(PMe_3)Rh$ system,[24] it is presumed that the initial C-H activation product (**44**) undergoes rearrangement to the corresponding C-C insertion product, rhodacyclobutane (**45**) (eq. 7-9).

Compound 45 decomposed at _ca_. 150°C during examination of its melting point. The IR of a hexane extract of the decomposed product indicated the presence of the dimer (**38**), which was also obtained during thermolysis of $(HBPz^*_3)Rh(CO)(\eta^2\text{-}C_3H_6)$ (**34b**) or $(HBPz^*_3)Rh(CO)(H)(C_6H_5)$ (**6**) in cyclohexane at 75°C.

Reaction of $(HBPz^*_3)Rh(CO)_2$ (1) with methylcyclopropane

When a yellow solution of 1 (2.19 _mM_) in purified cyclohexane was irradiated for ten minutes using a methylcyclopropane purge, the solution became colorless. The IR (cyclohexane) indicated a weak ν_{CO} band at 2033 cm^{-1} and a strong ν_{CO} band at 2022 cm^{-1}. After a few minutes, the IR showed complete disappearance of the 2033 cm^{-1} band and a corresponding increase in intensity of the 2022 cm^{-1} band. This observation is similar to the cyclopropane reaction. The band at 2022 cm^{-1} is assigned to the stable rhodamethylcyclobutane (**46**) (eq. 7-10).

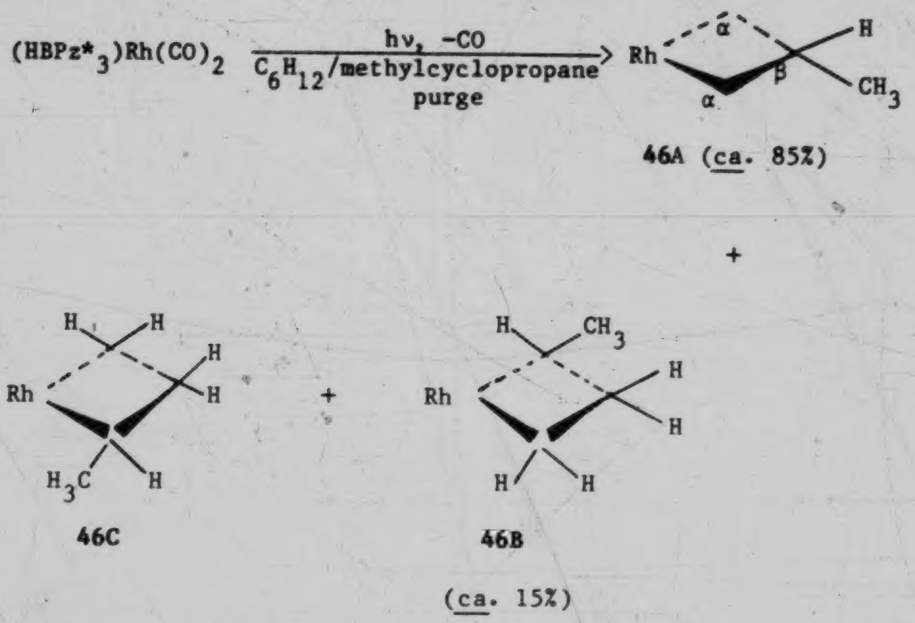
(HBPz*$_3$)Rh(CO)$_2$
hν, -CO
C$_6$H$_{12}$/methylcyclopropane
purge
Rh
α
α
β
H
CH$_3$
46A (ca. 85%)
+
Rh
H
H
H
H
H$_3$C
H
46C
+
Rh
H
CH$_3$
H
H
H
H
46B
(ca. 15%)

(7-10)

Compound **46** was isolated as colorless crystals in 65% yield and characterized by the usual spectroscopic and analytical techniques. Although the IR spectrum (hexane) exhibited only one ν_{CO} at 2023 cm^{-1}, the ^{1}H NMR suggested the presence of more than one isomer of **46** (eq. 7-10). The resonances due to the major isomer (**46A**) were well resolved (**46A** was identified as the major isomer by ^{13}C NMR, which will be discussed later). The ^{1}H NMR of **46A** showed two singlets in the 4-H region in a 2:1 ratio (δ 5.85, 5.58) and pairs of singlets in the 3- and 5-CH$_3$ region in a 6:3 ratio. H$_\beta$ appeared as a broad multiplet at δ 3.44 (1H). H$_\alpha$ appeared as multiplets at δ 2.00 (2H) and 1.00 (2H). The methyl group on C$_\beta$ appeared as a doublet (δ 1.13, J=7.0 Hz). Although most of the peaks of the minor isomers (**46B** and **46C**) were not well resolved, α-CH$_3$ signals at δ 1.17 (d, J=7.0 Hz) and 1.07 (d, J=7.0 Hz) were resolved; by integration of these signals, **46B** and **46C** comprise ca.

15% of the isomeric mixture.

APT ^{13}C NMR of the isomeric mixture of **46** is quite informative and a representative spectrum is shown in Fig. VII.1. It showed only the major isomer **46A**. Detailed assignments are given in experimental section. C_β of the metallacycle (assigned by means of its odd number of protons) appeared as a doublet at 40.77 ($^2J_{Rh-C}$=3.8 Hz). A doublet at δ -3.36 (J_{Rh-C}=14.3 Hz) was exhibited by C_α, assigned by means of the even number of protons attached. The methyl carbon bound to C_β of the ring appeared as a singlet at δ 23.07.

Prentice-Hall (PH) models show a crowded environment "above" the metallacyclobutane ring (i.e., on the boron side of the rhodium). An extremely hindered situation results when the β-CH_3 group of the metallacyle is directed towards the pyrazolylborate ligand. Less crowding results when the β-CH_3 is directed away from the pyrazolylborate ligand. The assignment of **46A** as the major isomer is based on these steric considerations.

It appeared from the PH models that a methyl group on the α-carbon of the ring can just be accommodated. It appeared to make little difference whether it was directed towards or away from the pyrazolylborate ligand. This would explain the presence of two minor isomers **46B** and **46C**.

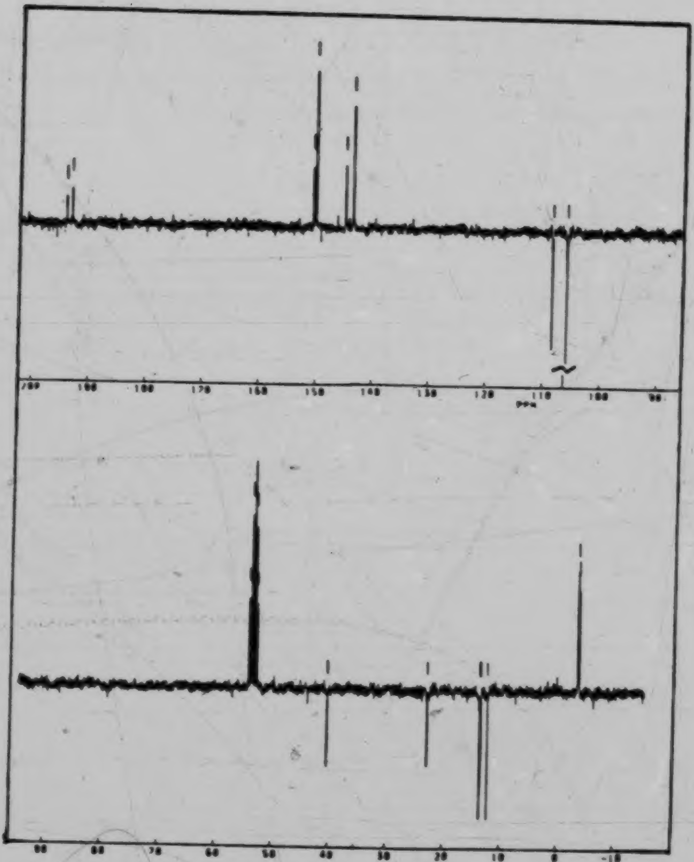

Figure VII.1 ^{13}C NMR spectrum (75.5 MHz, CD_2Cl_2) of methyl-substituted metallacyclobutane (**46A**).

Section 3

THERMOLYSIS OF METALLACYCLES

Thermolysis of 45

The thermolysis of metallacycle **45** was carried out in benzene-d_6 at 75°C in a sealed NMR tube. Hexamethyldisiloxane was used as internal standard. At specified times the NMR tube was withdrawn from the constant temperature bath and cooled, and NMR spectra were recorded at room temperature. Thermolysis was observed to proceed slowly and afforded mostly $(HBPz^*{}_3)Rh(CO)(D)(C_6D_5)$ (**8a**).

During thermolysis, the ^1H NMR indicated the formation of $(HBPz^*{}_3)Rh(CO)(\eta^2\text{-}CH_2CHCH_3)$ (**34b**), which slowly disappeared with the progress of reaction. This observation suggested the intermediacy of **34b** in the formation of **8a**. As described in Chapter VI, thermolysis of **34b** in benzene at 75°C yielded phenylhydride **6** and propylene. Fig. VII.2 shows the changes in concentration of **45**, **34b** and **8a** as a function of time. The organic products in the thermolysis reaction were propylene and cyclopropane, identified by ^1H NMR. The presence of propylene and cyclopropane suggested that two independent pathways might be involved for the formation of **8a**.

One route is presumed to be the direct conversion of **45** to **8a** with the reductive elimination of cyclopropane, supported by the presence of cyclopropane in the products. The second pathway involves the conversion of **45** to **34b**, which acts as an intermediate for the formation of **8a**. The overall scheme proposed for the conversion of metallacyclobutane (**45**) to **8a** is shown in eq. 7-11.

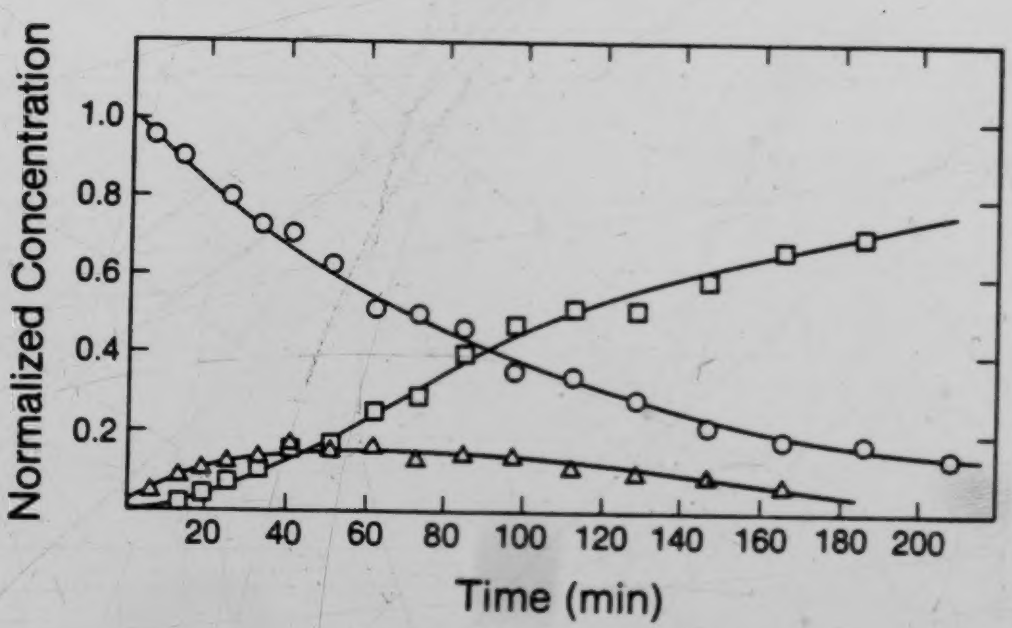

Figure VII.2 Plot of normalized concentrations of metallacyclobutane (**45**, O), pentadeuterophenyl deuteride (**8a**, □) and η^2-propylene complex (**34b**, Δ) at 75°C.

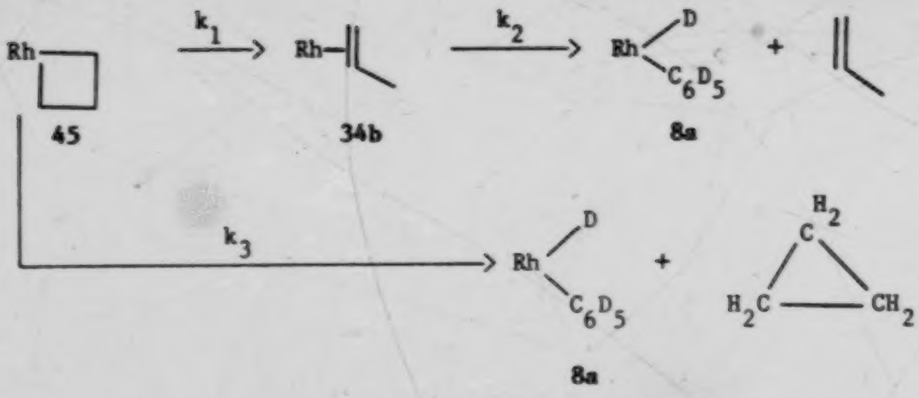

(7-11)

Examples of the rearrangement of metallacyclobutanes to olefin complexes are known.[30]

To evaluate k_1, k_2 and k_3 in eq. 7-11, a detailed kinetic study was carried out. The rate of disappearance of **45** was followed by heating the complex in C_6D_6 solvent at 75°C and monitoring the integral of one of the methyl resonances of the Pz* ring (δ 2.44) against the internal standard. Good first-order kinetics over three half-lives was observed. A typical plot of the ln(relative intensity) of the methyl pyrazole resonance versus time is shown in Fig. VII.3. The observed rate constant $(k_1 + k_3)$ is $(2.7 \pm 0.1) \times 10^{6}\ s^{-1}$.

To determine k_2 in eq. 7-11, an independent kinetic study of thermolysis of $(HBPz^*_3)Rh(CO)(\eta^2\text{-}CH_2CHCH_3)$ (**34b**) in C_6D_6 solvent at 75°C in a sealed NMR tube was carried out. The rate of disappearance of **34b** was followed by monitoring the integral of the methyl resonance of the propylene against the internal standard (hexamethyldisiloxane). A logarithmic plot of the relative intensity of the methyl resonance versus time yielded a straight line (Fig. VII.4) with slope equal to $-k_2$. The value obtained for k_2 is $(7.6 \pm 0.3) \times 10^{-6}\ s^{-1}$.

Integrated rate equations appropriate to the kinetic scheme of eq.

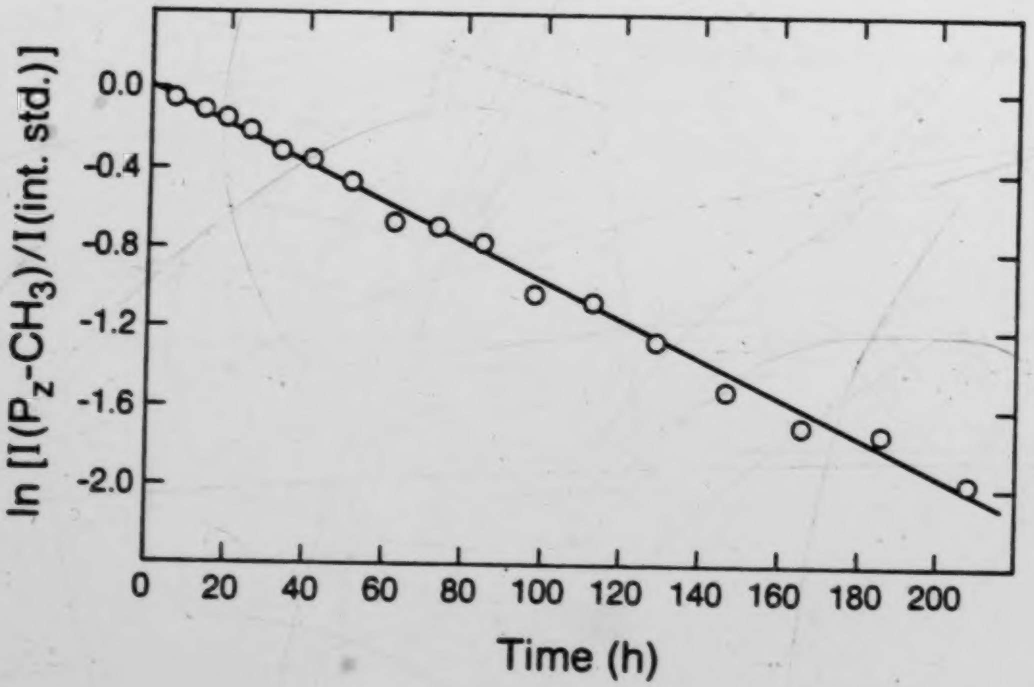

Figure VII.3 Pseudo-first-order plot for the disappearance of metallacyclobutane (45) in benzene-d_6 at 75°C.

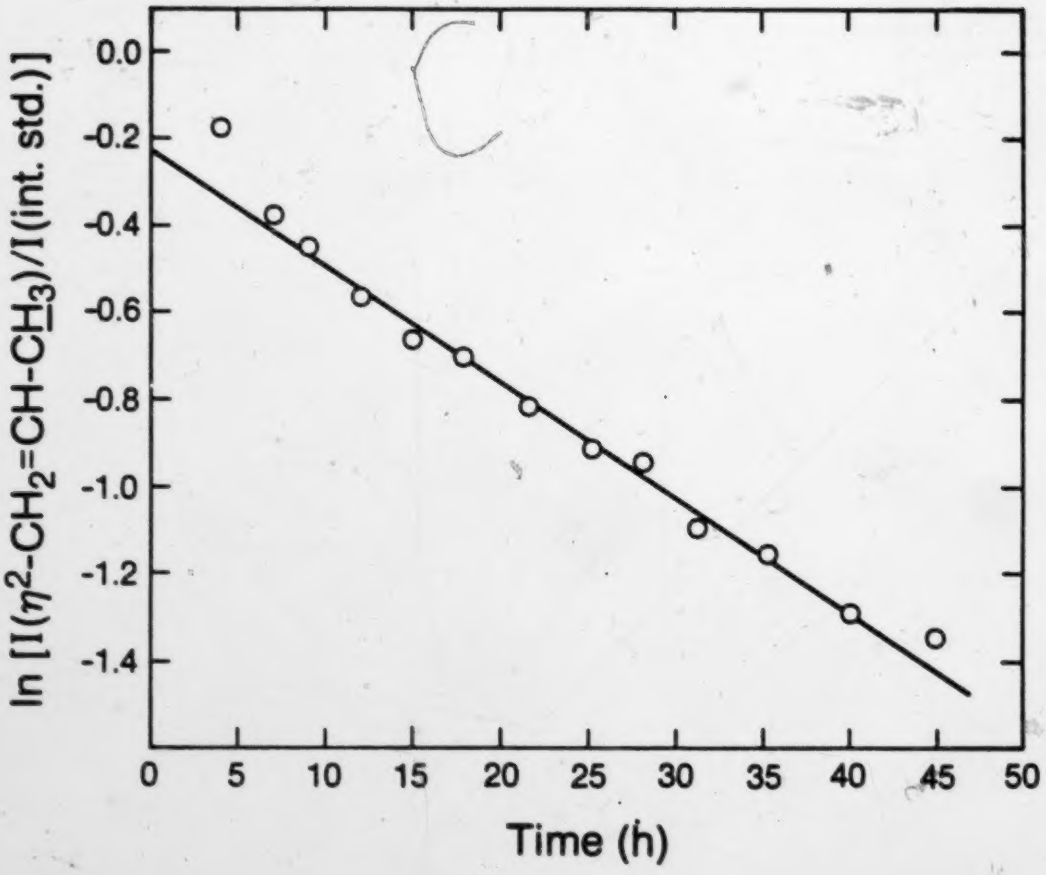

Figure VII.4 Pseudo-first-order plot for the reaction of η^2-propylene complex (**34b**) with benzene-d_6 at 75°C.

7-11 are available as a special case of more general solutions in the literature.[31]

$$\begin{tikzcd} A\ (\mathbf{45}) \arrow[r, "k_1"] \arrow[rr, bend right, "k_3"'] & B\ (\mathbf{34b}) \arrow[r, "k_2"] & C\ (\mathbf{8a}) \end{tikzcd}$$

$$A/A_o = e^{-(k_1+k_3)t}$$

$$B/A_o = \frac{k_1}{k_2 - (k_1+k_3)} \left[e^{-(k_1+k_3)t} - e^{-k_2t}\right]$$

$$C/A_o = \left[1 - e^{-k_2t}\right] + \frac{(k_3-k_2)}{k_2 - (k_1+k_3)} \left[e^{-(k_1+k_3)t} - e^{-k_2t}\right]$$

A_o is the initial (t=0) concentration of A (**45**), while the initial concentrations of B (**34b**) and C (**8a**) are zero.

A computer program written by Mr. Kam Kong of this Department took input values of (k_1+k_3), k_2, and the ratio k_1/k_3. The first two of these parameters were directly measurable. The program calculated [A], [B], and [C] at specified times, generating values that could be compared with the experimental concentrations for various assumed ratios k_1/k_3. The ratio k_1/k_3 could be selected that visually afforded the best fit of the data (cf. Fig. VII.5).

The k_1/k_3 ratio in effect gives the split betwen the direct and indirect pathways for conversion of A (**45**) to C (**8a**). It should be noted that k_2 is a pseudo-first order rate constant, the concentration of C_6D_6 being effectively constant.

It appeared that the concentration of **8a** was not very sensitive to

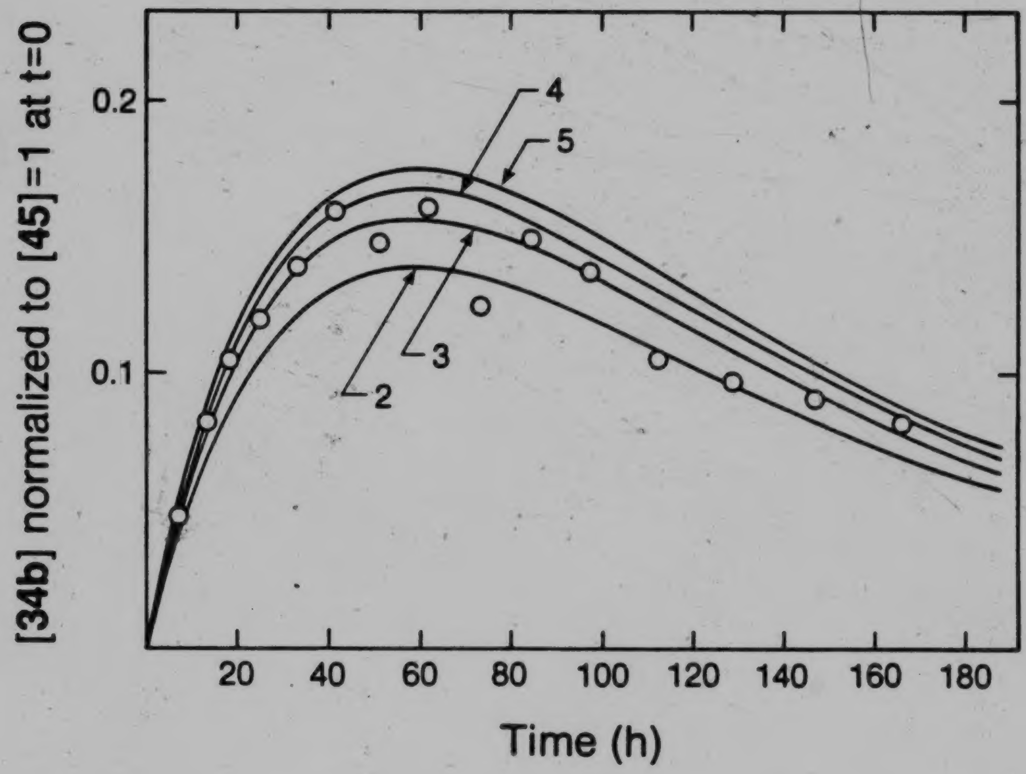

Figure VII.5 Calculated and observed concentrations of η^2-propylene complex (34b) when 45 is heated in C_6D_6 at 75°C. The numbers with arrows indicate k_1/k_3 ratios.

k_1/k_3 ratios. However, the concentration of **34b** was quite sensitive to k_1/k_3 ratios. The best fit of the normalized concentration of **34b** with the observed concentration was obtained using $k_1/k_3 = 3$. A typical plot of the observed and calculated (using $k_1/k_3 = 2\text{-}5$) concentration of **34b** as a function of time is shown in Fig. VII.5. From fitting kinetic data [$k_1 + k_3 = (2.7\pm0.1) \times 10^{6}\ s^{-1}$, $k_2 = (7.6\pm0.3) \times 10^{-6}\ s^{-1}$, $k_1/k_3 = 3$] the rate constants obtained are:

$$k_1 = (2.0 \pm 0.1) \times 10^{-6}\ s^{-1}$$

$$k_3 = (6.8 \pm 0.1) \times 10^{-7}\ s^{-1}$$

The ratio $k_1/k_3 = 3$ suggested that propylene/cyclopropane ratio would be ≅ 3 at the completion of reaction, assuming similar solubilities of the two gases in C_6D_6. From integration of cyclopropane and propylene resonances, the ratio of propylene/cyclopropane was 4.5±1. Considering the uncertainties involved, this value appeared to be in reasonable agreement with the expected ratio of 3.

It is concluded from the kinetic data analysis that 75% of the thermal decomposition of metallacyclobutane (**45**) proceeds via the intermediate η^2-propylene complex (**34b**) and 25% by direct reductive elimination of cyclopropane (eq. 7-12).

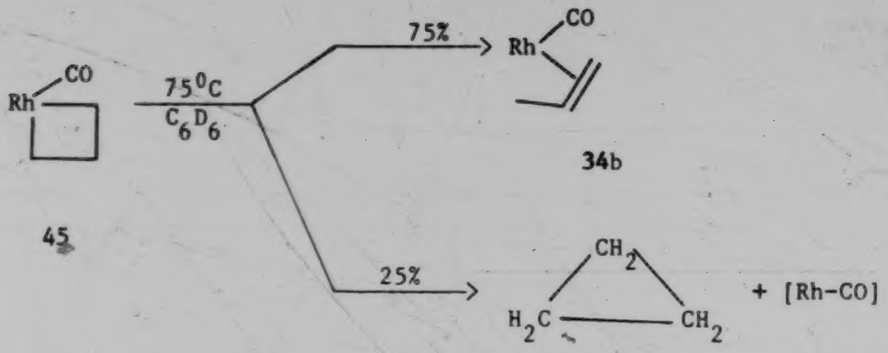
Rh
CO
75°C
C6D6
75%
Rh
CO
25%
CH2
H2C
CH2
+ [Rh-CO]

45

34b

(7-12)

The intermediate η^2-propylene complex (**34b**) may form by a β-elimination process facilitated by an η^3-η^2 shift of the (HBPz$^*_3$) ligand, as shown in eq. 7-13.

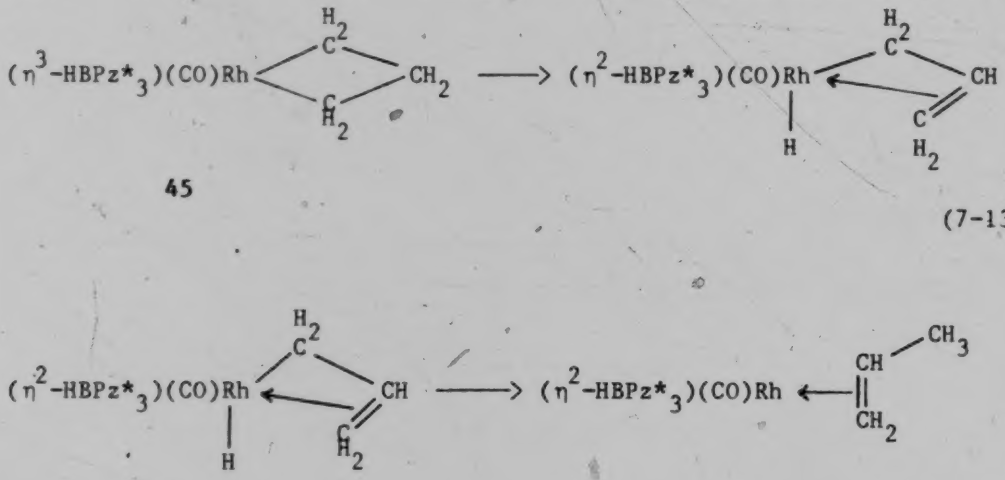
(η3-HBPz*3)(CO)Rh
H2
C
CH2
C
H2
(η2-HBPz*3)(CO)Rh
H
H2
C
CH
C
H2
(η2-HBPz*3)(CO)Rh
H
H2
C
CH
C
H2
(η2-HBPz*3)(CO)Rh
CH
CH3
CH2

45

(7-13)

34b

In the rearrangement of metallacycles to olefin complexes, it has generally been assumed[32] that the initial step is β-hydrogen elimination. However, no metallacycle has been directly observed to form an allyl hydride complex by β-hydrogen elimination.

An interesting question is whether β-hydrogen elimination could still occur with the major isomer of **46** (**46A**), which is considered to have methyl in the β-position of the ring and directed away from (HBPz$^*_3$) ligand. Thus thermolysis of **46** was carried out, and the results will be discussed in the following section.

Thermolysis of 46

Thermolysis of **46** was carried out in benzene-d_6 solvent at 75°C in a sealed NMR tube using hexamethyldisiloxane as an internal standard. The thermolysis was followed by recording ^{1}H NMR spectra at ambient temperature at specified times. The ^{1}H NMR indicated the formation of (HBPz$^*_3$)Rh(CO)(D)(C_6D_5) (**8a**) as the thermolysis proceeded. Qualitatively, the rate of disappearance of **46** was slower than that of **45**. No intermediate olefin complex was observed during the thermolysis. This is in contrast to the thermolysis of **45**, where an intermediate η^2-propylene complex (**34b**) was found.

The organic products in the thermolysis reaction were identified by ^{1}H NMR as methylcyclopropane and isobutylene. Isobutylene is considered to form from an unobserved η^2-isobutylene intermediate. The intermediate η^2-isobutylene complex was presumably not observed because of its more labile nature as compared with **34b**. The ratio of methylcyclopropane/isobutylene was approximately 4 by ^{1}H NMR. This ratio suggested that 80% of the reaction proceeded by direct elimination of methylcyclopropane and 20% of the reaction proceeded via the presumed η^2-isobutylene complex (eq. 7-14).

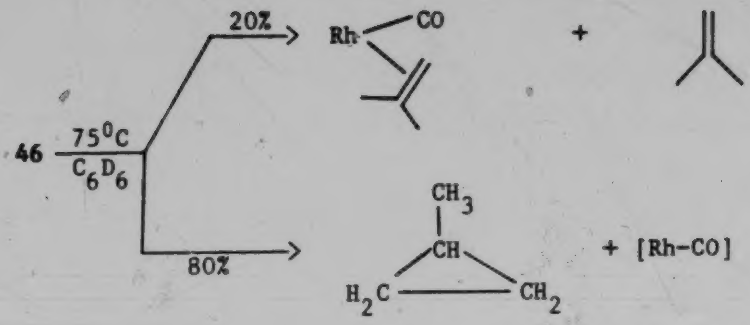

(7-14)

The results shown in eq. 7-14 are just the opposite to those obtained in case of thermolysis of **45** (eq. 7-12) where 75% of the reaction proceeded via the η^2-propylene complex and 25% by direct elimination of cyclopropane.

As described earlier, **46** contains ca. 15% of isomers that have two β-H atoms (the α-methyl isomers). Perhaps it is these (**46B** and **46C**) that are giving rise to olefin, while **46A** gives only methylcyclopropane. This possibility could be tested if a means to separate isomers of **46** could be found.

As discussed previously, PH models showed serious crowding "above" the metallacycle ring; it was considered that the major isomer, **46A** had a downward projecting β-CH_3 substituent. It appears reasonable that β-hydrogen transfer to the ring would require some folding of the ring (as shown below).

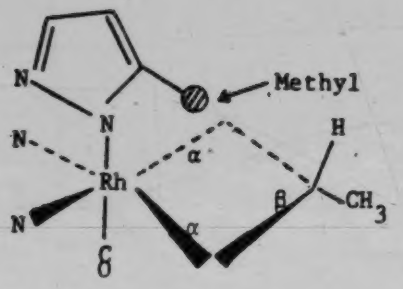

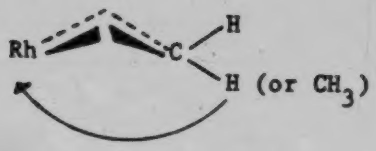

(46A)

For 46A, this would require folding into the crowded region, disfavouring olefin formation. For 45 on the other hand, there is a β-H on either side of the ring, which could fold away from the 3-methylpyrazole group in the transfer process.

This argument offers a rationale for the observed preponderance of methylcyclopropane in the thermolysis of 46A. These discussions are tentative, because it was not possible to obtain a pure sample of 46A. More intensive efforts at purification might be justified in future work.

Cyclopropane or methylcyclopropane formation from the metallacycle can be considered as a simple reductive elimination process (eq. 7-15).

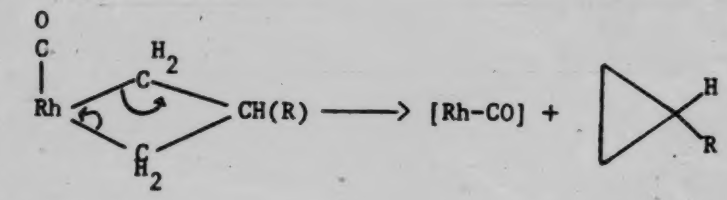

(7-15)

Since eq. 7-15 proceeds spontaneously as written, it implies that cyclopropanes will not react with the unsaturated intermediate to form the metallacyclobutane directly. Of course, they do not, the pathway instead involving C-H activation.

Section 4

FUNCTIONALIZATION OF METALLACYCLES

This section addresses some aspects of functionalization of metallacycles. As described in Chapter VI, one of the most important reactions in organometallic chemistry and in catalysis is the insertion of carbon monoxide into metal-carbon sigma bonds. Examples of stable carbon monoxide inserted metallacycles are rare. Grubbs and coworkers[33] reported the reaction of nickelacyclopentane with CO under mild conditions to give cyclopentanone (eq. 7-16).

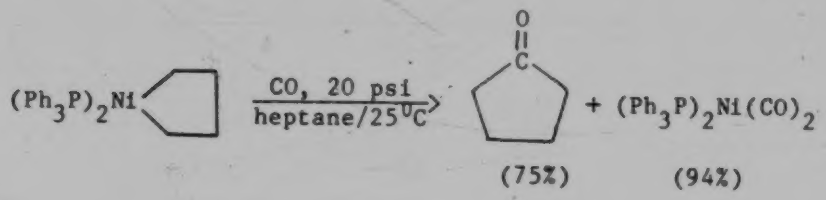

(7-16)

No metallacyclohexanone was detected in this reaction although it would be a plausible intermediate.

As an extension of the present work, carbonylation of metallacyclobutane (45) was investigated to determine whether it would afford a stable metallacyclopentanone, or whether cyclobutanone would form via the presumed CO inserted species. A general discussion on carbonylation reactions will be found in Chapter VI.

Carbonylation of $(HBPz^{*}_{3})(CO)Rh{-}CH_2{-}CH_2{-}CH_2$ (45)

The carbonylation of 45 was carried out in n-hexane at room temperature using 950 psig of CO. The reaction according to eq. 7-17 was complete in seven days.

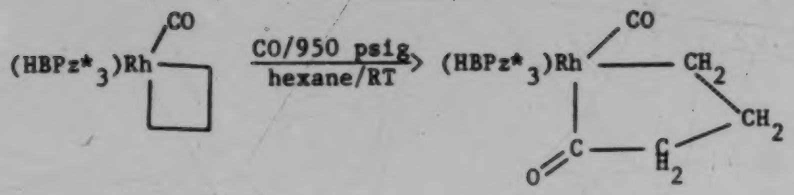

(7-17)

45 47

On the basis of the intensities of the ν_{CO} bands and assuming similar extinction coefficients, the IR indicated quantitative converstion of 45 to 47. Cyclobutanone was not detected in the reaction products.

Compound **47** was isolated as colorless crystals after chromatographic purification and crystallization and fully characterized by the usual spectral and analytical techniques. The IR (hexane) indicated a terminal and an acyl ν_{CO} at 2038 and 1707 cm^{-1} respectively. The MS showed the molecular ion and peaks due to successive loss of C_3H_6, CO, etc. were observed. All six methylene protons of the metallacycle are nonequivalent, and the ^1H NMR exhibited six multiplets in the range δ 3.37 - δ 2.04. The resonances at δ ca. 2.14 (m, 1H) and ca. 2.04 (m, 1H) showed some overlap with the methyl resonances of the Pz* rings. Coincidental overlap among the 4-H and 3- and 5-CH_3 resonances of the Pz* rings was also observed.

The APT ^{13}C NMR of **47** showed the acyl and terminal CO resonances at δ 241.5 (d, J_{Rh-C}=25.7 Hz) and 189.45 (d, J_{Rh-C}=72.5 Hz) respectively. The resonance at δ 24.45 (d, J_{Rh-C}=21.9 Hz) is assigned to C_α of the metallacycle.

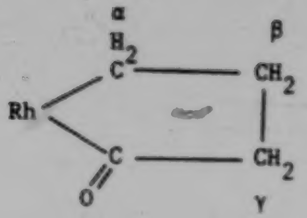

47 (ring only)

Judging from the chemical shift of C_β in 45 (δ 35.5), the resonance at δ 26.35 (s) is assigned to C_β in 47. One would expect the resonance due to C_γ to occur downfield relative to C_α and C_β since it is attached directly to CO; thus the resonance at δ 59.20 (d, $^2J_{Rh-C}$=8.3 Hz) can be asigned to C_γ. In view of its connection to rhodium via an sp^2 carbon atom, the observed J=8.3 Hz value is quite reasonable.

Attempt to eliminate cyclobutanone from 47

As shown in Chapter VI, the propionyl phenyl complex (**40**) reacted with $ZnBr_2$ to give propiophenone in good yield. Thus the reaction of 47 with $ZnBr_2$ in CH_2Cl_2 at room temperature was carried out with a view to eliminating cyclobutanone. The reaction of 47 with $ZnBr_2$ was fast and IR monitoring showed the growth of two bands at 2071 and 1731 cm^{-1}. Cyclobutanone was not observed among the reaction products. The new unidentified species did not survive chromatography under the experimental conditions.

Reaction of 45 with phenyldimethylphosphine

As discussed in Chapter VI, kinetic and mechanistic studies of carbon monoxide insertion reaction in $CH_3Mn(CO)_5$ and related compounds have revealed that the CO molecule that becomes the acyl-carbonyl is not derived from external CO but is one already coordinated to the metal atom. Since the carbonylation of **45** afforded the stable isolable acyl derivative **47**, it was of interest to examine the reaction of **45** with a phosphine with the expectation of obtaining an acyl complex. The formation of an acyl compound would be consistent with the migration mechanism.

Reaction of **45** with an excess of PMe_2Ph in CH_2Cl_2 was carried out at room temperature. The IR showed the complete disappearance of **45** in two days and indicated the formation in good yield of a new acyl complex (**48**) (eq. 7-18).

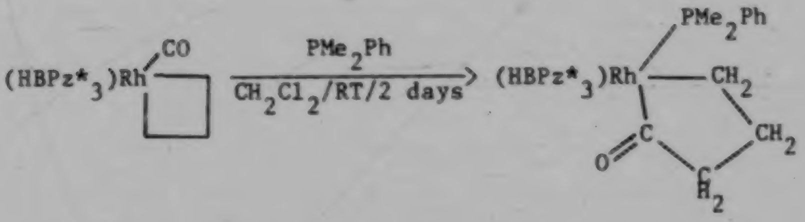

(7-18)

45 **48**

Qualitative observations indicated that the rate of formation of **48** increased with the phosphine concentration.

Compound **48** was isolated as colorless crystals in 75% yield after chromatography and crystallization and fully characterized by the usual spectroscopic and analytical techniques. The acyl carbonyl appeared at 1650 cm^{-1} (CH_2Cl_2) substantially lower than in **47** (1707 cm^{-1} in hexane).

The ^1H NMR spectrum of **48** showed three 4-H and six 3- and 5-CH_3 resonances of the Pz* rings, suggesting three nonequivalent rings in the octahedral geometry. Three multiplets at δ 7.15 (1H), 6.96 (2H) and 6.82 (2H) were found for the aromatic protons. The metallacycle methylene protons appeared as three multiplets at δ 3.15 (2H), 2.82 (2H) and 2.94 (2H). The phosphorus bound methyl groups are diastereotopic and appeared at δ 1.76 (dd, $^2J_{P-H}$=8.5 Hz, $^3J_{Rh-H}$=1.0 Hz) and 1.70 (dd, $^2J_{P-H}$=8.2 Hz, $^3J_{Rh-H}$=1.2 Hz).

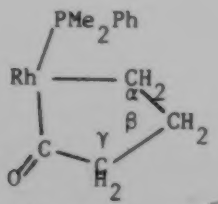

48 (ring only)

The APT ^{13}C NMR exhibited the acyl CO as a doublet of doublets at δ 251.55 (J_{Rh-C}=30.9 Hz; J_{P-C}=10.6 Hz). The phosphorus bound phenyl carbon appeared as a doublet at δ 135.75 (J_{P-C}=43.8 Hz). C_γ of the metallacycle appeared as a "triplet" at δ 57.11 (presumably overlapping double doublets, involving similar coupling constants to Rh and P). C_β appeared as a singlet (δ 25.06), while C_α was a doublet of doublets (δ 21.30, J_{Rh-C}=26.0 Hz; J_{P-C}=9.4 Hz). Two doublets were found for the diastereotopic methyl groups on phosphorus [δ 18.33 (d, J_{P-C}=30.9 Hz); δ 16.99 (d, J_{P-C}=33.2 Hz)]. Full details of ^{13}C NMR data for **48** will be found in the Experimental Section.

Carbonylation of (HBPz*$_3$)(CO)$\overline{\mathrm{Rh{-}C(O)CH_2CH_2CH}}\mathrm{_2}$ (47)

The carbonylation of **47** at an elevated temperature was carried out with the aim of forcing reductive elimination of cyclobutanone as shown in the hypothetical eq. 7-19.

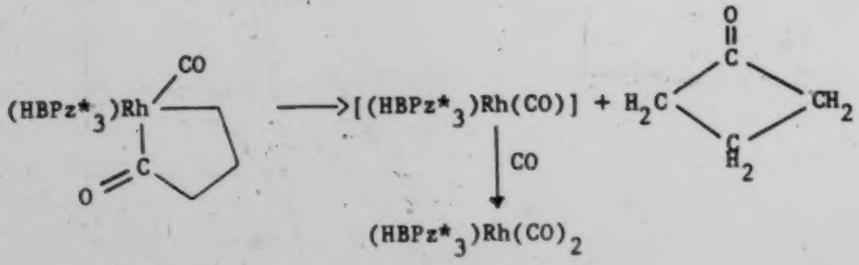
(HBPz*$_3$)Rh
CO
O
C
[(HBPz*$_3$)Rh(CO)] + H$_2$C
CH$_2$
C
H$_2$
O
C
CO
(HBPz*$_3$)Rh(CO)$_2$

(7-19)

Carbonylation of the acyl complex **47** in hexane at 75°C under 1000 psig of CO for eight days afforded no cyclobutanone. The IR spectrum indicated quantitative conversion of **47** to a new species, formulated as the six membered metallacycle **49** (eq. 7-20).

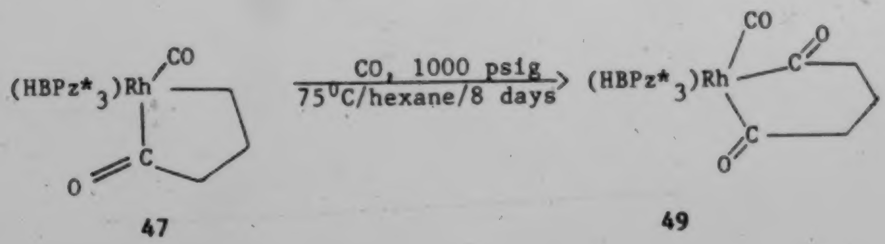
(HBPz*$_3$)Rh
CO
C
O
47
CO, 1000 psig
75°C/hexane/8 days
(HBPz*$_3$)Rh
CO
C
O
C
O
49

(7-20)

Compound **49** was isolated as colorless crystals in 81% yield. It is noteworthy that compound **49** does not survive chromatography. It was purified by careful crystallization. If a solution of **49** is allowed to stand (in hexane) at room temperature for several days, a small amount of **47** forms. Compound **49** was fully characterized by the usual spectral and analytical techniques.

The IR spectrum (hexane) (Fig. VII.6) exhibited the terminal ν_{CO} at 2045 cm^{-1} and the acyl ν_{CO} at 1702 and 1673 cm^{-1}. The two acyl bands are attributed to a coupling of the individual frequencies. The smaller splitting of acyl bands is presumed to be due to ring conformations.

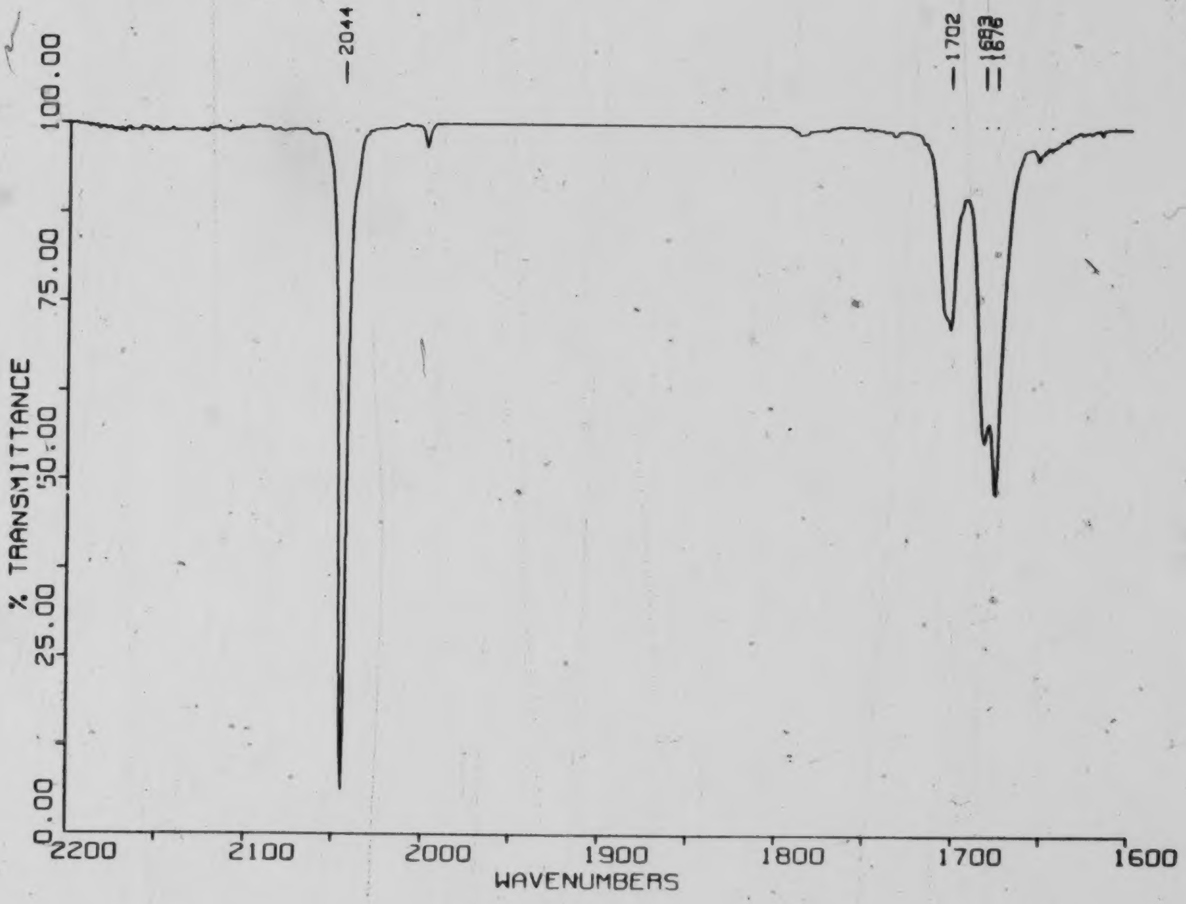

Figure VII.6 Infrared spectrum of rhodacyclohexadione (**49**) in hexane.

One might expect the six membered metallacycle to have a plane of symmetry (perhaps time averaged) containing Rh and C_γ. The ^1H NMR was consistent with this, exhibiting two singlets in the 4-H region of the Pz* region in a 2:1 ratio. The four β, β' protons appeared as a multiplet at δ 2.92. The γ protons overlapped with methyl resonances of the Pz* rings at ca. δ 2.40 and δ 2.18.

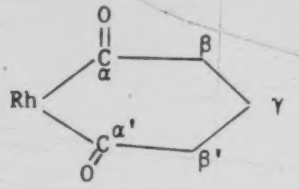

49 (only ring)

The APT ^{13}C NMR of **49** is shown in Fig. VII.7a. It showed the acyl and terminal CO at δ233.37 (d, J_{Rh-C}=25.7 Hz) and 189.92 (d, J_{Rh-C}=74.7 Hz) respectively. It exhibited two signals for the pyrazole 4-carbon in a 2:1 ratio and four signals for 3- and 5-pyrazole carbons in a 2:2:1:1 ratio. C_β was a doublet at δ 53.29 (J_{Rh-C}=3.7 Hz), (Fig. 7b) while C_γ appeared as a singlet at δ 21.31. The details of ^{13}C NMR data will be found in the Experimental Section.

Compound **49** decomposed at ca. 220°C during examination of its melting point. The IR of the hexane extract of the decomposed product showed mostly the five membered metallacycle (**45**).

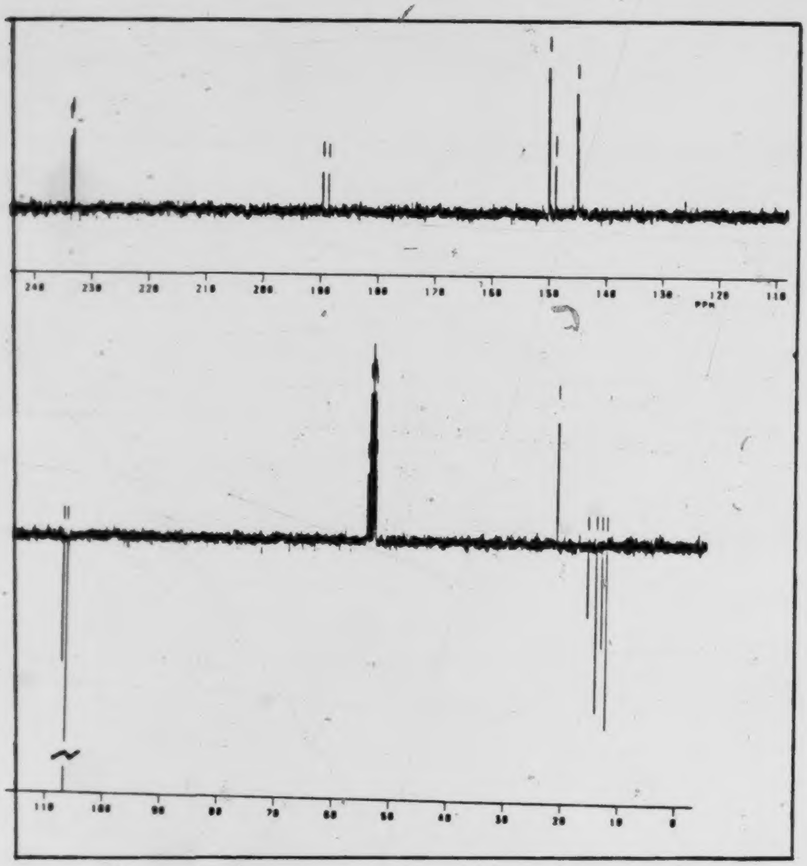

Figure VII.7a ^{13}C NMR spectrum (75.5 MHz, CD_2Cl_2) of rhodacyclohexadione (49).

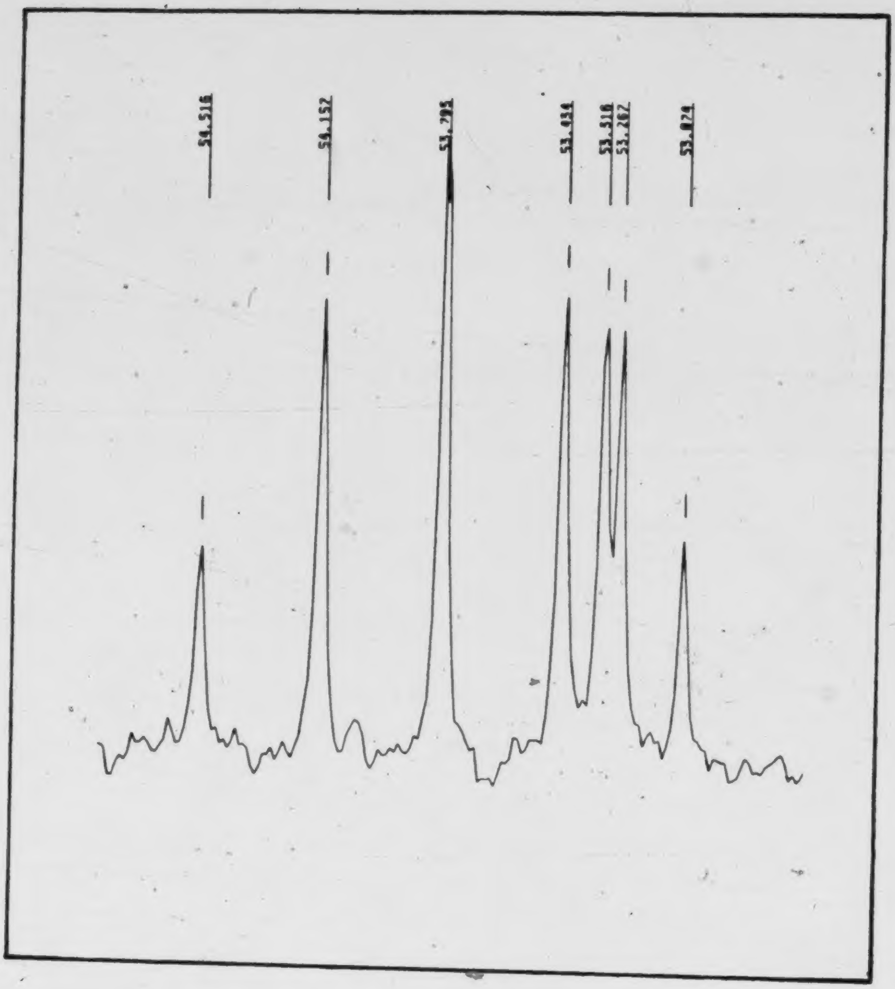

Figure VII.7b Expansion of ^{13}C NMR spectrum of **49** showing the doublet at δ 53.29 due to C_β of the ring. Other peaks are due to CD_2Cl_2 solvent.

Section 5

EXPERIMENTAL

Preparation of $(HBPz^*_3)(CO)Rh-CH_2CH_2CH_2$ (45)

Compound 1 (87.5 mg, 0.192 mmol) was taken up in purified cyclohexane (70 mL). The resulting yellow solution was irradiated for 9 min using a cyclopropane purge. The solution had become colorless at the end of this period. Removal of solvent under reduced pressure left a colorless solid which was dissolved in CH_2Cl_2 and chromatographed on a Florisil column (8 x 2.5 cm) eluting with CH_2Cl_2. Removal of solvent under vacuum afforded **45** as a colorless solid (68 mg, 75%) which decomposed at _ca._ 150°C without melting.

Characterization: IR (_n_-hexane) 2024 cm^{-1} (ν_{CO}). MS (140°C, 16 eV) $M^+-C_3H_6$ (428), $M^+-C_3H_6-CO$. ^1H NMR (CD_2Cl_2, ambient, 200 MHz) δ 5.80 (s, 1H), 5.68 (s, 2H), 3.15 (m, 1H (H_c/H_d, see text), 2.82 (m, 1H (H_c/H_d)], 2.50 (s, 3H), 2.30 (s, 3H), 2.25 (s, 6H), 2.20 (s, 6H), 1.65 (m, 2H (H_a/H_b)), 1.40 (m, 2H (H_a/H_b)). ^{13}C NMR (CD_2Cl_2, ambient, 75.5 MHz) δ 193.36 (d, J_{Rh-C}=74.2 Hz), 151.50 (s), 150.46 (s), 145.16 (s), 143.96 (s), 109.00 (s), 106.29 (s), 35.50 (d, $^2J_{Rh-C}$=3.7 Hz, $\underline{C}_\beta$), 13.83 (s), 13.58 (s), 13.31 (s), 12.50 (s), -13.31 (d, J_{Rh-C}=15.0 Hz, $\underline{C}_\alpha$). Anal. Calcd for $C_{19}H_{28}BN_6ORh$: C, 48.51; H, 5.96; N, 17.86. Found: C, 48.86; H, 6.05; N, 17.56.

Preparation of $(HBPz^*_3)(CO)Rh-CH_2CHCH_3CH_2$ (46)

Irradiation of 1 (80 mg, 0.175 mmol) in purified cyclohexane (80 mL) under a methylcyclopropane purge for 10 min afforded a colorless solution. The solvent was removed under reduced pressure and the resulting solid was dissolved in CH_2Cl_2 and then chromatographed on a Florisil column (8 x 2.5 cm) with CH_2Cl_2 eluent. Removal of solvent in vacuo yielded a colorless solid (55 mg, 65%). Attempts to separate the isomers of **46** (see discussion) by crystallization were not successful. MP darkens above 145°C.

Characterization: IR (*n*-hexane) 2023 cm^{-1} (ν_{CO}), MS (135°C, 16 eV) M^+-CO (428), M^+-CO-C_4H_8. ^{1}H NMR (CD_2Cl_2, ambient, 200 MHz) major isomer (**46A**): δ 5.85 (s, 1H), 5.78 (s, 2H), 3.44 (m, 1H), 2.57 (s, 3H), 2.36 (s, 3H), 2.32 (s, 6H), 2.25 (s, 6H), 2.00 (m, 2H), 1.13 (d, J_{H-H}=7.0 Hz, 3H, β-CH_3), 1.00 (m, 2H); minor isomers: most peaks of the minor isomers (**46B** and **46C**) were not well resolved, but methyl (bound to metallacycle) signals at δ 1.17 (d, J=7.0 Hz) and 1.07 (d, J=7.0 Hz) were reasonably well resolved and integrated (together) as *ca.* 15% of the products. ^{13}C NMR (CD_2Cl_2, ambient, 75.5 MHz) major isomer **46A**:

CO : δ 193.7 (d, J=74.0 Hz)
3,5 PzC : δ 150.95, 150.52, 145.31, 144.00
4 PzC : δ 108.64, 106.30
βC : δ 40.77 (d, J=3.8 Hz)
βC-CH_3 : δ 23.07
3,5 PzCH_3 : δ 13.82, 13.72, 13.65, 12.51
αC : -3.35 (d, J=14.3 Hz)

The minor isomers were not observed in the ^{13}C NMR spectrum. Anal. Calcd for $C_{20}H_{30}BN_6ORh$: C, 49.59; H, 6.20; N, 17.35. Found: C, 49.85; H, 6.38; N, 17.42.

Thermolysis of 45

Compound **45** (11.2 mg, 0.024 mmol), hexamethyldisiloxane (1 μL, 0.005 mmol) and benzene-d_6 (0.5 mL) were placed in an NMR tube sealed to a ground glass joint. After three cycles of freeze-thaw degassing, the NMR tube was sealed off under vacuum. A ^{1}H NMR spectrum was recorded to determine the relative intensities of hexamethyldisiloxane and methyl resonances of the Pz* rings.

The NRM tube was immersed in a 75°C bath (Lauda RK 20) and periodically removed to record the ^{1}H NMR spectrum. Before recording the NMR spectrum, the foil-wrapped NMR tube was allowed to cool to room temperature and shaken to dissolve the gaseous products formed during thermolysis. The rate of disappearance of **45** was followed by monitoring the integral of one of the Pz* methyl resonance (δ 2.44) against the internal standard. The change in concentration of the intermediate $(HBPz^*_3)Rh(CO)(\eta^2\text{-}CH_2CHCH_3)$ (**34b**) versus time was followed by monitoring the intensity of the methyl resonance of the η^2-propylene ligand (δ 1.83) against the internal standard. The rate of appearance of **8a** was followed by monitoring the rate of appearance of one of 4-H resonances of **8a** (δ 5.45). The resonance due to cyclopropane was at δ 0.16. Free propylene resonances appeared at δ 1.54 (m, 3H [$\underline{CH_3}$]), 4.96 (m, 2H) and 5.74 (m, 1H).

Thermolysis of $(HBPz^*_3)Rh(CO)(\eta^2\text{-}CHCHCH_3)$ (34b)

Compound **34b** (10 mg, 0.021 mmol) was dissolved in benzene-d_6 (0.5 mL) in a NMR tube, and hexamethyldisiloxane (1 μL, 0.005 mmol) was added to the solution. The NMR tube was sealed off under vacuum after three cycles of freeze-thaw degassing. The ^{1}H NMR spectrum of the resulting solution was recorded to determine the relative intensity of the internal standard and methyl resonance of the η^2-propylene ligand in **34b**. The NMR tube was heated in a bath [Lauda RK 20] at 75°C and removed periodically and cooled to room temperature and ^{1}H NMR spectra were recorded. The rate of disappearance of **34b** was followed by monitoring the integral of the methyl resonance of the η^2-propylene ligand. Propylene was detected as the organic product.

Thermolysis of 46

Compound **46** (11.5 mg, 0.024 mmol), hexamethyldisiloxane (1 μL, 0.005 mmol) and benzene-d_6 (0.5 mL) were placed in an NMR tube that was attached to a ground glass joint. After three cycles of degassing, the tube was sealed under vacuum. The thermolysis was carried out by heating the NMR tube in a constant temperature bath (Lauda RK 20) at 75°C. The NMR tube was removed from the bath from time to time, cooled to room temperature and shaken before taking NMR spectra. The ^{1}H NMR indicated methylcyclopropane and isobutylene as the organic products. Resonances due to methylcyclopropane appeared in the +1 to −1 ppm region. The resonances due to isobutylene were at δ 5.54 (septet, 2H) and 2.56 (t, 6H).

Preparation of $(HBPz^*_3)(CO)\overline{Rh-C(O)CH_2CH_2CH_2}$ (47)

Metallacyclobutane **45** (95 mg, 0.202 mmol) was taken up in n-hexane (60 mL). The resulting solution was pressurized with 950 psig of CO in a 150 mL Parr bench autoclave containing a stirrer bar and stirred magnetically at room temperature for 7 days. The IR indicated virtually quantitative conversion of **45** to the new acyl complex **47**. Removal of solvent under reduced pressure gave a colorless solid that was dissolved in CH_2Cl_2 and chromatographed on a Florisil column (8 x 2.5 cm) with CH_2Cl_2 eluent. Recrystallization from CH_2Cl_2/hexane by slow evaporation afforded colorless crystals (55.3 mg, 55%).

Characterization: IR (*n*-hexane) 2038 (ν_{CO} terminal), 1707 (ν_{CO} acyl) cm^{-1}. MS (195°C, 16 eV) M^+ (498), $M^+-C_3H_6$, $M^+-C_3H_6-2CO$. ^1H NMR (CD_2Cl_2, ambient, 200 MHz) δ 5.83 (s, 2H), 5.79 (s, 1H), 3.37 (m, 1H), 3.00 (m, 1H), 2.86 (m, 1H), 2.75 (m, 1H), 2.45 (s, 3H), 2.30 (s, 9H, coincidental overlap of three Pz* methyl resonances), 2.18 (s, 3H), *ca.* 2.14 (m, 1H, overlapped with methyl resonance), 2.08 (s, 3H), *ca.* 2.04 (m, 1H, overlapped with methyl resonance). ^{13}C NMR (CD_2Cl_2, ambient, 75.5 MHz) δ 241.51 (d, J_{Rh-C}=25.7 Hz), 189.45 (d, J_{Rh-C}=72.5 Hz), 151.02 (s), 150.52 (s), 149.92 (s), 145.21 (s), 144.95 (s), 144.25 (s), 108.55 (s), 107.07 (s), 106.45 (s), 59.20 (d, $^2J_{Rh-C}$=8.3 Hz, C_γ), 23.65 (s, C_β), 24.45 (d, J_{Rh-C}=21.9 Hz, C_α), 15.00 (s), 14.34 (s), 14.05 (s), 13.41 (s), 12.65 (s), 12.57 (s). Anal. Calcd for $C_{20}H_{28}BN_6ORh$: C, 48.15; H, 5.62; N, 16.68. Found: C, 47.80; H, 5.61; N, 16.81.

Preparation of $(HBPz^*_3)(PMe_2Ph)\overline{Rh{-}C(O)CH_2CH_2CH_2}$ (48)

Compound **45** (70 mg, 0.149 mmol) was taken up in CH_2Cl_2 (40 mL). Excess PMe_2Ph (0.2 mL, 1.5 mmol) was added and the reaction mixture was stirred at room temperature for two days. The IR indicated complete disappearance of **45** and the new ν_{CO} at 1650 cm^{-1} formed. Removal of solvent and excess phosphine under reduced pressure gave a colorless solid. The resulting solid was dissolved in CH_2Cl_2 and chromatographed on a Florisil column (8 x 2.5 cm) with acetonitrile eluent. The solid after evaporation of solvent was taken up in a minimal amount of CH_2Cl_2, and n-hexane added. Slow evaporation of the solution over a period of few days yielded colorless crystals (70 mg, 75%).

Characterization: IR (CH_2Cl_2) 1650 cm^{-1} (ν_{CO}, acyl). MS (230°C, 16 eV) $M^+-C_3H_6$ (566), $M^+-C_3H_6-CO$, $M^+-C_3H_6-CO-PMe_2Ph$. ^1H NMR (CD_2Cl_2, ambient, 200 MHz) δ 7.15 (m, 1H), 6.96 (m, 2H), 6.82 (m, 2H), 5.75 (s, 1H), 5.72 (s, 1H), 5.48 (s, 1H), 3.15 (m, 2H), 2.82 (m, 2H), 2.42 (s, 3H), 2.36 (s, 3H), 2.28 (s, 3H), 2.26 (s, 3H), 2.14 (s, 3H), ca. 2.94 (m, 2H), 1.87 (s, 3H), 1.76 (dd, $^2J_{P-H}$=8.5 Hz, $^3J_{Rh-H}$=1.0 Hz, 3H), 1.70 (dd $^2J_{P-H}$=8.2 Hz, $^3J_{P-H}$=1.2 Hz, 3H). ^{13}C NMR (CD_2Cl_2, ambient, 75.5 MHz) δ 251.55 (dd, J_{Rh-C}=30.94 Hz, J_{P-C}=10.6 Hz), 151.54, 150.42, 149.60, 145.12, 144.40, 143.64, 135.76 (d, J_{P-C}=43.8 Hz), 130.86, 130.73, 129.48, 127.86, 127.35, 107.94 (overlapped two pyrazolyl 4-C), 106.96, 57.11 ("t", presumably overlapping double doublet), 25.06, 21.30 (dd, J_{P-C}=33.2 Hz), 15.69, 15.42, 14.88, 14.29, 13.62, 13.06 (two Pz* methyls overlapping). Anal. Calcd for $C_{27}H_{34}BN_6OPRh.0.5\ CH_2Cl_2$: C, 50.73; H, 6.15; N, 12.91. Found: C, 50.73; H, 6.37; N, 12.23.

Preparation of (HBPz*$_3$)(CO)Rh-C(O)CH$_2$CH$_2$CH$_2$CO (49)

Compound **47** (100 mg, 0.200 mmol) in n-hexane (60 mL) was placed in a 150 mL Parr bench autoclave that contained a stir bar. The solution was first flushed with CO and then pressurized with 1000 psig of CO and heated at 75°C in an oil bath with magnetic stirring. After 7 days the IR indicated essentially complete conversion of **47** to **49**. Comparison of the IR spectrum of authentic cyclobutanone suggested that no cyclobutanone formed in the above reaction. Removal of solvent under reduced pressure yielded a colorless solid which was dissolved in a minimal amount of n-hexane. Cooling the hexane solution to -20°C afforded colorless crystals of **49** (85 mg, 81%) MP decomposed above 220°C.

Characterization: IR (n-hexane) 2045 (ν_{CO}, terminal), 1702, 1673 (ν_{CO}, acyl) cm^{-1}. MS (170°C, 16 eV) M^+ (526), M^+-CO, M^+-CO-C_3H_6, M^+-2CO-C_3H_6, M^+-3CO-C_3H_6. ^1H NMR (CD_2Cl_2, ambient, 200 MHz) δ 5.88 (s, 2H), 5.82 (s, 1H), 2.92 (m, 4H), 2.40 (10H: ca. 9H for three pyrazole methyl and 1H for H_γ of metallacycle), 2.18 (7H: 6H for two pyrazole methyls and 1H for H_γ), 1.80 (s, 3H). ^{13}C NMR (CD_2Cl_2, ambient, 75.5 MHz), δ 233.37 (d, J_{Rh-C}=25.7 Hz), 188.92 (d, J_{Rh-C}=74.7 Hz), 149.91, 148.82, 144.99, 107.45, 106.77, 53.29 (d, $^2J_{Rh-C}$=3.7 Hz), 21.31, 15.94, 14.45, 13.47, 12.64. Anal. Calcd for $C_{21}H_{28}BN_6O_3Rh$: C, 47.91; H, 5.32; N, 15.97. Found: C, 48.07; H, 5.38; N, 15.37.

References for Chapter VII

1. (a) J.X. McDermott, J.F. White and G.M. Whitesides, J. Am. Chem. Soc., 98 (1976) 6521.

   (b) G.B. Young and G.M. Whitesides, J. Am. Chem. Soc., 100 (1978) 5808.

   (c) T.M. Miller and G.M. Whitesides, Organometallics, 5 (1986) 1473.

2. J.P. Collman, L.S. Hegedus, J.R. Norton and R.G. Finke, "Principles and Applications of Organotransition Metal Chemistry", University Science Books, California, (1987), P459.

3. T.J. Katz, Adv. in Organometal. Chem., 16 (1977) 283.

4. C.G. Biefeld, H.A. Eick and R.H. Grubbs, Inorg. Chem., 12 (1973) 2166.

5. R.H. Grubbs and T.K. Brunck, J. Am. Chem. Soc., 94 (1972) 2538.

6. R.J. Haines and G.J. Leigh, Chem. Soc. Rev., 4 (1975) 155.

7. N. Calderon, J.P. Lawrence and E.A. Ofstead, Adv. Organometal. Chem. 17 (1979) 449.

8. L. Cassar, P.E. Eaton and J. Halpern, J. Am. Chem. Soc., 92 (1970) 3515.

9. T.J. Katz and N. Acton, Tett. Lett., (1967) 2601.

10. W. Hall, R.J. Puddephatt, K.R. Seddon and C.F.H. Tipper, J. Organomet. Chem., 81 (1974) 423.

11. K.C. Bishop III, Chem. Rev., 76 (1976) 461.

12. A.R. Fraser, P.H. Bird, S.A. Bezman, J.R. Shapley, R. White and J.A. Osborn, J. Am. Chem. Soc., 95 (1973) 597.

13. J. Doyle, J. McMeeking and P.J. Binger, J. Chem. Soc., Chem. Commun., (1976) 376.

14. M.A. Bennett, R.N. Johnson and I.B. Tomkins, J. Am. Chem. Soc., 96 (1974) 61.

15. G.K. Barker, M. Green, J.A.K. Howard, J.L. Spencer and F.G.A. Stone, J. Am. Chem. Soc., 98 (1976) 3373.

16. P. Diversi, G. Ingrosso, A. Immirzi, W. Porzio and M. Zocchi, J. Organomet. Chem., 125 (1977) 253.

17. P.W. Jolly, C. Kruger, R. Salz and J.K. Sekutowski, J. Organometal. Chem., 165 (1979) C39.

18. S.D. Chappell and D.J. Cole-Hamilton, Polyhedron, 1 (1982) 739.

19. C.F.H. Tipper, J. Chem. Soc., (1955) 2045.

20. S.E. Binns, R.H. Cragg, R.D. Gillard, B.T. Heaton and M.F. Pilbrow, J. Chem. Soc., (A) (1969) 1227.

21. R.J. Puddephatt, Coord. Chem. Rev., 33 (1980) 149.

22. (a) J.W.F.L. Seetz, G. Schat, O.S. Akkerman, F. Biekelhaupt, Angew Chem. Int. Ed. Engl., 22 (1983) 248.
    (b) J.W.F.L. Seetz, B.J.J. Van de Heisteeg, G. Schat, O.S. Akkerman and F. Bickelhaupt, J. Mol. Catal., 28 (1985) 71.

23. M. Ephritikhine, M.L.H. Green and R.E. MacKenzie, J. Chem. Soc. Chem. Commun., (1976) 619.

24. R.A. Periana and R.G. Bergman, J. Am. Chem. Soc., 106 (1984) 7272.

25. (a) J.A. Ibers, R. DiCosimo and G.M. Whitesides, Organometallics, 1 (1982) 13.
    (b) G.M. Whitesides, R.H. Reamey, R.L. Brainard, A.N. Izumi, T.J. McCarthy, Ann. N.Y. Acd. Sci., 56 (1983) 415.

26. (a) T.H. Tulip and D.L. Thorn, J. Am. Chem. Soc., 103 (1981) 2448.
    (b) J.C. Calabrese, M.C. Cotton, T. Herskovitz, U. Klabunde, G.W. Parshall, D.L. Thorn and T.H. Tulip, Ann. N.Y. Acad. Sci., 415

(1983) 302.

27. (a) J.W. Bruno, G.M. Smith, T.J. Marks, C.K. Fair, A.J. Schultz and J.M. Williams, J. Am. Chem. Soc., 108 (1986) 40.
    (b) C.M. Fendrick and T.J. Marks, J. Am. Chem. Soc., 108 (1986) 425.
28. R.A. Periana and R.G. Bergman, J. Am. Chem. Soc., 108 (1986) 7346.
29. R.G. Bergman, Science, 223 (1984) 902.
30. R.J. Al-Essa, R.J. Puddephatt, D.C.L. Perkins, M.C. Rendle and C.F.H. Tipper, J. Chem. Soc., Dalton Trans., (1981), 1738.
31. R.A. Alberty and W.G. Miller, J. Chem. Phys., 26 (1957) 1231.
32. J.P. Collman, L.S. Hegedus, J.R. Norton and R.G. Finke, "Principles and Applications of Organotransition Metal Chemistry", University Science Books, California, (1987) P471.
33. R.H. Grubbs, A. Miyashita, M. Liu and P. Burk, J. Am. Chem. Soc., 100 (1978) 2418.

CHAPTER VIII

DISCUSSION AND CONCLUSIONS

The work reported in the foregoing Chapters involves the compound $(HBPz^{*}_{3})Rh(CO)_{2}$ (**1**), its reactions and the characterization of various derivatives. Although **1** was first mentioned in the literature in 1971, it had received almost no attention until this work began. The investigations comprising this Thesis can be summarized under four major headings.

1. Coordination chemistry and dynamic behaviour

Tris(3,5-dimethylpyrazolyl)borato complexes, $(HBPz^{*}_{3})Rh(CO)(L)$ (L=CO, PR_3, olefin) have been synthesized and characterized. From a comparison of the ν_{CO} of the unambiguously four-coordinate 16-electron dicarbonyl rhodium compound, $(H_{2}BPz^{*}_{2})Rh(CO)_{2}$, it was concluded that $(HBPz^{*}_{3})Rh(CO)_{2}$ (**1**) has a five-coordinate 18-electron structure in hexane solution. However, the IR spectrum of 1 in CH_2Cl_2 suggested that a small (ca. 1%) amount of the four-coordinate $(\eta^{2}-HBPz^{*}_{3})Rh(CO)_{2}$ was present in equilibrium. Hence the energy difference between four- and five-coordinate forms of 1 is small.

Solution infrared spectra using the related bispyrazolylborates $(H_{2}BPz^{*}_{2})Rh(CO)(L)$ (L=PR_3, olefin) for comparison established that the $HBPz^{*}_{3}$ ligand was bidentate in $(HBPz^{*}_{3})Rh(CO)(L)$ (L=PR_3, olefin). ^{1}H NMR spectra of the latter complexes showed three equivalent Pz* rings at 25°C, going to two in a 2:1 ratio at low temperatures. Low temperature limiting spectra having three nonequivalent Pz* rings as expected for the static structures could not be obtained. The observed dynamic behaviour was explained on the basis of two kinds of fluxional process: a high temperature process, which averages all Pz* resonances at ambient temperature and is slowed in the -40° to -90°C range to produce two Pz* signals; and a low temperature process, which averages the two equatorial Pz* rings which are trans to different ligands. The latter has not been frozen out even at -90°C. It was proposed that the observed low temperature fluxional process involves a five-coordinate intermediate, which is trigonal bipyramidal and has a plane of symmetry. Activation parameters for the high temperature fluxional process were determined for two representative compounds, $(\eta^2$-$HBPz^*_3)Rh(CO)(PMe_2Ph)$, **4b**, and $(\eta^2$-$HBPz^*_3)Rh(CO)(\eta^2$-$C_2H_4)$, **34a**.

2. Photochemical C-H activation

a. Aromatic

Compound 1 [$(HBPz^*_3)Rh(CO)_2$] photochemically activates aromatic hydrocarbons with great efficiency at room temperature. Unlike previously reported photochemical systems, activation proceeds under daylight or tungsten illumination.

When a benzene solution of 1 was irradiated for five minutes under standard conditions, the conversion to $(HBPz^*_3)Rh(CO)(H)(C_6H_5)$ (**6**) was complete. Under the same conditions, conversion of $Cp^*Ir(CO)_2$ to the hydridophenyl complex was only ca. 60% after six hours irradiation, and there was a general degradation at longer times.[1] There was a significant barrier to phenyl rotation in this compound (**6**) and its derivatives due to the large steric requirements of the $HBPz^*_3$ ligand. Above room temperature solutions of **6** in benzene-d_6 underwent exchange forming $(HBPz^*_3)Rh(CO)(D)(C_6D_5)$ and followed pseudo-first order kinetics. The activation parameters for the exchange process are very similar to those of $Cp^*(PMe_3)Rh(H)(C_6H_5)$ with C_6D_6.[2] The similarity in activation parameters in the two systems is so striking that the mechanism for exchange is likely very similar in the two systems.

As it does benzene, compound 1 also efficiently activated other aromatic hydrocarbons. For example, it activated toluene sp^2-CH bonds at ambient temperature. The ^1H NMR of $(HBPz*_3)Rh(CO)(H)(C_6H_4Me)$ (**10**) at -80°C showed three hydride resonances which were presumed to be due to *para* and two *meta* conformers. Compound 1 also activated p-xylene and p-difluorobenzene to the corresponding hydrido species. A detailed study of the stability of p-difluoro compound, $(HBPz*_3)Rh(CO)(H)(C_6H_3F_2)$ (**13**), such as barrier to reductive elimination of $p\text{-}C_6H_4F_2$ would be of future interest.

Like compound 1, $(\eta^2\text{-}HBPz*_3)Rh(CO)(L)$ ($L=PR_3$, olefin) also activated aromatic C-H bonds. For instance, irradiation of $(\eta^2\text{-}HBPz*_3)Rh(CO)(PMe_2Ph)$ (**4b**) in benzene afforded mainly $(HBPz*_3)Rh(H)(Ph)(PMe_2Ph)$. One of the most significant discoveries was that photolysis of $(\eta^2\text{-}HBPz*_3)Rh(CO)(\eta^2\text{-}C_2H_4)$ (**34a**) in benzene yielded not only the hydridophenyl compound **6**, but the unexpected $(HBPz*_3)Rh(CO)(Et)(Ph)$ (**39**) in approximately equal amounts. The product ratio appeared to be sensitive to the wavelength used. Experimentation using other olefin complexes and hydrocarbons suggested that this combination of C-H activation and olefin insertion is *not* a general reaction, but imposes fairly definite requirements on both hydrocarbon and olefin.

b. Aliphatic

Photolysis of 1 in purified cyclohexane (CyH) for five minutes using a N_2 purge gave complete conversion of 1 to $(HBPz*_3)Rh(CO)(H)(Cy)$

(**17**). The N_2 purge was used during irradiation to prevent back reaction of **17** with released CO. In view of its lability and limited stability, **17** was not isolated but converted by reaction with CCl_4 to the chloro derivative $(HBPz^*_3)Rh(CO)(Cl)(Cy)$ (**18**) for characterization. The solution of **17** provided a thermal source of the reactive intermediate $[(HBPz^*_3)Rh(CO)]$ for activation of other molecules, such as C_6H_6, CH_4, H_2, C_2H_4, C_3H_6, $C\text{-}C_3H_6$ etc.

Addition of benzene to a cyclohexane solution of **17** at 25°C resulted in its quantitative conversion to phenyl hydride (**6**) within 10 minutes; **17** is a remarkably efficient scavenger for aromatic hydrocarbons. The kinetics of this reaction, in conjunction with the activation parameters of the exchange reaction of **6** with C_6D_6, enabled an estimate to be made of the relative strengths of Rh-Ph and Rh-Cy bonds in these molecules. The Rh-Ph bond is stronger by *ca*. 23 kcal mol^{-1}.

The dark reaction of CH_4 with **17** indicated thermal equilibrium between **17** and $(HBPz^*_3)Rh(CO)(H)(CH_3)$ (**19**) (eq. 8-1) at room temperature.

$$\underset{\textbf{17}}{(HBPz^*_3)Rh(CO)(H)(Cy)} + CH_4 \rightleftarrows \underset{\textbf{19}}{(HBPz^*_3)Rh(CO)(H)(CH_3)} + CyH \qquad (8\text{-}1)$$

The equilibrium constant for eq. 8-1 was *ca*. 190, indicating a reasonably high equilibrium selectivity favouring the primary rhodium-methyl bond. With the usual assumptions and known bond dissociation energies involved it was estimated that

$$D[Rh-Me] - D[Rh-Cy] \cong 13 \text{ kcal mol}^{-1}.$$

This implies, with the previous result, that $D[Rh-Ph] - D[Rh-Me] \cong 10$ kcal mol^{-1}.

Compound 1 also activated C-H bonds of a variety of acyclic hydrocarbons such as *n*-pentane, *n*-hexane, neohexane and *tert*-butyl methyl ether.

As noted earlier, (η^2-HBPz$^*_3$)Rh(CO)(PMe$_2$Ph) (**4b**) activated solvent benzene intermolecularly. However, photolysis of **4b** in cyclohexane resulted in *intra*molecular C-H activation (orthometallation of the phenyl ring). No *inter*molecular C-H activation product was observed in this case.

c. Olefins and cyclopropane

Photolysis of 1 in CyH under ethylene and propylene purge gave (HBPz$^*_3$)Rh(CO)(η^2-C$_2$H$_4$) (**34a**) and (HBPz$^*_3$)Rh(CO)(η^2-C$_3$H$_6$) (**34b**) respectively as the final products. **34a** was presumed to form via vinyl hydride (HBPz$^*_3$)Rh(CO)(H)(CH=CH$_2$). **34b** formed presumably through the intermediate allylic hydride (HBPz$^*_3$)Rh(CO)(H)(CH$_2$CH=CH$_2$).

Irradiation of 1 in CyH using cyclopropane purge yielded stable isolable rhodacyclobutane $(HBPz^*_3)(CO)\overline{Rh-CH_2CH_2CH_2}$ (**45**), presumed to be rearranged from the initial C-H activation product, (HBPz$^*_3$)Rh(CO)(H)(C$_3$H$_5$). An analogous reaction with methylcyclopropane afforded a mixture of methyl-substituted metallacyclobutanes (**46**).

3. Thermal C-H activation

1 activated benzene solvent in the dark forming

$(HBPz^*{}_3)Rh(CO)(H)(C_6H_5)$ (**6**). A reasonable rate was achieved only at 140°C, at which temperature the reaction was complicated by formation of two binuclear hydrides (**9**, **38**). The new olefin complexes $(\eta^2\text{-}HBPz^*{}_3)Rh(CO)(\eta^2\text{-olefin})$ (**34a**, olefin = C_2H_4; **34b**, olefin = CH_2CHCH_3) activated benzene cleanly in the yields of 90% or more in the 75-105°C range. Activation of an aromatic C-H bond by thermal loss of electron pair donor ligand is not a common process, and it usually does not proceed to a measurable extent unless combined with some other energetically favourable step. The uniqueness of this reaction is that benzene oxidative addition alone is enough to drive them to a measurable extent. The energies of M-H and M-Ph bonds formed must compensate for the M-L' and Ph-H bonds lost in eq. 8-2.

$$ML_nL' + Ph\text{-}H \xrightarrow{dark} [ML_n(H)(Ph)] + L' \qquad (8\text{-}2)$$

As mentioned earlier **34a** and **34b** exist in solution as the four-coordinate, 16-electron Rh (I), while there is little question of the tridentate character of $HBPz^*{}_3$ ligand in the Rh (III) product (**6**). Thus in the overall energetics, formation of a new Rh-N bond partly offset the loss of the Rh-olefin bond. This may be a significant factor in the effectiveness of the trispyrazolylborate system in C-H activation.

Thermolysis of **34b** in cyclohexane at 75°C afforded the binuclear hydride-bridged species (**38**), where intramolecular activation of one of the pyrazole methyl groups had occurred. This is in constrast to $Cp^*Rh(CO)_2$, where generation of the 16-electron fragment, $[Cp^*Rh(CO)]$ led to the dimer $[Cp^*Rh(\mu\text{-}CO)]_2$.[3]

Thermolysis of metallacyclobutane (**45**) in benzene at 75°C gave phenyl hydride (**6**) in good yield. Two pathways were involved in the formation of **6**. The major route involved the intermediacy of η^2-propylene complex $(HBPz^*_3)Rh(CO)(\eta^2$-propylene), **34b**, while the second involved direct reductive elimination of cyclopropane.

4. Functionalization using carbon monoxide

Carbonylation of $(HBPz^*_3)Rh(CO)(Et)(Ph)$ (**39**) in hexane afforded mainly $(HBPz^*_3)Rh(COEt)(Ph)$ (**40**) as a stable compound, while the minor product was presumed to be $(HBPz^*_3)Rh(COEt)(COPh)$ (**41**). **41** slowly converted in hexane solution at room temperature to **40**. Transformation of **40** into propiophenone in high yield occurred readily upon treatment with $ZnBr_2$. Similarly carbonylation of $(HBPz^*_3)Rh(CO)(Me)(Ph)$ (**9**) gave $(HBPz^*_3)Rh(COMe)(Ph)$ (**42**) as the major product. The minor product was presumed to be $(HBPz^*_3)Rh(COMe)(COPh)$ (**43**). **42** also reacted with $ZnBr_2$ with the elimination of acetophenone in good yield.

Carbonylation of metallacyclobutane (**45**) at room temperature yielded a stable isolable metallacyclopentanone (**48**). Further carbonylation of this five membered acyl complex at elevated temperature resulted in a six membered metallacyclic dione (**49**).

References for Chapter VIII

1. J.K. Hoyano and W.A.G. Graham, J. Am. Chem. Soc., 104 (1982) 3723.

2. W.D. Jones and F.J. Feher, J. Am. Chem. Soc., 106 (1984) 1650.

3. A. Nutton and P.M. Maitlis, J. Organomet. Chem., 166 (1979) C21.